GEOLOGY, ORE DEPOSITS AND APPLIED
ROCK GEOCHEMISTRY OF THE BUCHANS GROUP

JOHN GEOFFREY THURLOW
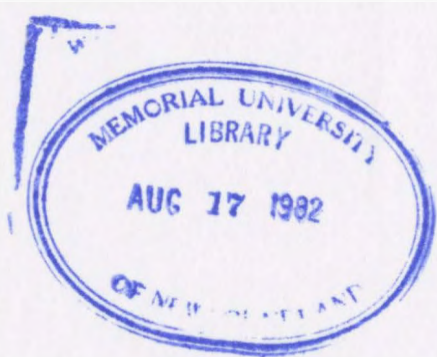
NOTICE

AVIS

The quality of this microfiche is heavily dependent upon the quality of the original thesis submitted for microfilming. Every effort has been made to ensure the highest quality of reproduction possible.

If pages are missing, contact the university which granted the degree.

Some pages may have indistinct print especially if the original pages were typed with a poor typewriter ribbon or if the university sent us a poor photocopy.

Previously copyrighted materials (journal articles, published tests, etc.) are not filmed.

Reproduction in full or in part of this film is governed by the Canadian Copyright Act, R.S.C. 1970, c. C-30. Please read the authorization forms which accompany this thesis.

La qualité de cette microfiche dépend grandement de la qualité de la thèse soumise au microfilmage. Nous avons tout fait pour assurer une qualité supérieure de reproduction.

S'il manque des pages, veuillez communiquer avec l'université qui a conféré le grade.

La qualité d'impression de certaines pages peut laisser à désirer, surtout si les pages originales ont été dactylographiées à l'aide d'un ruban usé ou si l'université nous a fait parvenir une photocopie de mauvaise qualité.

Les documents qui font déjà l'objet d'un droit d'auteur (articles de revue, examens publiés, etc.) ne sont pas microfilmés.

La reproduction, même partielle, de ce microfilm est soumise à la Loi canadienne sur le droit d'auteur, SRC 1970, c. C-30. Veuillez prendre connaissance des formules d'autorisation qui accompagnent cette thèse.

THIS DISSERTATION
HAS BEEN MICROFILMED
EXACTLY AS RECEIVED

LA THÈSE A ÉTÉ
MICROFILMÉE TELLE QUE
NOUS L'AVONS REÇUE

GEOLOGY, ORE DEPOSITS AND APPLIED ROCK

GEOCHEMISTRY OF THE BUCHANS GROUP, NEWFOUNDLAND

by

©

John Geoffrey Thurlow, B.A.Sc., M.Sc.

A Thesis submitted in partial fulfillment
of the requirements for the degree of

Doctor of Philosophy

Department of Geology
Memorial University of Newfoundland
St. John's, Newfoundland

April, 1981

ABSTRACT

The Buchans Group is a regionally extensive, sub-
marine, calc-alkaline volcanic suite erupted at a point in
time near the Ordovician-Silurian boundary. It is subdivided
into Lower and Upper Subgroups, each of which consists of
interbedded mafic to felsic flows, breccias, pyroclastics
and related sediments. The Lower Subgroup, which contains
the economic ores, consists of four volcanic formations which
have been repeated structurally by thrust faults, forming
seven major volcanic sequences. The economically barren
Upper Subgroup is subdivided into three major sequences.

Plutonic rocks associated with the Buchans
Group include the Feeder Granodiorite, Hungry Mountain
Complex and the Topsails Granite. The earliest of these,
the Feeder Granodiorite, is considered to be a time-
equivalent plutonic facies of the Buchans Group. Deformed
plutonic facies of the Hungry Mountain Complex were tecton-
ically emplaced upon the Buchans Group during a major
episode of southeast-directed Silurian thrusting. The Siluro-
Devonian Topsails Granite intrudes all older formations and,
in the Buchans area, consists of two main phases: a
high level alkali-feldspar phase and a coarser grained
equigranular peralkaline phase. Gently dipping alkali
amphibole-bearing ignimbrite forms roof pendants within the
Topsails Granite. These are interpreted as extrusive

equivalents of the Granite and may be outliers of the
Springdale Group.

The Buchans ores are high grade polymetallic
massive sulphide deposits associated with submarine felsic
volcanic rocks near the top of the Lower Buchans Subgroup.
Three genetically related ore types are recognized; stock-
work ore, in situ ore, and mechanically transported ore.
Stockwork ore consists of networks of veinlet and disseminated
base metal sulphides within highly silicified and locally
chloritized host rocks. In situ ore lies stratigraphically
above stockwork mineralization and is composed of banded
to streaky yellow ore, black ore and barite. Transported
ore consists of discrete sulphide and barite fragments
in breccias which flank in situ ores and form substantial
distinct orebodies. Their origin is interpreted as a
result of brecciation at source, transport down-slope
in paleotopographic channels by gravity-driven submarine
debris flows, and deposition in depressions. The Buchans
ores and their environment are similar to those of the
Japanese Kuroko deposits in almost all respects.

Whole-rock chemical analyses have shown that
Buchans Group volcanic rocks are similar in chemical
abundances and variations to other calc-alkaline volcanic
suites. There was apparently little chemical evolution in
Buchans Group flows through the stratigraphic column, and

flows within the ore horizon sequences are essentially similar to their counterparts elsewhere in the Buchans Group. Pyroclastic rocks of the ore horizon are chemically similar to those at other stratigraphic horizons and show no anomaly related to mineralization with the exception of high Ba content.

Study of the unaltered pyroclastic rocks of the ore horizon has shown that there are no regional variations in element concentrations, element ratios, discriminant scores or factor scores, either along or across stratigraphy, which bear relationship to mineralization. Erratic base metal concentrations are present in host pyroclastic rocks only within 50 m of ore. Visibly altered footwall rocks have undergone chemical changes typical of rocks in most massive sulphide terranes.

Anomalously high concentrations of Ba in ore horizon pyroclastics is a regional feature which provides a means of distinguishing ore horizon pyroclastics from similar lithologies at other stratigraphic horizons. The Ba anomaly is caused by microscopic barite which was widely distributed by subaqueous pyroclastic flows which transported most ore horizon pyroclastics.

TABLE OF CONTENTS

LIST OF FIGURES

Page

LIST OF PLATES

Page

CHAPTER ONE

GENERAL INFORMATION

1.1. Location and Access

The area of study is located in central Newfound-
land between latitudes 48°42'N and 48°58'N and longitudes
56°33'W and 57°00'W (Fig. 1-1). The town of Buchans is
accessible by 77 km of paved road which leaves the Trans
Canada Highway at Badger. A number of gravel surfaced
roads around the town of Buchans provide access to areas
up to 4.5 km from town.

Most parts of the study area are accessible on
a single day's outing on foot with transmission lines,
bogs and some stream beds providing best walking conditions.
All the lakes and ponds in the area are too small and
shallow for float plane operation and no rivers are navig-
able over significant distance by canoe.

1.2. Topography, Vegetation, Climate and Outcrop Exposure

The study area is a gently rolling upland area.
All parts of the area, except the extreme northwest, drain
into Red Indian Lake which forms the topographic low of
the area. Large areas to the north and west, underlain by
granitoid rocks, form a bog-covered and boulder-strewn
barren plateau. The area underlain by volcanic rocks, in
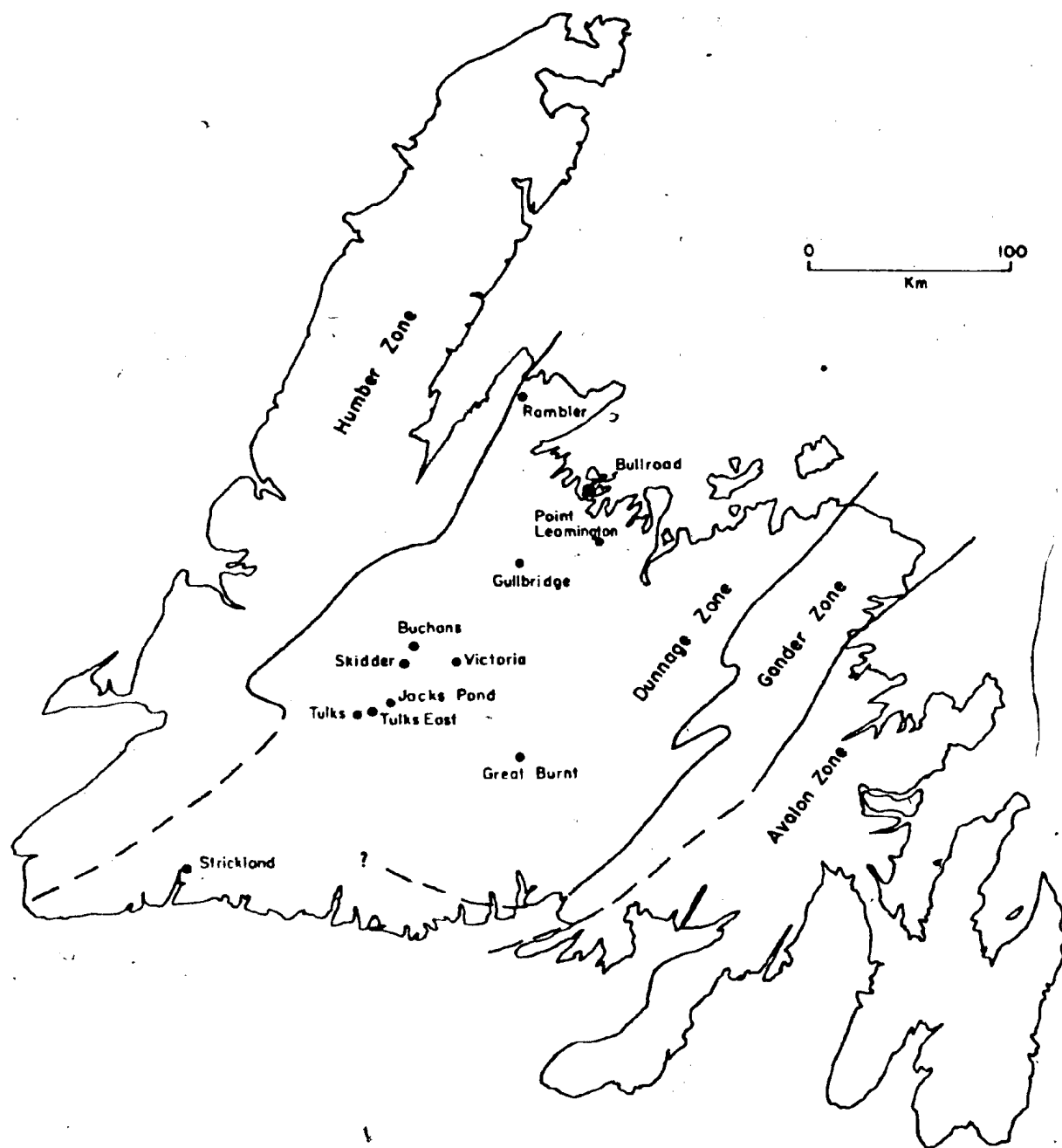
Figure 1 - 1 : Location of Buchans with respect to
tectonostratigraphic zones of New-
foundland and significant post-ophiolite
volcanogenic massive sulphide deposits.

general, slopes irregularly towards Red Indian Lake and is
covered with poorly drained bog and shallow ponds in low-
lying areas and dense spruce and fir forest on small
hummocks.

In general, the inland location of the Buchans
area results in a somewhat less moderated climate than
the rest of Newfoundland. Field work is comfortable from
May to October. Precipitation is moderate with summers
being somewhat drier than spring or fall. Mosquitos,
black flies and other biting insects are a problem for
much of the summer and rutting moose and their hunters
should be avoided during the fall.

Exposure of outcrop is, in general, very poor
and would average much less than one percent over the
study area. The best exposures are found in stream beds
and on small abrupt hills. The intervening bog and forest
normally contain a few widely scattered outcrops. Though
lichens may be thick and weathering may be deep, many
inland outcrop can be greatly enlarged and improved by
stripping off moss cover.

During the present study, at least half of the
350,000 m of Buchans drill core was logged and scores of
sections plotted. Although much of the core comes from
the immediate Buchans area, a number of holes have been
drilled at more distant localities. The location of drill

holes is shown on Fig. 1-2 (in pack pocket).

1.3. History of Mining

The history of the Buchans area has recently been compiled by Neary (1980).

The outcropping deposits at Old Buchans were discovered in 1905 by Matty Mitchell, a Micmac prospector employed by the Anglo Newfoundland Development Company.

Development work on the property was carried out between 1906 and 1911, but efforts were suspended due to metallurgical difficulties with the fine grained sulphide aggregate. Development began in earnest in 1926 by ASARCO as a result of their discovery of selective flotation, and production began in 1928 at a rate of 500 tons per day following the discovery of additional orebodies. In 1930 the milling capacity was increased to its present rate of 1250 tons per day.

The near-surface Oriental No. 1 and Lucky Strike Orebodies were discovered by equipotential surveys carried out in 1926 under the direction of Hans Lundberg (Lundberg 1957). (These discoveries represent the first successful application of geophysics in North America). The Rothermere and MacLean (formerly Rothermere #4) orebodies were discovered between 1947 and 1950 as a result of intensive

drilling under the direction of H.J. MacLean. E.A. Swanson became chief geologist in 1951 and was responsible for the discovery of the Oriental #2 orebody in 1953. Since that time the sub-economic Clementine and Sandfill prospects have been discovered but available tonnages are not sufficient to warrant production.

During the past twenty years virtually many methods of surface geochemistry and ground and airborne geophysics have been used in an attempt to outline new ore but with only limited success. Diamond drilling has always, and will continue to play a major role in the detailed local exploration, and over 350,000 m of drill core is stored in the core sheds in Buchans. The careful logging and re-logging of this core has made the Buchans area the most thoroughly studied local volcanic environment in the province.

1.4. Previous Geological Work in the Buchans Area

Murray (1871) described the rocks in the vicinity of Red Indian Lake in general terms and considered them to be correlative with "Silurian" rocks of the Exploits valley. He considered granites in the area to be of Laurentian (Archean) age.

Snelgrove (1928) implied the presence of two ages of granites in the Buchans area. The younger granites

cut the Buchans volcanics and he considered them to play
an important role in the mineralizing process. With
reference to the older granites, Snelgrove (1928, p. 1113)
states that "lavas actually abut against the granites
approximately five miles north of the lake (Red Indian),
although the age of the intrusives is probably later than
'Laurentian' as Murray mapped them". The occurrence of
Snelgrove's implied unconformity has not been mentioned
by subsequent workers. Snelgrove's thin section descrip-
tions of rocks from the mine area are the first published.

The paper by Newhouse (1931) represents the
first integrated descriptive work on the regional and
local geology and on the ore deposits. He considered the
volcanics to be of Cambro-Ordovician age and noted the
similarity of cherts of the Buchans area to those in
Notre Dame Bay. Plant remains collected by Newhouse
indicated that poorly indurated strata along the shores of
Red Indian Lake are of Carboniferous age.

After seven years of study, George (1937) describ-
ed both the regional and local geology of the Buchans area.
This excellent paper includes a number of maps, photo-
graphs, photomicrographs and cross sections made available
by further development of the Lucky Strike and Oriental
Orebodies. Description of the local stratigraphy, struc-
ture and mineralization occupies a prominent portion of

the paper and his account of the Lucky Strike and Oriental

Orebodies forms a valuable record of ores long since

removed by mining. He noted the association between

quartz porphyry (dacitic tuff) and ore, although he

considered this unit to be of intrusive origin. George

(1937) recognized the presence of two major stratigraphic

horizons favourable for mineralization, and considered

the Lucky Strike horizon to overlie the Oriental horizon.

Lamprophyre dykes described by George are considered by

later authors to be diabase.

The Buchans Staff (1955) provided the first

published general descriptions of the Rothermere Orebodies

as well as summaries of mining and milling practices.

Relly (1960) was responsible for the first compre-

hensive written report of the geology of the immediate mine

area. The bulk of this work is descriptive, based on field

observations and hundreds of thin and polished sections.

In addition, the thesis includes the first petrochemical

analyses aimed at understanding alteration related to the

mineralization. Despite amassing considerable evidence

in favour of a syngenetic origin for the ore, Relly con-

sidered the ore to be of epigenetic hydrothermal replace-

ment origin.

In a paper judged best of the year by the Canad-

ian Institue of Mining and Metallurgy, Swanson and Brown

(1962) reduced Relly's voluminous descriptive work to
publishable size integrating most of the ideas of the
mine staff at the time. They suggested an Ordovician
age for the Buchans Group and considered it to be correl-
ative with the Roberts Arm Group to the northeast. They
considered the ore to be of epigenetic origin but Anger
(1963) deduced from published descriptions that the ores
were similar to Meggen and Rammelsberg and, therefore,
probably syngenetic.

        Williams (1967) considered rocks of the Buchans
area to be of Silurian age, based on the presence of red
sandstones on the southeast shore of Red Indian Lake and
some lithologic similarities of the Buchans Group to the
Springdale Group. Mapping by Williams (1970) at 1:250,000
represented the first published regional geological map
which included the Buchans area.

        Anderson (1972a) carried out regional mapping at
1:50,000 but, to date, only preliminary maps are available.
Anderson (1972b) considered the Buchans Group to conformably
overlie plutonic boulder conglomerate of the Exploits Group
which he considered 'similar to Silurian Goldson Conglomer-
ate', and thus implied a Silurian age for the Buchans
Group.

        . Since the publication by Swanson and Brown (1962)

the ideas of the mine and exploration staff concerning ore genesis have changed and this has resulted in new advances in understanding the stratigraphy of the area. Entwistle and Barnes (1971) first suggested that the Oriental sequence was a fault repetition of the Lucky Strike sequence, an hypothesis supported by Walker and King (1975). The present author investigated the relationship between rock geochemistry and mineralization (Thurlow, 1973) and these findings and a geological summary were published by Thurlow, Swanson and Strong (1975) and Thurlow (1977).

In 1976, ASARCO Inc., and the Price Co. Ltd. commissioned a number of researchers to study various aspects of Buchans geology with the results published as a volume commemorative of fifty years of mining at Buchans. At the time of writing, most studies are near completion.

The coloured 1:50,000 geological map of the Buchans area accompanying this work (Fig. 2-2) was prepared to form part of a paper by Thurlow and Swanson (1980). A similar map of the Buchans sheet (12A/15) will be published shortly by Kean (1980).

In addition to the above mentioned workers, there exist several theses (e.g., Woakes, 1954; Catherall, 1960; Alcock, 1961) and a number of unpublished company reports (e.g., MacLean, 1941; Swanson, Perkins, and Higgins,

1955; Larsen, 1973).

1.5. Previous Lithogeochemical[1] Studies in the Vicinity
of Massive Sulphide Mineralization

The increasing difficulty of discovering massive
volcanogenic sulphide deposits has fostered abundant
lithogeochemical research. Govett and Nichol (1979) have
recently compiled a review of work to date. General
references such as Hawkes and Webb (1962), Bradshaw et al.
(1970), Boyle and Garrett (1970), Sakrison (1971), and
Levinson (1974) discuss the techniques and problems
encountered in economic lithogeochemical surveys and
refer to the various successes and failures of numerous
individual studies. Regional lithogeochemical surveys in
areas of massive sulphide mineralization have met with
some academic success in areas such as the Archean of the
Canadian Shield (e.g., Davenport and Nichol, 1972;
Descarreaux, 1973; Bennett and Rose, 1973; Larson and
Webber, 1977; McConnell, 1976; Sopuck, 1977; Lavin, 1976),
New Brunswick (Govett et al., 1974; Graf, 1977) and Cyprus
(Govett and Pantazis, 1971). Similarly, local studies in
the immediate vicinity of massive sulphide mineralization
have resulted in the detection of anomalies of varying
extent and intensity in such areas as the Canadian Shield
(e.g., Sakrison, 1967; Spitz and Darling, 1978; Marcotte
and David, 1978), Cyprus (e.g., Govett, 1972; Pantazis

1. The terms "lithogeochemistry" and "rock geochemistry"
    are used synonymously in this study.

and Govett, 1973), Japan (e.g., Tatsumi and Clark, 1972; Tono, 1974), the Scandinavian Caledonides (e.g., Nilsson, 1968; Gjelsvik, 1968; Nairis, 1971) and the Appalachians (e.g., Gale, 1969; Thurlow, 1973; Whitehead, 1973; Whitehead, 1973; Whitehead and Govett, 1974; Goodfellow, 1975; Govett and Goodfellow, 1975).

In spite of the apparent ability of many rock geochemical studies to be capable of guiding massive sulphide exploration, the exploration community in general, have been hesitant in applying such methods. This has been, in part, due to costs but is more a function of the relative speed and efficiency of applied geophysical, geochemical and geological techniques in unequivocally pinpointing specific targets.

Rock geochemistry is plagued by a number of other deficiencies largely related to its relative infancy. Some of these include:

1) a lack of universally applicable parameters to areas of unknown mineral potential,

2) a general lack of research into the mode of occurrence of base metals in silicate rocks and minerals,

3) a lack of integrated regional and local lithogeochemical surveys,

4)   a lack of integrated stratigraphic, petro-

logical and lithogeochemical data,

5)   a general lack of convincing demonstration

that anomalies are indeed related to mineral-

ization (especially in regional surveys),

6)   the presence of very subtle (and sometimes

dubious) anomalies often identified only

by advanced statistical techniques,

7)   the presence of obvious alteration and/or

mineralization (especially in local surveys)

which requires no geochemical analysis to

identify the anomalous situation.

Rock geochemical studies have been successful
in characterizing the nature of chemical change in massive
sulphide alteration zones; particularly the near universal
removal of Na_2O and addition of MgO due to breakdown of
plagioclase and chlorite formation (Table 1-1). This has
proven most useful in areas where deformation and meta-
morphism have masked original textures. Also successful,
has been the ability of rock geochemical studies to assist
in local and regional correlation of mineralized horizons.

1.6.   Present Study

This study stems from earlier work by the author
(Thurlow, 1973) which indicated that applied rock

Table 1-1 (after Govett and Nichol. 1979)

Summary of major element dispersions in relation to
volcanogenic massive sulphide deposits

Deposit	Alteration mineralogy	Elements enriched	Elements depleted	Elements unchanged	Age
Kuroko, Japan Lambert & Sato (1974)	Mon, Ser, Chl, Kaol	K, Mg, Fe, Si	Ca		Cenozoic
Kuroko, Japan Tatsumi & Clark (1972)	Ser, Qtz, Cal	Mg, K	Na, Ca, Fe	Al	Cenozoic
Hitachi, Japan Kuroda (1961)	Cord, Anthoph.	Mg, Fe, Ba	Na, Ca, Sr		Cenozoic
Buchans, Canada Thurlow et al. (1975)	Chl, Ser, Qtz	Mg, Fe, Si	Na, Ca, K		Paleozoic
Heath Steele, Canada Wahl et al. (1975)	Chl, Ser	Mg	Na, Ca		Paleozoic
Brunswick No. 12 Canada Goodfellow (1975)	Chl, Ser, Qtz	Mg, Fe, (Mn), (K)	Na, Ca (Mn), (K)	Al	Paleozoic
Killingdal, Norway Rui (1973)	Chl, Bio, Qtz	Mg, K, Mn	Na, Ca, Si	Al, Ti, Fe (total)	Paleozoic
Skorovass, Norway Gjelsvik (1968)	Chl, Ser	Mg	Na, Ca		Paleozoic
Boliden, Sweden Nilsson (1968)	Chl, Ser, Qtz, Andal	Mg, K, Al	Na, Ca		Proterozoic
Mattabi, Canada Franklin et al. (1975)	Qtz, Carb, Ser, Chld, Chl, Andal, Gar, Kyan, Bio	Fe, Mg	Na, Ca		Archean
Millenbach, Canada Simmons et al. (1973)	Chl, Ser, Anthoph, Cord.	Mg, Fe	Na, Ca, Si		Archean
Mines de Poirier Canada Descarreaux (1973)	Chl, Ser,	Mg, K	Na, Ca	Si	Archean
Lac Dufault, Canada Sakrison (1966)	Chl, Ser	Mg, Fe, Mn	Na, Ca	Al, Ti K, Si	Archean
East Waite, Mobrun, Joutel, Poirier, Agnico-Eagle, Mattabi, Sturgeon Lake, South Bay McConnell (1976)	Qtz, Ser, Chl, Carb, Sauss, Epidote	Mg, Fe	Na, Ca	Si, Al	Archean

geochemistry may be of use in exploration at Buchans. It
was realized, that in order to be properly interpreted,
the geochemistry had to be expanded to a more regional
scale and that a thorough understanding of the complex
stratigraphy of the area was required. The purpose of
this study is therefore:

1) to establish the relationships of the Buchans Group
   to surrounding lithologies,

2) to refine the volcanic stratigraphy of the Buchans
   Group

3) to determine the nature of the ore occurrences and
   to compare them with other volcanogenic sulphide
   deposits,

4) to establish the general petrochemical character of
   the Buchans Group, and

5) to determine whether rock geochemical techniques have
   practical exploration application at Buchans.

1.7. Acknowledgments

CHAPTER TWO

THE STRUCTURAL AND STRATIGRAPHIC SETTING OF
THE BUCHANS GROUP

2.1. Introduction

The Buchans Group and adjacent formations form
part of the Dunnage Zone (Williams, 1979); one of four
tectonostratigraphic sub-divisions of the Newfoundland
Appalachians. Regional compilation and correlation within
the Dunnage Zone by Dean (1977) and Kean et al. (1980)
have shown that a pre-Caradocian "early island arc"
volcanic sequence overlies Cambro-Ordovician oceanic crust.
The "early arc" volcanics are in turn overlain by a wide-
spread graptolitic Caradocian shale which is succeeded by
flych and post-Caradocian volcanics, including the Buchans
Group.

Rocks bounding on the Buchans Group in space
and time include a large area of granitoid rocks to the
east, north and west (the Topsails Granite of Baird, 1960),
foliated plutonic rocks of the Hungry Mountain Complex
to the north, Carboniferous rocks along Red Indian Lake (Fig. 2-2)
and the thick volcano-sedimentary terrane south of Red
Indian Lake (Fig. 2-1). These units have been examined in
this study mainly to determine their stratigraphic relation-
ships to the Buchans Group.
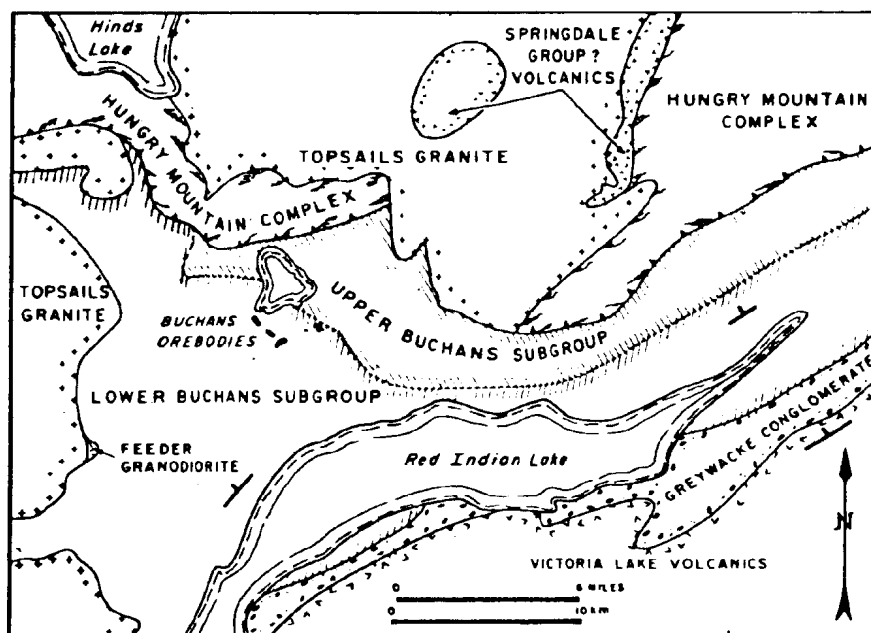
Figure 2-1.   Generalized geological map of the Buchans
              area.

2.2. The Relationship of the Buchans Group to Structurally
     Underlying Formations

The relationship between the Buchans Group and
underlying rock units is not known with certainty though
recent mapping at 1:50,000 by Kean (1977, 1979, 1980) has
elucidated many aspects.

Southeast of Red Indian Lake, volcanic and
sedimentary rocks of the pre-Caradocian Victoria Lake
Group are overlain by fossiliferous Caradocian black shales,
slates and argillites (Kean and Jayasinghe, 1980). These
are in turn overlain by a plutonic boulder-bearing grey-
wacke-conglomerate sequence, lithologically similar to
the Sansom Greywacke and Goldson Conglomerate in Notre
Dame Bay (Anderson, 1972). The Buchans Group structurally
overlies this sequence. Though the contact, or contact
zone, is not exposed, it has been considered both a fault
by Williams (1970) and a conformable contact by Anderson
(1972). Through mapping and regional correlations, Kean
(1977, 1980) interprets the Buchans Group as younger than
the greywacke-conglomerate sequence but also in fault
contact with it. The author considers this the most
reasonable interpretation though uncertainties exist as
to the signficance of a major structural lineament travers-
ing Red Indian Lake and a red sandstone sequence on the
southeast shore of the Lake. These uncertainties cannot

be dismissed until fossil evidence of the age of the
Buchans Group is obtained.

2.3. Buchans Group Correlatives

With few exceptions, geologists have considered,
and still consider, the Buchans Group to be a time-
equivalent regional correlative of the Roberts Arm Group
of Notre Dame Bay (e.g., Swanson and Brown, 1962). There
are many arguments in support of this contention despite
a lack of fossil control. The Roberts Arm and Buchans
Groups are both regionally extensive and lithologically
similar submarine volcanic sequences. Both appear to
conformably overlie a post-Caradocian flysch sequence and
stratigraphically underlie the dominantly subaerial
Springdale Group. Both are chemically similar mafic to
felsic calc-alkaline suites (Strong, 1977). Both have
undergone a similar structural history of thrust faulting
and Acadian folding. Both contain a variety of base
metal sulphide deposits, some of which are remarkably
similar (e.g., Buchans and the Bull Road showing at
Pilleys Island).

To date, the Buchans Group has proven barren of
fossils diagnostic of its age. The best estimate of the
age of the Buchans Group is Rb-Sr whole rock isochron of
447 ± 18 Ma, essentially on the Ordovician-Silurian

boundary (Bell and Blenkinsop, 1980). A similar age of
448 ± 7 Ma has recently been derived from the Roberts
Arm volcanics (Bostock, 1978; Bostock et al., 1979).

2.4. Granitoid and Related Rocks (Topsails Granite and
Feeder Granodiorite)

Granitic to gabbroic rocks underlie the area
north and west of the Buchans Group (Fig. 2-1) and comprise
a portion of a larger plutonic complex which underlies
approximately 7200 sq. km (3000 sq. mi.) of west central
Newfoundland. Brief study by the author has led to
subsequent more detailed work, recently published by
Taylor et al. (1980).

During the present study, the following plutonic
rock types were identified (nomenclature after Streckeisen
(1976), reproduced in Appendix 1).

1) Pink medium grained granodiorite with prominent (5-10
mm) rounded quartz (hereinafter called the "Feeder
Granodiorite").

2) Fine grained gabbro and related hybrid granite

3) Pink to reddish orange to brick red, fine to medium
grained, equigranular, biotite-bearing alkali-feldspar
granite to alaskite (the "biotite granite" of Taylor
et al., 1980)

4) Aegirine and/or alkali-amphibole-bearing peralkaline
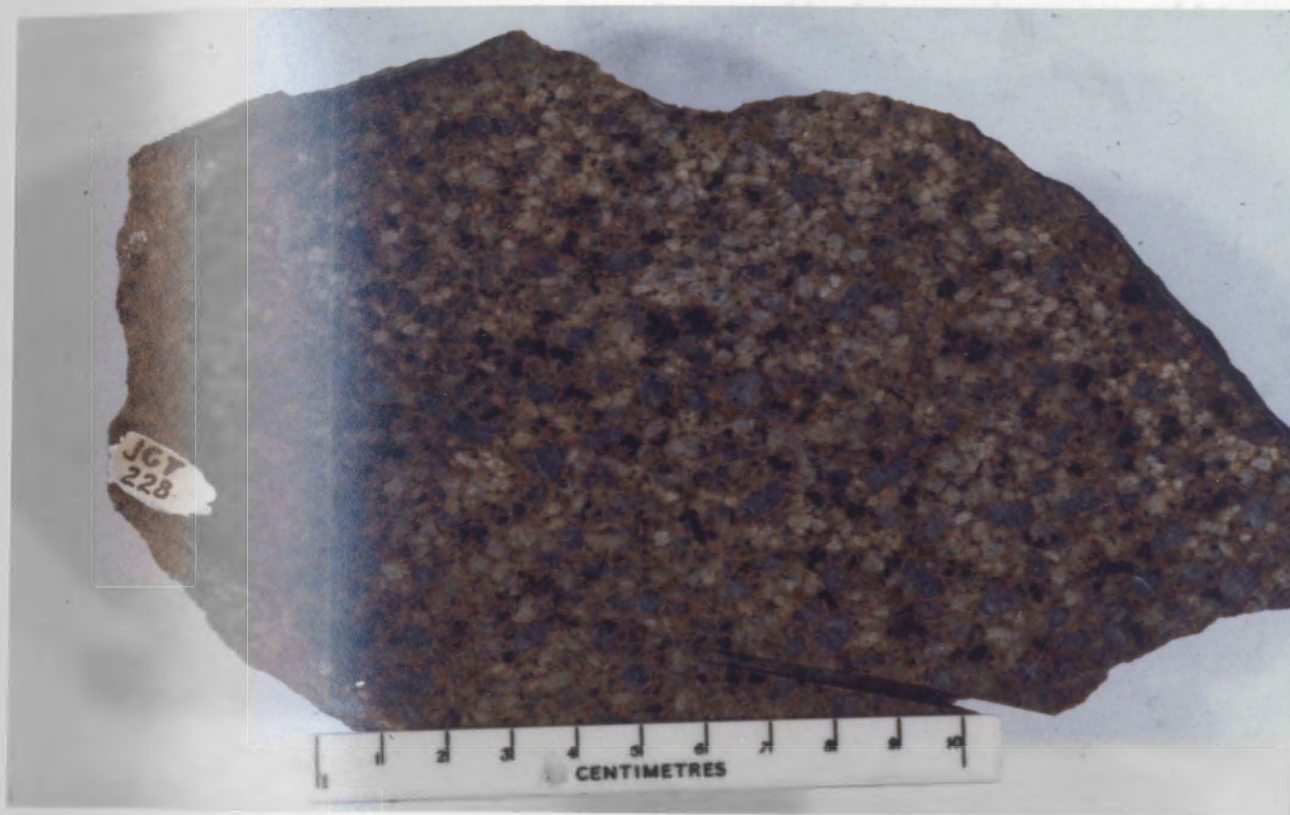
Plate 2-1: Feeder Granodiorite with rounded to
subhedral, cracked quartz, plagioclase
(white) and altered biotite.

granite and related quartz-feldspar porphyry.

In addition, Taylor et al. (1980) have
identified a metaluminous biotite-hastingsite granite
which is cut by dykes of peralkaline microgranite.

Bell and Blenkinsop (in press) have established
whole rock Rb/Sr isochrons as follows:

a) Feeder Granodiorite, 480 ± 80 Ma, initial $^{87}Sr/^{86}Sr$ =
    0.754

b) Peralkaline Granite, 419 ± 5 Ma, initial $^{87}Sr/^{86}Sr$ =
    0.707

c) Alkali-feldspar granite, 386 ± 9 Ma, initial $^{87}Sr/^{86}Sr$ =
    0.7067

The Feeder Granodiorite is restricted to two
small parts of the study area (Fig. 2-2). The distribution
of these occurrences around the margins of the Topsails
Granite suggests that the Feeder Granodiorite was once
more extensive but is now largely obliterated by later
granite intrusions.

The Feeder Granodiorite is distinctly more
calcic than later granites and contains strongly zoned
plagioclase generally in excess of two thirds of feldspars
(Plate 2-1). Perhaps the most characteristic feature of
these rocks is the presence of prominent (up to 1.5 cm)
quartz phenocrysts generally equant and rounded or slightly

Plate 2-2: Core samples, right to left; Feeder granodior-
ite-like boulder from pyroclastic breccia,
rhyolite, dacitic crystal-vitric tuff, volcan-
ic conglomerate. All samples are characteriz-
ed by large, rounded to subhedral, cracked
quartz and are considered to be facies
equivalents.

resorbed but locally with sharply defined hexagonal
crystal faces (Plate 2-1). The quartz crystals commonly
have poor to well developed irregular to radial cracks.
The equant nature of the quartz crystals is indicative of
early quartz crystallization under low pressure (i.e.,
high crustal level) (Tuttle and Bowen, 1958). The locally
preserved hexagonal crystal outlines are characteristic of
high temperature beta quartz and the radial to irregular
cracks in quartz may be due to density increase and con-
sequent volumetric decrease during transformation from
beta to alpha quartz. The complex zoning of plagioclase
crystals is indicative of instability of pressure and
temperature in the magma chamber, a characteristic most
likely to be developed at the margins of a high level
intrusive body.

Textural and geochemical comparison of the Feeder
Granodiorite and certain rhyolitic volcanics of the Buchans
Group lead the author to conclude that these lithologies
are genetically related. Massive pink to grey rhyolite
flows of the Prominent Quartz Sequence contain large zoned
plagioclase phenocrysts and texturally distinctive prominent
(5-10 mm) rounded to hexagonal quartz phenocrysts with
radial to irregular cracks (Plate 2-2). Both macroscopi-
cally and microscopically, the phenocryst mineralogy and
distinctive morphology (especially of quartz) are identical
in these flows to those present in the Feeder Granodiorite.
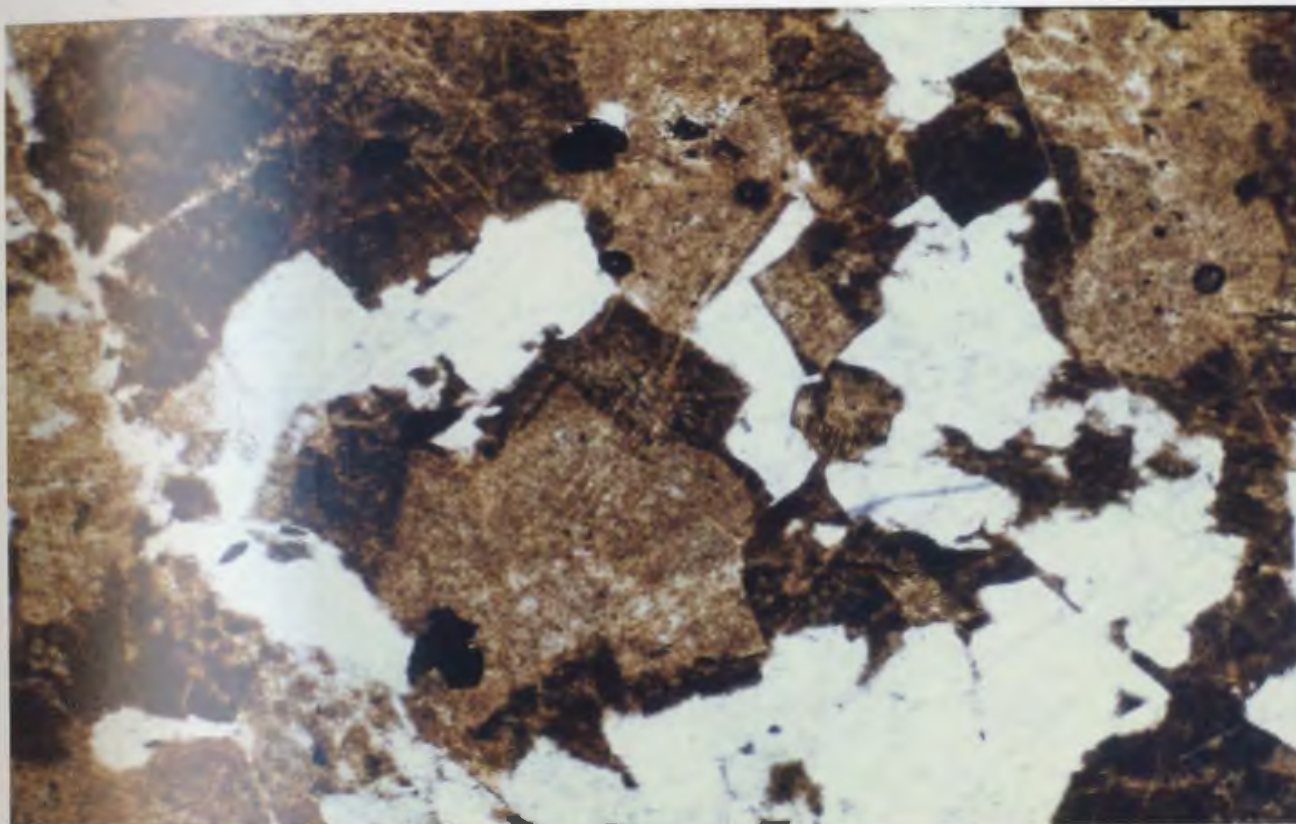
Plate 2-3:   Typical alkali-feldspar granite with quartz,
             albite and K-feldspar.   Albite is much less
             clouded by minute hematite than K-feldspar.

This striking textural similarity, geochemical similarities presented in Chapter Five, the occurrence of cobbles and boulders of Feeder Granodiorite-like material in the Buchans Group and the similarity of radiometric ages of the Feeder Grandiorite and Buchans Group suggest that magmas of the Feeder Granodiorite fed certain rhyolitic volcanics of the Buchans Group.

The Topsails Granite can be subdivided into peralkaline and non-peralkaline suites. The non-peralkaline suite is further divisible into the alkali-feldspar granite with associated mafic rocks and the biotite-hastingsite granite.

The alkali-feldspar granite (terminology after Streckeisen, 1973) is composed of approximately equal quantities of quartz, albite and K-feldspar with lesser altered biotite and minor hornblende. The granite is characterized by moderate to strong hematitization of feldspars imparting a deep pink to brick-red appearance in hand specimen. In all cases, K-feldspar is distinctly more clouded by minute hematite than is albite, facilitating distinction of these two minerals (Plate 2-3). Fluorite, apatite, zircon, allanite and magnetite are common accessories. Quartz and biotite contents vary and the granite locally approaches syenite and elsewhere, alaskite.

Plate 2-4:   Peralkaline granite containing quartz,
             perthite and black alkali amphibole.

Massive fine grained mildly alkaline gabbroic to dioritic rocks are intimately associated with the alkali-feldspar granite within the area of study. These mafic rocks are areally much more restricted than associated granites but regional magnetic and gravity data suggest that they are volumetrically more important than their surface exposure would indicate. Gabbroic bodies are surrounded and intruded by later granite except at one locality in the northwest of the area where gabbro is faulted against rhyolite of the Upper Buchans Subgroup.

The biotite-hastingsite granite crops out east of Hinds Lake and consists of K-feldspar and quartz with lesser plagioclase, hastingsite and biotite. Taylor et al. (1980) consider this granite to be comagmatic with the biotite-bearing alkali-feldspar granite.

Peralkaline granitic rocks crop out in the north-eastern portion of the area in close association with volcanic roof pendants in the granite. These are medium to coarse grained, equigranular and weather in various shades of red, reddish yellow, light purple and white. They are characterized by alkali ferromagnesian minerals (aegirine, riebeckitic-arfvedsonite and aenigmatite), perthite and quartz (Plate 2-4) i.e., are hypersolvus granites. At the contact with the volcanic roof pendants red phenocryst-rich dykes, mineralogically similar to

the peralkaline granite, with aphanitic to granophyric
groundmass, cut the volcanics.

Considerable evidence exists to suggest that
all granitoid rocks were intruded into, and crystallized
at a high level in the crust. Miarolitic cavities are
common in the alkali-feldspar granite and may be filled
with fluorite, siderite and a green phylosilicate
(lepidolite?). The hypothesis that the Feeder Granodiorite
feeds rhyolites of the Prominent Quartz Sequence and sub-
sequently intrudes its own ejecta, suggests a high level
of intrusion. A similar relationship between the peralka-
line granite and the volcanic roof pendants in the granite
is suggested in the next section. The presence of roof
pendants and wide chill zones in the granites with the
development of strongly porphyritic granites is further
evidence of a high level of intrusion. The low grade
metamorphism of the host rocks indicates that they were
never buried to great depth and thus granites must have
intruded into a high level. The brittle behavior of the
host rocks at granite contacts and the lack of metasomatism
of the host rocks at granite contacts are, further evidence
of a high level of intrusion. Within both the Lower and
Upper Buchans Subgroups there exist boulders of the
Feeder Granodiorite in density flow deposits, further suggest-
ing a high level of intrusion.

Although no contacts are exposed between the various types of granitoids, or granitoids and the Buchans Group, a sequence of igneous intrusion can be inferred from relationships previously presented and from apophyses which maintain the characteristic mineralogy, chemistry and, in some cases, texture of their parent rocks. The Feeder Granodiorite feeds and subsequently intrudes volcanic rocks of the Lower Buchans Subgroup and is evidently the earliest exposed plutonic body in the Buchans area. It will be shown in a later section that intrusion of the Feeder Granodiorite is separated in time from later igneous activity by a period of major thrust faulting.

Relationships between the various later granitoid suites are not yet fully resolved though it is evident that all post-date the Buchans Group. Gabbroic rocks feed numerous diabase dykes which cut all portions of the Buchans Group and the Feeder Granodiorite. These dykes are petrographically and geochemically identical to the gabbros. The alkali-feldspar granite feeds porphyritic red "rhyolite" dykes which cut the Buchans Group and again, the mineralogical and geochemical character of the dykes is similar to the source plutonic body.

Dykes of alkali-feldspar granite also cut the gabbroic bodies. The contacts between the two are, in some cases, sharp but generally a diffuse zone of "hybrid

granite" is developed. Thin dykes intruding gabbro have thin hybrid zones at the contact whereas the contact between large gabbro and granite bodies is commonly marked by "hybrid" zones on the order of hundreds of meters in width. Within the Buchans Group, dykes of both "rhyolite" cutting diabase and vice versa can be observed. This suggests a temporal link between magmas of gabbroic and granitic composition. Furthermore, the gabbros exhibit mildly alkaline characteristics (see Section 5.2.) suggesting a genetic link between the gabbros and the alkali-feldspar granite.

Fine grained, spherulitic to flow-banded dykes with alkali ferromagnesian minerals, presumably apophyses from the peralkaline granite, cut the Buchans Group. Taylor et al. (1980) observe that dykes of peralkaline granite cut the hastingsite-biotite granite, in apparent conflict with the reported isotopic ages. They suggest that both criteria may be correct and that oscillatory peralkaline-peraluminous magmatism may have been operative.

2.5. Volcanic Outliers Within the Topsails Granite
    (Springdale Group?)

Volcanic rocks within the Topsails Granite (Fig. 2-1) were briefly examined in order to compare their gross lithologic character with volcanic rocks of the Buchans

Group. Little similarity was observed between these groups of volcanic rocks. They consist of reddish sub-aerial ignimbrite, non-welded pumice flows, breccias, pyroclastics and flow banded rhyolite, intruded by porphyritic dykes emanating from the peralkaline granite. Gently dipping ignimbrites overlying the peralkaline granite contain alkali ferromagnesian minerals suggesting an intrusive-extrusive relationship between the granite and volcanics. Non-peralkaline volcanics are reported by Taylor et al. (1980). The relationship between these and the peralkaline volcanics and granites is not clear.

Vertically cleaved, gently dipping ignimbrite on Barren Mountain occupies an area near the core of a synclinal trough and is probably an outlier of a once more extensive subaerial felsic volcanic sequence. The litho-logic similarity to volcanic rocks of the Springdale Group as described by Kalliokowski (1955), Neale and Nash (1963) and Williams (1967) suggests that parts of the volcanic rocks associated with the Topsails granite are related to the Springdale Group. The major synclinal axis in the Springdale Group as mapped by Kalliokowski (1955), can be traced southward through the Topsails Granite, through the Barren Mountain outlier and into the Buchans Group.

2.6. Hungry Mountain Complex

Two belts (Western and Eastern) of deformed plutonic rocks exist approximately 5 km north and 15 km east-northeast of Buchans and occupy an area between the Topsails Granite and the Buchans Group (Figs. 2-1, 2-2). These rocks have been called the Hungry Mountain Complex (Thurlow, 1975) after a prominent hill in the area. The author considers the Western and Eastern Belts to be lateral equivalents of a once larger sheet which has subsequently been dissected into two parts by intrusion of the alkali-feldspar facies of the Topsails Granite. Mapping by Riley (1957), Anderson (1972) and Kean (1979) indicates that rocks correlative with the Western Belt of this Complex extend from the northern boundary of the present study area in a northwesterly direction along the west shore of Hinds Lake (Figs. 2-1, 2-2). Mapping by ASARCO exploration crews in the later 1940's and scattered observations by the present author indicate that the Eastern Belt extends northward at least to a point several kilometers east of Quarry.

Bell and Blenkinsop (1980) have established two Rb-Sr whole-rock isochrons of 660 ± 70 Ma and 400 ± 60 Ma from separate localities in the Western Belt.

Rocks of the Hungry Mountain Complex range in composition from gabbro to granite and are characterized

by a complex deformational history. Within the Western
Belt, foliated rocks of granodioritic composition are
most abundantly exposed. These are light grey to white
weathering and consist of quartz, zoned plagioclase (with
albite-oligoclase rims) and alligned biotite with minor K-
feldspar and hornblende. Dykes of foliated granodiorite
locally cut bodies of deformed diorite and hornblende gabbro.
Elsewhere the foliated granodiorite contains slightly to
moderately flattened, angular to rounded, resorbed horn-
blende quartz diorite xenoliths with diffuse margins. At
one locality a hornblende-plagioclase inclusion (similar
to the larger mafic portions of the Complex) contains a
fabric which is not parallel to the fabric in the enclosing
host rock. This is taken as evidence that some of the more
mafic portions of the Complex have undergone an earlier
deformational history before intrusion of the granodioritic
phase.

The Western Belt of the Hungry Mountain Complex,
though generally similar to the Eastern Belt, contains a
greater abundance of massive medium to coarse grained
gabbro. The degree of deformation is more variable
ranging from locally intense to essentially undeformed.
Deformed granodioritic dykes locally cut pre-deformed
gabbro but in at least one locality, the opposite sequence
is observed.

Plate 2-5:   Hornblende gabbro breccia, intrusive into
the Hungry Mountain Complex.

The deformational fabric within the Complex is typically defined by abundant flattened quartz and aligned biotite (or chlorite after biotite) which form augen of altered plagioclase.

In more mafic phases, tabular hornblende defines the foliation. At several localities this main foliation is openly folded with interlimb angles of approximately 120 degrees. No cleavage is associated with this later folding.

A steeply dipping spaced fracture cleavage of probable Acadian age is visible locally and overprints the main foliation within the Complex.

The Hungry Mountain Complex is cut by a number of intrusives that post-date the main fabric. The earliest of these is an intrusive breccia composed of coarse horn-blende gabbro in a light feldspathic matrix (Plate 2-5). Amphibole-rich portions consist of coarse hornblende (over 1 cm) with less abundant clinopyroxene, orthopyroxene and interstitial highly altered feldspars. Deuteric alteration especially of orthopyroxene, to tremolite is common. Macroscopically a strong textural similarity to the Brighton Gabbro (Hussey, 1974) is noted.

The hornblende gabbro and the entire Complex are cut by grey to red aplite and "rhyolite" dykes emanating

Plate 2-6: Flow banded peralkaline dyke (top) cutting
deformed Hungry Mountain Complex. Small
circled xenolith of host rock occurs in
dyke below lens cap.

from the alkali-feldspar granite, dark brownish-red,
aegerine-bearing dykes from the peralkaline granite
and less abundant diabase dykes related to the gabbro.
Chilled contacts against the foliated rocks of the
Complex are abundantly exposed and the foliation in the
latter is truncated by dyke intrusion (Plate 2-6).
Locally, angular fragments of foliated granodiorite
are included in the dykes.

The contact between the Hungry Mountain Complex
and the main body of the Topsails Granite is not exposed
on surface but probably exists in DDH 2856 (location on
Fig. 1-2). The upper .153 m of this drill hole consists
of typical foliated granodiorite cut by abundant (greater
than 1/3 of the volume) red "rhyolite" dykes of the alkali-
feldspar Topsails Granite. At 153 m depth the foliated
granodiorite is cut by a thicker body of "rhyolite" with
a wide chilled margin. Near the contact, the matrix is
aphanitic but this coarsens with depth until at 296 m.
depth (end of hole) the "rhyolite" has graded into a fine
grained, slightly porphyritic granite with matrix crystals
of 1-2 mm size. This is considered to be a portion of the
main body of the Topsails Granite intruding the Hungry
Mountain Complex. The width of the chilled margin (in
excess of 140 m) indicates that the Hungry Mountain Complex
was relatively "cold" at the time of the Topsails Granite
intrusion.

Plate 2-7:   Mylonite from the base of the Hungry Mountain
             Complex.

2.7.   Contact Relationships Between the Hungry Mountain
       Complex and the Buchans Group

   2.7.1.   Relationship Within the Hungry Mountain Complex

       The contact between the Hungry Mountain Complex
and the Buchans Group is neither exposed in outcrop nor
in drill core but several areas of outcrop near the contact
are present.   Within a few hundred meters of the contact,
foliated granitoid rocks of the Complex become noticeably
more deformed and acquire a protomylonitic texture.   This
passes gradationally towards the contact into mylonitic
fabric characterized by extreme stretching of quartz
resulting in a strong lineation (Plate 2-7).   Quartz
exhibits sutured grain boundaries, the development of
sub-grain boundaries and commonly forms augen with chlorite
around more resistant plagioclase.   Less commonly, a planar
fabric defined by flattened quartz is developed.   North
of Buchans the lineation trends north-northwest and plunges
gently at 10 to 20 degrees.   The strike of the foliation,
where present, parallels a topographic break which is inter-
preted as the contact with the Buchans Group.

       At one locality small folds are generated by the
transposition of the main foliation in the Complex by
the mylonitic fabric.   These folds are defined by flatten-
ed quartz and biotite passing around the hinges of

isoclinal folds with attenuated limbs. They indicate
that the main foliation in the Complex pre-dates the
mylonitic fabric. This is further substantiated by the
presence of sub-vertical foliations in the Complex which
are highly discordant to the mylonite zone within several
hundred meters of the mylonite.

2.7.2. Relationships Within the Buchans Group

Rocks of the Buchans Group near the contact with
the Hungry Mountain Complex are exposed in the bed of
Harry's River and form sporadic outcrops for a distance of
about 2 km from the contact (Fig. 2-2). Within 650 m of
the contact these consist of a sequence of dark green to
black fine grained basaltic and andesitic tuffs. Stratigra-
phically below this is a sequence of subaqueous pyroclastic
flows and related arkose of the Prominent Quartz Sequence
(see Section 3.2.). These units strike northeast and
dip to the northwest at 45 degrees.

Within 650 m of the contact with the Complex
the mafic tuffs of the Buchans Group have undergone low
greenschist facies metamorphism. At distances greater
than 650 m from the contact, the Buchans Group exhibits
its typical prehnite-pumpellyite facies of metamorphism.
Moving towards the contact, chlorite decreases at the
expense of actinolite and a penetrative mineral fabric
at a slight angle to bedding (approximately 25°) becomes

Plate 2-8: Shallowly dipping penetrative foliation in
felsic tuffs of Upper Buchans Subgroup, below
Hungry Mountain thrust. Later, steeply
dipping, spaced fracture cleavage is typical
of all Buchans area rocks.

visible within these greenschist facies rocks. Small
recumbent folds with axial planes parallel to the foliation
are developed. Within 50 m of the inferred contact, horn-
blende appears and increases at the expense of actinolite.
Within 20 m of the contact, the mineral assemblage consists
of quartz, blue-green hornblende in excess of actinolite,
epidote, altered plagioclase (of unknown composition) and
minor chlorite and sphene, an assemblage typical of the
epidote-amphibolite facies of Miyashiro (1973).

Basaltic to rhyolitic rocks of the Upper Buchans
Subgroup occupy a large area to the northeast of Buchans
(Fig. 2-2). These rocks contain a subhorizontal to
gently northward dipping penetrative fabric (Plate 2-8)
which increases gradually in intensity towards the contact
with the Complex. This foliation is visible throughout a
large area of the Upper Buchans Subgroup for distances
up to 6 km from the contact with the Hungry Mountain
Complex. This foliation is cut by a vertical spaced
fracture cleavage, typical of Acadian deformation through-
out the Buchans Group (Section 3.3). In contrast to this
gradual lateral change in intensity of fabric, a much
more rapid change in intensity of fabric and metamorphic
grade is observed in vertical drill holes penetrating
this sequence. For instance, DDH 2837 (location on Fig. 1-2)
penetrates over 1.2 km of mafic to felsic flows, pyroclastics
and arkosic sediments. From the bottom of the hole to

within 150 m of surface, the sequence is characterized by
the presence of prehnite-pumpellyite-chlorite vesicles
in basalts and matrix prehnite in acid pyroclastics and
arkosic sediments. No foliation is present in this
sequence. However, within 150 m of surface, an initially
weak but upward increasing foliation at a slight angle
to bedding becomes evident. Prehnite and pumpellyite
disappear and a quartz-albite-epidote-chlorite-calcite
assemblage is present. The disappearance of pumpellyite
above 150 m in this drill hole and the presence of typical
low grade greenschist assemblage is taken to indicate
that the prehnite-pumpellyite: greenschist isograd
exists, with a sub-horizontal attitude, slightly below
150 m of the present erosional surface.

In view of the evidence presented (i.e., the
mylonite zone in the Hungry Mountain Complex at the contact
with the Buchans Group, the intensifying foliation at a
low angle to bedding near the contact with the Complex and
the stratigraphically inverted metamorphic zonation in
the Buchans Group from sub-greenschist to epidote
amphibolite facies, it is suggested that the Hungry
Mountain Complex was thrust upon the Buchans Group. The
thrust plane is at a moderate angle to the present
erosional surface in the Harry's River area but at a
very low angle in the Upper Buchans Subgroup to the east.
By comparison with the width of the aureole in the Harry's

River area, it is suggested that the thrust plane existed approximately 500 m above the present erosional surface in the area of DDH 2837, i.e., had an average northward dip of approximately 10° in this area (Fig. 2-3). These variations in the present attitude of the thrust plane are attributed to a post-thrusting open Acadian folding (see Section 3.3.).

The time of thrusting can be fairly accurately determined from the relationships previously discussed. Thrusting occurred after deposition of the Buchans Group. Unfoliated "rhyolite" dykes akin to the alkali-feldspar Topsails Granite cut the mylonite zone in the Complex, indicating a pre-Topsails Granite age of thrusting. The wide chill zone in the Topsails Granite against the Complex (DDH 2856) provides further evidence that the Complex was relatively "cold" at the time of Topsails Granite intrusion. Radiometric age dates (Bell and Blenkinsop, 1980) concur with the geological data and suggest a Silurian age of thrusting.

The gently plunging north-northwest trending lineation both in the mylonite zone and in the Buchans Group is interpreted as stretching in the direction of thrusting. The thrusting direction was from north-northwest to south-southeast as indicated by facing directions of small recumbent folds in the aureole beneath

N   S

mylonite

Hungry Mountain Complex

Topsails Granite

folded and foliated Buchans Group greenschists

undeformed Buchans Group volcanics
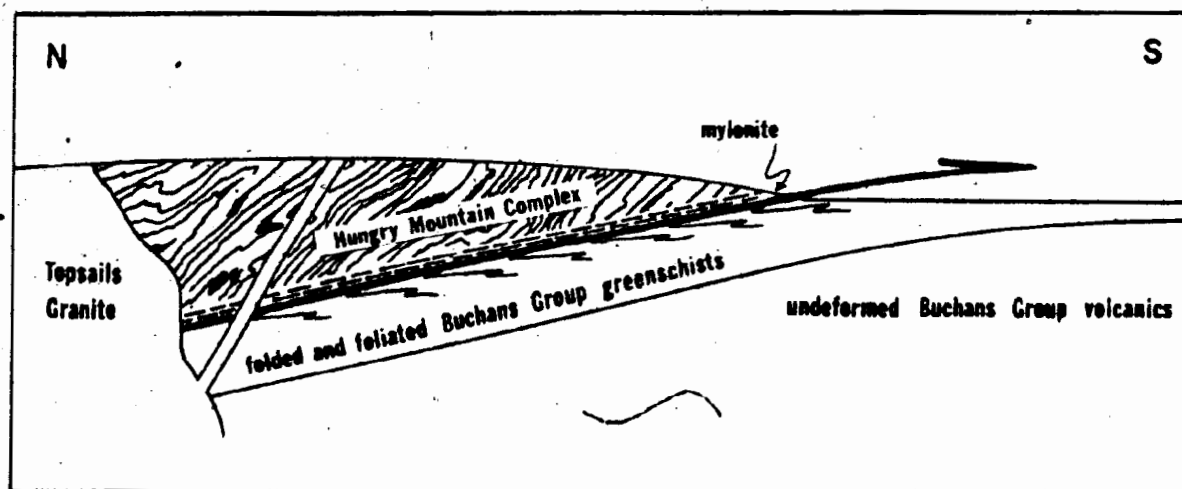
Figure 2-3. Schematic cross section showing relationships between the
Hungry Mountain Complex, Topsails Granite and Buchans Group.

the thrust in the Buchans Group.

Due to the lack of systematic study of the
Hungry Mountain Complex, its geological significance and
pre-thrust disposition are obscure. It is evidently a
package of rocks very foreign to the volcanic and plutonic
evolution of the Buchans area. The remarkable similarity
of gabbros in the Complex to gabbros of the Annieopsquotch
igneous complex (recently interpreted as ophiolitic by
Dunning and Herd, 1980), and the inversly zoned metamorphic
aureole beneath the Complex, suggests that the Hungry
Mountain Complex might represent part of a dismembered
ophiolite suite.

2.8. Siluro-Devonian Deformation

The Buchans area has been subjected to two major
structural events: 1) the pre-Topsails Granite Silurian
episode of thrusting, discussed earlier, and 2) a period
of Devonian broad open folding. The latter event imparting
a weak northeast-striking subvertical fracture cleavage
to all existing lithologies and is axial planar to a
broad open syncline within the Buchans Group. The inten-
sity of this cleavage varies considerably and is directly
related to the competency of the affected rocks. In
many exposures, the cleavage is not visible but it can be
identified in several parts of the Buchans Group, Hungry
Mountain Complex, Topsails Granite and the subaerial

- 49 -

Plate 2-9:   Shallowly dipping red sandstone and conglomer-
             ate of presumed Carboniferous age.   Upright
             hammer is approximately one meter length.

volcanic roof pendants on the Granite. The deformation related to this cleavage is nowhere sufficiently intense to cause visible effects of strain. The cleavage does not affect dated Carboniferous strata and is thus post-granite and pre-Carboniferous in age, i.e., Devonian.

Folds related to this deformation are broad, open and of regional extent. The axis of one major syncline within the Buchans Group can be traced through flat lying and vertically cleaved ignimbrite within the Topsails Granite and subsequently into a major syncline within the Springdale Group, a distance of approximately 100 km.

2.9. Carboniferous

Rocks of presumed Carboniferous age crop out in several small areas along Red Indian Lake and in a number of drill cores along the contact between the Footwall Arkose and the Upper Buchans Subgroup in the center of the map area. Similar rocks are reported to have been present on Buchans Island before construction of the Exploits Dam (E.A. Swanson, pers. comm. 1975).

These strata consist of flat lying to gently-dipping, poorly indurated, polymictic red conglomerate and red crossbedded sandstone (Plate 2-9). Some boulders in the conglomerate are very similar to parts of the Buchans Group, others can be confidently related to the Topsails

Granite. Similar conglomerates and sandstone are present
in the banks of the Shanadithit River and underlie thin
coal seams and limestone (D. Barbour, pers. comm. 1975).
Plant remains collected from the latter area are of
Carboniferous age (Newhouse, 1931) and miospores (Belt,
1969) reveal an assemblage typical of the Missippippian
Horton Group. Palynological analysis of a single silty
mudstone sample from the present study area revealed the
presence of vegetal matter but no diagnostic age was
determinable (J. Utting, pers. comm. 1975).

Although the contact is not exposed, there is
little doubt that these Carboniferous rocks unconformably
overlie the Buchans Group. Steeply dipping, deformed
rocks of the Buchans Group occur within meters of gently
dipping poorly indurated Carboniferous strata at several
localities. Relationships suggest angular unconformity
of nearly 90 degrees in these areas. The poorly indurated
nature and lack of cleavage indicate that these Carbonifer-
ous rocks have not undergone Acadian or subsequent deforma-
tion. This lack of deformation provides the best evidence
that the upright fracture cleavage and associated folding
of the Buchans Group, Hungry Mountain Complex, Topsails
Granite and Springdale Group is indeed of Acadian age.

The occurrence of pods of Carboniferous strata
along the contact between the Footwall Arkose and the
Little Sandy Formation is used as evidence for a pre-

Carboniferous fault contact between these lithologies.

2.10.   Summary of Chapter Two

The geological history of the Buchans area and relationships between various rock units can be summarized as follows:

Middle to Late Ordovician (Caradocian and/or later)	Deposition of greywacke and conglomerate on southeast side of Red Indian Lake
Latest Ordovician or earliest Silurian	Extrusion of Buchans Group – Roberts Arm Group volcanics with cogentic intrusion of Feeder Granodiorite; deposition of massive sulphide ores
Silurian	Southeasterly directed thrust faulting of pre-deformed Hungry Mountain Complex upon the Buchans Group
Late Silurian to early Devonian	Intrusion of the various phases of the Topsails Granite with extrusion of cogenetic subaerial volcanics
Late Devonian	Open folding, uplift, erosion

Early Mississipian

Formation of the Red Indian
Lake basin and deposition of
red beds

CHAPTER THREE

GEOLOGY OF THE BUCHANS GROUP

3.1. Introduction

Within this chapter an integrated account of
the geology of the Buchans Group is presented. A conse-
quence of the author's earlier work (Thurlow, 1973) was
the realization that further geochemical data could be
interpreted properly only if a detailed understanding of
the stratigraphy, structure and modes of deposition of
the Buchans Group could be gained. Within the scope of
this thesis it is not possible to document all the complex-
ities of Buchans geology and this account, although
lengthy, is considered by the author to represent only a
surficial summary. At the time of writing, several major
structural-stratigraphic difficulties still exist and
will be solved only by further detailed work with existing
data and new data from ongoing diamond drilling.

The concept of volcanic cycles has been modified
and the Buchans Group is subdivided into Lower and Upper
Subgroups, each consisting of several sequences. The
Lower Buchans Subgroup is a "volcanic cycle" consisting
of voluminous basaltic volcanics overlain by arkosic
rocks followed by intermediate and felsic volcanics which
contain the major ore deposits. The Upper Buchans Subgroup

comprises a second "volcanic cycle" initiated with relative-
ly minor mafic volcanism and arkose deposition overlain by
voluminous, dominantly felsic volcanics. In this sense,
the entire Buchans Group is a single dominantly mafic to
dominantly felsic sequence composed of lesser internal
increasingly felsic volcanic cycles. In detail, the
nature of these cycles is different from typical Archean
cycles (e.g., Goodwin, 1968) and volcanic cycles of the
Horkuroko district of Japan (as described by Takahashi
and Suga, p. 111-112).

The geology of the Buchans Group is extremely
complex. The understanding of the stratigraphy is hamper-
ed by lack of outcrop, rapid lateral facies changes, a
lack of marker beds, local subsidence, uplift, contempor-
aneous block faulting and diabase intrusion. Although
metamorphism in the area is relatively mild, interpretation
of the structure (and thus stratigraphy) is consequently
hampered by a lack of bedding-cleavage relationships.
Perhaps the major complicating factor is the postulated
presence of major thrust faults. Without fossil control
it is impossible to prove the existence of these faults
but the possibility of their presence demands the building
of a stratigraphic sequence based on observed indisputably
conformable contacts. Such contacts are not common as
most are characterized by late diabase sills or more
commonly by "innocent-looking" shears, the magnitude of

which is not possible to judge. The stratigraphy presented
in the following sections is based upon structurally
conformable contacts which allow no possibility of alter-
nate interpretation. This stratigraphy is schematically
shown in Fig. 3-1 and summarized in Table 3-1. The
stratigraphy of the Buchans Group has not been formalized
into formations, members, etc. because of the uncertain-
ties attached to the effects of thrust faulting.

3.2. Stratigraphy of the Buchans Group

3.2.1. Stratigraphy of the Lower Buchans Subgroup

3.2.1.1. Footwall Basalt: The Footwall
Basalt is the lowermost unit of the Buchans Group and is
thought to conformably overlie a greywacke-conglomerate
sequence which bears lithologic similarities to the Sansom
Greywacke and Goldson Conglomerate of Notre Dame Bay (Anderson,
1972a). Lithologically and stratigraphically the Basalt
is considered by most workers to be correlative with basalts
of the Roberts Arm Group to the northeast. The Footwall
Basalt is continuous throughout the study area and crops
out sporadically on hills, ridges, river beds and along
the north shore of Red Indian Lake, dips northward and
faces consistently northward. Basaltic rocks thought
to form part of the Footwall Basalt are the host rocks
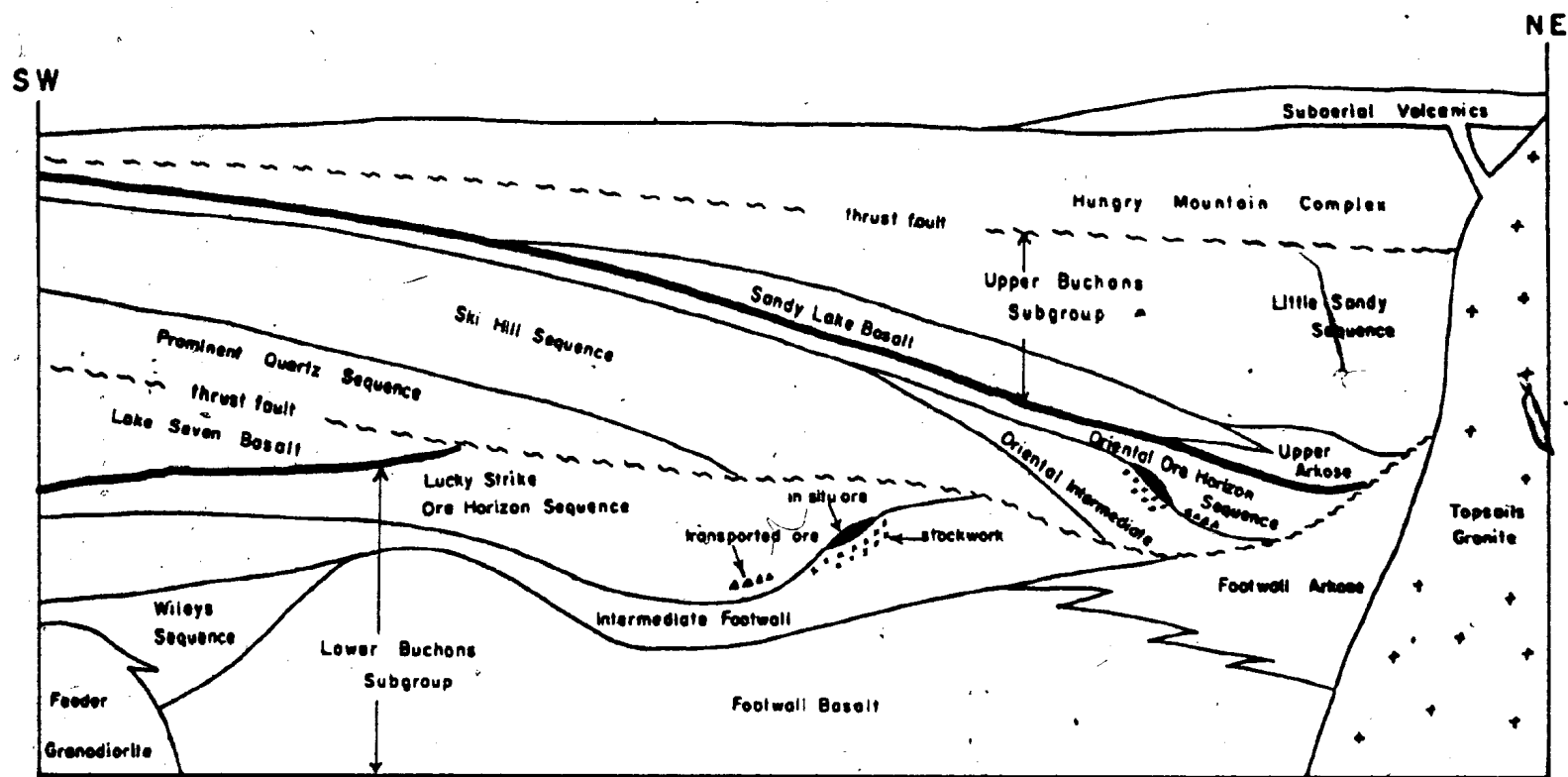for the Skidder Prospect (see next Section). .

FIGURE 3-1: Schematic post-thrusting stratigraphy of the Buchans Group.

Table 3-1 Stratigraphy of the Buchans Group

Unit	Lithologies	Max. Thickness	Mineralization
Upper Buchans Subgroup	Mafic to felsic pyroclastics and breccia with lesser flows, minor volcanic sediment. Includes a basal member (Upper Arkose) of reworked conglomerate.	2000 m (?)	Little Sandy Prospect (Cu) and several areas of weakly to heavily disseminated pyrite, trace chalcopyrite.
Lower Buchans Subgroup			
Oriental Ore Horizon Sequence	Dacitic tuff, rhyolite breccia domes, pyritic siltstone and wacke, pyroclastic breccia, polylithic volcanic breccia-conglomerate, "granite conglomerate".	400 m	High grade massive sulphide orebodies; Oriental #1 and #2, Old Buchans Conglomerate and possibly Old Buchans East and West. Sandfill and Middle Branch Prospects.
Oriental Intermediate	Pendacees felsic pyroclastic breccia, flows; altered intermediate and mafic flows, pyroclastics and breccias.	300 m	Minor ore grade stockwork mineralization with larger areas of subeconomic epigenetic Pb-Zn-Cu.
Old Mill Sequence	Mainly andesitic pyroclastics and breccias; minor basaltic flows, dacitic flows.	1000 m	Local isolated black ore clasts.
Prominent Quartz Sequence	Mainly dacitic pyroclastics, pyroclastic breccias related tuffaceous sediments, lesser rhyolite. Interbedded basaltic and andesitic units, jasper chert.	2000 m	Local disseminated pyrite, Pb-Zn and traces Pb-Zn veining.
Fault			
Lake Seven Basalt	Basaltic pillow lava, pillow breccia and lesser pyroclastics.	350 m	Barren
Lucky Strike Ore Horizon Sequence	Dacitic tuff, massive rhyolite, pyritic siltstone and wacke, pyroclastic breccia, polylithic volcanic breccia-conglomerate, "granite conglomerate", basal basaltic and andesitic horizons.	600 m	High grade massive sulphide orebodies; Lucky Strike, MacLean, Rothermere #1 and #2, Clementine Prospect. Subeconomic veins and isolated occurrences of sulphide clasts.
Intermediate Footwall	Completely interbedded and altered mafic to felsic flows, pyroclastics and breccias, related tuffaceous pyritic siltstone and wacke.	250 m	Localized ore grade pyritic stockwork Zn-Pb-Cu mineralization. Small, stratiform, high grade, polymetallic massive sulphides. Larger areas of subeconomic disseminated and veinlet mineralization.
Footwall Arkose and Wiley's Sequence	Mainly lithic arkose; lesser arkosic conglomerate, siliceous greywacke; minor siltstone, mudstone, chert. Facies equivalent Wiley's Sequence is dominantly felsic pyroclastics with lesser flows and tuffaceous sediments.	2500 m	Carmel Sector; very small bedded pyritic Pb-Zn occurrences; otherwise barren.
Footwall Basalt	Basaltic pillow lava, pillow breccia, lesser pyroclastics, massive flows, interbedded chert. Very minor felsic pyroclastics.	2000 m (?)	Skidder Brook pyritic massive sulphide deposit (Cu-Zn).

Plate 3-1:   Pillow lava of the Footwall Basalt with
             poorly developed radial cracks and amygd-
             ule-rich bands concentrated along pillow
             top.

The base of the Footwall Basalt has not yet been
observed north of Red Indian Lake and thus the thickness
is not known with confidence. Thickness estimates are
also complicated by paleotopographic irregularities on top
of the Basalt and by an essentially unknown component of
the structural repetition by thrust faulting. Despite
these complications, the exposed thickness of the Footwall
Basalt probably exceeds 2000 m within the study area.
Outside the study area it may attain a total thickness of
8300 m, barring unknown repetition by folding or faulting.

The Footwall Basalt consists dominantly of
basaltic pillow lavas and related pillow breccias. Pillows
range from spherical to elongate and are normally from
1.0 to 1.5 m in diameter. Amygdules are common and are
normally filled with calcite although various combinations
of prehnite, pumpellyite, silica, chlorite and epidote
also occur. Large calcite and smaller chlorite-filled
amygdules commonly coexist in the same pillow. In some
areas, amygdules are concentrically arranged only along
the tops of pillows (Plate 3-1) and may facilitate "tops"
determinations (similar pillows are described by Jones,
1969). Amygdules are normally spherical and 5 mm in
diameter although in some localities abundant giant
amygdules (over 3 cm) are present. If amygdule proportion
and size are related to water depth as suggested by Jones
(1969), then shallow water is indicated in these cases.

Plate 3-2: Nearly whole pillows in pillow breccia,
Footwall Basalt. Note concentric amygd-
ule-rich bands near pillow margins.

Plate 3-3: Highly disaggregated pillow breccia,

Footwall Basalt.

Plate 3-4:   Graded pillow breccia, Footwall Basalt.

The pillow lavas are normally feldsparphyric with laths less than 2 mm long and of andesine-labradorite composition. Colourless to light brown unaltered augite phenocrysts are locally present and may attain sizes up to one centimeter, although those of 1-2 mm are most common. The groundmass consists of a fine grained intergrowth of plagioclase, clinopyroxene and much less abundant magnetite. Matrix plagioclase is variably altered to various combinations of epidote, calcite, clay minerals and sericite and is locally replaced by pumpellyite. Clinopyroxene may be altered to epidote and chlorite.

Outcrops of broken-pillow breccia (terminology after Carlisle, 1963) are, in general, poorly exposed but textural variations can be seen best in numerous polished boulders that occur in river beds cutting the basalts. Pillows occur in various stages of disruption from near whole pillows (Plate 3-2) to highly disaggregated varieties (Plate 3-3) which are locally size-graded (Plate 3-4). Isolated-pillow breccia is volumetrically much less significant than broken-pillow breccia.

Pillow lavas are commonly interbedded with chert lenses and locally contain abundant interpillow chert. Cherts occur in a variety of colours ranging from black to dark grey to green although bright red jasper chert predominates in some areas. Chert beds are normally

Plate 3-5: Spheroidal banded rhyolite within Footwall Basalt unit.

less than one meter thick although a major exception
to this generalization occurs in the Skidder Brook
area. Here, in a small area of limited strike length,
there occurs a sequence composed mainly of jasper chert
in excess of 125 m thick. These are interbedded with
less abundant green chert, red cherty mudstone, grey
siltstone, greywacke and lithic arkose and a few massive
basaltic flows. The Skidder Cu-Zn prospect (see next
Section) is associated with similar, but thinner, jasper
chert several hundred meters stratigraphically above the
chert sequence at Skidder Brook.

A number of volumetrically less significant
lithologies occur throughout the Footwall Basalt. These
include pyroclastics (tuff, lapilli-tuff, lapillistone,
agglomerate), tuff-breccias, hyaloclastic breccias,
explosion breccias, blocky flow breccias and massive flows.
Fine grained pyroclastics locally grade imperceptibly
into greywacke and black fine grained bedded volcanic
siltstone of basaltic composition.

Volcanic rocks more felsic than basalt occur
at a small number of isolated localities in the Footwall
Basalt. A few bodies of massive aphyric to feldsparphyric
dark grey rhyolite occur northeast of Skidder Brook.
These are characterized by a peculiar well developed
spheroidal structure (Plate 3-5) which consists of thin

concentric colour banding which defines distinct spheroids of approximately 20 cm diameter. The banding becomes less distinct and eventually disappears both towards the center of individual spheroids and towards the massive rhyolite matrix between spheroids. The origin of this texture is not known but is suspected to be a cooling-related phenomenon.

Other types of felsic volcanic rocks within the Footwall Basalt include small lenses of strongly hematitized rhyolite breccia and thin beds of dacitic tuff. Most of these are of too small scale to be represented on the geologic map (Fig. 2-2).

Alteration of basaltic rocks of the Footwall Basalt is patchy in distribution and shows no recognizable pattern. Pervasive hematitization is present in some areas and may, or may not be combined with abundant vein and amygdule calcite. Such alteration occurred at, or shortly after, deposition as interbedded sedimentary units show no effects of alteration and many non-hematitized breccias contain strongly hematitized fragments. Epidotization is locally intense but usually occurs independently of hematitization and calcite introduction. Various combinations of silicification, pyritization and chloritization are found in some areas but are generally weak and of limited extent. Traces of

disseminated pyrite occur throughout the Footwall Basalt.

In the mine area, the distribution of the Foot-
wall Basalt undergoes some changes that are not evident
elsewhere as an anomalous inlier of the Basalt exists
in the immediate Buchans area (Fig. 2-2). The rocks of
this Buchans Inlier are known (through diamond drilling)
to extend entirely beneath a shallow cover of later rocks
(the Prominent Quartz Sequence) and to be contiguous
with rocks which comprise the main portion of the Footwall
Basalt south of Buchans (Fig. 2-2). The basaltic rocks
of the Inlier strike east-northeast, dip consistently to
the north-northwest at 30 to 50 degrees and face north-
northwest, much like their counterparts to the south.
Although previously thought to be an anticlinal structure
(George, 1937; Relly, 1960; Swanson and Brown, 1962),
these facts dictate that folding cannot be the sole
cause of the presence of the Inlier.

With a few modifications, the lithologies of
the Buchans Inlier are similar to those of the rest of
the Footwall Basalt. Broken-pillow breccia is the most
common rock type. Pillow fragments, some with chilled
rims, range in size from 0.5 m down to tuff size and
are normally separated by a few centimeters of fine
grained matrix. Elongate fragments lie parallel to
bedding with no tendency toward imbrication (cf. Carlisle,

1963, p. 64). Many fragments are highly amydgaloidal (over
50%), some so much so that they initially had densities
close to that of water or may even have floated. Broken-
pillow breccia horizons are locally intercalated with
thin (up to a few meters) aquagene tuff beds or more
rarely with isolated-pillow breccia. Although not exposed
on surface, thin beds of arkose, chert and red mudstone
are interbedded with basalts of the Buchans Inlier.

3.2.1.1.1. Skidder Prospect: The Skidder Cu-
Zn Prospect, though not within the immediate study area,
is briefly mentioned here as it characterizes the type of
mineralization found at the base of the Buchans Group.
It occurs as at least two massive stratiform sulphide
lenses conformable within basaltic rocks of the Footwall
Basalt in close association with jasper chert. Mineralogy
consists mainly of pyrite with minor chalcopyrite and
sphalerite and rare galena. A zone of strong silicifica-
tion and disseminated mineralization exists in the
stratigraphic footwall of the deposit with less intense
alteration in the hangingwall.

3.2.1.2. Footwall Arkose and Wiley's Sequence:
The Footwall Arkose, and the presumed time-equivalent
Wiley's Sequence, form a major regional volcanic and
sedimentary horizon which conformably overlies the Footwall
Basalt. The term "Arkose" is derived from the abundantly

exposed pinkish, fine to coarse grained massive lithic
arkose of volcanic derivation exposed in the mine area.

The Footwall Arkose occurs on surface along a
strike length of more than 20 km from the area near the
east end of Red Indian Lake to the Buchans mine area.
It has been intersected downdip in hole BJ-44 3 km north
of the northernmost outcrop. The unit strikes east to
northeast, dips northward at 5° to 80° and faces consist-
ently northward. Felsic tuffs within the Arkose form the
host rocks for the Connel Option massive sulphide body
(see next Section) but all economic massive sulphide
deposits in the Buchans area occur stratigraphically
above the Arkose.

The felsic volcanic Wiley's Sequence conformably
overlies the Footwall Basalt southwest of Buchans and
contains many lithologies in common with the Footwall Arkose.
It is therefore considered a time-equivalent more proximal
volcanic facies of the Footwall Arkose though the exact
correlation in the critical area south of Buchans is
tenuous. It is further considered to be a stratigraphic
equivalent of the Prominent Quartz Sequence, a unit which
is a structural repetition in a higher thrust slice.

The conformable nature of the contact between
Footwall Arkose and the Footwall Basalt is displayed in a
number of drill cores in the mine area and in outcrop in

the Buchans River due south of Oriental. Indeed the
upper portion of the Footwall Basalt is characterized
by a number of arkosic horizons which are indistinguish-
able from lithologies of the Footwall Arkose proper.
In this sense, the contact between the two formations
on a large scale may be termed "interbedded". The upper
contact of the Arkose is bounded by a bedding plane
(thrust?) fault throughout large areas of the formation,
although (rarely) in the mine area the Arkose is conform-
ably overlain by the Intermediate Footwall (e.g., DDH 885).

In the eastern portion of the study area, the
Footwall Arkose attains a maximum thickness of 2500 m
(barring structural repetition) from the base to the fault-
bounded top.

The Arkose is exposed in over 200 drill cores
in the mine area and in a few additional holes throughout
the strike length of the formation. It is best exposed
in the Buchans Inlier in the bed of the Buchans River.

The Footwall Arkose is a multi-lithologic volcano-
sedimentary sequence. In general, the lower parts of the
formation consist of interbedded green greywacke, tuffaceous
wacke, resedimented conglomerate, sharpstone breccia, silt-
stone, mudstone and multicoloured cherts. Shales are
conspicuous in their absence (or lack of exposure). Inter-
bedded with these are pumiceous felsic lithic-crystal
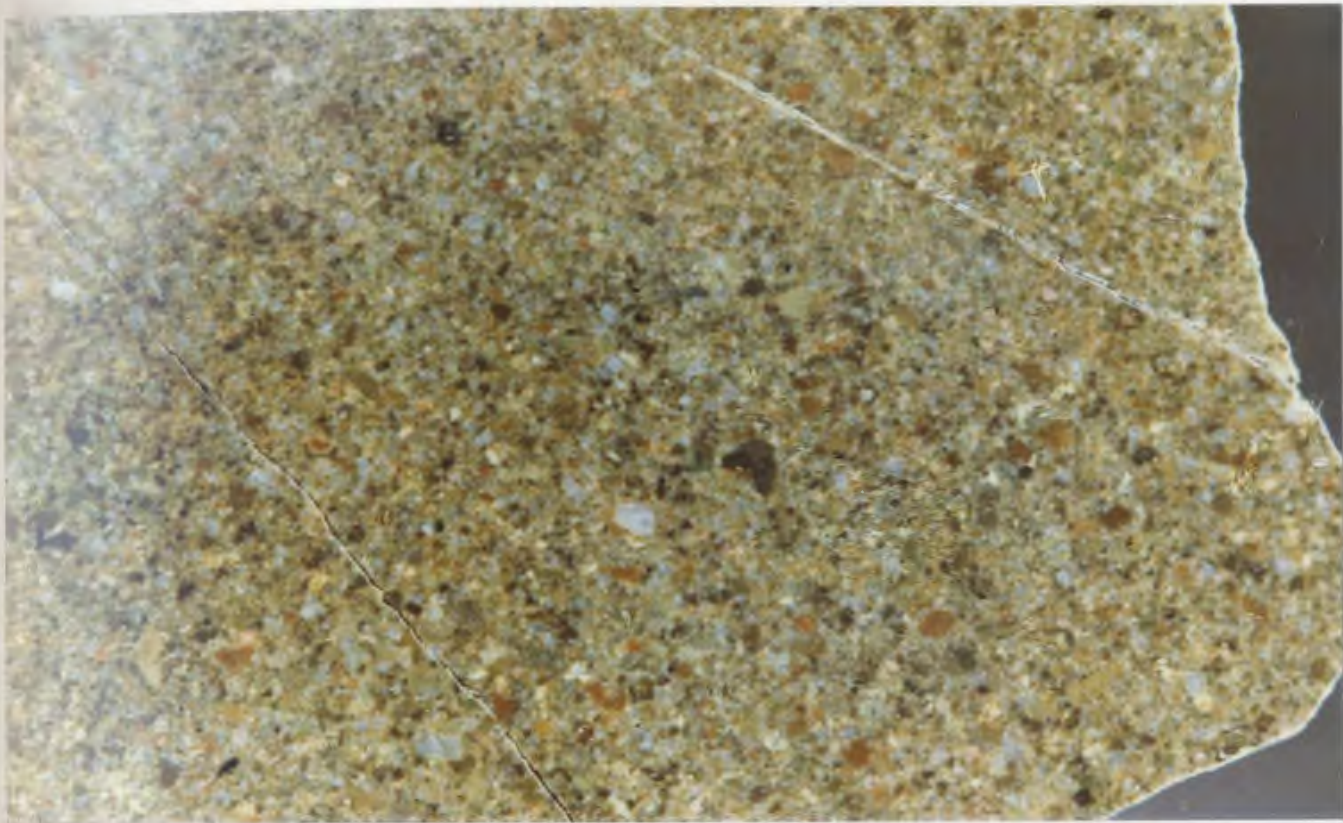
Plate 3-6:   Typical lithic arkose from Footwall Arkose

unit composed of quartz, plagioclase and

reddish rhyolitic grains.   Enlargement

approximately 2X.

tuffs locally containing quartz crystals larger than 1 cm,
a characteristic feature of the Wiley's and Prominent
Quartz Sequences.

The upper parts of the formation contain a
relatively greater proportion of chert and siltstone and,
especially in the mine area, lithic arkose. This rock is
pinkish, fine to coarse grained and is normally massive
and devoid of sedimentary structures, including bedding
(Plate 3-6). It consists of varying proportions of quartz,
plagioclase (oligoclase-andesine), reddish rhyolitic rock
fragments and lesser K-feldspar. Crystal fragments range
in size from less than 1 mm to 8 mm although those of
0.5 to 1.5 mm are most common. Sorting is normally fair
to poor. A weak hematitization of feldspars and the pre-
sence of small red rhyolite fragments imparts the character-
istic light pinkish colour to the arkose.

Massive arkosic rocks contain a number of types
of rounded, isolated pebbles, cobbles and boulders.
Pink to red rhyolites up to several centimeters in diameter
are most common and may be quartz and/or feldsparphyric
and flow-banded. Some varieties contain prominent (greater
than 5 mm) quartz phenocrysts, a characteristic of rhyolites
of the Wiley's and Prominent Quartz Sequences.

Rare occurrences of granitoid boulders are known
(e.g. DDH 247). Isolated pebbles of jasper and rounded

basaltic fragments are found locally. Rounded boulders
of lithic arkose which contain rhyolite pebbles are found
within normal arkosic rocks at some localities in the
mine area. The presence of these boulders suggests instab-
ility during arkose deposition with canibalization of
previously deposited arkose.

In considering the mode of transport and depos-
ition of arkosic rocks of the formation, the thick, coarse
grained, massive nature of the units and the presence of
outsize clasts are of importance. The haphazard occurrence
of these clasts within massive beds devoid of sedimentary
structures rules out deposition either from suspension
or from traction currents. Alternatively, the arkose
displays many of the features of grain flow deposits as
described by Stauffer (1967). Deposition from non-
turbulent mass flows of this nature satisfactorily explains
the thick, massive and homogeneous nature of the arkose,
its textural immaturity, the presence of isolated boulders
of variable composition, the lack of sedimentary structures
including bedding, the interbedding of such divergent
lithologies as basalt and arkose with relatively little
basaltic detritus in the arkose and the presence of thin
interbeds of siltstone and mudstone between the mass flows.

Lithic arkosic rocks of the Footwall Arkose were
probably not derived from an exposed granitic terrane. The

relative lack of alteration of plagioclase feldspars,
the lack of clastic biotite or hornblende and the scarcity
of granite boulders dictate against this possibility.
Conversely, the presence of felsic pyroclastics inter-
bedded with lithic arkose, of "arkose" with a locally
vitric matrix and of lithic arkose with abundant pink
rhyolite fragments suggests that rhyolitic pyroclastics
are the probable source rock for arkosic portions of
the formation. The presence of rhyolite boulders with
prominent (5-10 mm) quartz and feldspar phenocrysts
suggests that the stratigraphically equivalent Wiley's
Sequence is the source. A single current direction
on imbricated rip-up clasts indicates a westerly source
and therefore supports this hypothesis.

    The Wiley's Sequence forms an extensive felsic
volcanic horizon southwest of Buchans, overlying the
Footwall Basalt and underlying the Intermediate Footwall.
Lithologies include massive porphyritic to flow banded
rhyolite, dacitic to rhyolitic pyroclastics and breccias,
tuffaceous sediments, lithic arkose, wacke, siltstone,
mudstone, jasper chert and local basaltic horizons. Several
rhyolite and pyroclastic horizons are characterized by
large (5 mm to 10 mm) quartz and plagioclase phenocrysts
and crystals. Also occurring is a spectacular sequence
of graded subaqueous pyroclastic flow deposits.

3.2.1.2.1.   Connel Option: The Connel Option (Fig. 2-2)
is a small uneconomic distal massive sulphide sheet which
occurs within the Footwall Arkose.   It was discovered
in September 1928 by trenching on an "electrical indication".
The deposit is a conformable bed of chalcopyrite, sphaler-
ite, galena and pyrite; approximately 200 m long and
with a maximum width of 60 cm.

The mineralized horizon is underlain by a
series of thinly interbedded, laterally extensive, multi-
coloured chert, siltstone and fine grained dacitic crystal-
vitric dacitic tuff and ash.   A single contorted Mn-rich
bed up to 30 cm thick occurs within jasper cherts approx-
imately 90 m in the stratigraphic footwall of the deposit.
In the vicinity of the mineralization this sequence is
overlain by a sequence of fine grained bedded dacitic
ash, 15 cm of grey chert and subsequently by massive
sulphides.   The deposit is overlain by up to 1.5 m of
unmineralized grey-green chert.

The deposit is not underlain by an altered and
sulphide impregnated stockwork.   Chert and tuff in the
footwall locally contain disseminated traces of Pb-Zn-Cu-
pyrite mineralization and thin (on the order of 1 mm) beds
of sulphide.   A thin (30 cm) highly sericitic alteration
of fine grained vitric dacite occurs in the footwall in
a single drill core.

The massive sulphides consist of very fine grained high grade sphalerite, galena and chalcopyrite with abundant pyrite exhibiting colloform texture. Faint banding of sulphides is visible in some areas. The principle gangue minerals are pyrite and silica. No barite is present.

Unlike the major massive sulphides of the Buchans area, the Connel Option cannot be related to any known nearby volcanic center. Indeed, the thin blanket shape of the sulphides and their occurrence in a thinly bedded, laterally extensive sequence of chert, siltstone and fine grained volcanic ash suggests a lack of significant paleo-relief and implies that the deposit is distal to the volcanic source.

The source of metal for the deposit is unknown. The lack of known stockwork alteration and mineralization in the footwall suggests that a local fumarole was not the source of the metals. Either of Sato's (1972) Type 1 or Type 3 brines could satisfy the geologic constraints on the source of the ore metal. In this regard it is interesting to speculate on the ore-forming potential of the volcanic center which was responsible for deposition of the Footwall Arkose.

3.2.1.3. Intermediate Footwall: The Intermed-iate Footwall is a sequence of mafic to intermediate

with minor felsic volcanic and volcaniclastic rocks.
Unlike the underlying regionally extensive units, the
Intermediate Footwall occupies a total surface and sub-
surface area of approximately 130 km^2. The term "Inter-
mediate" is derived from the intermediate stratigraphic
position between the underlying units and the overlying
ore-bearing sequence and the intermediate bulk composition
as compared to the felsic ore horizon sequence and the
mafic Footwall Basalt. ·The broadness of the term "inter-
mediate" is also convenient because of pervasive alteration
in the mine area which renders recognition of original
compositions difficult. The Intermediate Footwall
is especially important in terms of ore genesis in that
it is host for the stockwork mineralization below the
massive sulphide orebodies and itself contains at least
two small stratiform massive sulphide bodies.

The Intermediate Footwall originally conformably
overlay the Footwall Arkose (e.g., DDH 885). Locally,
the Intermediate Footwall appears to discoformably over-
lie the Footwall Basalt (e.g., DDH 1038). This discon-
formity is marked by a mixed breccia zone several meters
thick consisting of numerous fragments of basalt of the
Footwall Basalt and fragments of the Intermediate Footwall.
The proportion of basaltic fragments decreases rapidly
with distance above the contact and the proportion of
altered fragments of the Intermediate Footwall

sympathetically increases. Apart from this local discon-
formable relationship and the above-mentioned conformable
contact in DDH 885, the basal contact of the formation
is a bedding plane fault and/or is occupied by diabase
or "rhyolite" sills. The upper contact of the Intermediate
Footwall is also commonly marked by a bedding plane fault
although pyritic siltstone of the Lucky Strike ore horizon
sequence locally conformably overlies the Intermediate
Footwall (e.g., DDH 435).

Thickness estimates in the mine area are complic-
ated by both faulting of the upper and lower contact and
elsewhere by paleo-erosion at the upper contact which
yielded rather uneven paleotopograhy. Regardless of these
complications the formation attains a maximum thickness
of at least 250 m in the area beneath Rothermere and Lucky
Strike orebodies and exceeds 1000 m thickness in areas
more remote from mineralization. Further description of
the nature and role of the Intermediate Footwall in the
mineralizing process is given under the heading "Ore
deposits of the Lucky Strike ore horizon sequence".

3.2.1.4. Lucky Strike Ore Horizon Sequence:
The paleotopography following deposition of the Intermed-
iate Footwall was characterized by a number of topographic
highs, channels and depressions on the volcanic surface
(Figure 3-2). The largest of these, MacLean Depression,
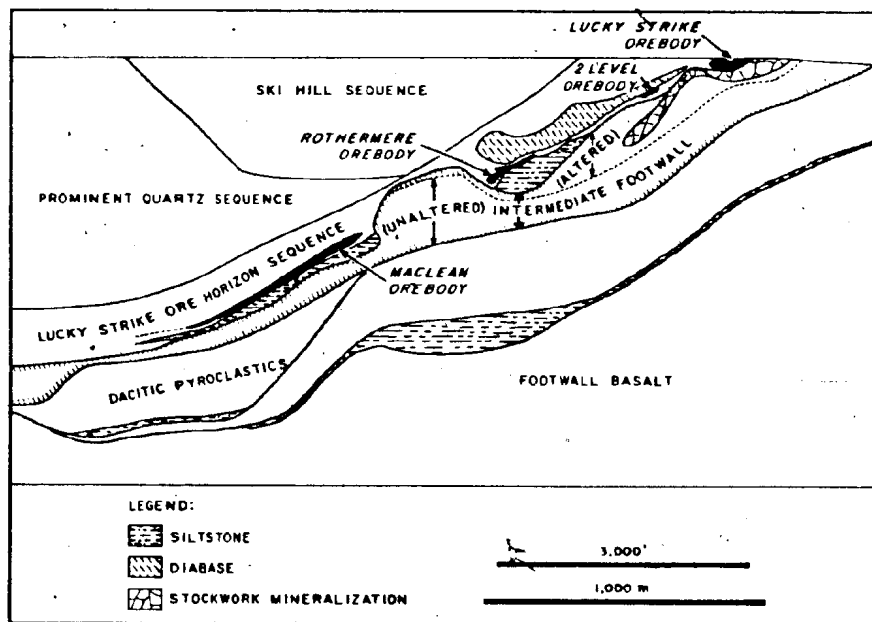
Figure 3-2. Vertical cross section through Lucky
Strike, Two Level, Rothermere and
MacLean Orebodies. Section line is
shown in plan on p. 133.

reaches a maximum width of 800 m, a length in excess of
1 km and a depth locally exceeding 200 m. Smaller
depressions underlie Rothermere, Two Level and Lucky
Strike Orebodies. Felsic volcanic and sedimentary
units of the Lucky Strike ore horizon sequence overlie
the Intermediate Footwall, filled the paleotopographic
depressions and subsequently levelled the existing topo-
graphy. These units form the host rocks of the high
grade stratiform polymetallic sulphide bodies including
Lucky Strike, Two Level, Rothermere, MacLean and the
Clementine Prospect.

The Lucky Strike ore horizon sequence is confined
to the Buchans area roughly between Old Buchans and Clemen-
tine, and occupies a total known surface and subsurface
extent of approximately 50 sq. km. It reaches a maximum
thickness locally exceeding 1000 m. The sequence is
exposed on surface only in rare outcrops and in the Lucky
Strike open pit but is cored top to bottom in hundreds of
drill holes. The sequence conformably overlies the Inter-
mediate Footwall (e.g., DDH 435) although the basal contact
has commonly acted as the locus for low angle faulting.
The upper contact of the sequence with the Ski Hill and
Prominent Quartz sequences is a major low angle shear
zone which has been traced for more than 25 km across
the Buchans area. The Lucky Strike ore horizon sequence
is conformably overlain by the Lake Seven Basalt. This
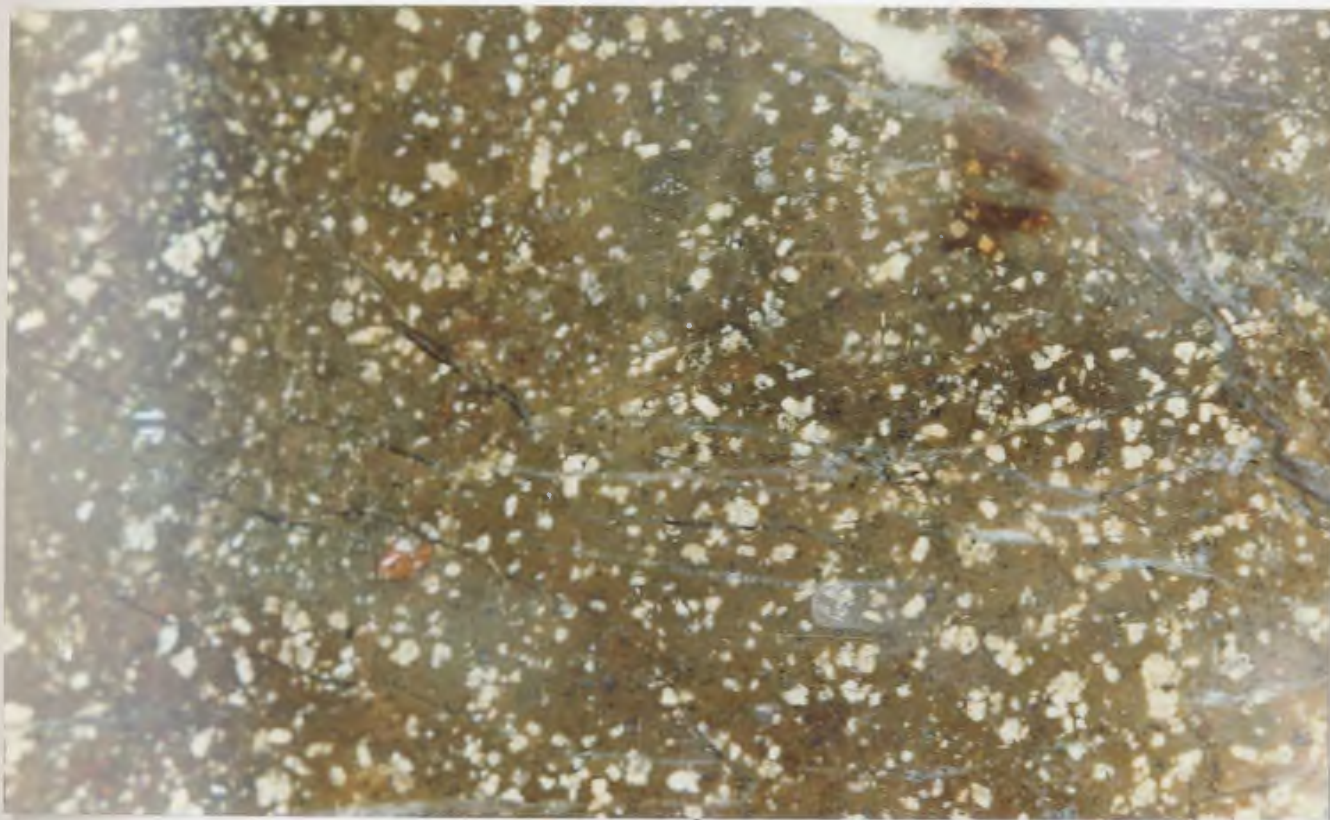
Plate 3-7: Hematitized ore horizon rhyolite with white
            plagioclase and somewhat smaller clear
            quartz. Enlargement approximately 2X.

latter contact defines the top of the Lower Buchans Subgroup.

The lithologies of the Lucky Strike ore horizon
sequence are described in some detail in the following
sections. In general the sequence consists of basal
rhyolite, pyritic siltstone, wacke and dacitic tuffs over-
lain by the massive and transported orebodies with associa-
ted volcanic breccia-conglomerate which are in turn overlain
by a sequence of dacitic tuffs with minor basaltic and
andesitic volcanics.

3.2.1.4.1. Rhyolite: Massive rhyolite occurs
at the base of the Lucky Strike ore horizon sequence in
the area north (downdip) of the Lucky Strike Orebody. The
rhyolite is normally structureless to autobrecciated and
is only rarely interbedded with other lithologies.

The rhyolite is characterized by moderate hematiti-
zation imparting maroon to pinkish hues to the rock (Plate
3-7). Most rhyolite is feldsparphyric though aphyric
varieties and those containing feldspar and small resorbed
quartz phenocrysts also occur. Oligoclase-andesine
phenocrysts (1 mm) are normally clouded by minute hematite
and partially altered to flecks of sericite and epidote
with less common pumpellyite. In more hematitized rhyolites,
calcite alteration of feldspar is dominant. The groundmass
is normally holocrystalline, equigranular and very fine
grained though local granophyric patches exist. Accessory

zircon, sphene, apatite, magnetite and traces of altered
amphibole are common.

3.2.1.4.2. Pyritic Siltstone: Pyritic siltstone
and wacke flank and overlie rhyolite but more commonly
directly overlie the Intermediate Footwall (e.g., DDH 435).
These sediments are restricted to the immediate vicinity
of mineralization and occur in troughs and depressions in
the volcanic surface. Thickness is controlled by this
paleotopography and locally exceeds 100 m.

At the contact, the Intermediate Footwall consists
of typically altered, veined and mineralized polylithic
breccia. This is overlain by pyritic siltstone with no
veins and containing numerous altered fragments of Inter-
mediate Footwall "floating" in a matrix of siltstone.
These fragments die out rapidly above the contact but
small lithic fragments of the Intermediate Footwall are
common throughout the remainder of the siltstone unit.

The siltstone is typically light to dark grey,
siliceous, poorly sorted and massive to locally thinly
bedded, but rarely cherty (Plate 3-8). Slump structures,
small scale cross beds, graded beds, cut and fill structures,
load casts, flame structures, intraformational siltstone
breccias, and small penecontemporaneous faults are common.

The siltstones and coarser volcanic wackes are

Plate 3-8:   Sample from footwall pyritic siltstone unit of
             Lucky Strike ore horizon sequence exhibiting
             ball and pillow structures, flame structures
             and graded bedding.

composed of quartz and plagioclase crystals, a high propor-
tion of rock fragments, minor volcanic glass and a small
proportion of detrital zircon and apatite. Quartz and
plagioclase are normally broken or shattered and feldspars
are commonly altered to calcite. Locally there occur very
thin dacitic crystal-vitric ash horizons with strongly
resorbed quartz in a matrix of altered and flattened pumice
shreds and shards. These horizons are harbingers of on-
coming felsic volcanic activity of the ore horizon dacitic
tuff.

Rock fragments include a wide variety of silicic,
chloritic, pyritic, sericitic and clay mineralized fragments
derived from the Intermediate Footwall, rare jasper chert
and basaltic fragments. Breccias composed entirely of
siltstone (termed siltstone breccia) occur locally. In
some cases it is demonstrable that the siltstone fragments
were transported to their ultimate site of deposition. In
other areas, zones of bedded siltstone have been severely
disrupted to form very coarse and tight packed breccias
that evidently developed in place. These breccias suggest,
a very unstable depositional environment during siltstone
deposition.

The most characteristic feature of all siltstones
below the ore horizon is the presence of very fine grained
disseminated matrix pyrite. This pyrite is euhedral to

broken to subrounded and is normally slightly finer grained
than the siltstone in which it occurs. Pyrite forms
distinct beds in cross bedded siltstone and pyrite grains
are graded in size in graded silt beds. These features
suggest that the pyrite was in hydrodynamic equilibrium
with associated silicate grains and that the pyrite is
detrital. Pyrite constitutes from less than one percent
to five percent of most of the siltstone, though locally
there occur very thin (less than one mm) beds composed
virtually entirely of pyrite. Also present throughout
the siltstone are traces of broken to rounded sphalerite
and barite crystals and rare specks of chalcopyrite.
These sulphide and sulphate minerals are also considered
to be detrital and derived from the underlying Intermediate
Footwall. The presence of these sulphides and the lack of
alteration in the siltstone similar to that of the Inter-
mediate Footwall at the contact provides further evidence
that some stockwork mineralization and related alteration
predated the major massive sulphide mineralization.

3.2.1.4.5. Dacitic Pyroclastics: Dacitic
pyroclastics form the most widespread lithology of the ore
horizon sequence. They are interbedded with, and overlie
the rhyolite and pyritic siltstone (e.g., DDH 2704).
Beyond the limits of these units, the pyroclastics
directly overlie the Intermediate Footwall (e.g., DDH 1406).

Plate 3-9: Dacitic pyroclastic composed of fragments of
dacitic crystal-vitric tuff in chloritic
crystal-vitric matrix. Quartz and white
plagioclase are clearly visible. This is one
of several common types of ore horizon dacitic
tuff.

The bulk of the dacitic pyroclastics occur in the hangingwall of the major orebodies but a thin unit does occur in the footwall. This latter unit varies markedly in thickness, being thin to locally absent in the Lucky Strike area but reaching thicknesses in excess of 100 m below MacLean. The distinction between footwall and hangingwall dacitic pyroclastics is difficult in areas more remote from Lucky Strike due to a lack of alteration in the footwall, the lack of a marker bed defining the ore horizon and the lithologic similarity of footwall and hangingwall tuffs. Due to this lithological similarity, these units will be described together in this section.

Dacitic tuffs and lapilli tuffs are the most common lithology in the ore horizon. These are light to dark green and contain widely varying proportions of quartz and plagioclase crystals with essential and accessory lithic fragments set in a fine grained matrix of variably altered volcanic glass. Bedding is locally visible and is defined by diagenetic flattening of glass shards and pumice shreds or by alteration of vitric-rich and vitric-poor beds (Plate 3-9).

Quartz crystals comprise up to 30% of the tuffs (most commonly 10-20%) and range in size from microscopic to 3 mm (average 1-2 mm). Quartz is rarely euhedral,

normally being resorbed, embayed, broken or a combination
of these. Halos.of secondary quartz are common around
quartz crystals.

Feldspar crystals generally comprise the same
proportion of the dacite as quartz and exhibit the same
size range and average size as quartz. Feldspars are
mainly plagioclase with much less common K-feldspar.
Accurate determination of feldspar composition is hindered
by alteration, normal and oscillatory zoning, broken crystals
and locally by lack of twinning. In general, feldspar
compositions as determined by the Michel-Levy method
and on rare combined Carlsbad-albite twins is andesine.
Plagioclase is variably altered to a fine grained inter-
growth of sericite and clay minerals or less commonly
calcite, pumpellyite, prehnite or epidote.

Hornblende crystals are normally absent though
locally form up to two percent of the tuffs. In general,
hornblende is more common in the Oriental area than in
the Lucky Strike area and is generally more abundant in
more vitric-rich tuffs. Alteration of hornblende to
chlorite with anomalous lilac birefringence is common.

Apatite, sphene, rutile, zircon and leucoxene
are ubiquitous but minor constituents of the tuff. Traces
of pyrite are microscopically visible in most samples.
Traces of biotite occur rarely.

Matrix volcanic glass and its altered equivalents
form from 30 to 70% of most portions of the dacitic tuffs
(though all extremes from glass-poor crystal-lithic tuff
to 100% vitric ash or pumice tuff exist). Alteration of
glass to a fine grained sericite-clay mineral-chlorite
aggregate imparts the characteristic grey to green colours
of the dacite. Despite complete alteration of glass,
characteristic shard shapes are commonly visible microscop-
ically and pumice shreds and larger long tube pumice frag-
ments are normally visible with the hand lens or naked eye.

Volcanic glass, from microscopic shards to pumice
fragments several centimeters in length, is almost invar-
iably flattened into the bedding plane imparting a psuedo-
foliated appearance which is characteristic of virtually
all vitric-ash pyroclastics in the Buchans area. This
feature previously led the author (Thurlow, 1973; Thurlow
et al., 1975) to consider that portions of the dacitic
tuffs were deposited subaerially. However, such tuffs
are locally interbedded with laminated mudstone and silt-
stone (which in some cases is graded-bedded and displays
small scale cross beds and load casts). Elsewhere, vitric
dacitic tuff with strongly flattened pumice is interbedded
with pillow lava. On the basis of these observations the
occurrence of flattened pumice and glass shards is not
considered to represent collapse due to load in a glowing
sheet of subaerial volcanic ejecta. Similarly flattened

1

pumice in vitric pyroclastics of demonstrable submarine origin have been described by Fiske (1963), Fiske et al. (1963), Fiske and Matsuda (1964), Mutti (1965), Fiske (1969) and in no less than five papers in Ishihara (1974) describing Miocene volcanic rocks in the vicinity of the Kuroko deposits of Japan. Fiske (1969) states that pumice can be flattened into the bedding plane to produce "a highly compact rock that, in some cases, superficially resembles welded tuff" and Ohtagaki et al. (1974) state that "in appearance, it resembles the pumice found in common welded tuffs". Ohtagaki et al. consider that flattened pumice in subaqueous sequences is a result of compaction during dewatering and diagenesis of pumice which has been depositionally and diagenetically altered to soft clay minerals. A similar mode of origin of flattened pumice in the Buchans area is considered likely.

The most common fragment types within dacitic tuffs are fragments of dacitic tuff and rhyolite grains and clasts. Fragments of dacite crystal-vitric tuff are diffuse to well defined, rounded to angular and have a composition and texture very similar to the matrix material. The colour of these fragments is normally slightly different from the matrix and serves to distinquish the fragments. Accessory lithic fragments are common especially at the base of graded subaqueous pyroclastic flows. The base of such flows consists of tightly packed

breccias with a crystal-vitric matrix and contains angular
to rounded fragments of virtually every lithologic type
below the dacite (i.e., basalt, jasper chert, numerous
varieties of altered Intermediate Footwall, rhyolite,
siltstone, granodiorite and (rarely) boulders of Feeder
Granodiorite. Lithic fragments in these pyroclastic
debris flows become finer grained and less abundant upward
as the flow grades into crystal-vitric tuff and may be
overlain by vitric ash or tuffaceous siltstone.

In the vicinity of the in situ massive sulphides
the distinction between footwall and hangingwall dacite is
not difficult. Near Lucky Strike and Rothermere Orebodies,
the footwall dacite is normally greyer and more hydrother-
mally altered (to clay minerals) and may contain traces
of galena, sphalerite and pyrite. However, beyond the
area of significant alteration (e.g., beyond the vicinity
of MacLean Orebody) the author has been unable to find
any consistent macroscopic, microscopic or geochemical
difference between the footwall and hangingwall dacite.

Although most portions of the dacitic tuffs are
sufficiently similar such that recognition of any internal
stratigraphy is difficult, there exists one distinctive
type. Locally known as the "coarse-quartz dacite", this
crystal-vitric tuff is characterized by quartz crystals
somewhat coarser than normal (average 2-4 mm) and conformably

Plate 3-10:   Typical dacitic pyroclastic from the "coarse quartz" unit. Sample contains 1-3 mm quartz, 1 mm plagioclase in matrix of black chloritic altered glass. Pinkish lithic fragments are rhyolite; dark lithics are basalt and andesite.

overlies the normal hangingwall dacite (e.g., DDH 827).
It is best developed in a depositional basin which occurs
between the Lucky Strike - MacLean and Clementine areas
and locally exceeds 100 m in thickness. The coarse-quartz
dacite is intimately associated with graded subaqueous
debris flows and itself contains more lithic fragments than
the normal tuff. Locally the coarse-quartz dacite is
interbedded with more normal dacitic tuff but is is emphas-
ized that the first appearance of the coarse-quartz dacite
occurs well in the hangingwall of the major ore deposits.
This relationship is important as this dacite locally
contains scattered pebbles of high grade black ore and is
conformably overlain by polylithic breccia-conglomerate
which also locally contains sulphide fragments.

The coarse-quartz dacite contains a variety of
lithic fragments with pinkish massive rhyolite and aphyric
aphanitic andesite fragments being more common (Plate 3-10).
Lithic-rich beds are commonly separated by vitric-rich beds
imparting a diffuse banding to the rock.

The coarse-quartz dacite is conformably overlain
(e.g., DDH's 799, 827) by a complex polylithic breccia-
congldmerate unit which, like the coarse-quartz member,
occupies the depositional basin between the Lucky Strike -
MacLean area and the Clementine area. This unit is
characterized by an abundance of pink aphyric, to quartz and

Plate 3-11: Tight packed pyroclastic breccia from coarse-
quartz member of Lucky Strike ore horizon
sequence. Angular to rounded fragments are
mainly rhyolite.

feldsparphyric rhyolite fragments (Plate 3-11) although a
lesser proportion of basaltic and andesitic fragments
(most of which are of unknown origin) are also normally
present. Less abundant fragment types include cherty
siltstone, pyritic siltstone, rare granodiorite boulders,
pumice fragments, dark grey carbonate fragments (e.g., DDH's
629, 799) of unknown origin and sulphide fragments.
Fragments are moderately to tightly packed in a lithic
quartzo-feldspathic matrix with only a local significant
vitric component. Breccia-conglomerate beds are normally
massive although thick graded beds ranging from coarse
breccia-conglomerate to cherty siltstone are not uncommon
(e.g., DDH's 2210, 629). These debris flows are interbed-
ded with greywacke, siltstone (locally pyritic), vitric
tuff and spectacular graded pumiceous pyroclastic flows
(e.g., DDH's 1562, 932).

Sulphide fragments in this horizon and (less
commonly) in the underlying coarse-quartz member are of
interest. Sulphide clasts have been recognized macro-
scopically in at least 10 drill holes, i.e., DDH's 191,
1442, 2681, 2243, 2332, 2224, 2210, 1406, 2214 and 2778.
Black ore clasts are most common with much less abundant
yellow ore and stockwork fragments. Sulphide clasts
range from angular to rounded, competent to plastic and
reach a maximum size of 13 cm (although the average is

less than one cm). They are especially concentrated in
the thickest portion of a basin which existed in the area
between Lucky Strike and Clementine.

The source of the sulphide fragments is of
interest in exploration. Since the fragments occur in a
stratigraphic horizon at least 200 m (diabase removed)
above the Rothermere ore horizon it is unlikely that the
Lucky Strike Orebody provided the sulphide fragments in
this breccia conglomerate. The relative rarity of fragments
which are so abundant in the main ore horizon (i.e.,
granodiorite, pyritic siltstone and varieties of Inter-
mediate Footwall) as well as the presence of basaltic,
andesitic and carbonate fragments of unknown origin further
suggest that the lithologies in the breccia-conglomerate
are not from the Lucky Strike area. The decrease in
abundance of sulphide fragments towards the Lucky Strike
area further dictates against this area as a source.
Some of the extraneous fragment lithologies can be
matched with those in the Clementine clastic ore horizon,
although the sulphide-bearing horizon lies above Clementine
as well.

3.2.1.4.4. Lucky Strike Ore Horizon: Massive
sulphide, transported ores and facies-equivalent breccia-
conglomerate and "granite-conglomerate" overlie dacitic
pyroclastics. These are described in Chapter Four.

The ores are overlain by a thick sequence of
dacitic pyroclastics, as described in the previous section,
and subsequently overlain by the Lake Seven Basalt.

3.2.1.5. Lake Seven Basalt: The Lucky Strike
ore horizon sequence is conformably overlain by the Lake
Seven Basalt (e.g., DDH 799) which subcrops west of
Rothermere Orebody (Fig. 2-2). Though it forms the base
of the Upper Buchans Subgroup, the Lake Seven Basalt is
described in this section as it is the uppermost member
of the Lucky Strike thrust block. The unit is areally
restricted and consists dominantly of basaltic pillow lava,
pillow breccia, pyroclastics and massive flows. Flows
contain small phenocrysts of fresh augite and labradorite
largely altered to calcite, sericte and epidote. The
phenocrysts occur in a fine grained diabasic-textured
matrix of plagioclase and clinopyroxene, the latter altered
to chlorite. Locally flows are black and very fine grained
and contain quenched plagioclase with swallow tail termin-
ations and hollow cores, i.e., similar to those described
by Pearce (1974).

Several features of the Lake Seven Basalt are
similar to those of the Footwall Basalt and indeed, distinc-
tion of the two units on a hand specimen basis is impossible.
Pink to white calcite amygdules are common in the Lake
Seven Basalt and the unit has locally been affected by weak

to strong hematitization. Pyroclastic units commonly have
a pink to white crystalline calcite-rich matrix (e.g.,
DDH 1562) and may show size grading of individual beds.

3.2.1.6. A Stratigraphic Discontinuity at the
Top of the Lake Seven Basalt: The
interpretation of the uppermost contact of the
Lake Seven Basalt with overlying units has far-reaching
effects both in terms of understanding the stratigraphy
and in terms of exploration. Despite hundreds of drill
penetrations, an indisputably conformable contact has not
yet been observed. Normally, the contact is occupied by
one of the innumerable diabase sills which cut the Buchans
Group, or is a zone of poor core recovery or, in some cases,
a zone of obvious shearing. The same comments apply in
areas where the Lake Seven Basalt is absent and where the
overlying Prominent Quartz or Ski Hill sequences lie
directly on the Lucky Strike ore horizon sequence.

Two opposing interpretations are based upon the
nature of this contact: 1) the contact is a zone of local-
ized bedding plane shearing developed during regional
folding and is of no regional consequence in understanding
the stratigraphy, and 2) the contact represents a thrust
fault superimposing older on younger lithologies. The
significance of the latter hypothesis is discussed more
fully in Section 3.3.1.1.
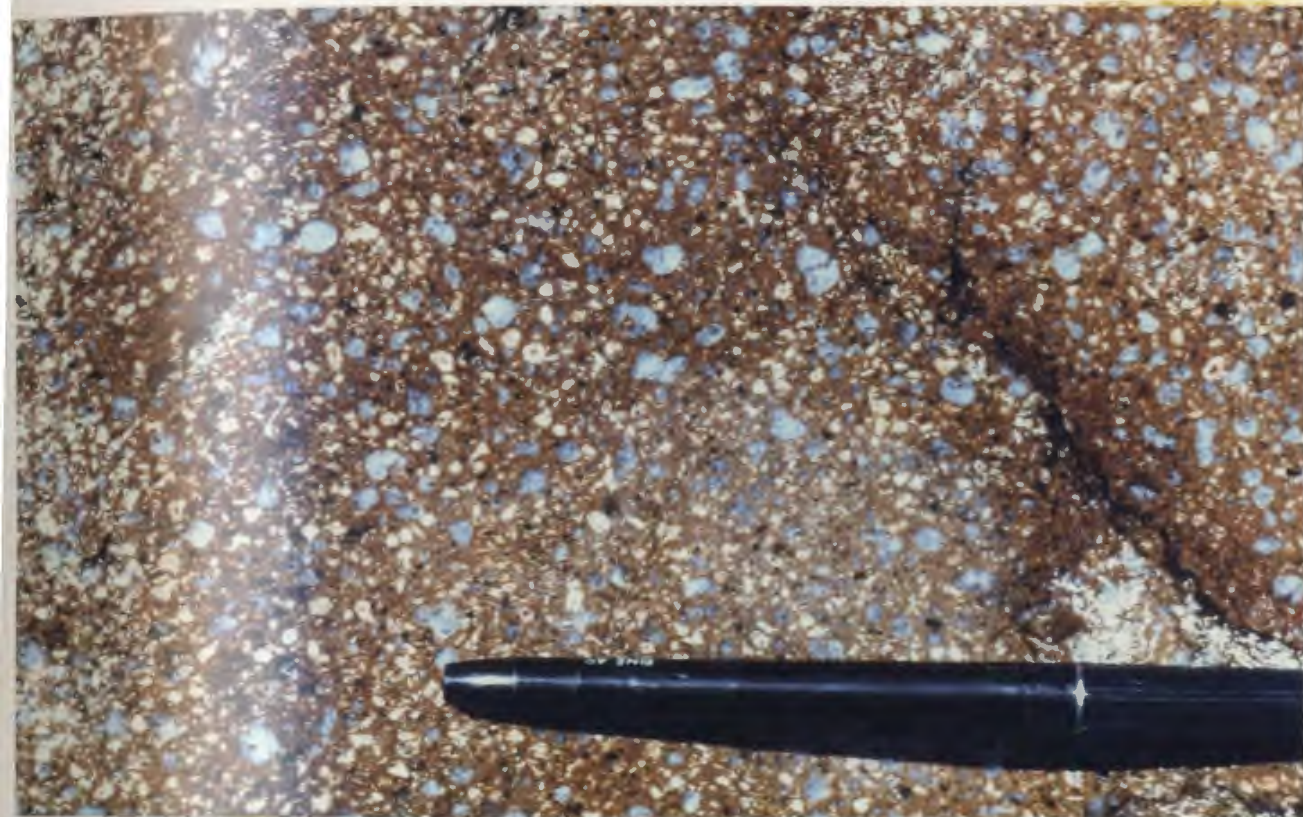
Plate 3-12:   Porphyritic rhyolite of Prominent Quartz
              Sequence containing large rounded to sub-
              hedral quartz and smaller zoned plagioclase
              phenocrysts.

3.2.1.7. Prominent Quartz Sequence: Rocks of
the Prominent Quartz sequence are the lowermost units
recognized above the stratigraphic discontinuity discussed
in the previous section. The sequence is widely distributd
to the north and west of Buchans and occupies a known
surface and subsurface area of approximately 100 square
kilometers. Outcrop exposures are extremely sparse but
the sequence is fairly well known through drilling designed
to penetrate the underlying ore horizon. The sequence is
absent in areas east of Buchans but reaches thicknesses in
excess of one kilometer to the west. Field, petrographic
and geochemical evidence suggests that felsic volcanics of
this sequence were derived from magmas of the Feeder
Granodiorite. The Prominent Quartz Sequence is considered
to be a thrusted repetition of the Wiley's Sequence and
Footwall Arkose.

The Prominent Quartz sequence consists dominantly
of rhyolitic flows and pyroclastics which are commonly
characterized by the presence of "prominent" (5-10 mm)
quartz phenocrysts (Plate 3-12). These are normally rounded
and somewhat embayed though locally well preserved hexagonal
crystal outlines exist. They range in size up to a maximum
of 3 cm. Irregular to radial cracks are common. Zoned
plagioclase phenocrysts are normally present in approximately
the same abundance as quartz but are generally smaller,
reaching a maximum size of 1 cm. Oscillatory zoning is

common and even in flows plagioclase crystals are commonly
broken. Plagioclase is commonly partly altered to pumpell-
yite, epidote, calcite and sericite.

Small (less than 1 mm) hornblende phenocrysts
commonly comprise less than 5% of rhyolite flows and are
normally altered to chlorite with lesser pumpellyite,
epidote and calcite. Associated with these, there is
normally a small proportion of magnetite which also may
occur as small isolated crystals in the matrix. The matrix
to flows is aphanitic and quartzofeldspathic in a wide
variety of colours ranging from salmon pink to black.

Individual rhyolite flows of the Prominent Quartz
sequence have been traced over areas exceeding a square
kilometer. Locally thick (greater than 100 m) massive
structureless rhyolite flows (e.g., DDH 2090) display no
flow banding or autobrecciation and are overlain with sharp
conformable contact by lithic-crystal-vitric tuff with
some fragments of massive rhyolite. The sharp nature of
such contacts, the lack of autobrecciated flow tops, the
widespread distribution of the flows and their coarsely
porphyritic nature are evidence in support of unusually
fluid rhyolite magmas.

Rhyolite flows, especially those south of Lucky
Strike, have locally undergone strong silicification,
sericitization and pyritization but no significant

mineralization is known.

Crystal-vitric tuffaceous rocks of the Prominent Quartz sequence contain an identical phenocryst assemblage to the flows, i.e., prominent cracked quartz, zoned plagioclase and hornblende, but the matrix consists of anastomosing flattened glass shards and larger pumice shreds. Volcanic glass is commonly altered to dark green to black chlorite.

Also included in the Prominent Quartz sequence are important members of rhyolite and (related?) pumiceous pyroclastics which do not contain prominent quartz and feldspar phenocrysts but instead normally contain smaller (1 mm) quartz crystals. Particularly important are widespread, distinctive and spectacular subaqueous pyroclastic flows which are apparently confined to the northern and western portions of the Buchans Group. These are thick graded deposits ranging from coarse polylithic breccias with fragments locally in excess of 1 m at the base (but normally less than 10 cm). These grade upward into finer grained breccias with abundant multicoloured long tube pumice and further upward into finer grained lithic-crystal-vitric tuff overlain gradationally by siltstone and cherty mudstone. Individual deposits may be tens of meters thick and the entire sequence consists of several tens of individual pyroclastic flows. Double grading such as that

described by Fiske and Matsuda (1964) is locally developed.
The thickness of these deposits and the abundance of
pumiceous material suggests that they were triggered by
violent volcanic explosions. The coarsest facies of these
units are developed in the Wiley's Sequence whereas finer
grained more distal facies exist in numerous drill cores
to the north (e.g., DDH's 2666, 724). This suggests
northerly directed pyroclastic flow from an active (now
eroded) felsic volcanic centre to the south.

A variety of tuffaceous sediments are interbedded
with the volcanics of the Prominent Quartz sequence. The
most unusual of these is a sequence composed dominantly
of black, locally pyritic and carbonaceous mudstone which
occur south of Lucky Strike (e.g., DDH's 1908, 1904).
These are massive to thinly laminated and generally do not
break parallel to bedding, hindering the search for macro-
fossils. Several samples of this material were sent for
detailed microfossil analysis but proved barren (J. Utting,
pers. comm., 1975).

A number of basaltic horizons are included within
rocks of the Prominent Quartz sequence. These horizons
are macroscopically and chemically similar to rocks of
the structurally underlying Lake Seven Basalt and Footwall
Basalt.

3.2.1.8.   Ski Hill Sequence: The Ski Hill sequence consists of a thick pile of black to dark green breccias, pyroclastics and pillow lava of basaltic to andesitic composition.   It conformably overlies the Prominent Quartz sequence (e.g., DDH's 2925, 2927, 2841) but where the underlying Prominent Quartz sequence is absent, the Ski Hill sequence rests with sheared contact directly upon the Lucky Strike ore horizon sequence.   Sporadic outcrops of the Ski Hill sequence occur in an east-west trending belt extending from the Buchans River approximately 4 km west to the Lake Seven area (Fig. 2-2).   The sequence occupies a known surface and subsurface area of approximately 30 square kilometers and reaches a maximum known thickness of approximately 1 kilometer.

The Ski Hill sequence consists mainly of andesitic breccias and pyroclastics interbedded with massive and pillowed flows of basaltic to andesitic composition.   In general, flows of the sequence consist of plagioclase (andesine-labradorite) and augite phenocrysts set in a very fine grained diabasic-textured groundmass.   Like the Footwall and Lake Seven Basalts, augite phenocrysts are normally much less altered than plagioclase phenocrysts or matrix pyroxene.   Plagioclase phenocrysts are commonly zoned, aligned or felted and generally partially altered to combinations of epidote, calcite, pumpellyite or clay minerals.   Most flows and blocks of massive andesite in

Plate 3-13:   Typical Ski Hill Sequence breccia with both
              elongate and spherical quartz amygdules.
              Elongate vesicles at top of larger fragment
              (near center of photograph) are filled with
              matrix material.   Approximately true size.

breccias contain zoned amygdules filled with combinations
of prehnite, quartz, pumpellyite, chlorite and calcite.
Spherical, flow-stretched and amoeboid amygdules are common
(Plate 3-13).

The top of the Ski Hill sequence is normally
characterized by an upward increase in the abundance of
exotic accessory fragments which grade upwards into poly-
lithic breccias of density flow origin. These breccias
contain a variety of lithic fragments ranging in composition
from basalt to rhyolite and locally contain rounded grano-
diorite pebbles and cobbles (e.g., DDH's 885, 1003, 1038,
1185). In places, these breccias are characterized by a
siliceous siltstone matrix bearing detrital pyrite, much
like siltstones of the overlying Oriental ore horizon
sequence. Rare occurrences of Pb-Zn beds (?) and of high
grade black ore fragments in breccias (e.g., DDH's 1911,
1884) are also known in these upper portions of the Ski
Hill sequence.

The distinction between rocks of the Ski Hill
sequence and Footwall Basalt is locally difficult and,
although some empirical generalizations can be made,
there are many exceptions. Rocks of true andesitic compos-
ition are dominant in the Ski Hill sequence and rare in
the Footwall Basalt. No arkosic rocks similar to the
Footwall Arkose are known within the Ski Hill sequence and

the sequence is nowhere immediately overlain by arkosic
rocks. Interpillow chert and chert interbeds are much
more common in the Footwall Basalt than in the Ski Hill
sequence. In general, calcite amygdules (especially
pink calcite) are more common in the Footwall Basalt and
amygdule abundance is also generally greater. Distinctive
small elongate amygdules stretched during flow are common
in the Ski Hill sequence and rare in the Footwall Basalt.
Quartz-prehnite-pumpellyite amygdules are generally more
common in the Ski Hill sequence. Pervasive hematitization
is somewhat more common in the Footwall Basalt. In general,
pillow lava is somewhat more common in the Footwall Basalt
whereas true pyroclastics and a variety of breccia types
are more common in the Ski Hill sequence. Breccias of the
Ski Hill sequence are commonly polylithic (in varieties
of basalt and andesite) whereas breccias of the Footwall
Basalt are most commonly monolithic. Polylithic breccias
such as those that occur at the top of the Ski Hill sequence are
not known in the Footwall Basalt. Pyritic siltstone,
plutonic pebbles and black ore occurrences are also not
known in the Footwall Basalt.

3.2.1.9. Oriental Intermediate Footwall: A unit
known as the Oriental Intermediate Footwall conformably
overlies the Ski Hill Sequence and forms the host for
epigenetic stringer and stockwork mineralization associated

with the Oriental #1 orebody. The Oriental Intermediate
consists dominantly of an areally restricted pile of altered
intermediate to felsic pyroclastics and especially pumice
tuff, pumice breccia and vitric tuff.

Though this sequence is dominantly felsic, the
term "intermediate" is convenient in that the more felsic
end members of the sequence are quartz-poor to quartz-free
in contrast to the quartz-rich pyroclastics of the Oriental
ore horizon sequence. Also, as at Lucky Strike, the
"intermediate" volcanics occupy a stratigraphic position
intermediate between underlying mafic and overlying felsic
sequences.

The Oriental Intermediate is discussed more fully
in Section 4.4.

3.2.1.10. Oriental Ore Horizon Sequence: The
Oriental ore horizon sequence is a significant felsic vol-
canic accumulation which conformably overlies the Oriental
Intermediate. It forms the host rocks for the in situ
Oriental #1 Orebody and the transported Oriental #2 and
Old Buchans Conglomerate Orebodies as well as the subeconomic
transported Sandfill and Middle Branch Prospects.

The sequence is shallowly northward-dipping and
occupies a known surface and subsurface area of less than
10 square kilometers in an area north of Old Buchans and

Oriental. The sequence reaches a maximum thickness of approximately 400 meters in an area north of Oriental but thins rapidly both to the east and west. The northerly downdip extensions of the sequence have not been fully outlined by diamond drilling.

The lithologies and stratigraphy of the Oriental ore horizon sequence are remarkably similar to their counterparts at Lucky Strike. Detailed discussion of the sequence is given in Chapter Four.

3.2.2. Stratigraphy of the Upper Buchans Subgroup. The Upper Buchans Subgroup is characterized by mafic, intermediate and felsic volcanic rocks with the latter predominant. In keeping with the generally northerly dips in the area, it is generally distributed in the north part of the study area. The stratigraphy is less well known than that of the Lower Buchans Subgroup largely because of the lack of economic incentive to drill these rocks systematically. Information is largely derived as a consequence of drilling of the underlying Oriental ore horizon sequence. The understanding of the stratigraphy is further hampered by significant thrust faults, the effects of which are not yet fully understood.

There was no recognizable break in volcanism-sedimentation between Lower and Upper Subgroups but the

boundary marks the end of the Oriental ore horizon felsic
volcanic sequence and the upper stratigraphic limit of
known economic mineralization. It also marks the onset of
renewed mafic volcanism on a widespread scale and concurrent
influx of arkosic density flows containing detritus
extraneous to the intermediate Buchans area. As such,
the boundary marks the beginning of a second volcanic
cycle, not totally dissimilar to that of the Lower Buchans
Subgroup.

The Oriental ore horizon sequence is conformably
overlain by two separate units which interfinger in complex
fashion at their margins. The Sandy Lake Basalt conformably
overlies the Oriental ore horizon sequence in the west
(e.g., DDH's 2853, 1582) whereas the Upper Arkose forms
the base of the Upper Buchans Subgroup to the east
(conformable contacts in DDH's 1683 and 1872, among others).

The Sandy Lake Basalt consists of basaltic pillow
lava, pillow breccia and pyroclastics all characterized by
abundant calcite amygdules, labradorite and/or augite pheno-
crysts and locally intense diagenetic calcite-hematite
introduction. As such, this basaltic unit is virtually
indistinguishable from basalts of the Lower Buchans Subgroup.

On the other hand, the Upper Arkose is among one
of the more unique and interesting units in the Buchans
area. The Upper Arkose occupies and levels the remnants

Plate 3-14: Volcanic conglomerate of Upper Arkose.
Rounded cobbles are varieties of rhyolite,
some with large quartz phenocrysts.

of a deep paleotopographic trough in the underlying Oriental ore horizon sequence. Towards the western margin of Arkose deposition, the Upper Arkose conformably overlies (e.g., DDH's 1582, 1758) and interfingers with the Sandy Lake Basalt. The Upper Arkose reaches a maximum unsheared thickness in excess of 100 m and locally attains a total thickness in excess of 300 m.

The Upper Arkose is composed almost entirely of lithic arkose and arkosic conglomerate. The conglomerate is polymictic and contains boulders of massive rhyolite and dacitic crystal-vitric tuff, both with prominent (5-10 mm) quartz phenocrysts and pink rhyolite with or without small quartz and feldspar phenocrysts (Plate 3-14). Less common are calcite amygdaloidal basalt (very similar to those of the Sandy Lake Basalt), arkosic conglomerate boulders, and minor granitoid boulders. Relly (1960, p. 82, 97) reported an occurrence of a sulphide boulder in the Upper Arkose in the Oriental east pit though none have been noted by the author, E.A. Swanson or other workers. Most boulders are well rounded with moderate sphericity and vary from tightly to loosely packed. The matrix is normally immature and poorly sorted, consisting of small lithic fragments and quartz and feldspar crystals. The conglomerates are normally massive and devoid of all sedimentary structures, though local thick graded beds exist and rare inverse to normally graded beds occur (e.g., DDH 1492). Near the base

of the conglomerate in the Oriental area, there exists at
least one horizon of dacitic crystal-vitric tuff macroscop-
ically, microscopically and geochemically identical to
that of the underlying Oriental ore horizon sequence
(e.g., DDH 1606). The presence of this interbedding at
the upper contact of the Lower Buchans Subgroup provides
strong evidence that there was no depositional break at
this juncture.

Rocks of this arkosic conglomerate horizon and
those of the Footwall Arkose Formation are virtually
indistinguishable. Only the stratigraphic position is
diagnostic in identifying these lithologies. However, in
general the Upper Arkose normally contains a greater
abundance of conglomerate and a greater variety of boulder
lithologies. Felsic volcanic boulders with prominent
quartz (5-10 mm), granitoid boulders and basaltic boulders
are relatively more common in the Upper Arkose than in
the Footwall Arkose.

The Upper Arkose is considered to have been
deposited by the same mechanism as the Footwall Arkose
(i.e., density flow) and evidence supporting this hypothesis
is similar to that quoted for the Footwall Arkose. Indeed,
their textural and lithologic similarity suggests that the
same volcanic source may have supplied detritus in both
units. The vast difference in lithologies between those

of the Footwall-Upper Arkose and those of the ore horizon
sequence suggests that the volcanic sources for these
sequences were spatially separated. The occurrence of ore
horizon dacitic crystal-vitric tuff identical to that of
the Lucky Strike Formation interbedded with the Upper
Arkose probably represents an interfingering of volcanic
materials from these two sources and further represents
the last volcanic gasp from the source which produced
the Oriental ore horizon sequence. Evidently volcanic
activity shifted back and forth between these two centers
with very little temporal overlap.

The Upper Arkose is conformably overlain by the
Little Sandy sequence (e.g., DDH's 1606, 1683). This
dominantly volcanic unit is the uppermost sequence of the
Buchans Group and, although widely distributed to the north
and east of Buchans (Fig. 2-2), is probably the most poorly
known in the area. The sequence forms the host rocks for
the Little Sandy copper mineralization several kilometers
east of Buchans.

The base of the Formation in the east is every-
where fault-bounded, juxtaposing rocks of the Little Sandy
sequence and Footwall Arkose. The contact is marked by
shearing, fault gouge, diabase dykes or by discontinuous
linear patches of poorly indurated red sandstone and conglo-
merate containing abundant boulders of peralkaline rhyolite
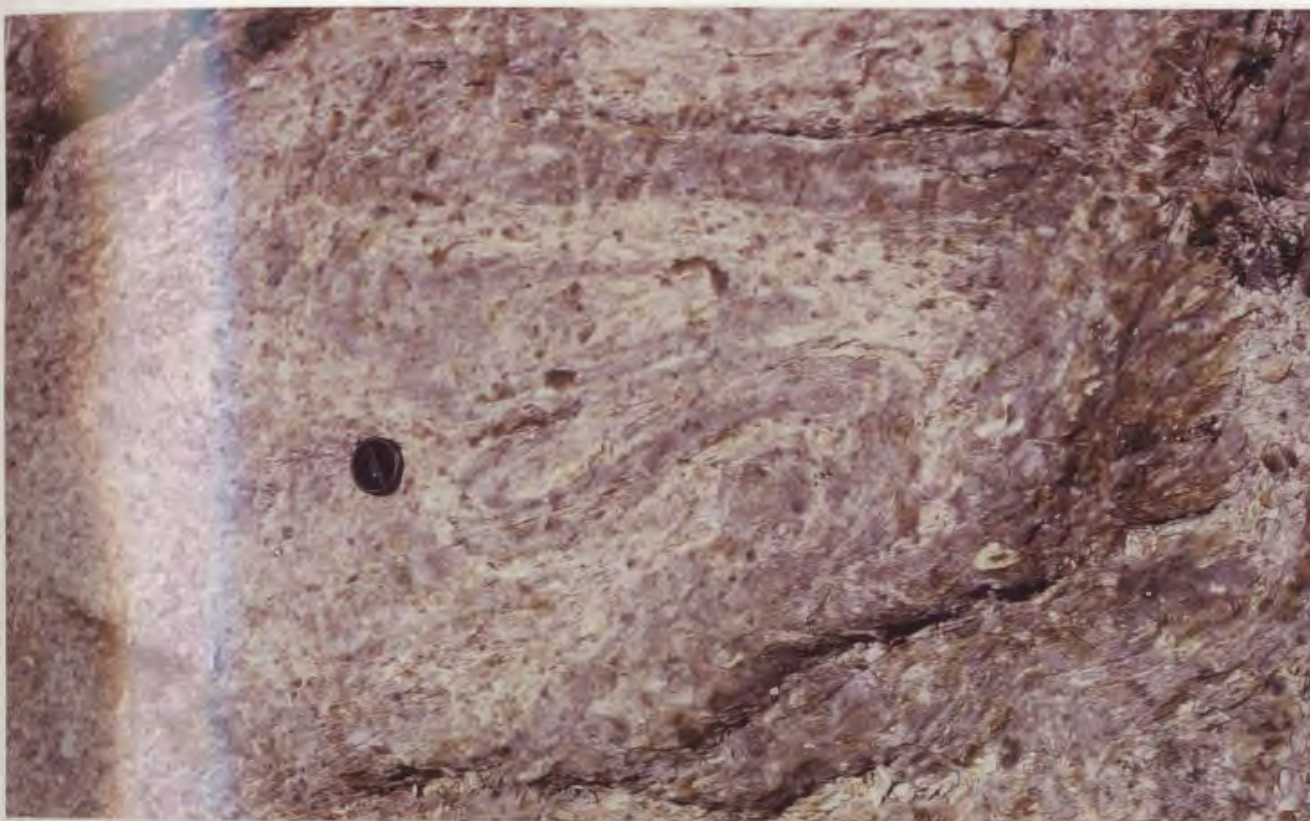
Plate 3-15: Rhyolite of the Little Sandy sequence, Upper
            Buchans Subgroup. Note contorted flow
            banding.

and related lithologies (e.g., DDH BJ-24). MacLean (1943)
considered (with some reservations) these lithologies to
be interbedded with the Buchans Group but they are herein
interpreted as remnants of presumed Carboniferous age
deposited unconformably upon the Buchans Group along the
paleo-eroded fault contact.

The upper contact of the Little Sandy sequence
is marked either by a thrust contact juxtaposing the Hungry
Mountain Complex and the Little Sandy sequence or by
intrusive contact with the alklai-feldspar phase of the
Topsails Granite. In the poorly known northwestern portion
of the study area, the Hungry Mountain Complex may origin-
ally have been absent and lithologies thought to be correl-
ative with the Springdale Group may lie unconformably upon
the Buchans Group (this relationship is present between
the Springdale Group and Roberts Arm Groups in Notre Dame
Bay, c.f. Strong, 1973).

The Little Sandy sequence consists of abundant
fine grained andesitic to rhyolite pyroclastics with less
abundant volcanogenic sediments and basaltic flows and
volcaniclastics.

Intermediate and felsic volcanics are much more
common than mafic varieties. Massive rhyolite flows with
wildly contorted flow banding (Plate 3-15), pumice flows,
pyritic tuff, rhyolitic autobreccias and thick units of

bedded andesitic tuff are the most common lithologies.
Locally there occurs a distinctive dacitic crystal-vitric
tuff indistinguishable from that of the ore horizon sequences
(e.g., DDH 1606).

Strong alteration is characteristic of large
portions of felsic sequences yielding typically rubbly,
white to rusty weathering outcrops. Alteration consists
of varying degrees of silicification, chloritization, seric-
itization, clay mineral alteration and ubiquitous pyritization.
Interbedded breccias locally contain fragments which display
alteration rims similar to those in the ore horizon sequences.
The Little Sandy copper prospect occurs in such a sequence
of altered intermediate to rhyolitic rocks as thin, reticul-
ating, chalcopyrite-bearing chloritic quartz veins and open
space filling between breccia fragments. The deposit,
though epigenetic in detail, is stratiform on a large scale
and considered to be a product of near surface or surface
fumarolic activity.

3.2.3. Diabase and Related Intrusives: All units
in the Buchans area are cut by fine to coarse grained,
dark green to black diabase dykes and sills. These bodies
range in size from small dykelets to large intrusives
locally in excess of 700 m in thickness. They consist of
porphyritic to sub-ophitic labradorite and augite with
traces of opaques, sphene, leucoxene and green amphibole

(hornblende?) normally replaced by chlorite. Quench
textures in pyroxene and plagioclase are common and chlor-
ite locally replaces matrix glass. Grain size varies
sympathetically with diabase thickness and may exceed
1 cm in thicker intrusions. Chlorite-calcite-quartz-
filled amygdules are common, indicating a shallow depth
of emplacement. Locally in thicker sills, amygdule size
and proportion are related to stratigraphic height.
Chilled margins are common and cumulus layering is notice-
able in thicker dykes and sills. Macroscopically visible
contact metamorphism is restricted to the margins of thick-
er intrusions.

The author's previous work (Thurlow, 1973) deter-
mined the presence of two chemically distinct diabase types,
i.e., a relatively more abundant "high titanium diabase"
characterized by brownish to purplish to pinkish (titani-
ferous?) augite and "low titanium diabase" which exhibits
many features in common with the Buchans Group volcanics.
These two diabase types are easily separable on many
geochemical plots, e.g., Fig. 5-4. Petrographic examination
of diabase and gabbro related to the alkali-feldspar phase
of the Topsails Granite indicates that these are mineral-
ogically and texturally indistinguishable from the high
titanium diabase and a temporal and genetic link of these
mildly alkaline intrusives is suggested. In contrast, the
low titanium diabase is geochemically identical to the

Buchans Group volcanics and thus may represent feeders to basaltic rocks of the Buchans Group. Locally, difficulty exists in separating sills from massive flows in drill core.

Diabase occurs commonly as sills associated with gouge zones at important geological contacts. Some of these contacts can nowhere be demonstrated to be conformable despite hundreds of penetrations, raising the possibility of low-angle thrust faulting, a hypothesis that finds support in a number of geological contexts. Consequently, diabase distribution may be controlled to some degree by the presence of earlier-formed thrust faults. Some sills have themselves undergone shearing which, according to this model, must have occurred as rejuvenations along old fault zones, probably during regional flexural folding. Detailed study of the distribution of high and low titanium diabase dykes has not been undertaken but, according to the present model, only high titanium diabase could be present as thrust fault-plane fillings.

Dykes of felsite and granite also cut the Buchans Group, commonly in association with diabase. Mutual cross-cutting relations of felsite and diabase have been observed at several localities. Granitic dykes are macroscopically, microscopically and geochemically identical to the alkali-feldspar phase of the Topsails Granite and are almost certainly apophyses from this body.

3.3.   Structure and Metamorphism of the Buchans Area

 3.3.1.   Structure of the Buchans Area: The structure
of the Buchans area, though relatively simple on a regional
scale, is complex on the detailed scale used in exploration.
The Buchans area has been subjected to two structural
events of regional consequence, i.e., a period of Silurian
thrust faulting and a later period of Devonian (?) folding.

  3.3.1.1.   Silurian Thrust Faulting in the Buchans
  Group: The evidence supporting an
important regional event of Silurian thrust faulting has
been presented in Section 2.7.   This southeastward directed
event caused the present superposition of the Hungry
Mountain Complex upon the Buchans Group.   As far as the
Hungry Mountain Complex is concerned, there seems to be
general acceptance of this hypothesis.   However, the sugges-
tion that similar major faults occur within the Buchans
Group has been the subject of debate.   The author is of
the opinion that such faults do exist though, as for opinions
to the contrary, no proof can be offered.   The possibility
and implications of such faulting are outlined in this
section.

  The relative stratigraphic positions of the Lucky
Strike and Oriental orebodies and their original positions
within the stratigraphy are at the crux of the thrusting
problem.   In the past, various workers have interpreted the

Lucky Strike ore horizon sequence to either overlie the
Oriental ore horizon sequence (e.g., George, 1937), or to
be overlain by the Oriental sequence (e.g., Swanson and
Brown, 1962; Thurlow, Swanson and Strong, 1975) or to be
stratigraphically equivalent to the Oriental sequence
(e.g., Relly, 1960). According to a thrust hypothesis,
the Oriental sequence now structurally overlies the
Lucky Strike sequence but represents a thrusted repetition
of sequences that were originally stratigraphic equivalents.

The thrust hypothesis is based upon two undeniable
facts; 1) that the Oriental ore horizon sequence represents
a remarkable lithologic and stratigraphic repetition of
the Lucky Strike ore horizon sequence, and 2) that no
indisputably conformable contact has been observed between
the blocks of rock containing the Lucky Strike and Oriental
orebodies.

The remarkable stratigraphic repetition of
lithologies formed the basis for the concept of volcanic
cycles at Buchans. This same repetition led Entwistle
and Barnes (1971) to suggest that the Oriental sequence
is a faulted repetition of the Lucky Strike sequence.
Walker and King (1975) provided the first hard evidence
in support of this concept by demonstrating a lack of
stratigraphic conformity between the Ski Hill and Lucky
Strike ore horizon sequences. The possibility of such

faults has demanded the construction of a stratigraphic
column based on indisputably conformable contacts. This
stratigraphy has been outlined in previous sections and
summarized in Fig. 3-1.

The suggestion that Lucky Strike and Oriental
orebodies originally lay at the same stratigraphic horizon
implies that certain rock sequences are also stratigraphic
correlatives. These are outlined in Table 3-2. Without
exception, these implied correlations are extremely
plausible and provide further circumstantial evidence of
thrust faulting.

A second possible stratigraphic reconstruction
is presented in Table 3-3. This model implies not only
that Lucky Strike and Oriental are correlative but also that
the Footwall and Upper Arkose are correlative. Whether or
not this reconstruction is valid, hinges on the interpre-
tation of contact relations in DDH 885. It is beyond the
scope of this thesis to elaborate fully on this point.
This second model has far-reaching implicatins both in
terms of regional and local stratigraphy and in terms of
exploration.

The hypothesis that thrust faulting is an import-
ant element in Buchans geology is supported also by the
following points:

Table 3-2: Buchans Group Thrust Correlatives - Model A

Lucky Strike Fault Block	Oriental Fault Block
	Little Sandy Sequence
~~ fault ~~~	
Lake Seven Basalt ——————	Sandy Lake Basalt and Upper Arkose
Lucky Strike Ore Horizon ————— Sequence	Oriental Horizon Sequence
Intermediate Footwall —————	Ski Hill Sequence and Oriental Intermediate
Footwall Arkose and Wiley's ————— Sequence	Prominent Quartz Sequence
	~~ fault ~~~
Footwall Basalt	

Table 3-3: Buchans Group Thrust Correlatives - Model B

Block A	Block B	Block C
		Little Sandy Sequence
~~ fault ~~~		
Footwall Arkose —————————		Upper Arkose
	~~ fault ~~~	
Footwall Basalt —— Lake Seven Basalt ——		Sandy Lake Basalt
Victoria Lake Volcanics ____ {	Lucky Strike Sequence—Oriental Sequence	
	Intermediate Footwall—Ski Hill and Oriental Intermediate	
	Wiley's Sequence ————— Prominent Quartz Sequence	
	~~ fault ~~~	

1) the anomalously rapid pinching out of some units

    along sheared contacts,

2) the occurrence of minor shears repeating lithologies,

    especially in the Clementine area, and areas north

    of MacLean Orebody, and

3) the occurrence of apparent Footwall rocks overlying

    the West orebody.

     The suggestion that thrust faults are not a

significant factor in Buchans geology can also be force-

fully argued. The bedding plane shears visible at many

important contacts can be interpreted as bedding plane

slip developed during regional folding.

     The fact that demonstrably similar lithologies

represent definite stratigraphic repetitions is a further

argument in favour of cyclic volcanism and the lack of

any need to invoke thrust faulting. The prominent quartz-

bearing Upper Arkose is stratigraphically hundreds of

meters above the Prominent Quartz sequence and represents

a remarkable stratigraphic repetition of similar litholog-

ies. Other such examples can be cited; e.g., dacitic

crystal-vitric tuffs of the Oriental and Little Sandy

sequences.

     3.3.1.2. East-West Fold Axes Related to Thrusting:

In several parts of the Buchans Group there is some

evidence which implies an early period of small scale

folding.   Open warps with east-west trending axes of
several kilometers length have become evident through recent
diamond drilling and stratigraphic re-interpretations.
Because of generally shallow dips, these folds have given
rise to unusual map distributions of some sequences,
especially in the area west of Lucky Strike (Fig. 2-2).

Apart from limited areal extent, there exists
some instances where these folds have only limited vertical
extent and are confined to units overlying a postulated
thrust fault.   It is noteworthy also that the axes of these
small folds are perpendicular to the proposed direction
of Silurian thrusting and that the folds are subsequently
"cross-folded" by broad Devonian folding (see next section).
In light of these facts it is postulated that these small
warps with east-west axes are genetically related to the
episode of Silurian thrusting.

3.3.1.3.   Devonian Folding: All rocks of the
Buchans area, except Carboniferous strata, have been affect-
ed by open Devonian folding.   This event produced a weak,
subvertical, spaced, fracture cleavage in most lithologies,
the strength of which varies according with location.
Many of the more competent lithologies do not bear this
cleavage.

The cleavage generally strikes northeast and

is axial planar to a broad synclinal structure whose axis
can be traced from the Buchans Group, through the Topsails
Granite and into the Springdale Group (see Section 2.3.).
Northwest dipping and facing sequences on the southeast
side of Red Indian Lake appear to constitute a deeper
structural level exposed on the south limb of this same
broad structure.

Flattening related to this deformation is neglig-
ible to not detectable throughout the study area. Fragments
within pyroclastics, breccias and conglomerates throughout
the Buchans Group show no visible effects of strain.
Beyond the study area to the southwest, deformation
increases in intensity within the Footwall Basalt to the
point where noticeably flattened pillows occur.

3.3.2. Metamorphism of the Buchans Area: The
metamorphism of the Buchans Group is a complex topic, a
full discussion of which is beyond the scope of this thesis.
The Buchans Group has evidently been subjected to burial
metamorphism, local dynamothermal metamorphism during
thrusting, a possible subsequent episode of re-equilibration
of burial metamorphic facies and subsequent regional meta-
morphism during open folding. Whereas the details of
these events must await future study, the general metamorphic
environment is discussed below such that the effects of
metamorphic alteration on rock chemistry can be reasonably

evaluated.

Greenschist facies rocks occur only in the lower-
most exposed portions of the Footwall Basalt in the extreme
southwest of the study area. Here, foliated and slightly
flattened pillow lavas contain chlorite, albite, actinolite,
calcite and epidote, mineralogy characteristic of the
greenschist facies. This rapid southwestward increase in
tectonic flattening of pillows and of metamorphic grade
continues in a regular fashion beyond the study area.

Prehnite-pumpellyite facies metamorphism, (Coombs,
1960) is by far the most widespread metamorphic grade
achieved by the Buchans Group. Metamorphic alteration
is heterogeneous on outcrop scale with pyroclastics display-
ing considerably more extensive mineralogical change than
that of associated massive basaltic flows and blocks in
breccias. Within the latter lithblogies calcic plagioclase
phenocrysts are commonly partially altered to combinations
of sericite, calcite, epidote and pumpellyite. Augite
phenocrysts are normally fresher than plagioclase though
incipient alteration to epidote, chlorite and calcite
along fractures is common. Amygdules are filled with
various combinations of quartz, chlorite, calcite, epidote,
prehnite and pumpellyite, all of which may occur in a single
thin section. Mafic pyroclastic rocks contain all of the
above-mentioned metamorphic minerals in greater abundance
than in flows, with the addition of minor authigenic

albite and sphene.   Within felsic pyroclastics, illite,
and mixed-layer illite-montmorillonite, and montmorillonite-
chlorite commonly replace vitric material (Henley and
Thornley, 1980).

Monomineralic metadomains as described by Jolly
and Smith (1972) and Jolly (1974) are poorly developed in
the Buchans Group.   Numerous thin veinlets of probable
synmetamorphic age transect the volcanic rocks in several
areas but these are normally polymineralic (combinations
of quartz, epiodte, calcite, prehnite) and do not show
gradational transitions into albite basalts as do metadomains.
Nevertheless, these fractures probably acted as important
fluid channelways during metamorphism.

Locally, near the top of the stratigraphic
sequence, zeolite-like minerals fill amygdules in massive
basaltic flows.   Other amygdules in the same rock are
filled with epidote, calcite, prehnite and pumpellyite and
plagioclase phenocrysts display partial alteration to
pumpellyite.   The occurrence of zeolite (?) in these
prehnite-pumpellyite facies rocks attests to the sluggish
reaction rates so typical of low grade metamorphic
assemblages and concurs with the observation by Jolly
and Smith (1974) that the stratigraphic range of secondary
void filling minerals is commonly somewhat greater than
the range in which they replace rock forming minerals.

The presence of the zeolite implies that the stratigraphic top of the Buchans Group existed near the boundary between zeolite and prehnite-pumpellyite metamorphic facies. The lack of pervasive low grade metamorphic alteration (such as that described by Smith, 1968) and the lack of equilibrium even on thin section scale (as evidenced by the above-mentioned zeolites) further implies that the duration of metamorphism of the Buchans Group was insufficent to allow reactions to proceed to completion.

Henley and Thornley (1980) have compared the metamorphic mineral assemblages of the Buchans Group to thoroughly studied areas elsewhere, and concluded that metamorphic temperatures were in the $260^{\circ} - 300^{\circ}$ C range.

CHAPTER 4

ORE DEPOSITS OF THE BUCHANS GROUP

4.1. Introduction

The ore deposits of the Buchans Group and their host rocks are described in this chapter. Three genetically related ore types occur at Buchans, i.e., 1) stockwork ore, 2) in situ ore, and 3) mechanically transported ore. All three types of mineralization are known to occur in two distinctly separate horizons, the Lucky Strike ore horizon sequence and the Oriental ore horizon sequence.

In terms of economic importance, in situ and transported ores are of approximately equal significance and together have provided about 98% of production. Large tonnages of subeconomic stockwork mineralization are present but only local zones attain ore grade.

The distribution of the various ores is shown in Fig. 4-1. Tonnages, grades and other features of the Buchans ore zones are summarized in Table 4-1.

4.2. Intermediate Footwall and Stockwork Mineralization

4.2.1. General Comments: The Intermediate Footwall is a thick, localized volcanic sequence which, beyond the area of stockwork mineralization and alteration, consists
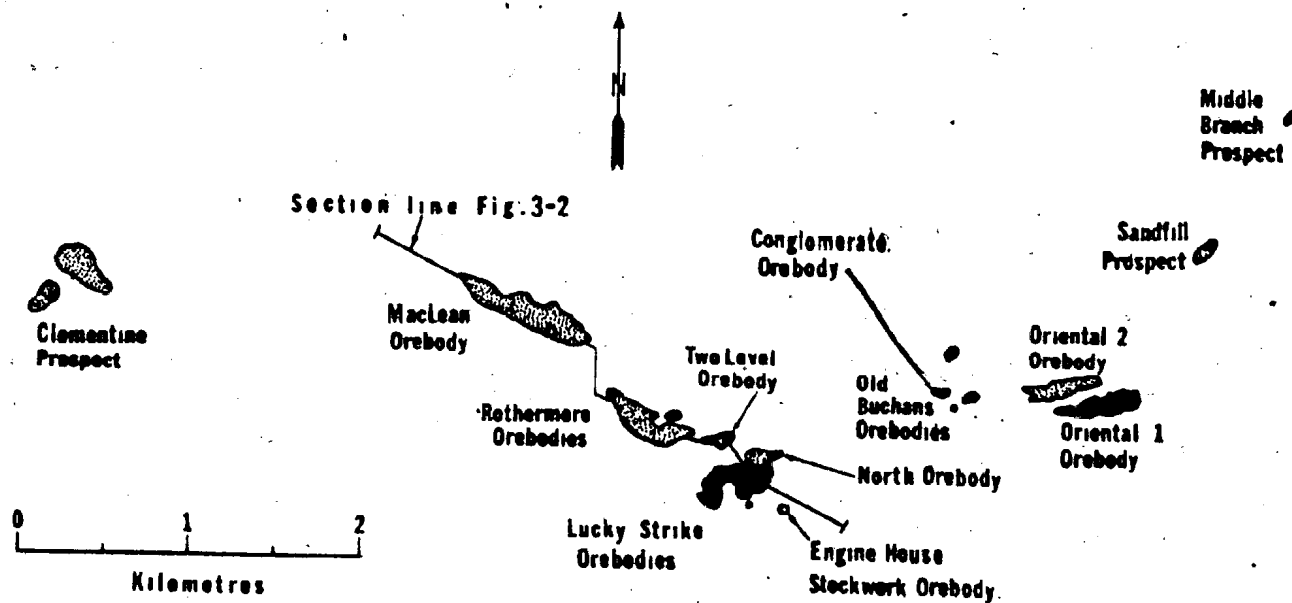
Figure 4-1: Distribution of in situ (solid black) and transported fragmental (stippled) mineralization at Buchans.

Orebody	Gross Tonnage		Au[3]	Ag[3]	Cu	Pb	Zn	[1]Fe	Cp	Ga	Sl	Py	Ba	Sulfide Plus Barite
Lucky Strike Ore Horizon Sequence														
In Situ Ores														
Lucky Strike Main	4,752,373		.050	3.29	1.67	8.42	18.36	9.3(8.0)	4.8	9.7	27.4	14.0	26	81.9
Lucky Strike - New Year	803,112		.041	3.23	1.40	9.75	18.76	5.5(4.7)	4.0	11.3	28.0	7.4	26	76.7
Sub-total In Situ	5,555,485		.049	3.28	1.63	8.61	18.42	(7.5)						
Transported Ores														
Lucky Strike - North	620,510		.049	3.58	0.46	4.54	8.20	1.8(1.5)	1.3	5.2	12.2	2.4	55	76.1
Two Level	328,596		.047	3.64	0.50	4.56	8.02	2.5(2.2)	1.4	5.3	12.0	3.8	55	77.5
	949,106		.048	3.60	0.47	4.55	8.14	(1.7)						
Rothermere #1	3,402,000		.033	3.94	1.15	7.73	12.68	4.3(3.8)	3.3	8.9	18.9	6.0	31	66.1
Rothermere #2	195,615		.034	3.59	1.44	7.65	13.73	6.6(5.7)	4.2	8.8	20.5	9.5	30	73.0
	3,597,615		.033	3.92	1.16	7.72	12.74	(3.9)						
MacLean	3,653,000		.028	3.84	1.13	7.46	13.50	4.3(3.8)	3.3	8.6	20.1	6.0	24	62.0
Sub-Total Transported	8,199,721													
Oriental Ore Horizon Sequence														
In Situ Ores														
Oriental #1	2,738,664		.061	3.93	1.71	8.47	15.80	6.0(5.1)	4.9	9.8	23.6	7.7	24	70.0
Old Buchans East	133,353		.067	4.55	1.65	7.57	14.27	10.0(8.5)	4.8	8.7	21.2	15.1	24	73.8
Old Buchans West	19,907		.045	3.00	1.70	10.40	16.80	6.0(5.1)	4.9	12.0	29.0	7.7	24	73.6
Sub-Total In Situ	2,891,924		.061	3.95	1.70	8.44	15.73	(5.2)						
Transported Ores														
Oriental #2	928,863		.046	6.15	0.76	6.20	9.41	3.2(2.8)	2.2	7.2	14.0	4.6	30	58.0
Old Buchans Conglomerate	72,763		.045	3.70	0.76	5.88	9.47	2.6(2.3)	2.2	6.8	14.1	3.5	31	57.6
Sub-Total Transported	1,001,626		.046	5.97	0.76	6.18	9.47	(2.7)						
Total In Situ	8,447,409	48%	.053	3.51	1.66	8.55	17.50	6.74	4.8	9.8	26.0	14.4	25	86%
Total Transported	9,201,346	52%	.034	4.08	1.04	7.12	12.20	3.51	3.0	8.3	18.2	7.5	30	67%
Total Gross Tonnage	17,648,756	100%	.043	3.81	1.33	7.81	14.74	5.06	3.8	9.0	22.0	8.2	28	73%
Total Milled To December 31/78	17,426,000		.043	3.69	1.34	7.60	14.62							

1. Fe in sulphide assays from drill holes. Assay in brackets based on 15% dilution to conform more closely with mill assays.
2. Percentages of major ore-forming minerals (chalcopyrite, galena, sphalerite, pyrite, barite) as calculated from grades.
3. Au and Ag in oz./ton.

Table 4-1: Ore deposits of the Buchans Area
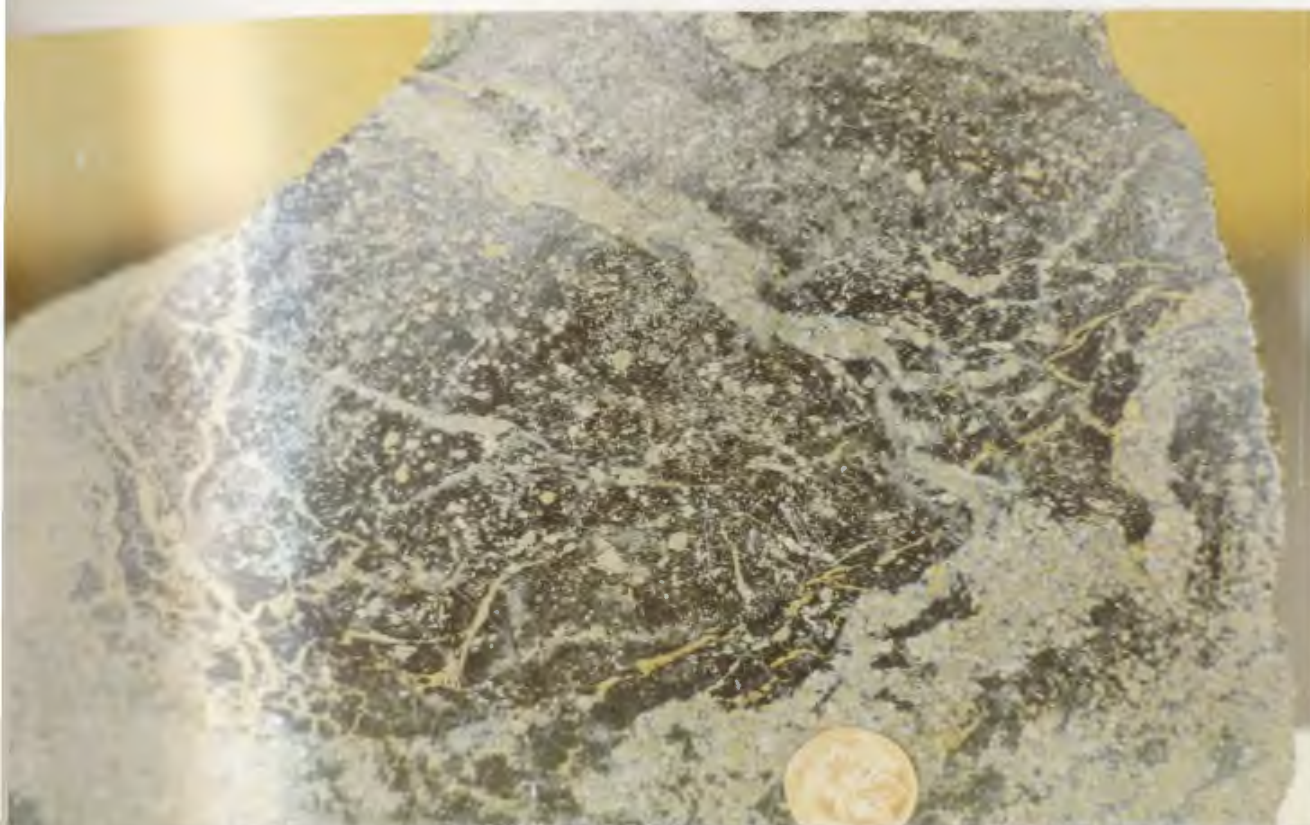
Plate 4-1: Stockwork mineralization, Lucky Strike area.
Top; chalcopyrite-pyrite veinlets cutting sulphide-
impregnated chloritized host. Bottom; silicified
and chloritized stockwork.

mainly of andesitic pyroclastics and breccias. However,
within 1 km of Lucky Strike, the unit gradually changes
character into a complex mound of pyroclastics and breccias
ranging from basaltic to rhyolitic composition. These
rocks have undergone progressive alteration and mineraliza-
tion which increases in intensity towards the Lucky Strike
area and obscures the original character of the host rocks.
The Intermediate Footwall is the host for several zones of
stockwork mineralization and ore and at least two small
syngenetic massive sulphides.

Strong stockwork mineralization consists of a
network of quartz-sulphide veins and veinlets cutting
strongly altered and sulphide-impregnated host rocks
(Plate 4-1). The largest concentration of stockwork miner-
alization in the Buchans area occurs at Lucky Strike. Fine
to coarse grained euhedral pyrite is the most abundant
sulphide within the stockwork with much lesser quantities
of chalcopyrite, sphalerite and galena. Quartz, chlorite,
barite and calcite are the dominant gangue minerals. Compared
to the overlying massive sulphide, stockwork mineralization
is more pyrite-rich and, in terms of metal ratios, contains
proportionally more Cu. Only small zones of stockwork
contain economic quantities of base metal sulphides.

In general, the development of the Intermediate
Footwall in the Lucky Strike area is one of continuous

volcanism with concurrent mineralization and alteration. Within the overall alteration envelope, internal centers of hydrothermal activity migrate both areally and stratigraphically with time, resulting in several partially over-lapping alteration zones. The major period of stockwork mineralization which fed Lucky Strike entirely post-dates this earlier mineralization and alteration history.

The strongly altered and mineralized zone is shaped like a thin flat-topped mushroom with most of the underlying stem cut off by faults. The zone of strongest alteration and mineralization is crudely concordant with stratigraphy and is approximately 600 m wide and up to 100 m thick. The overall alteration zone covers an area of several square kilometers but rarely exceeds 100 m thickness, and is thus more blanket-shaped. This distribution pattern of stockwork mineralization and alteration is unlike many massive sulphide deposits worldwide (c.f. Sangster, 1972).

In plan view, three roughly concentric zones consisting of varying degrees of alteration and sulphide mineralization can be outlined (Fig. 4-2). Peripheral zones of the alteration halo are characterized by a clay mineral-pyrite assemblage, the intensity of which increases inward towards zones of stronger alteration. Henley and Thornley (1980) have identified illite as the most abundant clay
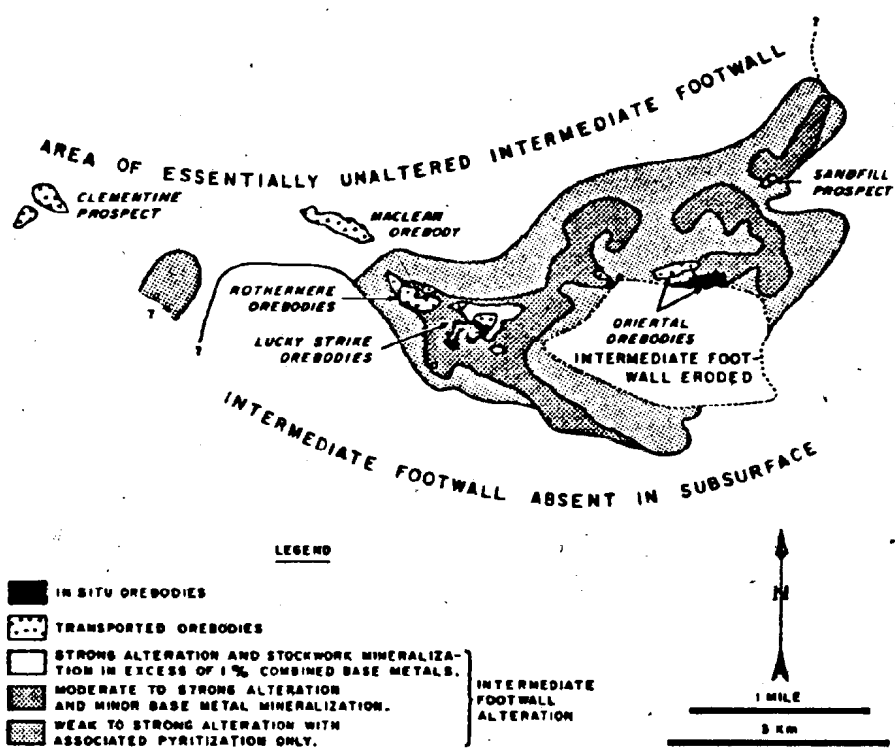
Figure 4-2. Distribution of alteration zones within the Intermediate Footwall.

mineral with lesser montmorillonite and mixed layer clays.
This peripheral alteration zone passes gradually into a
zone of strong clay mineral-pyrite alteration with local sil-
icification, chloritization and minor base metal mineral-
ization (Fig. 4-2). This in turn passes gradually into a
zone of strong silicification and chloritization containing
consistently in excess of 1% base metals. This latter zone
is confined to areas immediately adjacent to in situ mineral-
ization and contains all the significant stockwork occurren-
ces (Fig. 4-2). This generalized alteration pattern is
presently one of the major criteria used in guiding explor-
ation for deeply buried in situ deposits.

Kowalik et al. (1980) have recently completed a
stable isotope study of the stockwork zone. They conclude
that: 1) sea water was the dominant fluid involved in the
alteration and mineralizing process, 2) sea water sulphate
was the source of sulphur in the deposits, 3) temperatures
in the stockwork zone range from 140° C to 370° C, with
temperatures increasing both laterally and vertically towards
Lucky Strike.

4.2.2. Stratigraphy and Mineralization in the
Lucky Strike Area: The early history of the Intermediate
Footwall has largely been obliterated by subsequent explosion
and alteration. The lowermost member of the formation above
the fault base consists of tightly packed, coarse polylithic

(in varieties of intermediate composition) breccias, locally
pumiceous breccias interbedded with minor amygdaloidal flows
and related breccias of probable basaltic to andesitic
composition. Some fragments in these breccias display
altered rims, a feature which is common at higher strati-
graphic levels in the pile and there can be shown to be
caused by alteration along fractures with subsequent
explosion (see Section 4.3.). Thus the earliest consolidated
rocks of the formation were fractured, altered and exploded
to form polylithic breccias. These breccias were subsequent-
ly strongly and pervasively altered. This alteration
varies in intensity, composition and style and consists of
varying degrees of silicification, sericitization, chloriti-
zation, pyritization, clay mineralization and less common
carbonate alteration. Alteration occurs both as veins and
as pervasive alteration away from veins such that the
original breccia texture is locally obscured. Introduction
of vein material has locally caused brecciation of the host
rock. For the most part, sulphide mineralization associated
with this alteration is pyrite, though minor sphalerite,
galena, chalcopyrite and less abundant barite are common.
No massive sulphide mineralization is known to be related
to this episode of alteration and mineralization.

Overlying the earlier mineralized and altered
portion of the Intermediate Footwall Formation is a second
unit which is characterized by the presence of abundant

altered fragments derived from the underlying unit. This
unit is the most extensive unit of the altered
Intermediate Footwall. Polylithic breccias are the most
abundant constituent of this unit and contain numerous
varieties of strongly altered fragments of original basaltic
to rhyolitic composition. Evidence that these breccias
are in part derived from the previously mineralized and
altered breccias includes 1) the presence of strongly
altered fragments with variable degrees and types of
alteration, locally in a much less altered matrix, 2) the
presence of fragments composed of coarse euhedral pyrite
(interpreted as vein pyrite from the underlying unit),
3) the presence of numerous fragments composed entirely of
black chlorite and euhedral pyrite, similar to some
pervasively altered material of the underlying unit, .
4) some altered fragments contain pyrite-sphalerite-galena-
chalcopyrite mineralization.in thin fractures and veins
which are terminated at fragment boundaries.

A number of other fragment types are present in
the breccias including pink rhyolite fragments, locally
with altered rims. The polylithic breccias commonly
contain a visible vitric component in the matrix and
normally contain varying proportions of angular to flattened
long tube pumice. All variations exist between vitric
polylithic breccias (pyroclastic breccias) and breccias
composed almost entirely of tightly packed pumice fragments

and wispy shreds (pumice breccias). Recognizable vitric
ash horizons have locally escaped pervasive alteration
and obliteration of primary texture. The breccias are
normally moderately to well packed and poorly sorted,
with average fragment size usually less than 5 cm. Breccia
beds locally display a crude size grading over a few
meters. The presence of abundant vitric material in the
breccias suggests that the brecciation of the previously
altered unit was accomplished by explosion related to
violent frothy eruption. The products of eruption and
exploded lithic fragments were subsequently redeposited as
homogenized subaqueous density flows.

This second member of the Intermediate Footwall
suffered locally intense alteration and stockwork mineral-
ization which fed two small stratiform massive sulphide
bodies; the Rothermere Footwall Orebody and the West
Orebody. Tonnages and grades of these deposits are given
in Table 4-1. The Rothermere Footwall Orebody is a small,
thick, massive polymetallic lens concordant with bedding
and some 15 m below the upper contact of the formation.
The footwall to the deposit consists of strongly altered
polylithic breccia locally containing vein sulphide clasts.
The alteration varies from strong sericitization, pyritiza-
tion and clay mineralization although the most strongly
altered and veined portions consist of virtually 100%
chlorite and disseminated and vein euhedral pyrite and traces

of base metal sulphide. Elsewhere, intense silicification
is dominant, emanating from milky, pyritic, fine grained
quartz veins and cutting the above-mentioned earlier alter-
ations. Alteration evidently continued after the major
period of sulphide deposition, as hangingwall breccias are
moderately altered and contain minor disseminated sulphide
and local sulphide veins. The deposit itself is lens-
shaped, high grade and polymetallic. Ore mineralogy, in
order of abundance, consists of sphalerite, galena, chalco-
pyrite, pyrite and tetrahedrite. Dark grey to white barite
occurs throughout the deposit but, towards the top,
becomes increasingly common and forms a massive mainly
baritic cap. Apart from the obvious barite zoning, no base
metal zonation is evident within the deposit. A unique
feature of the sulphide portion of the deposit is the
occurrence of numerous rounded chalcopyrite-pyrite
aggregates with diffuse outlines. These may represent
sulphide flocculates which settled into the accumulating
sulphide mud.

The West Orebodies, a group of small sulphide
deposits, occur within the Intermediate Footwall approximately
150 to 250 m southwest of Lucky Strike Orebody. Their strat-
igraphic position with respect to the Rothermere Footwall
Orebody is uncertain. The footwall of the deposits consists
of strongly altered and pyritized breccias and tuffs,
locally of probable original dacitic composition. Minor

pyritic and base metal-rich veins cut this altered unit.
The contact with the ore zone is characterized by a rapid
increase (normally over less than one meter) of disseminated
and vein sulphide until a sulphide mass consisting dominantly
of coarse euhedral pyrite with finer grained chalcopyrite,
galena and sphalerite is attained. This sulphide mineral-
ization is associated with strong calcite alteration of
completely obliterated host rock. Commonly there occur
zones of very fine grained massive high grade Pb-Zn ore
which display considerable textural similarity to syngenetic
ores in the major massive sulphide deposits. These massive
sections are locally cut by coarse grained pyritic stringers.
The deposit is one of the few areas in the Buchans camp
where stockwork ore and related syngenetic massive sulphide
can be seen to merge. The average base metal content of
the entire deposit (Table 4-1) displays characteristics of
both stockwork and syngenetic sulphide. The hangingwall
contact of the deposit is normally sharp and consists of
strongly altered tuffs and breccias probably of original
dacitic composition. Pyritic veins, similar to that in the
stockwork portion of the deposit, locally cut hangingwall
rocks.

The Engine House Orebody, the largest deposit of
stockwork ore, occurs approximately 200 m southeast of
Lucky Strike. Tonnage and grade figures are given in
Table 4-1. The deposit occurs entirely within the Intermediate

Plate 4-2: Green mariposite-like sericite after plagio-
clase; a typical feature of proximal areas of
the clay mineral alteration envelope.

Footwall and no connection is known between this strong
stockwork mineralization and Lucky Strike Orebody. Both
the footwall and hangingwall contacts of the deposit are
marked by a rapid gradation from normally altered and
mineralized Intermediate Footwall tuffs and breccias into
pervasively altered and mineralized ore. The deposit
consists dominantly of coarse euhedral vein and disseminated
pyrite with local enriched zones of sphalerite, galena,
chalcopyrite and tetrahedrite in a pervasively silicified
and/or chloritized host (Plate 4-1). On the whole, silicic
alteration is dominant, although local zones of 100%
chlorite-pyrite with minor base metal are present. Barite
is of minor importance and is generally more closely
associated with silicic than chloritic alteration. Calcite
is minor but ubiquitous throughout the deposit.

   The character of the immediate host rock for the
Engine House deposit has been largely obliterated by pervasive
alteration and mineralization. However, local occurrences
of somewhat less obscured host are known. Most commonly,
these occur as fragments of greyish aphanitic altered flow
(?) of compositions originally ranging from basalt to
rhyolite. Relict plagioclase in these flows is commonly
altered to waxy green illite or locally to a bright green
mariposite-like mineral (Plate 4-2). Samples of the latter
material submitted for X-ray diffraction are apparently
sericite and show no chromium enrichment (R. Henley, pers.

comm., 1976). Larger fragments of flow are locally
brecciated by intrusion of quartz-sulphide veins producing
breccia aggregates consisting of fragments with altered rims.

The second unit of the Intermediate Footwall and
the related small massive sulphide orebodies are conformably
overlain by another sequence of altered polylithic breccias
and pumiceous tuffs. These are interbedded with fine grained,
pyritic, light grey, tuffaceous, siliceous siltstone and
wacke, in part derived from reworking of previously deposited
breccias. Detrital sulphides (especially pyrite) are
characteristic of the unit. The unit displays a gradual
facies change from dominantly breccia with minor inter-
calated sandy tuff and tuffaceous siltstone in the Lucky
Strike area, to dominantly tuffaceous pyritic siltstone
in the area 500 m east of Lucky Strike (e.g., DDH 2520).
The breccias of this unit are similar to underlying breccias
and will not be discussed further. The interbedded and
facies-equivalent tuffaceous siltstone and siliceous wacke
are generally light grey and normally massive with bedding
faint to absent. These tuffs are locally vitric and may
grade into subaqueous pumice flows similar to those
described by Yamada (1973). Graded beds ranging from fine
grained breccia to pyritic siltstone occur locally, as does
small scale cross bedding. The unit locally contains a few
isolated pebbles of strongly altered material derived from
the underlying breccias, small (2 mm) pyritic pebbles and

reddish rhyolite pebbles. Minor silica-pyrite-carbonate veining is common and the entire unit has been slightly, but pervasively silicified.

4.3. Lucky Strike Ore Horizon Sequence

4.3.1. Footwall Rocks: Rhyolite with flanking and overlying pyritic siltstone and dacitic tuff form the base of the Lucky Strike ore horizon sequence (see Chapter Three) and overlie the earlier altered and mineralized Intermediate Footwall. The stockwork which fed Lucky Strike Orebody post-dates the earlier alteration in the Intermediate Footwall and the basal rocks of the ore horizon sequence. Alteration related to this mineralization consists of strong silicification and chloritization, similar to the previous alteration assemblages. Pyritic and baritic base metal-bearing veins cut the altered and sulphide impregnated host rocks. Henley and Thornley (1980) have identified the black chlorite of the stockwork as clinochlore-penninite, a variety more magnesian than ambient Buchans Group chlorites.

Lucky Strike Orebody overlies the stockwork though the critical contact zone is poorly known due to shearing and removal of this material from the Lucky Strike glory hole.

4.3.2. Lucky Strike Orebodies: The Lucky Strike
Orebodies consist of a number of contiguous ore zones
which together form the largest single body of massive
sulphide within the Buchans area. They were discovered
in suboutcrop in 1926 as a result of equi-potential pros-
pecting by Hans Lundberg. From 1928, when mining began,
until 1957 the mine produced 6,175,995 tons of ore with an
average grade of 26% BaSO$_4$, 17.40% Zn, 8.20% Pb, 1.51% Cu,
3.31 oz/ton Ag and 0.049 oz/ton Au. The average mineral
percentages by weight, as derived from the grade, are
given in Table 4-1. It consists both of in situ massive
sulphide and mechanically transported sulphides intimately
associated with stockwork mineralization in the underlying
Intermediate Footwall. Information regarding the ore
itself and contact relations with surrounding rocks is
scarce due to the early practice of assaying of entire
drill cores. Nevertheless, valuable information can be
gained from the Lucky Strike open pit and from excellent
early descriptions of the ore (e.g., George, 1937).

The ore overlies either altered dacitic crystal-
vitric tuff or strongly altered and mineralized stockwork
of the Intermediate Footwall. Contacts are generally
not cored due both to shearing and to generally poor core
recovery of most early drilling. Locally, conformable
contacts of ore on dacitic tuff or of ore on Intermediate
Footwall are visible. The deposit is conformably overlain

by dacitic crystal-vitric tuff or by diabase sills.
(possibly filling fault planes).

In cross section, the deposit has a thick lens
shape (Fig. 3-2), a characteristic peculiar to Lucky Strike
and in keeping with its largely in situ origin. It consists
of a zoned aggregate of sphalerite and barite with lesser
galena, chalcopyrite and pyrite with minor tetrahedrite and
bornite. Secondary smithsonite, native silver, and Zn, Cu,
Pb and Fe sulphates occurred locally. George (1937) noted
the presence of mineralogical zoning within the deposit and
the following description is derived partly from his work.
The Main Orebody consisted of approximately 90% Pb-Zn ore
(black ore) and 10% Cu-Zn ore (yellow ore) with the latter
confined mainly to the base of the deposit. In general,
Cu-Zn ore contained more pyrite, chalcopyrite and sphalerite
and less barite and galena than Pb-Zn ore. Gold and silver
were concentrated towards the hangingwall (i.e., in the Pb-Zn
ore). Although no ferruginous chert bed is known in the
hangingwall of the deposit, it is locally overlain by red
(hematitized) barite containing minor pyrite and commonly
also by hematitized dacitic crystal-vitric tuffs. This
zoning bears a remarkable similarity to that of many of the
Kuroko deposits.

Ore textures, as preserved in a few drill cores
and in exposures in the Lucky Strike Pit, indicate that the

Plate 4-3: Typical in situ wispy and streaky very high grade
ore. Yellow areas are chalcopyrite, light grey
are fine grained galena-sphalerite and dark grey
to black is barite.

bulk of the deposit consisted of fine grained massive struc-
tureless ore and of "streaky ore" (Plate 4-3). These latter
ores consist of thin, discontinuous wispy yellow streaks
of chalcopyrite-pyrite-rich ore within more abundant
black galena-sphalerite-rich ores. Elliston (1963) has
described and illustrated similar textures within mudstones.
He calls the process responsible for this texture "fluidal
wisping" and gives evidence to suggest that it forms as a
result of lateral flow in unconsolidated watery plastic muds.
In view of evidence presented in subsequent paragraphs, a
similar origin for streaky ore at Buchans is plausible.

Well developed compositional banding was not common
at Lucky Strike but, according to Relly (1960), it existed
locally. Portions of Lucky Strike Orebody consist dominantly
of discrete sulphide and sulphate fragments associated
with the breccia-conglomerate and "granite conglomerate".
The occurrence of these ores is discussed in detail in the
following sections.

4.3.3. Ore Horizon Breccias: The ore horizon of
many worldwide massive volcanogenic sulphide deposits is
commonly marked by a weakly mineralized cherty tuffaceous
exhalite horizon (e.g., Sangster, 1972; Ridler, 1973;
Sangster and Scott, 1976). In contrast the Lucky Strike
and Oriental ore horizons are characterized by a complex
series of beds composed of coarse polylithic rudaceous rocks

with associated volcanic arenites and wackes. Within the
rudaceous fraction all gradations exist from volcanic
breccia to volcanic conglomerate with breccia-conglomerate
being most abundant (terminology after Fisher, 1960).
Because of the lithologic similarity of these rocks in the
Lucky Strike and Oriental ore horizon sequences, they are
described together in this section.

The horizons occupy an area in excess of 3 sq. km
in the mine area and are intimately associated with the
transported massive sulphide orebodies. Thickness varies
sympathetically with underlying paleotopography from zero
on paleotopographic highs to over 100 m in paleotopographic
lows. Within the unit there is a common gradation from
underlying volcanic breccia and breccia-conglomerate to
overlying granitoid-bearing volcanic breccia-conglomerate
(hereinafter referred to as "granite conglomerate"). This
sequence is best displayed in the Oriental area, particularly
in the vicinity of Oriental No. 2 Orebody.

The breccia-conglomerate beds overlie either
pyritic siltstone or dacitic crystal-vitric tuff. They
consist of a polylithic assemblage of rounded to angular
fragments ranging from silt size to fragments over two
meters in diameter. Scores of locally derived fragment
types can be identified and can be grouped into eight
basic lithologic categories, i.e.,

1) various altered lithologies of the Intermediate Footwall including stockwork and vein sulphide fragments,

2) pyritic siltstone and wacke fragments,

3) varieties of massive rhyolite fragments,

4) varieties of ore horizon dacitic tuff as fragments,

5) fragments of basalt, andesite, jasper chert, etc., possibly derived from the Footwall Basalt,

6) rare fragments of volcanic arenites and wackes derived from the breccia-conglomerate itself

7) varieties of rounded granitoid pebbles, cobbles, and boulders, and

8) fragments of barite and massive sulphide ore (black ore and yellow ore).

The proportion of these various fragment types varies dramatically within individual beds and between separate beds such that the breccia-conglomerate is locally composed almost entirely of one lithologic type. The transported orebodies (e.g., MacLean) are an example of breccias composed mainly of massive sulphide fragments and are one of several facies within the unit. However, more commonly the breccia-conglomerate is an intimate mixture of numerous fragment types with those of types one to four (above) being most common. It is anomalous, and perhaps significant, that fragments of all lithologies underlying the breccia-conglomerate occur within the unit except fragments that can be confidently related to the Footwall

Plate 4-4:   Typical polylithic granitoid-bearing breccia
conglomerate. Both photos from hangingwall
of Old Buchans Conglomerate Orebody.

Plate 4-5:   Granodiorite cobble in ore breccia; MacLean

            Extension deposit, 20-4 drift.   Cobble is textur-

            ally identical to the Feeder Granodiorite.

Arkose.

The "granite conglomerate" (Plate 4-4) conformably
and gradationally overlies the breccia-conglomerate and is
especially well developed in the Oriental area. The "contact"
between the two is normally characterized by a gradual
stratigraphic increase in plutonic boulders until a breccia-
conglomerate composed of approximately 20% (average)
granitoid boulders is achieved. In contrast to other litho-
logies, granitoid boulders are <u>invariably</u> well rounded with
moderate to high sphericity. Numerous granitoid types
exist, ranging in composition from (rare) diorite to quartz
monzonite but pink to grey varieties of granodioritic com-
position normally predominate. Granodiorite boulders range
in size from up to a maximum of 5.8 m (Swanson and Brown,
1962) but those of 25 cm and less are most common. Granitoid
boulders are commonly the largest fragment type within the
"granite conglomerate". Many granitoid boulders are textur-
ally identical to the Feeder Granodiorite (Plate 4-5).

Textures and structures of the "granite conglomerate"
and breccia-conglomerate are similar and will be discussed
together below. The basal contact of the breccia-conglomerate
with the underlying siltstone or dacite is normally sharp
but locally characterized by scouring or channeling of
underlying lithologies. Initial deposits of the unit vary
locally from fine grained volcanic arenites to coarse

breccia-conglomerate. The breccia-conglomerate is normally
polylithic, coarse grained (average 2-20 cm) and very poorly
sorted. Only locally can a bimodal size distribution be
recognized. Most fragments are angular to subrounded and
any given fragment type can vary from angular to rounded.
Fragments of Intermediate Footwall, pyritic siltstone and
dacite are rarely rounded whereas rhyolite fragments (though
normally subangular) are more commonly rounded than the
previous lithologies. Only granitoid boulders are every-
where rounded. Sphericity of all fragment types (except
granodiorite) is low. Packing varies dramatically but the
coarser units are normally matrix-supported, to somewhat
fragment-supported. Where elongate tabular fragments are
present a chaotic clast fabric is locally visible, though
more normally clasts are elongate subparallel to the base
of the unit, thus defining a crude bedding. In rare under-
ground bedding plane exposures in MacLean, the long axes of
pebbles parallel the long axis of the orebody. A weak
imbrication of larger elongate fragments is locally visible
and defines current directions from the vicinity of the
Buchans Inlier. Although sorting is normally poor, some
thick beds display a gradual vertical grading over several
meters. Elsewhere, chaotic unsorted breccia beds several
meters thick grade rapidly over the uppermost meter from
coarse breccia to fine grained arenite or wacke. In some
instances some beds are graded inversely at the base and
normally graded at the top (e.g., DDH 1440).

The matrix of the breccia-conglomerate consists of
a heterogeneous arenaceous mixture of quartz, plagioclase and
small lithic fragments similar in composition to the larger
breccia fragments. Fine grained detrital pyrite is common
and small massive sulphide fragments occur locally.
Pumice shreds are a rare local occurrence. Thin beds
(1 m and less) of arenaceous material are locally inter-
bedded with breccia-conglomerate and may be massive, or
display a crude stratification or be graded. Cross
stratification has not been observed.

Further comments on the ore horizon breccias
accompany and follow description of the transported ores.

4.3.4. MacLean, Rothermere Two Level Orebodies and
Lucky Strike North; transported ores: The MacLean,
Rothermere, and Two Level Orebodies occur in a linear
arrangement extending northwest from Lucky Strike (Fig. 4-1).
Two Level Orebody was discovered shortly after the discovery
of Lucky Strike, Rothermere in 1947 and MacLean (formerly
Rothermere No. 4) in 1950. MacLean and Rothermere have
provided the bulk of production during recent years. Tonnage
and grade figures are given in Table 4-1. Because of the
gross similarity of the occurrence of these deposits, they
are discussed together in this section.

The orebodies occur within dacitic crystal-vitric
tuffs of the Lucky Strike ore horizon sequence at a

stratigraphic horizon very near to that of the Lucky Strike
deposit (Fig. 3-2). They occur within paleotopographic
depressions within a sinuous paleo-channel and are intimate-
ly associated with pyritic siltstone, breccia-conglomerate
and "granite conglomerate". The ores comprise several
breccia beds composed dominantly of sulphide fragments.
MacLean Orebody consists of at least four major, distinct
breccia beds and Rothermere, of at least three. Lucky
Strike North, Two Level, Rothermere No. 2 and a bed along
the northern edge of MacLean are characterized by an
abundance of granitoid boulders and barite and are probably
genetically linked. This linear arrangement of ores lies
slightly northward and parallel to the later major Rother-
mere-MacLean ores. Ore mineralogy consists of a high
grade assemblage of low-Fe sphalerite, galena and barite
with lesser chalcopyrite, pyrite and minor tetrahedrite
and bornite (Strong, 1980). Numerous lines of evidence
presented in the following paragraphs indicate that these
orebodies consist of mechanically transported sulphide
fragments deposited from rapidly moving subaqueous density
flows derived from the Lucky Strike Orebody.

The orebodies are a series of elongate tabular
deposits conformable within the enclosing host rocks. This
conformability is evident both in cross section (Fig. 3-2)
and on a detailed scale underground where primary features
in the ores may be seen to parallel ore-host contacts and

Plate 4-6:   Typical low grade transported ore breccia.   Two
             high grade black ore fragments in centre.   Note
             also siltstone fragment with altered rim and
             "mariposite"-bearing fragment at bottom right.
             Large fragments at upper left and right are
             varieties of rhyolite.

bedding in the host rocks. The author has seen no examples
where ore transgresses the host rocks, an observation also
recorded by Relly (1960, p. 95). The ore rests directly
on either dacitic crystal-vitric tuff, pyritic siltstone
or "barren" breccia-conglomerate. The footwall contact is
normally knife sharp where ore lies on dacite or siltstone
and may be sharp or gradational where ore lies on breccia-
conglomerate. Any given orebody may rest on all these
lithologies throughout its length. The hangingwall contacts
of ore against dacitic crystal-vitric tuff or late diabase
sills are sharp whereas contacts with overlying breccia-
conglomerate or "granite conglomerate" may be sharp or
gradational. Where gradational contacts of ore against
breccia, in the footwall or hangingwall are observed
the "contact" is marked by an increase in discrete high
grade sulphide or barite fragments towards the orebody.
These fragments texturally occupy a position in the breccias
identical to other lithic fragments (Plate 4-6) and are
considered to have been deposited at the same time and by
the same mode as the lithic fragments. Locally where ore
rests on siltstone or dacitic tuff, scour channels within
the underlying rocks are visible. In some places at the
hangingwall contact, very fine grained clastic ores are
load-casted into hangingwall dacitic crystal-vitric tuff.
Late diabase dykes locally cut the ore, display chilled
margins and have caused varying degrees of contact meta-
morphism in the ore.
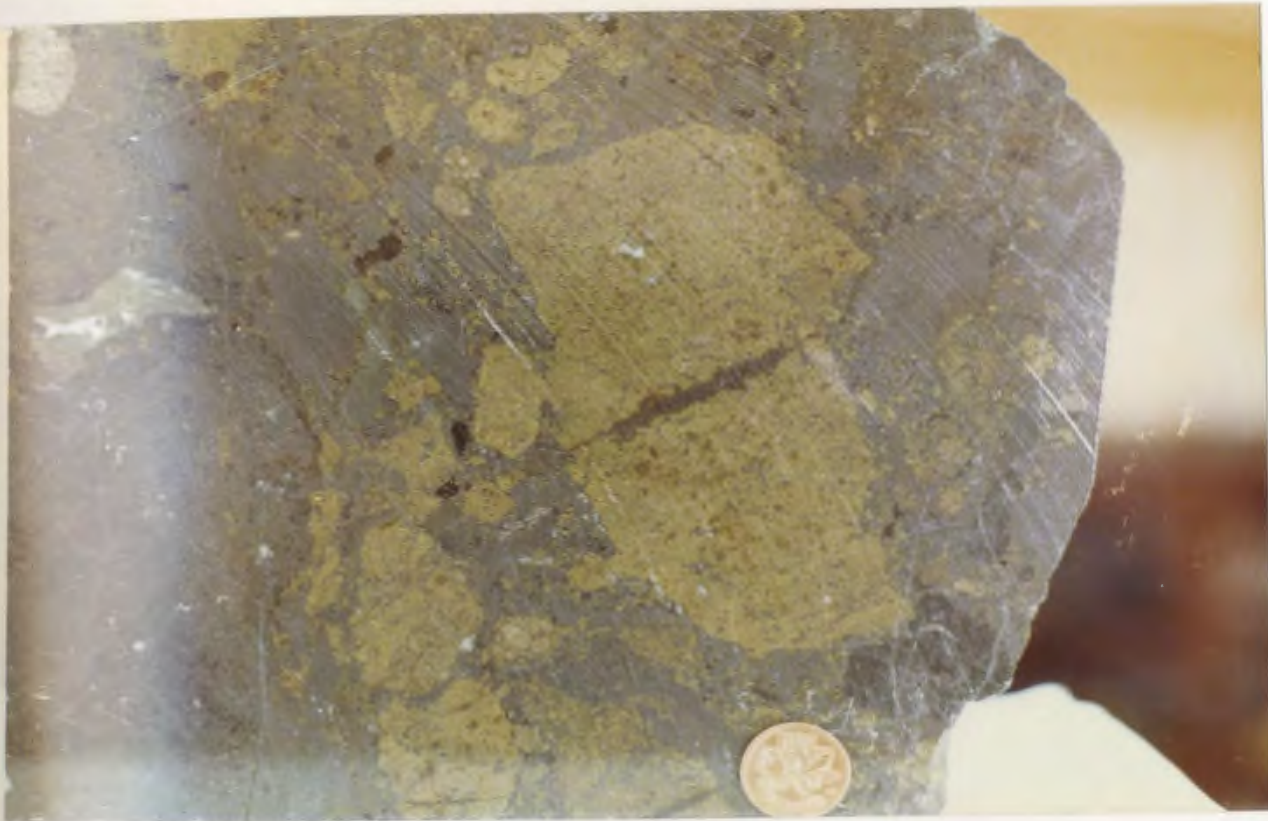
Plate 4-7: High grade transported ore. Yellow ore fragments and darker, smaller, less distinct black ore clasts. Darker clast above coin is barite.

Plate 4-8: Plastically deformed ore fragments. Light grey
irregularly shaped galena clast at right center
adjacent to darker galena-sphalerite clast
(center) with wispy, frayed edge.

The ore itself is a series of breccia beds com-
posed of varying proportions of sulphide and lithic
fragments (Plate 4-7). All fragment types which occur in
the breccia-conglomerate and "Granite conglomerate" occur
in the orebodies and vice versa. In effect then, the
orebodies are members of the "granite conglomerate" -
breccia-conglomerate horizon. The sulphides occur as dis-
crete fragments from (probably) submicroscopic grains to
boulders in excess of 2 m in diameter. Fragments less than
10 cm in diameter are most common. Many sulphide fragments
display a distinct streaky aspect and rarely may be termed
banded. Streaky banding within fragments is invariably
truncated sharply at fragment margins and is commonly
oriented randomly with respect to streaks in adjacent frag-
ments, bedding in enclosing matrix and ore-host rock contacts.
Some sulphide fragments vary from angular to rounded to
tabular and were evidently coherent and competent fragments
at the time of deposition. Tabular fragments are commonly
aligned parallel to the margins of the orebody though
locally a weak imbrication is visible (indicating transport
directions from the southeast). Other sulphide fragments
are elongate with wavy but sharp contacts with matrix along
their long axes, but with wispy, frayed terminations along
their short ends. These fragments are commonly moulded
plastically around adjacent more competent sulphide and
lithic fragments (Plate 4-8). Streaky banding in these
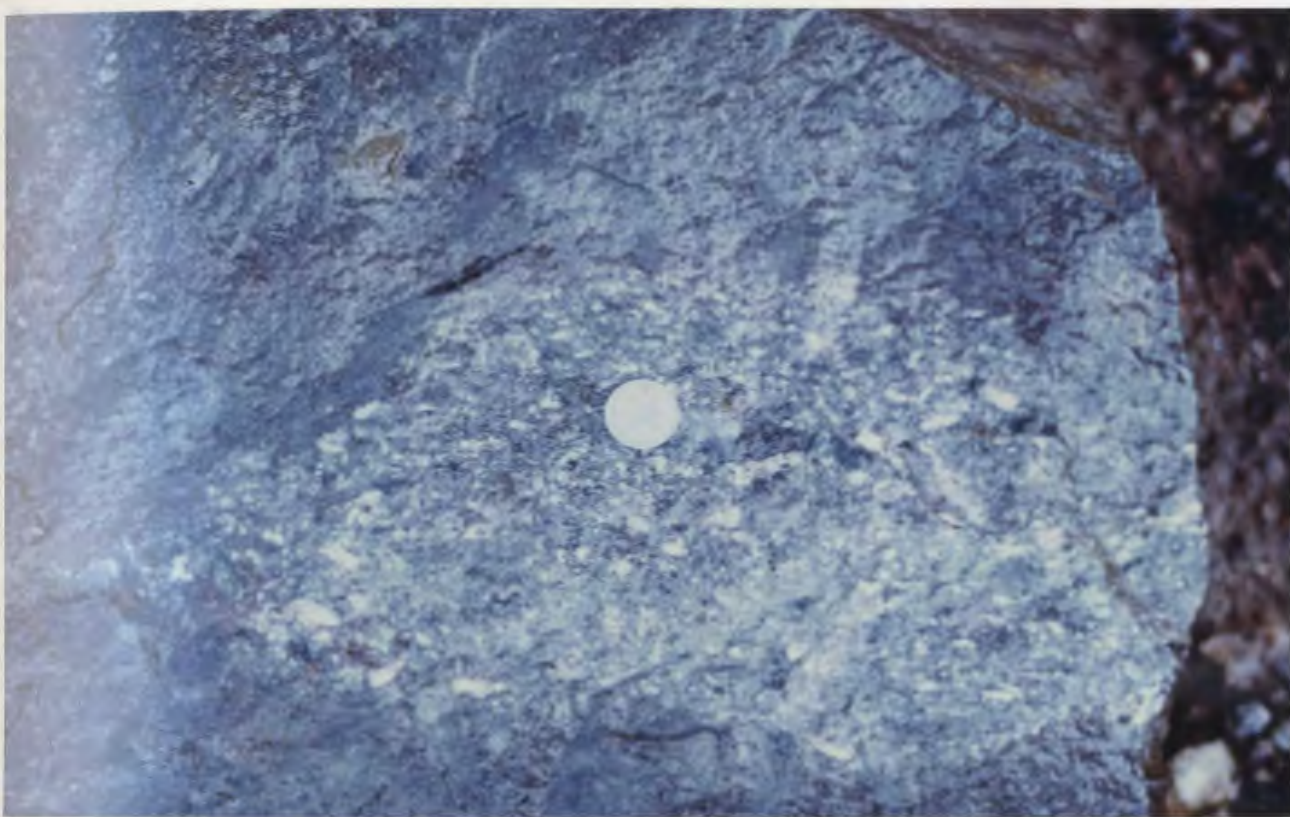
Plate 4-9: Coin rests on fragment of baritic fragmental ore
within fragmental black ore matrix.

fragments normally parallels the long axis of the fragment
and mimics any contortions of the fragment margin. These
are interpreted as sulphide fragments deposited while still
in an only partially indurated, plastic condition. The
presence of ores composed of sulphide fragments indicates
that induration of sulphides of the source orebody was
rapid, a conclusion also reached by Spence (1975). They
further indicate that the streaky sulphide banding was
produced at, or shortly after, deposition and not by a
later stage process.

Fragments composed largely or wholly of barite
occur throughout the orebodies. In general, these fragments
are better rounded and more spherical than the sulphide
fragments and, in the case of MacLean and Rothermere, are
concentrated towards the top of the orebodies where they
form a discrete transported baritic cap. Spectacular
fragmental baritic ore is also exposed in the Lucky Strike
glory hole and consists of massive to crudely graded beds
composed both of fine grained baritic and massive sulphide
fragments and less common large (up to 5 cm) broken barite
crystals. These clastic crystals indicate that at least
portions of the barite were coarsely crystalline at deposition.

Another feature indicative of rapid lithification
is the very rare occurrence of fragments composed of
fragmental ore (Plate 4-9). This texture has been observed

only in the Lucky Strike glory hole, a testimony to the
probable depositional friability of these boulders.

Lithic fragments in the ore are of identical
nature and occurrence to those in the associated "granite
conglomerate" and breccia-conglomerate, the only difference
being that their proportion has been significantly diluted
by the greater abundance of sulphide fragments. All lithic
fragments (except granodiorite) can be confidently related
to nearby rocks in the footwall. Lithic fragments display
the same textures and structures in the ore as in the.
associated breccia-conglomerate and "granite conglomerate".
Locally, lithic fragments in the ore display a crude vertical,
size grading but due to the difficulty in distinguishing
ore fragments from matrix while underground, only rare
samples of grading of sulphide fragments have been observed.

The matrix of the fragmental ores appears to
consist both of more finely divided clastic particles and
possibly of some sulphide chemical precipitate. Sulphide
and lithic fragments form part of a completely gradational
size sequence from less than 1 mm to the largest boulders.
Some of this finer grained material is probably derived
from attrition and comminution of larger fragments by
collisions during density flow. Several polished slabs
of fine grained ore exhibit a sand-sized clastic texture
which is highlighted by fine grained lithic fragments
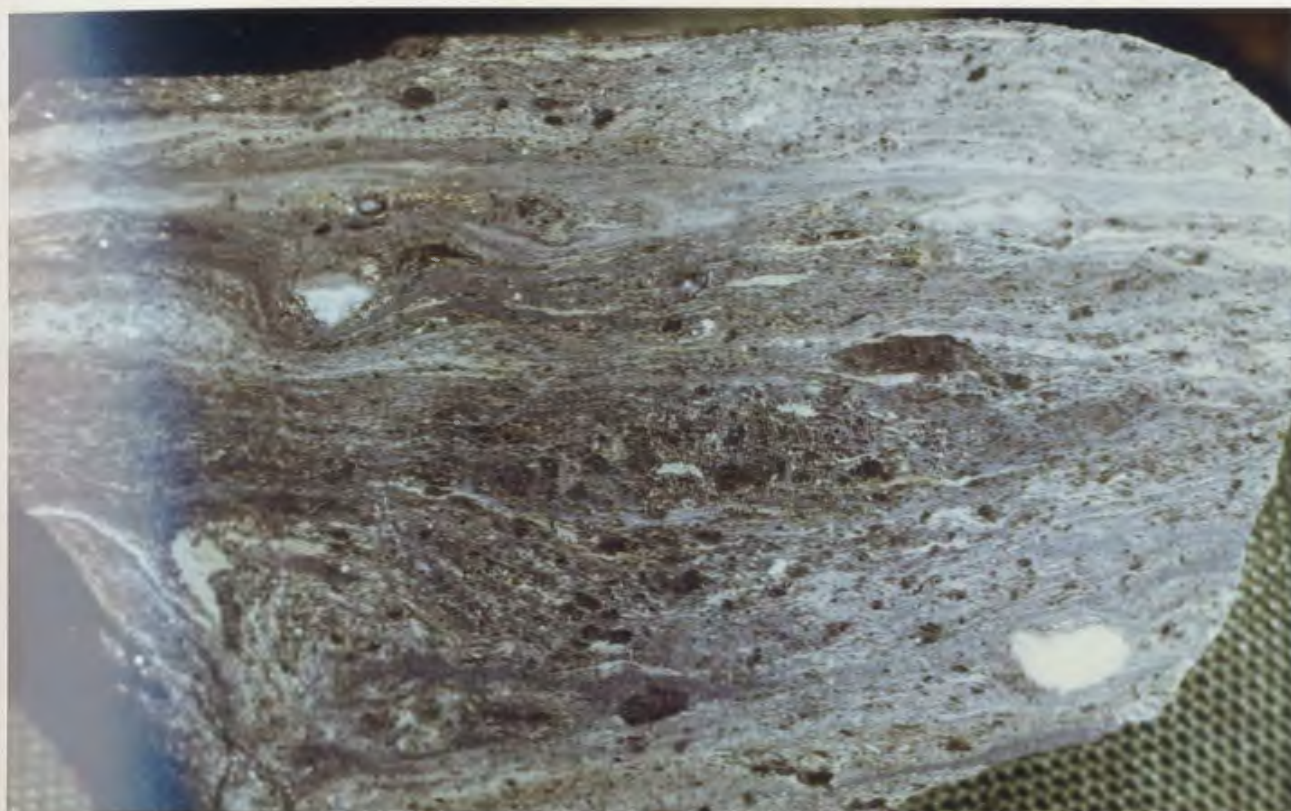
Plate 4-10: Fine grained bedded high grade clastic ore

containing some larger silicate and sulphide

clasts.
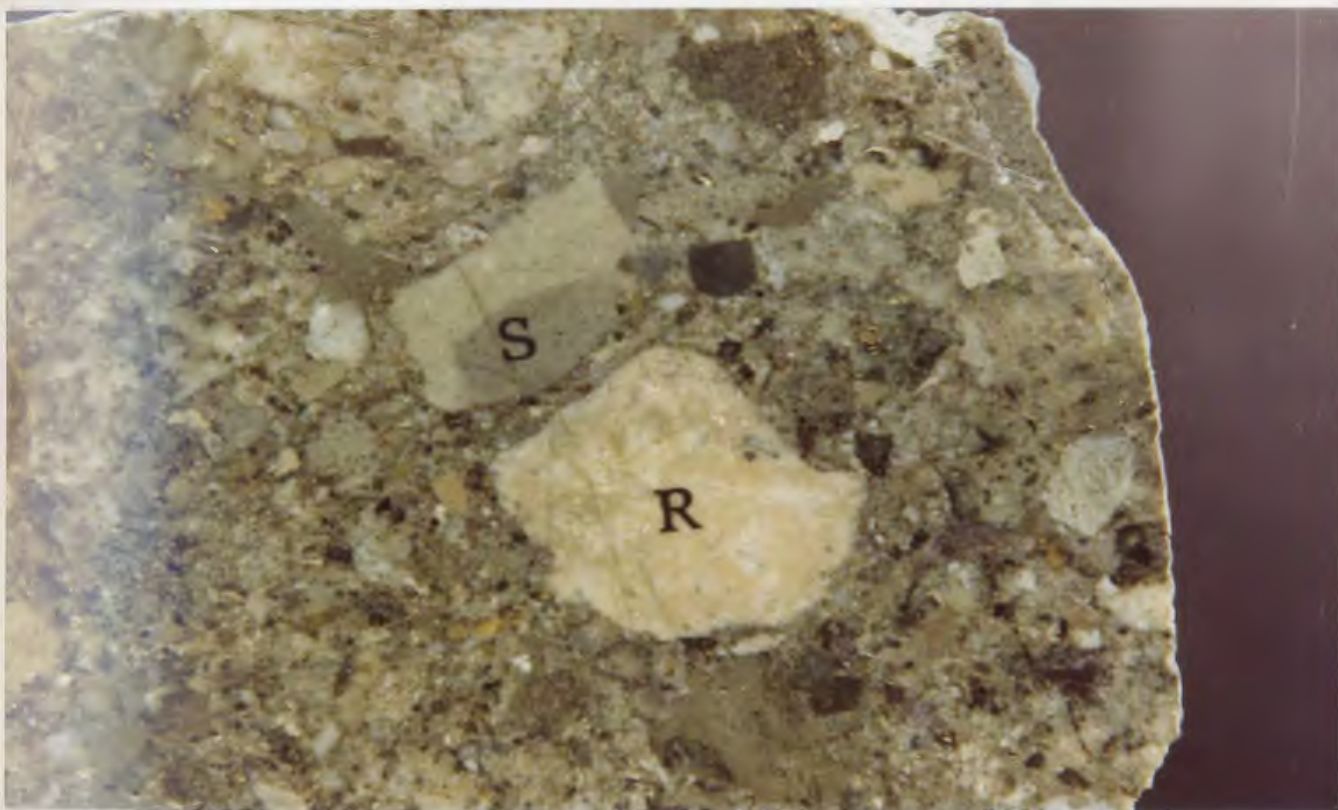
Plate 4-11: Siltstone fragments (S) with altered rims. Larger rhyolite (R) and altered Intermediate Footwall (I) fragments in top photo. Alteration rim on siltstone clast in bottom photo is broken.

(Plate 4-10). However, many samples of lithic-free, fine grained, high grade, streaky black ore show no evidence of clastic textures. All ore sulphides have been slightly annealed during low grade metamorphism and thus, destruction of silt sized (and finer) clastic textures during metamorphism has probably occurred.

If some chemically precipitated matrix sulphide exists it may have been deposited from heavy brines which collected in the depressions which host the ores (c.f. Sato, 1972).

One important feature common to lithic fragments in the ore, breccia-conglomerate and "granite conglomerate" is the presence of alteration rims on some fragments (Plate 4-11). This feature is most commonly developed in pyritic siltstone fragments, with less common development of rims on fragments of rhyolite and Intermediate Footwall and rare rims on dacitic tuff. Very rare rims have been observed on granitoid and sulphide fragments. Siltstone fragments with altered rims are of three types, i.e.,

1) fragments with altered rims and fresh cores

2) fragments with concentric alteration zones (rare), and

3) broken fragments with only partial alteration rims.

In addition to these types there occur siltstone fragments which have been homogeneously altered from rim to core and fragments which have undergone no alteration. In fragments of

Plate 4-12: Pyritic siltstone cut by fractures with adjacent alteration. See text and Fig. 4-3 for schematic and explanation.

Intermediate Footwall with altered rims, the alteration
rim is superimposed on previously pervasively altered
lithologies, indicating formation of the rim after a period
of significant alteration. The similarity of the occurrence
of these types of alteration rims to those in the Shitabanhi
Orebodies in Japan (Lee et al., p. 61, 1974) is remarkable.

The origin of these fragments has important
implications regarding the mode of fragmentation of lithic,
sulphide and sulphate fragments in the ore horizon. In
several drill cores (e.g., DDH 1910) and underground the
author has seen massive, competent, non-brecciated, bedded
pyritic siltstone which is transected by hairline fractures
in a reticulate pattern (Fig. 4-3, Plate 4-12). Extending
in from these fractures is the same light greyish alteration
visible in the rimmed fragments in the ore. It is evident
that if this rock was broken into fragments along the
hairline fractures, a breccia composed of fragments with
altered rims would result. The author proposes that
hairline fracturing, permeation by hydrothermal fluids
and subsequent violent explosion are responsible for the
rimmed siltstone, rhyolite and Intermediate Footwall
fragments in the ore horizon. These same explosions may
have been largely responsible for fragmentation of all
other lithologies which occur as clasts in the ore horizon,
including massive sulphide. In the case of the Kuroko
deposits of Japan, there is evidence of deep-rooted explo-
sions within the white rhyolite domes which have explosively
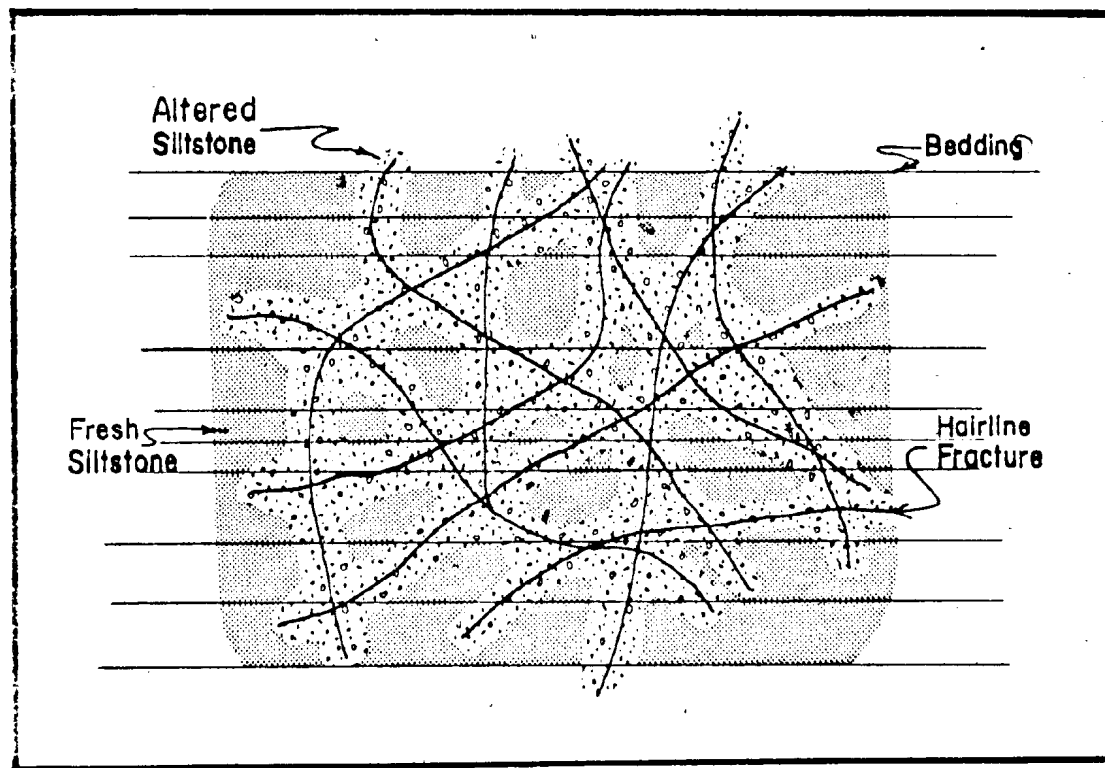
Figure 4-3: Sketch showing bedded siltstone transected by hairline fractures with alteration extending into the siltstone from the fractures. Fragmentation of this rock would produce breccia fragments with altered rims.

transported a variety of lithic fragments (including accidental basement fragments) to surface with subsequent deposition in the ore horzion (T. Satō, pers. comm. 1975).

The evidence presented in the preceeding paragraphs suggests that the Lucky Strike North, MacLean, Rothermere and Two Level Orebodies and their related breccias were emplaced as sulphide fragments from rapidly moving subaqueous density flows. The most compelling evidence in favour of this interpretation is the universal presence of competent to plastic sulphide fragments with chaotically disoriented streaky banding truncated at the fragment margins. The presence of chaotic internal structure, to crude grading to imbrication, the presence of scour channels in underlying rocks and the close association with sulphide-bearing polylithic breccia-conglomerate of density flow origin is further evidence in support of this hypothesis.

The interpretation of the ores as mechanically transported sulphides deposited from a series of subaqueous debris flows explains a large number of features, i.e.,

1) the tabular, elongate shape of the deposits in a south-east-northwest direction,

2) the occurrence of the ores in paleotopographic depressions within a paleo-channel,

3) the lack of directly associated stockwork mineralization (Fig. 4-2),

4) the lack of significant alteration (especially at
   MacLean) which can be confidently and consistently
   related to the presence of sulphide mineralization,

5) the progressive thinning of MacLean Orebody away from
   Lucky Strike,

6) the presence of coarse breccia beds on finer breccia
   beds,

7) the abundance and variety of lithic fragments in the
   ore and the presence of fragments with altered rims,

8) the occurrence of the sulphides at the same stratigraphic
   horizon as a major "in situ" deposit,

9) the presence of unmineralized siltstone and tuff beds
   within the ore,

10) the absence of well banded (bedded) massive sulphide,

11) the relative scarcity of yellow ore fragments,

12) the presence of a transported baritic cap and preferen-
    tial accumulation (in the MacLean case) of barite
    towards the proximal (southeast) end of the deposit, and

13) the occurrence of metal ratios at MacLean and Rothermere
    which are consistent with their being derived from the
    upper portions of the zoned Lucky Strike Orebody.

The general mode of transport of the fragmental
ores and related breccias can be deduced from previous
description. The size of the breccia fragments, thickness
of the breccia beds, distances of transport and scour
channels at the base are indicative of a powerful and fast-
moving transporting agent.

The generally poorly sorted, chaotic, and polylithic
nature of the breccias and ores is further evidence of
deposition from rapidly moving flows. The occurrence of
long axes of clasts parallel to the direction of flow
indicates that clasts did not roll on the bed as in fluvial
deposits (e.g., Rust, 1972) but instead were alligned in
suspension by clast collisions similar to that proposed
by Rees (1968). The author invisages transport by a series
of rapidly moving debris flows, not unlike the submarine
equivalents of landslides. Calculations by Davies and
Walker (1974) on deposits of this type in Quebec indicate
flow velocities on the order, of tens of meters per second.

The following interpretive sequence of events at
Buchans can be constructed from all the preceeding:
1) Near-surface explosions occurred in the vicinity of
    Lucky Strike during black ore formation. Exploded
    lithic and sulphide fragments collected on the slope
    and were dislodged by subsequent explosions, by earth-
    quakes or simply by instability of the accumulation
    on the volcanic slope. The direction of mass flow was
    controlled by a topographic channel which existed in a
    northwesterly direction downslope from Lucky Strike.
    Density flows scoured the underlying beds picking up
    additional fragments during transport. Debris was
    preferentially deposited in depressions along the path
    of flow.

2) Black ores continued forming at Lucky Strike and sub-
   sequent explosions resulted in further debris flows.

3) As baritic ores formed at Lucky Strike, subsequent
   explosions resulted in transport of increasingly more
   baritic debris flows which collected on top of under-
   lying transported black ores.

4) Explosions in the vicinity of Lucky Strike ceased.

5) Red hematite-rich barite formed a cap on Lucky Strike
   and formation of the orebodies was complete.

4.3.5. Clementine Prospect: The Clementine Prospect
is a significant transported sulphide deposit occurring
on the Lucky Strike ore horizon, approximately 4 km west
of Lucky Strike (Fig. 4-1). The deposit has recently been
studied by Calhoun (1979) and Calhoun and Hutchinson (1980)
and further description will not be undertaken here.

4.4. Oriental Ore Horizon Sequence .

4.4.1. Oriental No. 1 Orebody: The Oriental No. 1
Orebody was discovered in 1926 and produced 2,738,664 tons
of ore with an average grade of 15.8% Zn, 8.47% Pb, 1.71% Cu,
3.93 oz/ton Ag and 0.061 oz/ton Au. Apart from Lucky Strike
and the small, fault-disrupted Old Buchans deposit it is the
only other known major massive sulphide deposit containing
"in situ" sulphides associated with stockwork mineralization.
However, study of the deposit is hampered by post-ore

Plate 4-13:   Banded Oriental No. 1 ore.   Interbanded very
              high grade chalcopyrite and darker galena-
              sphalerite with minor bornite filling fractures.

imbricate (thrust?) faults of small displacement which have
effectively sliced the ore zone into hundreds of sulphide
bodies.

The Oriental deposits occur along the north side
of the Buchans Inlier and lie above a major (thrust?) fault
which separates rocks of the Inlier from the Oriental ore
horizon sequence (Fig. 2-2). This same fault may be
responsible for repetition of the Lucky Strike ore horizon
sequence in the Oriental area, implying that the Oriental
deposits lie in approximately the same stratigraphic
position as the Lucky Strike deposits.

Virtually all lithologic contacts in the Oriental
area are sheared and thus the original stratigraphic relation-
ships are obscured. The deposit is closely associated with
altered dacitic crystal-vitric tuffs of the Oriental ore
horizon sequence and with highly silicified and mineralized
breccias of the Oriental Intermediate Footwall. The ores
consist of both "in situ" banded massive sulphide and mechan-
ically transported ores. Ore mineralogy consists of sphal-
erite, barite and galena with less abundant chalcopyrite,
bornite, pyrite and tetrahedrite. Sulphides of the Oriental
No. 1 deposit are among the finest in grain size in the
Buchans area and banded sulphides are better displayed at
Oriental No. 1 than anywhere else in the area (Plate 4-13).
Oriental ores display a number of sedimentary structures
including slump folds and bedding sag structures.

4.4.2.   Oriental No. 2 Orebody: The O-2 deposit is a complex sulphide body located 150 m north of O-1 and occurs at, or very nearly in, the same stratigraphic horizon as O-1. The deposit produced 928,863 tons of massive and fragmental ore at 9.41% Zn, 6.20% Pb, 0.76% Cu, 6.15 oz/ton Ag, and .046 oz/ton Au.   The deposit was discovered in 1953, commenced production in 1955 and was mined out in 1969.   At present the mine is flooded and information is available only from drill-core.   The deposit is tabular, varying in thickness up to 10 m and averaging about 5 m.   It is approximately 500 m long, 75 m wide and ranges in depth below surface from 40 m to 120 m (Swanson, Perkins and Higgins, 1955).

The ore-bearing sequence conformably overlies dacitic crystal-vitric tuffs which everywhere form the footwall of the deposit.   These tuffs vary from green to grey and normally consist of 1-2 mm quartz and plagioclase crystals in a variably sericitized and clay mineralized vitric matrix.   This footwall dacite tuff may be overlain conformably in the immediate O-2 area by any one, or combination of six distinctive rock types, i.e., massive sulphide, polylithic breccia-conglomerate, monolithic breccia, clastic ore, pyritic siltstone or dacitic vitric-crystal tuff.   The relationships between these units are complex.

The footwall polylithic breccia-conglomerate, clastic ore and siltstone are all underlain and overlain by dacitic tuffs in the immediate footwall of the deposit. The polylithic breccia-conglomerate consists of angular to rounded fragments of basalt, andesite, dacitic pyroclastic, silicified sugary-textured acid (?) volcanic fragments, fragments similar to portions of the Intermediate Footwall and rare granitoid and jasper pebbles. Pink rhyolite fragments are absent in this horizon. Baritic black ore, yellow ore and less common siliceous or chloritic stockwork fragments occur in varying quantity and sizes up to 25 cm and locally reach ore grade over 60 cm thickness. The footwall breccia-conglomerate is thick between 0-1 and 0-2 but thins rapidly northward. The horizon is very poorly sorted and bedded, although a few graded beds with fragments grading from 50 mm to 1 mm over 2 m are present. The lack of very fine grained sediments at the top of such beds suggests that these debris flows were very dense (i.e., contained little water) and that minimal mixing with water occurred during transport.

Less than one meter of grey pyritic siltstone occupies the same stratigraphic horizon as the breccia-conglomerate in the footwall of the western portion of the orebody.

The polylithic breccia-conglomerate-clastic ore-siltstone horizon is commonly overlain by a few centimeters

of variably altered dacitic vitric-crystal tuff which is in turn locally overlain by a monomictic breccia containing fragments of strongly altered rocks derived from the Inter-mediate Footwall. This breccia apparently thickens northward, possibly suggesting a northerly source.

Massive sulphides of the 0-2 orebody everywhere lie in sharp conformable contact with footwall rocks which variably consist of the main footwall dacitic tuff, poly-lithic breccia-conglomerate, the thin dacitic tuff above the breccia-conglomerate or monomictic breccia. The ore contains both massive (chemically?) deposited sulphide and clastic sulphide facies. Black ore and baritic black ore are dominant in both clastic and massive facies as yellow ore fragments in clastic ore and as wisps in massive ore are volumetrically much less significant. The ore mineralogy consists of barite, sphalerite, galena, pyrite and chalco-pyrite with lesser tetrahedrite and bornite (Alcock, 1960).

Massive 0-2 ore, like most other massive sulphides in the area is poorly banded and contains local discontin-uous streaks of chalcopyrite-rich ore in black ore. These streaks are commonly randomly oriented in core, suggesting large scale slumping of massive ore. The massive ore commonly contains a variety of strongly altered lithic fragments possibly incorporated into the slumping sulphide during movement. Near the transition from massive to clastic ore,

massive ore commonly takes on an autobrecciated appearance
and grades into clastic ore containing both competent
angular sulphide fragments and flattened and frayed sulphide
fragments which apparently behaved plastically. Local thin
fine grained lithic-rich beds are present in clastic ore.
In general, clastic sulphide ore is more common at the
base and top of the orebody and occurs virtually to the
exclusion of massive ore at the northern (distal) periphery
of the orebody. The hangingwall contact between high grade
clastic ore and overlying volcanic breccia-conglomerate is
locally sharp but is commonly characterized by a gradual
decrease in abundance and size of sulphide fragments with
increasing dilution of lithic fragments. Zoning in the
orebody is very poorly developed. Barite-rich zones occur
randomly throughout the ore and show little consistent
enrichment towards the top of the orebody. No chalcopyrite-
rich yellow ore zones are known in the orebody. The ore is
not underlain by stockwork mineralization.

All of the above evidence suggests that O-2 is a
transported orebody derived from the nearby O-1. The dis-
tribution of massive and clastic facies and textures in both
suggest that O-2 moved as a large, slowly advancing sulphide
mud flow.

The immediate hangingwall of the O-2 orebody may
consist of any of three distinct lithologies which from

stratigraphic bottom to top include 1) monomictic volcanic breccia with fragments derived from the Intermediate Footwall, b) polylithic volcanic breccia-conglomerate and c) granitoid-bearing volcanic breccia-conglomerate. Strongly altered felsic pyroclastics also locally form the immediate hangingwall but their exact stratigraphic relationship to other hangingwall lithologies is unknown.

The monomictic Intermediate Footwall-bearing breccia is only locally present and contains numerous black ore fragments and boulders. It is conformably overlain by a polylithic volcanic breccia-conglomerate which bears a lithologic similarity to its counterpart in the footwall. This unit is the most common hangingwall lithology and normally contains a few granitoid pebbles but only rare pink rhyolite pebbles. Angular and plastically deformed sulphide clasts are ubiquitous and yellow ore fragments are normally relatively more abundant than in the orebody itself. The breccia-conglomerate is conformably, and in most places gradationally overlain by a similar breccia-conglomerate but containing abundant subrounded to rounded, pink to white granitoid boulders up to several centimeters in diameter. Other fragment and boulder lithologies in the "granite conglomerate" include green dacitic crystal-vitric tuff, basalt, a variety of fragments derived from the Intermediate Footwall Formation (some bearing the mariposite-like sericite), and rare chert and pumice

fragments. Sulphide fragments less than one centimeter
in diameter are common and may consist of baritic black
ore, black ore, yellow ore and rare fine grained siliceous
pyritic stockwork fragments. Rare isolated sulphide
boulders may exceed 10 cm diameter. Sulphide fragments
generally decrease in abundance with distance above the
ore zone. The unit on the whole is poorly sorted and bedded
although a crude sorting into relatively boulder-rich and
boulder-poor zones is locally observed. Graded bedding and
reverse grading are rare occurrences. Fragments and
boulders are most commonly matrix-supported though local
fragment-supported zones are present.

North of the 0-2 zone, the "granite conglomerate"
rests conformably on footwall dacite and the unit is
conformably overlain by hangingwall dacite.

4.4.3. Sandfill Prospect: The Sandfill Prospect
is an subeconomic sulphide deposit which occurs 1 km north-
northeast of Oriental (Fig. 2-1) and at approximately the
same stratigraphic horizon as the Oriental deposits. The
deposit, which is exposed only in drill core, occurs at
350 m depth and comprises 75,000 possible tons of 1.5% Cu,
4.7% Pb, 10.0% Zn, 0.01 oz/ton Au and 2.5 oz/ton.Ag. It is
a mechanically deposited "orebody" consisting of a concentra-
tion of sulphide fragments surrounded by a lower grade zone
of sulphide fragments diluted by abundant lithic fragments.

The Sandfill and Middle Branch deposits provide excellent examples of the paleotopographic control exerted on the distribution of the transported ores.

The deposit occurs in a sequence of debris flows of the Oriental ore horizon sequence and lies approximately 100 m above the fault-bounded upper contact of Footwall Arkose. In the footwall of the deposit there occurs a small (100 m long and 15 m thick) pervasively silicified and lightly pyritized grey-white rhyolite body with a strongly brecciated top. This rhyolite breccia grades upward into a thin (less than 10 m) sequence of white rhyolitic lapillistone and lesser bedded rhyolitic wacke with lightly disseminated pyrite and rare films of galena and sphalerite in the matrix. Matrix pyrite is generally coarser in coarser wackes suggesting a detrital origin. Within a few meters of the overlying "ore", extraneous lithic fragments become abundant. These include pyritic siltstone (with altered rims), altered intermediates (with "mariposite") and a few small Cu-Pb-Zn sulphide fragments which increase upwards in size and abundance to a maximum of 80% sulphide fragments. (Weak silicification occurs for one meter below "ore" in a single drill core.) This "ore" consists mainly of galena-sphalerite-chalcopyrite fragments up to 10 cm in size, with lesser chalcopyrite and/ or pyrite, barite and barite-sphalerite fragments. Many of the fine grained banded sulphide fragments bear a strong

resemblance to Oriental ores. Lithic fragments occur throughout the ore and a few fine grained (1 cm) essentially barren, polylithic breccia beds are intercalated with the "ore". Within one meter of the top of the "ore" the size of both lithic and sulphide fragments decreases dramatically and the ratio of lithic to sulphide fragments increases rapidly as the sequence grades into a pyritic wacke bed. This "ore" sequence is subsequently overlain by at least nine graded breccia beds ranging in thickness from less than one meter to 20 m thick, each of which grade from polylithic breccia at the base to greywacke or siltstone at the top. Small sulphide fragments are a component of each breccia bed but their abundance and size decreases with each successive breccia bed above the major sulphide concentration. This sequence of subaqueous debris flows is subsequently overlain by dacitic pyroclastic flows which locally contain a few granitic pebbles.

Considerable evidence exists to suggest that the Sandfill Prospect is a mechanically deposited sulphide accumulation. This evidence includes:

1) the presence of angular sulphide fragments

2) banding in sulphide fragments is terminated at fragment boundaries

3) the abundance of silicate fragments

4) the vertical and lateral, increase in size and relative abundance of sulphide fragments towards "ore"

5)   the lack of metal zoning in the sulphide-body

6)   the absence of stockwork mineralization

7)   the lack of visible alteration consistently related
     to the presence of sulphides

8)   the occurrence of graded sulphide and silicate frag-
     ments at the top of the "ore"

9)   the occurrence of the ore in a sequence of graded
     sulphide-bearing subaqueous debris flows.

4.4.4.   Middle Branch Prospect: The Middle Branch
prospect is a small sulphide deposit exposed in a single
drill hole at a depth of 555 m.   The single intersection
over 2 m assayed 0.4% Cu, 3.1% Pb, 4.8% Zn, 0.02 oz/ton Au,
1.4 oz/ton Ag and 8.0% Fe in sulphides.

The deposit occurs at a stratigraphic horizon
very close to that of the Sandfill deposit although rapid
lateral facies changes and minor faults filled with diabase
have hampered detailed correlation.   The deposit is bounded
on both the footwall and the hangingwall by diabase dykes.
Beneath the footwall diabase there occurs a sequence of
fractured and altered siliceous siltstones which contain
detrital pyrite and traces of epigenetic galena-sphalerite
in thin fractures.   A distinct whitish alteration of silt-
stone occurs adjacent to the network of epigenetic fractures
and pervades into the siltstone for short distances.
These siltstones are interbedded with rhyolitic tuff-
breccia containing grey to pink rhyolite fragments with

lesser siltstone fragments and minor pyrite and galena-
sphalerite fragments up to one centimeter. Traces of Pb-Zn
veining as films in fractures occur locally and a single
vein of pyrite-barite occurs 15 m below "ore".

The sulphide body itself is not so obviously
fragmental as the Sandfill although a transported origin
is suspected. The "ore" contains 20% lithic breccia frag-
ments but no sulphide fragments are macroscopically visible.
The gangue minerals are much coarser grained than Sandfill
with pyrite commonly of 1-2 mm size and barite up to 1 cm.
Galena and sphalerite are fine grained and the ore contains
relatively little chalcopyrite. Overlying the hangingwall
diabase there occurs a polylithic breccia which contains a
few sulphide-bearing fragments.

The ultimate source of the Sandfill and Middle
Branch Prospects is of considerable exploration interest.
As with all transported ores, an analysis of paleotopography
may be valuable in tracing such ores to their sources.
An isopach map of the Oriental ore horizon sequence, a
schematic cross section of the Sandfill-Middle Branch
area and a paleotopographic plan are presented in Figures
4-4, 4-5 and 4-6, respectively. It can be seen from these
diagrams that the Sandfill and Middle Branch Prospects
occupy opposite flanks of a ridge of coalescing rhyolite-
breccia domes which traverse the length of a deep paleo-
trough. This trough extends from Old Buchans to Oriental
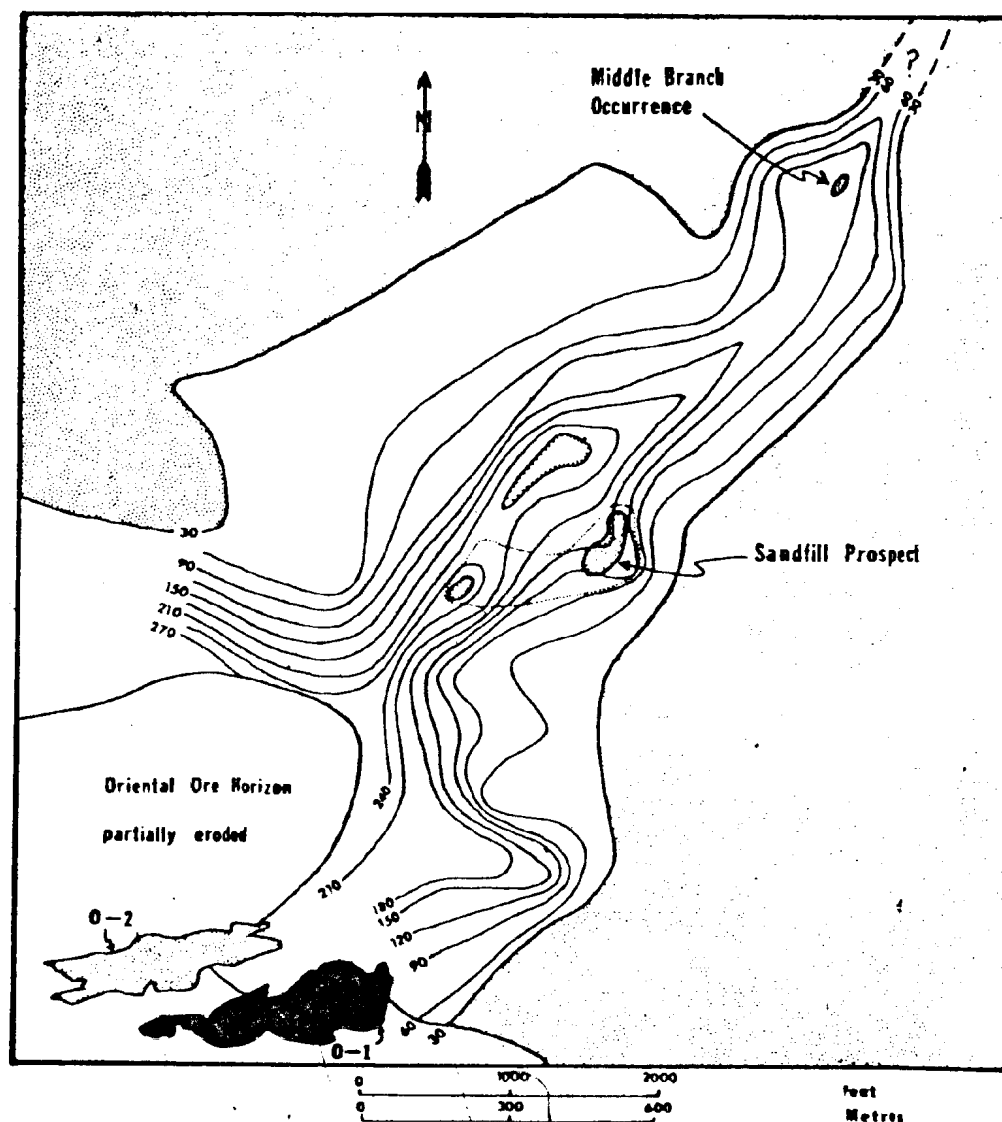
Figure 4-4. Isopach map of the Oriental ore horizon sequence
illustrating the nature of the Oriental-Sandfill
Middle Branch channel. In situ ore, solid black:
transported ore, stippled. Contour interval = 30 m

NW

SE

Unseparated Upper Buchans Subgroup

Upper Arkose

Ski Hill Polylithic Breccia

quartz and feldsparphyric rhyolite

Dacitic
Pyroclastics

Felsic Pumice Tuff
and Pumice Breccia
(Intermediate Footwall)

arkose

Ski Hill Andesitic
Breccia

Middle Branch
Channel

Sandfill Channel

Rhyolite
Breccia

Siltstone,
Breccia

Lower Sulphide Clast-Bearing Sequence

fault

fault

Footwall Arkose

- 192 -

Figure 4-5

Schematic stratigraphy in the Sandy Lake - Sandfill - Middle Branch Area
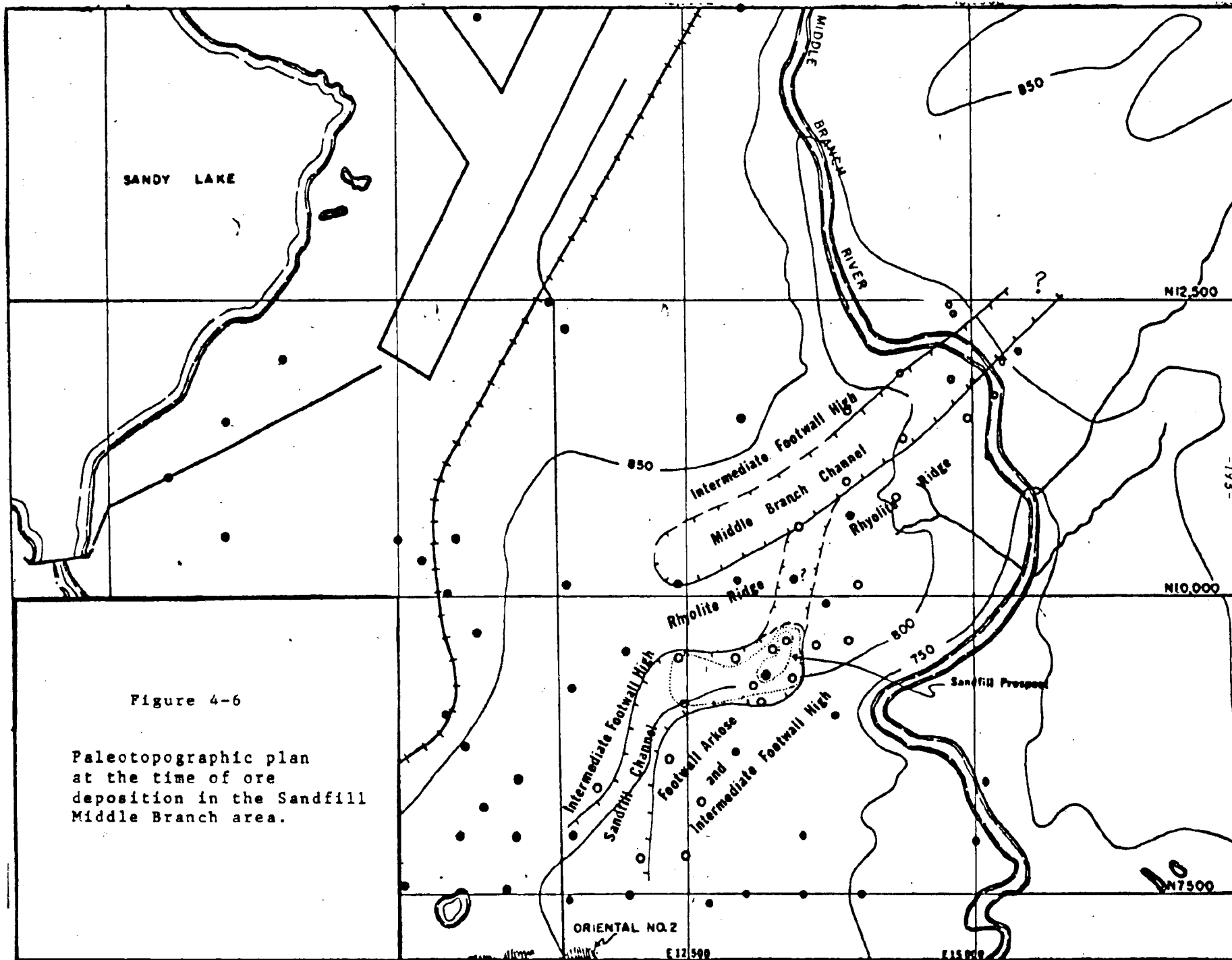
Figure 4-6

Paleotopographic plan at the time of ore deposition in the Sandfill Middle Branch area.

SANDY LAKE

MIDDLE BRANCH RIVER

850

N12,500

Intermediate Footwall High

850

Middle Branch Channel

Rhyolite Ridge

Rhyolite Ridge

N10,000

800

750

Sandfill Prospect

Intermediate Footwall High

Sandfill Channel

Footwall Arkose and Intermediate Footwall High

N7500

ORIENTAL NO. 2

E 12,500

E 15,000

-193-

and subsequently northward to the Sandfill-Middle Branch
area, and beyond. The presence of this trough linking
the in situ Oriental No. 1 orebody to the Sandfill-Middle
Branch Prospects provides compelling evidence that Oriental
No. 1 constitutes the source of the transported Prospects.
Other arguments in favour of an Oriental source are listed
below:

1) Correlation between Middle Branch-Sandfill and Oriental
   indicate that all three zones occur at essentially
   the same stratigraphic horizon.

2) The Oriental and Sandfill-Middle Branch transported ores
   both consist of mainly black ore fragments in polylithic
   breccias.

3) The broad thick sequence which hosts the Oriental ores
   funnels rapidly northward into a relatively narrow,
   northeast trending trough which hosts the Sandfill-
   Middle Branch mineralization (Fig. 4-4).

4) Though alteration and minor sulphide veining exist in
   the Sandfill area, typical stockwork similar to that
   at Oriental or Lucky Strike is not known to occur.

5) Sorting and grading of host rocks in the Sandfill-
   Middle Branch zones is better than that at Oriental.
   This, combined with the relatively lithic-diluted
   nature of the ores, suggests that they are relatively
   distal deposits and that Oriental could be the distant
   source.

Evidence in favour of an undiscovered source is
as follows:

1) Points 1), 2), and 5) above, could be equally explain-
ed by an undiscovered source.

2) Altered rhyolite fragments are abundant in the Sandfill-
Middle Branch ore horizon and are relatively much less
abundant in breccias of the Oriental area. These
fragments are demonstrably of local origin, and there-
fore suggest that the sulphide fragments could also be
local

3) The size of lithic fragments (some over 120 cm, or
approximately 2600 kg) and sulphide fragments (up to
45 cm in diameter or approximately 225 kg) in the ore
horizon breccias is suggestive of a local source.

4) It can be seen from Fig. 4-2 that zones of sulphide
veining and alteration in rhyolite occur near the Sand-
fill and Middle Branch deposits. If these deposits
were derived from Oriental this would have to be ascribed
to coincidence.

5) Metal ratios of the Sandfill deposit are dissimilar from
the Oriental No. 1 or Oriental No. 2 orebodies. In
comparison, metal ratios from Rothermere and MacLean
are virtually identical to their presumed source at
Lucky Strike.

6) Barite-pyrite boulders occur in the ore breccias and
Barite-pyrite veinlets occur in altered rhyolite in the

Sandfill-Middle Branch area. This barite-pyrite assoc-
iation is relatively poorly developed at Oriental.

7) It is entirely possible that the Middle Branch channel
(Fig. 4-6) does not connect with the Sandfill-Oriental
channel. A separate source might thus be suggested
for at least the Middle Branch prospect.

8) If a major thrust fault is present on top of the Footwall
Arkose a number of further arguments can be invoked.
It is beyond the scope of this thesis to fully document
the reasoning for these arguments.

4.4.5. Old Buchans Orebodies: The Old Buchans Orebodies
are among the most poorly understood deposits in the Buchans
area due to the antiquity of mine workings, poor core
recovery, strong faulting and lack of study. The Old Buchans
Conglomerate Orebody was transported, occurring on the
Oriental horizon and grossly similar to O-2. The Old
Buchans East and West Orebodies are associated with stock-
works and numerous faults. Their stratigraphic position
is uncertain and conceivably they could lie in the Lucky
Strike thrust block, or even possibly in a lower thrust block.

4.5. Selected Comments

4.5.1. Miscellaneous Occurrences of Sulphide Clasts:
A noteworthy feature of the Buchans area is the widespread
distribution of sulphide clasts occurring over several
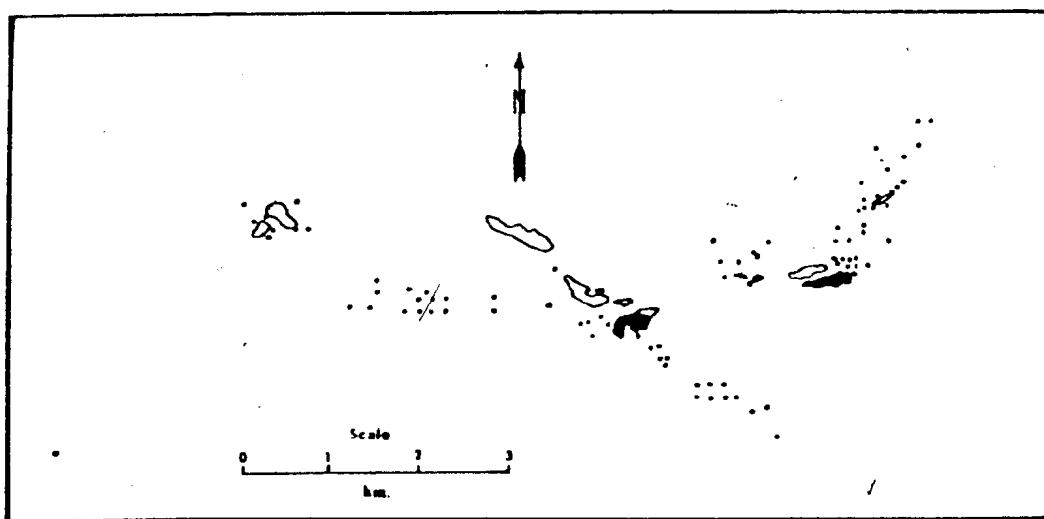
Figure 4-7: Plan showing distribution of high grade sulphide
clasts in the Buchans area. Dots indicate vertical
drill holes which have intersected sulphide clasts.
In situ orebodies are shown in solid black, transported
orebodies as outlined.

Plate 4-14:   Central greyish black ore pebble and smaller
clastic sulphide grains in pyroclastic breccia.
Enlargement approximately 1.5X.

square kilometers in the Lucky Strike and Oriental ore
horizon sequences. The distribution of such clasts as
intersected in drill core is shown in Fig. 4-7. They range
from grains and pebbles to 30 cm boulders of high grade
black ore (Plate 4-14). Clasts of yellow ore are much
less common. They normally occur in polylithic breccias
or pyroclastic breccias at the same stratigraphic horizon
as major in situ and transported orebodies, but significant
concentrations of clasts are also found within the ore
horizon sequences, at stratigraphic positions in which no
in situ ore is known.

Many such clasts display diffuse, dark rims of
alteration suggestive of diagenetic chemical attack.
Smaller grains locally are almost entirely degraded. The
significance of this is discussed in Chapter Seven.

Minor occurrences of sulphide clasts are known
within the Intermediate Footwall and Ski Hill Sequence.
These are grossly explicable in terms of the minor stratiform
mineralization occurring at these horizons. An inexplicable
occurrence of small, high grade sulphide grains and pebbles
occur within the Wiley's Sequence, 6.7 km distant from
Lucky Strike Orebody.

4.5.2. Comments on Granitoid Boulders at Buchans:
The Feeder Granodiorite is lithologically and chemically
similar to some Buchans Group rhyolites and to granitoid

boulders in the ore horizon. It probably represents the source of the granitoid boulders occurring throughout the Buchans Group and in the ore horizon.

Granitoid boulders in volcanic terranes are not uncommon (e.g., Cady, 1975; Helwig and Sarpi, 1969) and in some instances, such boulders are thought to represent the plutonic equivalents of cogenetic volcanics (e.g. Gabrielse and Reesor, 1974). Cobbing and Pitcher (1972) suggest that magma pressure may force up fault blocks of solidified magma chamber thus exposing them to erosion at the same time as intrusion-extrusion. However no such fault blocks and no logical source, exposed during ore deposition, are known at Buchans.

More plausibly, the author suggests that the granitoid boulders were rounded during gas-transport to surface in "pebble dykes", such as those that occur in close association with the Japanese Kuroko deposits and many porphyry Cu-Mo deposits. No such dykes are known at Buchans, but the most likely source area, in the Lucky Strike region, is now eroded. An origin of this nature would explain the unique sphericity and rounding of the granitoid boulders as well as their anomalous abundance in the areally and stratigraphically restricted ore horizon breccias.

4.5.3. Buchans as Compared to Other Occurrences of
Mechanically Transported Ores: The occurrence of mechani-
cally transported ores was predicted as early as 1965 (Suffel,
1965, p. 1062) and since have been recognized in association
with several massive sulphide deposits, e.g. at Noranda,
Sinclair (1971); Spence (1975); at Kidd Creek, Walker et al.
(1975); in the Iberian pyrite belt (Schermerhorn 1970, 1971);
and in the Kuroko deposits (see next section). Sulphide
fragments have been noted in many other deposits, some of
which may be transported.

The Buchans transported ores are proximal by
comparison to those of the Iberian pyrite belt. Within
this class, they represent (to the author's knowledge)
the world's best preserved, most extensively developed,
farthest travelled and highest grade transported ores.

4.6. Comparison of Buchans and Kuroko Deposits

The Buchans deposits and the famous Kuroko deposits
of Japan are so very similar that a few words of comparison
are warranted. Both types occur as stratiform polymetallic
deposits associated with breccia horizons in felsic vol-
canic rocks (Sato, 1974; Lambert and Sato, 1974). The ore
and gangue mineralogy of both types is similar, although
neither gypsum nor anhydrite have been identified at Buchans.
Both types have generally sharp boundaries with their wall

Plate 4-15:   Fragmental ore from the Japanese Ainai Kuroko
deposit.   The bulk of the same is composed of
black and yellow ore clasts.

rocks and display numerous internal submarine sedimentary structures and textures consistent with a volcanic-exhalative mode of origin. Both appear to be relatively shallow water phenomena though this has been questioned in the Kuroko case by Urabe and Sato (1978). Stringer and stockwork mineralization is common to the footwall of both types. Sediments associated with both types are dominantly volcaniclastic as opposed to chemical. Some Kuroko ore-bodies (e.g., Shakanai Mine, Ohtagaki et al., 1974, p. 135) contain interbedded barren sedimentary layers like Rothermere and MacLean Orebodies. Though not a commonly mentioned feature, some Kuroko deposits occupy depressions in the underlying volcanic surface (e.g., Ohtagaki et al., 1974, p. 137; N. Sato and Kusaka, 1974, p. 146; Tanimura et al., 1974, p. 153; Hirabayashi, 1974, p. 200; Honishi, 1974, p. 218). Pebbles of granitic basement rock occur in close association with ores of the Yoshino Mine (Osada et al., 1974, p. 185) and are apparently related to contemporaneous block faulting with basement uplift. It is interesting to note that these same deposits are not associated with white rhyolite domes and contain no gypsum.

Mechanically transported sulphide ores have been described from several Kuroko mines (Plate 4-15), e.g., Shakanai Mine, (Kajiwara, 1970; Ohtagaki et al., 1974), Kosaka Mine (Sato, 1968; Oshima et al., 1974), Ainai Mine (Ishikawa and Yanagisawa, 1974), Hanaoka Mine (Takahashi
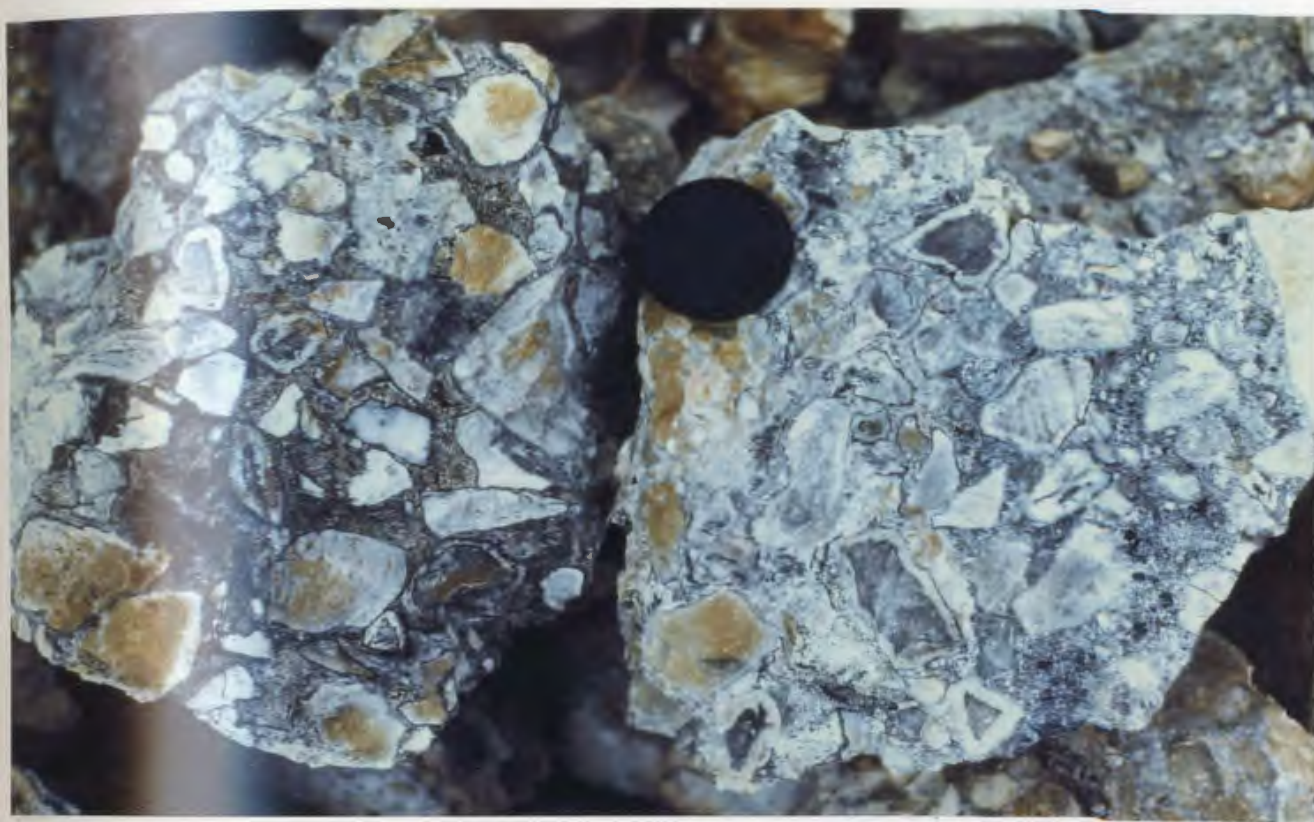
Plate 4-16:   Motoyama volcanic breccia, Kosaka Mine.   Note
altered rims on rhyolite fragments, similar to
those occurring at Buchans.

and Suga, 1974; Ito et al., 1974), Kamikita Mine (Lee et al., 1974), Kurosawa Mine (Motegi, 1974) and Fukazawa Mine (Tanimura et al., 1974). Imbrication, bedding sag struc- tures, graded sulphide breccias, scouring at the base of the deposits and ore balls surrounded by clay are features of transported Kuroko ores which have also been identified at Buchans. Both plastic and competent sulphide fragments have been identified in both the Kuroko (e.g., Ishikawa and Yanagisawa, 1974, p. 87) and Buchans deposits. The occurrence at Buchans of lithic fragments with all three types of alteration rims as described by Lee et al. (1974, p. 61) is remarkable (Plate 4-16).

Despite the absence of gypsum and anhydrite at Buchans and the limited development of yellow ore, zoning is very similar to that of a typical Kuroko deposit as described by T. Sato (1974). The stratigraphically lowest stockwork mineralization at Buchans is pyritic, much like that of the Kuroko deposits. Stratigraphically higher stockwork mineralization at Buchans is pyritic and poly- metallic like some Kuroko stockworks. Such mineralization at Buchans is associated with strong chloritization and/or silicification; where silicification is dominant the Buchans stockwork closely resembles Keiko. Copper is relatively more abundant in the stockwork at Buchans than in the over- lying massive sulphide, a feature in common with the Kuroko deposits. Yellow ore is poorly developed at Buchans but,

where present, is concentrated towards the base of the massive sulphide (George, 1937), i.e., in a similar position to the Oko. Pb-Zn-rich black ore occupies the upper portion of the "in situ" deposits at Buchans in a similar stratigraphic position to the Kuroko. Gold and silver minerals are concentrated in this zone in both cases. Bedded barite overlies the black ore in both Buchans and Kuroko examples. Though no red hematite-quartz layer is present at Buchans, this horizon is locally occupied by hematitized barite and hematitized tuff. Several Kuroko deposits are subsequently overlain by tuffaceous felsic volcanic rocks.

Several features of the Buchans deposit differ from those of typical Kuroko deposits. Though present at Buchans, white rhyolite bodies do not display the intimate spatial relationship to mineralization which is so character- istic of the Kuroko deposits. Gypsum is absent at Buchans. Yellow ores are poorly developed and the abundance of pyrite throughout is less than that of typical Kuroko deposits. Well banded ores and ores displaying colloform banding are relatively less abundant at Buchans. Though mechanically transported sulphide ores are characteristic of both examples, the Buchans deposits are anomalous in both the high quantity and quality of transported ores as well as transport distances which exceed any of the Kuroko deposits (T. Sato, pers. comm., 1975).

CHAPTER FIVE

GENERAL PETROCHEMICAL NATURE OF THE BUCHANS GROUP

5.1.   Post-Magmatic Chemical Changes of Buchans Group Rocks

The ongoing spilité debate (e.g., Amstutz, 1974) and an interest in ocean floor chemical changes has fostered abundant research into post-depositional changes in submarine volcanics (especially basalts). Documented chemical changes as a result of low temperature depositional and diagenetic alteration range from essentially nil (e.g., Clarke, 1975) to substantial additions and removals of certain elements. On the basis of petrographic, geochemical and experimental data (and with a few discrepancies), SiO_2, CaO, MnO, total Fe and Cu are commonly leached during low temperature submarine alteration of basaltic rocks whereas H_2O, K_2O, MgO, Rb, Cs, Fe^{+++}/Fe^{++} and K/Rb commonly increase (e.g., S.R. Hart, 1969, 1973; Philpotts et al., 1969; Cann, 1970; R. Hart, 1973; Hajash, 1975; Bischoff and Dickson, 1975). The same authors have generally concluded that Ti and Al have remained relatively inert during alteration but little consensus has been reached on the behavior of more mobile elements such as Na.

Under conditions of prehnite-pumpellyite metamorphism, such as that experienced by the Buchans Group, volcanic sequences commonly undergo varying degrees of

hydration and redistribution of elements, especially Na
and Ca (Smith, 1968; Jolly and Smith, 1972; Jolly, 1972).
Among the base metals, Jolly (1974).demonstrated consider-
able redistribution of Cu and removal of Zn in low rank
basaltic rocks.

In view of the variety of probable post-magmatic
chemical changes, any attempt to relate rock chemistry
to mineralization must demonstrate that anomalous conditions
are indeed a function of mineralization and not due to
other processes. Apart from the effects of mineralization
in proximity to ore, rocks of the Buchans Group have
undoubtedly been subject to chemical changes as a result of
depositional, diagenetic and metamorphic alteration. Perhaps
the most obvious effect of post-magmatic alteration is the
widespread depositional-metamorphic introduction of water
combining to form hydrous minerals (chlorite, sericite,
pumpellyite, prehnite, etc.). Apart from increasing loss
on ignition, this has the effect of "diluting" the abundance
of other elements.

Local diagenetic redistribution of several elements
is evident in virtually all lithologies. Concordant
hematitization and calcite introduction and abundant vein
and amygdule calcite are characteristic of many mafic
pyroclastics and breccias. In these rocks crustification,
comb and cockade structures, indicative of open space

filling, are visible locally. Such volcaniclastics commonly alternate with finer grained tuffaceous rocks which show no such alteration, indicating that calcite introduction occurred at, or shortly after deposition. The variety of vesicle-fillings further indicate post-depositional mobility of H_2O, Si, Ca, Mg, Fe and Al. Analyses of rocks containing significant vesicle and fracture filling was not attempted in this study. It is shown in subsequent sections that diagenetic-metamorphic alteration of crystal-vitric tuffs involved hydration and addition of MgO with removal of Na_2O. Secondary quartz halos around quartz crystals in these rocks indicate mobility of silica probably during diagenetic alteration of glass to clay minerals. Dispersion of very mobile elements such as Hg from the orebodies possibly provides an indication of the extent of secondary migrations. In the case of Hg, depositional, diagenetic and metamorphic processes have caused dispersion only on the scale of a few meters (Thurlow, 1973). If this is the case, then elements much less mobile than Hg have probably migrated proportionally shorter distances.

With respect to the elemental abundances discussed in subsequent sections, it is apparent that an average of a large number of samples will tend to nullify the effects of local migrations as the population will presumably include samples at all phases of migration. In this regard, the averages are probably a reasonable approximation of the

original composition. However, the effects of depositional
enrichments of elements and of hydration are superimposed
on the averages and quantitative estimates of their contri-
bution are difficult if not impossible.

5.2. General Elemental Abundances and Chemical Variations
of Buchans Group Rocks

The average chemical composition of all significant
lithologic units of the Buchans Group analysed in this study
are given in Table 5-1.

The volcanics of the Buchans Group display little
alkaline affinity. Neither olivine nor feldspathoids are
present in the mode or the norm and pyroxenes are neither
sodic nor titaniferous. Phosphorus and titanium are present
in abundances well below normal for any alkaline suite and
the Buchans volcanics are generally subalkaline on the
alkali: silica diagram of Irvine and Baragar (1971) (Fig. 5-1).

Similarly, the volcanic rocks of the Buchans
Group bear little lithologic or chemical resemblance to
oceanic tholeiites. The relatively shallow water environ-
ment, the relative abundance of felsic volcanics and the
total absence of ultramafic rocks and sheeted dykes render
an ocean floor origin extremely unlikely. Chemically, the
Buchans Group volcanics display abundances of large cations
(K, Rb, Ba, Sr, etc.) which are much greater than those of

Table 5-1: Average Chemical Composition of Buchans Area Rocks

	Footwall Basalt Flows	Footwall Basalt Fragmentals	Prominent Quartz Sequence Rhyolites	Prominent Quartz Sequence Dacitic Tuffs (Large Quartz)	Prominent Quartz Sequence Dacitic Tuffs (Small Quartz)	Prominent Quartz Sequence Tuffaceous Siltstone	Ski Hill Sequence Flows	Ski Hill Sequence Fragmentals	Intermediate Footwall	Mineralized Intermediate Footwall	Pyritic Siltstone Rothermere-Maclean
n=	3	8	9	11	19	8	18	51	29	14	18
SiO_2	48.8	46.6	69.0	68.5	69.8	67.4	57.4	55.4	54.4	47.2	65.4
TiO_2	.83	.87	.39	.35	.33	.33	.70	.66	.53	.21	.34
Al_2O_3	15.47	16.81	13.36	14.02	14.44	13.93	15.23	16.18	16.15	8.61	13.58
Fe_2O_3	8.63	11.54	3.78	3.95	2.73	4.25	8.31	9.20	9.84	17.16	3.86
MnO	.14	.13	.11	.06	.05	.17	.16	.16	.32	.35	.11
MgO	5.86	6.72	1.25	1.53	1.47	2.61	3.50	3.65	6.34	7.17	3.18
CaO	9.90	6.27	2.39	2.48	2.27	2.06	6.20	6.42	1.95	2.09	2.13
Na_2O	3.06	1.82	3.69	2.66	2.32	1.96	3.54	2.58	1.90	.29	2.87
K_2O	.97	1.40	2.52	2.46	2.62	4.13	1.04	1.38	2.00	.79	2.18
P_2O_5	-	-	-	-	-	-	-	-	.10	.09	.08
Loss. Ig.	5.41	7.12	2.83	3.46	3.27	2.99	2.93	3.91	5.58	11.78	4.07
Total	98.92	99.13	99.32	99.47	99.30	99.44	99.16	99.74	99.11	95.74	97.72
Ba (ppm)	410	721	708	493	688	873	617	1062	1541	1898	1848
Ba (SO_4=)	-	-	-	-	-	-	-	-	29	3492	1327
Pb	25	30	13	7	8	14	19	28	79	5470	88
Pb (S=)	7	6	16	18	11	10	13	14	70	5400	113
Zn	64	90	36	52	33	37	75	88	235	11700	364
Zn (S=)	13	16	13	15	12	12	19	21	68	12000	325
Cu	52	66	3	3	5	14	49	59	64	1670	21
Cu (S=)	45	45	6	5	4	7	43	51	63	1514	16
S	-	-	-	-	-	-	-	-	-	-	-
Ag	-	-	-	-	-	-	-	-	.93	4.1	.43
Hg (ppb)	-	-	-	-	-	-	-	-	44	234	67
Rb	22	34	45	61	69	71	18	32	39	28	34
Sr	256	245	153	144	265	144	267	310	129	68	219
Zr	72	60	122	140	127	110	87	82	81	59	129
Mo	<3	<3	-	-	<3	<3	<3	<3	<3	92	<3
Ni	48	40	4	6	5	3	21	12	13	27	5
Co	25	34	27	18	9	5	27	22	20	19	7
Cr	243	134	10	13	16	40	76	47	53	122	20
V	177	326	25	24	21	27	170	249	245	136	54
Th	-	-	11(4)	10(8)	14(3)	-	-	-	11	-	-
U	-	-	3(4)	1(8)	2(3)	-	-	-	2	-	-
Ga	-	-	13(4)	15(8)	17(3)	-	-	-	18	-	-
n =	5	8	9	11	19	8	18	51	29	14	18

Table 5-1 (continued)

Table 5-1 (continued)

	Granite Boulders In Ore Horizon	Feeder Granodiorite	Low Titanium Diabase	High Titanium Diabase	Alkali-Feldspar Granite	Peralkaline Granite	Hungry Mountain Complex
n=	5	3	9	18	12	5	3
SiO_2	72.8	74.5	48.3	46.8	74.7	76.0	70.6
TiO_2	.30	.23	.81	2.01	.20	.18	.34
Al_2O_3	12.45	12.59	15.84	15.48	12.68	11.32	13.96
Fe_2O_3	1.65	2.14	10.45	11.75	1.66	2.39	3.06
MnO	.05	.04	.18	.20	.02	.05	.05
MgO	.91	.48	7.07	6.25	.15	.01	1.11
CaO	1.27	1.38	8.69	8.97	.43	.23	2.30
Na_2O	4.02	4.08	2.32	3.05	3.84	3.90	3.45
K_2O	1.54	2.58	.94	.46	4.88	4.51	3.34
P_2O_5	-	-	.23	.36	-	-	-
Loss. Ig.	2.18	.66	5.48	4.77	.73	.62	1.19
Total	97.17	98.68	100.31	100.10	99.29	99.21	99.40
Ba (ppm)	1758	983	593	450	416	403	1454
Ba(SO_4=)	806	0	-	-	0	0	0
Pb	571	7	17	24	17	24	16
Pb(S)	683	8	8	15	10	13	14
Zn	849	21	70	96	34	65	28
Zn(S)	587	5	19	19	12	44	9
Cu	60	3	57	40	1	3	3
Cu(S)	58	2	42	37	1	3	3
S	-	-	-	-	-	-	-
Ag	-	-	-	-	-	-	-
Hg (ppb)	-	-	-	-	-	-	-
Rb	18	54	21	19	139	108	85
Sr	172	114	314	345	42	19	255
Zr	117	107	81	168	248	386	116
Mo	-	-	=3	=3	-	-	-
Ni	4	5	56	48	2	3	17
Co	35	49	31	31	43	48	36
Cr	10	9	163	77	7	8	10
V	14	45	356	262	14	10	41
Th	-	16(1)	-	-	23(1)	14(1)	-
U	-	0(1)	-	-	3(1)	4(1)	-
Ga	-	12(1)	-	-	14(1)	24(1)	-
n =	5	3	9	18	12	5	3

Figure 5-1: Alkali: silica diagrams for Buchans Group flows
(small dots), low-titanium diabase (stars) and
Feeder Granodiorite (large dots). Dividing line
between alkaline and subalkaline fields after
Irvine and Baragar (1971).

oceanic tholeiites and have correspondingly lower Ni, Cr
and K/Rb (Table 5-1).

In contrast, the lithologies and depositional
environments of the Buchans Group volcanics, combined with
the general chemical nature of Buchans Group flows, indicate
that these rocks are most similar to modern calc-alkaline
suites. A triangular FMA diagram, presented in Fig. 5-2
demonstrates a lack of iron enrichment, a characteristic
of calc-alkaline suites.

The general elemental abundances of Buchans Group
flows are also similar to those of calc-alkaline suites of
modern island arcs. K_2O, an important element in discrimina-
ting volcanic suites, averages uniformly around 1% in
Buchans Group mafic flows, similar to that of high alumina
basalts (Fig. 5-3). According to the classification scheme
of MacKenzie and Chappel (1972) for calc-alkaline rocks,
Buchans Group mafic and intermediate flows span a range from
high Alumina basalt to dacite. Other elemental abundances
of Buchans Group flows are closely comparable to those of
calc-alkaline suites of modern island arcs.

Diagrams involving the relatively immobile elements
Ti, Zr (Figs. 5-4 and 5-5) show the bulk of Buchans Group
mafic flows plotted in the field of calc-alkali basalts.

K:Rb ratios of Buchans Group flows encompass a
range from 250 to 900, centering around 450 (Fig. 5-6), a
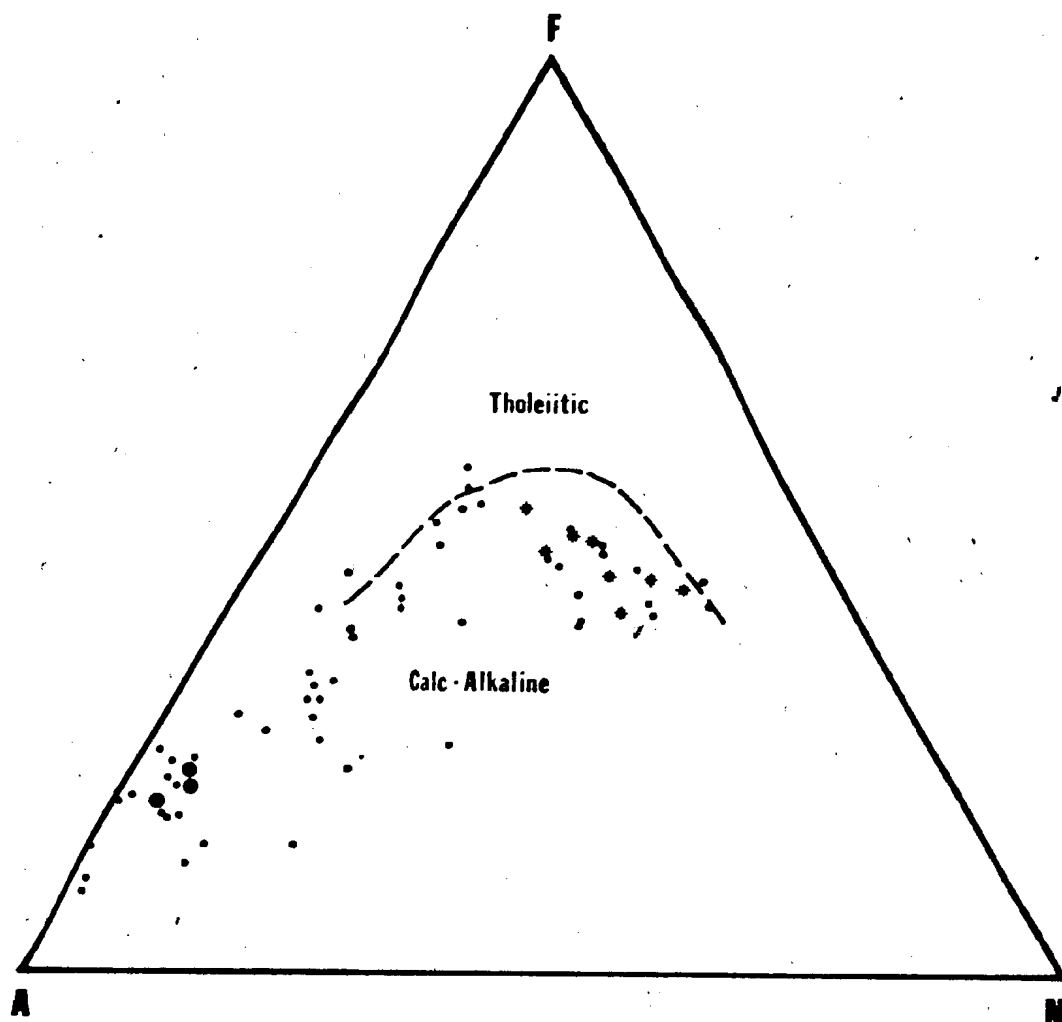
Figure 5-2: AFM diagram for Buchans Group flows (small dots), low-titanium diabase (stars) and Feeder Granodiorite (large dots). $A = Na_2O + K_2O$, F = total Fe as FeO, $M = MgO$. Dividing line between calc-alkaline and tholeiitic suites after Irvine and Baragar (1971).
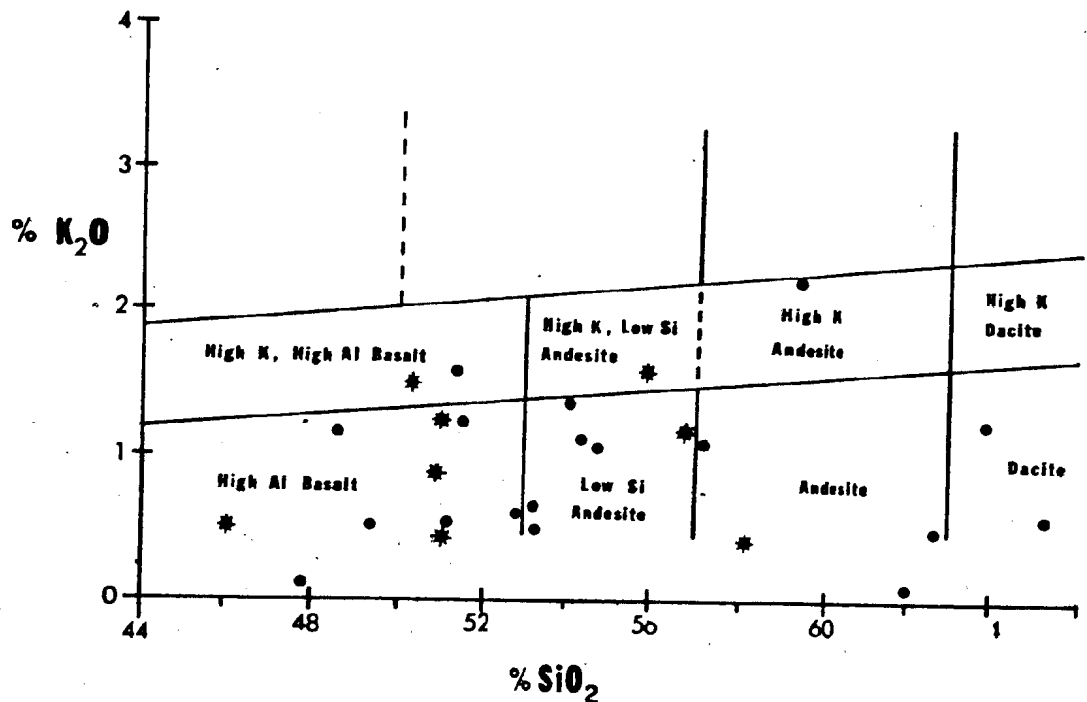
Figure 5-3: K_2O: SiO_2 classification of calc-alkaline rocks after MacKenzie and Chappel (1972). Buchans Group flows (dots) and low-titanium diabase (stars).
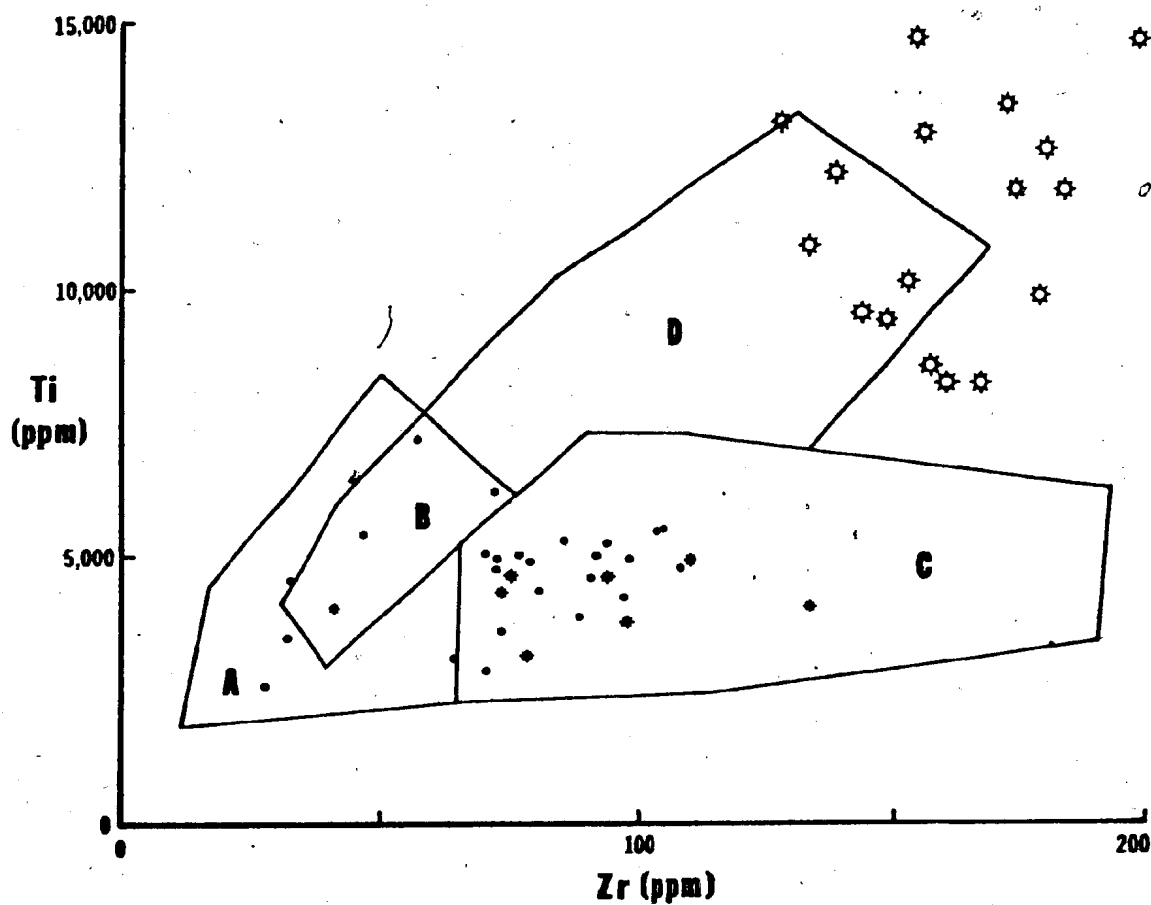
Figure 5-4: Ti:Zr diagram for Buchans Group basalts (dots),
low-titanium diabase (solid stars) and high-
titanium diabase (open stars). Fields A to D
after Pearce and Cann (1973). A = low potash
tholeiites, C = calc-alkali basalts, D = ocean
floor basalts, B = overlap of fields A, C and D.
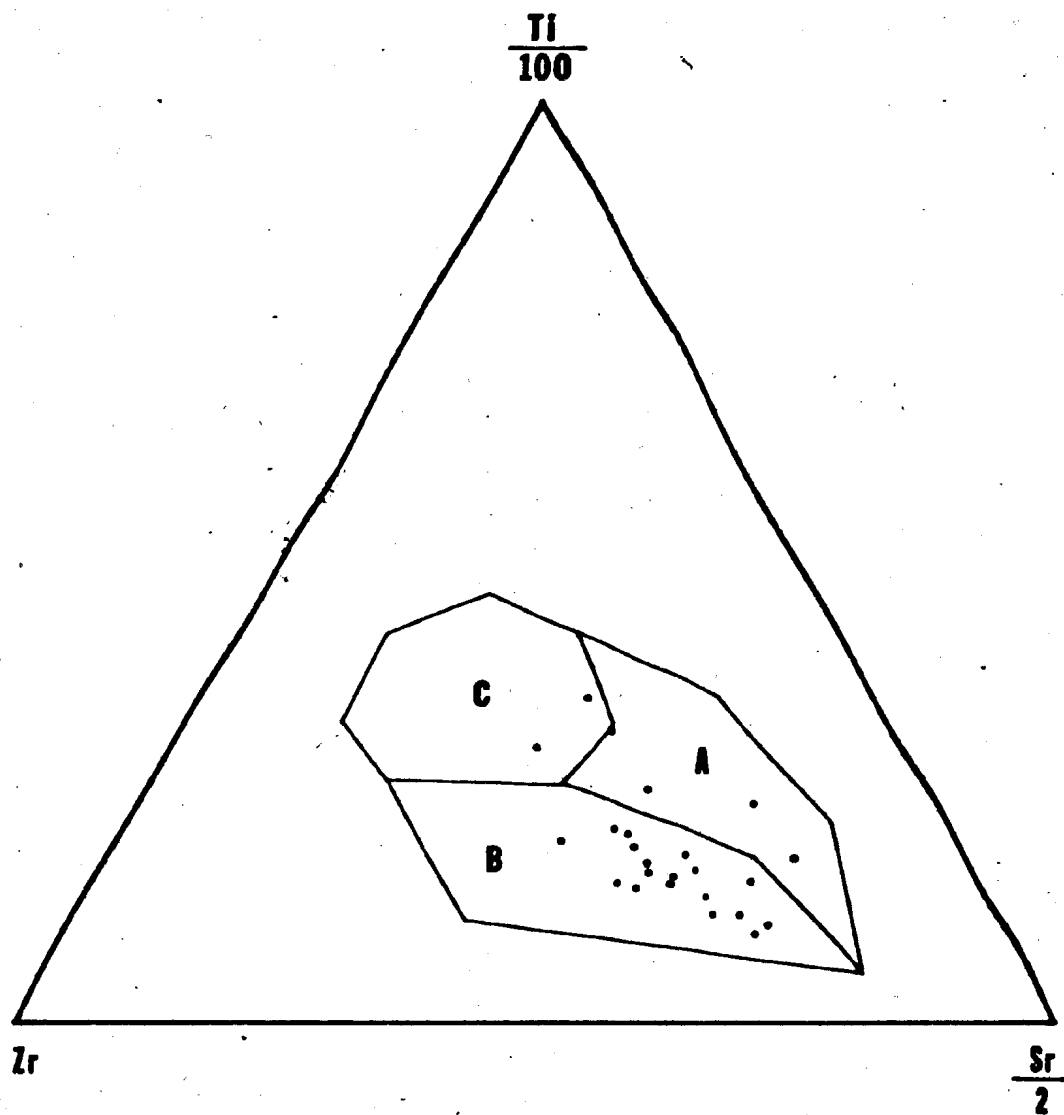
Figure 5-5: Ti/100: Zr: Sr/2 diagram for Buchans Group
basalts. Fields A, B and C after Pearce and
Cann (1973). A = island arc basalts, B =
calc-alkali basalts, C = ocean floor basalts.
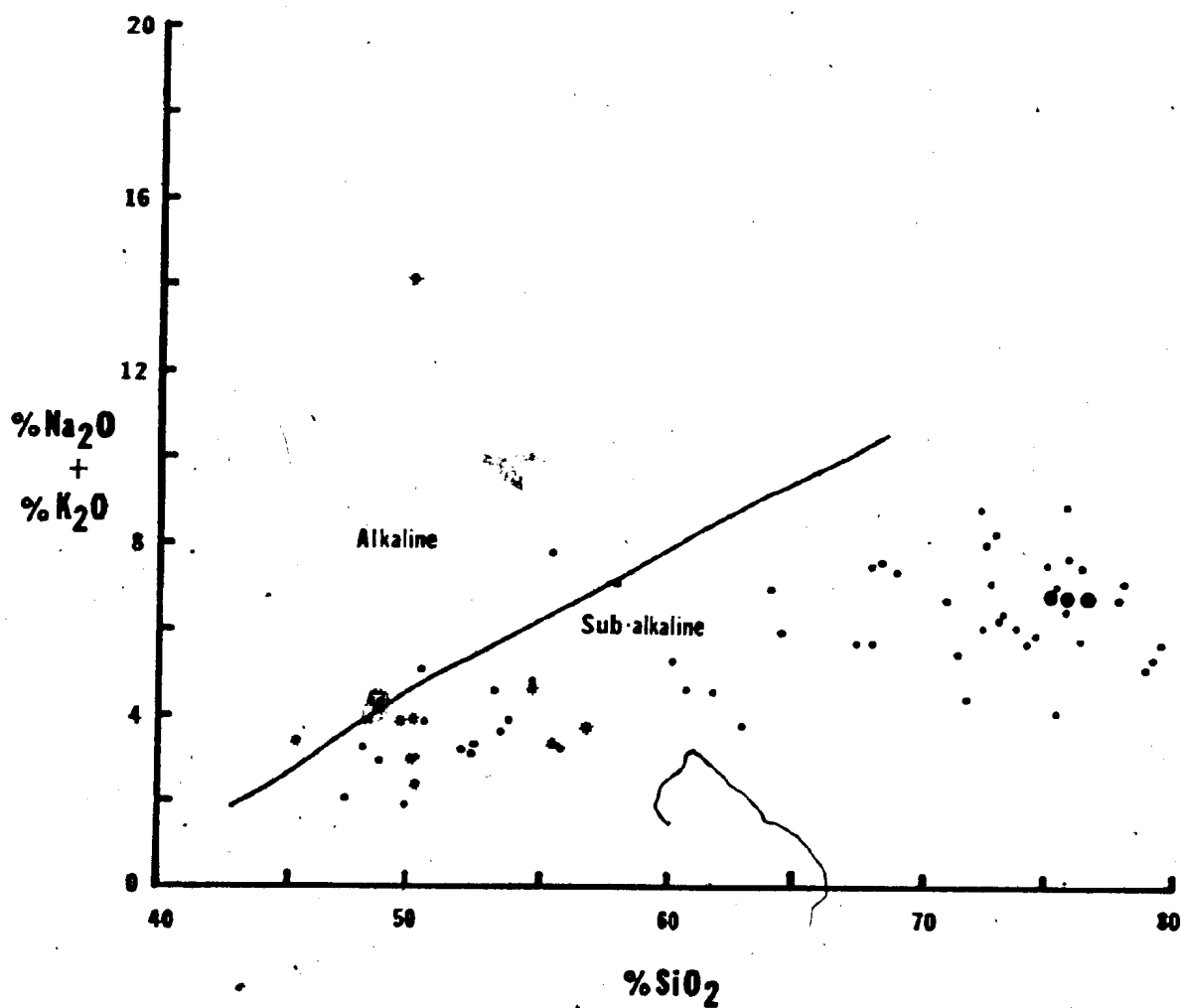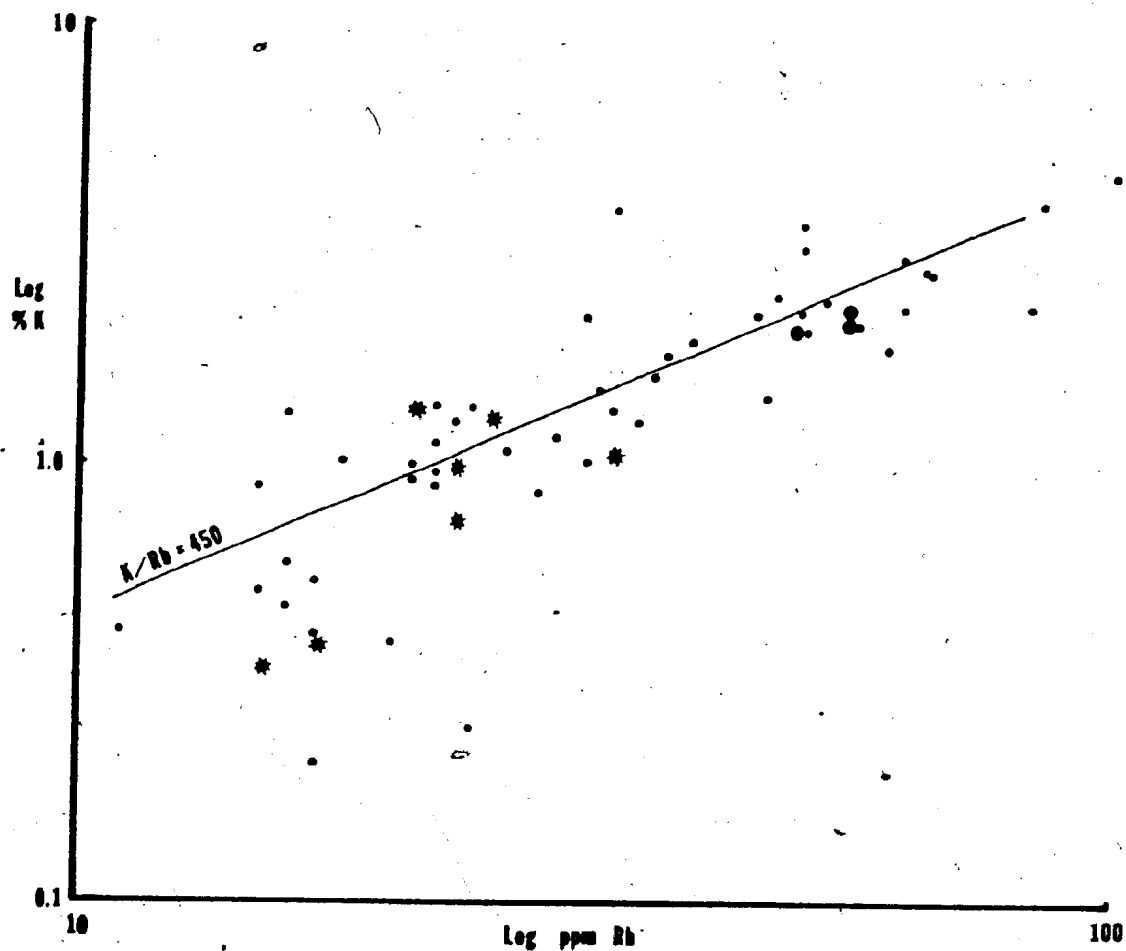
Figure 5-6: K: Rb diagram for Buchans Group Flows (small dots) low titanium diabase (stars) and Feeder Granodiorite (large dots).

fairly typical average for modern island arc sequences.

A histogram of SiO_2 abundances in Buchans Group flows is given in Fig. 5-7. The diagram shows a relative paucity of samples of "intermediate" composition yielding a weakly bimodal distribution. Sampling bias obviously has a major effect on this diagram, however from general observation the author considers the dominance of mafic and felsic volcanics over those of intermediate composition to be a reality. Compared to other Newfoundland calc-alkaline mafic to felsic volcanic suites, the Buchans Group has relatively more abundant intermediate volcanics (Strong, 1975).

A correlation matrix for Buchans Group flows is given in Table 5-2. In general, the predictable elemental associations are observed amongst both major and trace elements. Of particular interest to this study is the behavior of the base metals and barium. Pb shows a near perfect correlation with Pb(S) and little correlation with any other element. This would seem to indicate that the bulk of Pb in Buchans Group flows occurs almost exclus-ively as minute sulphides which show preference for no specific host mineral phase. Cu shows a very strong correlation with Cu(S) and weaker association with Fe, Ca and Mg. This seems to indicate that it occurs as minute sulphide within Fe, Ca and Mg-bearing phases (e.g. chlorite,
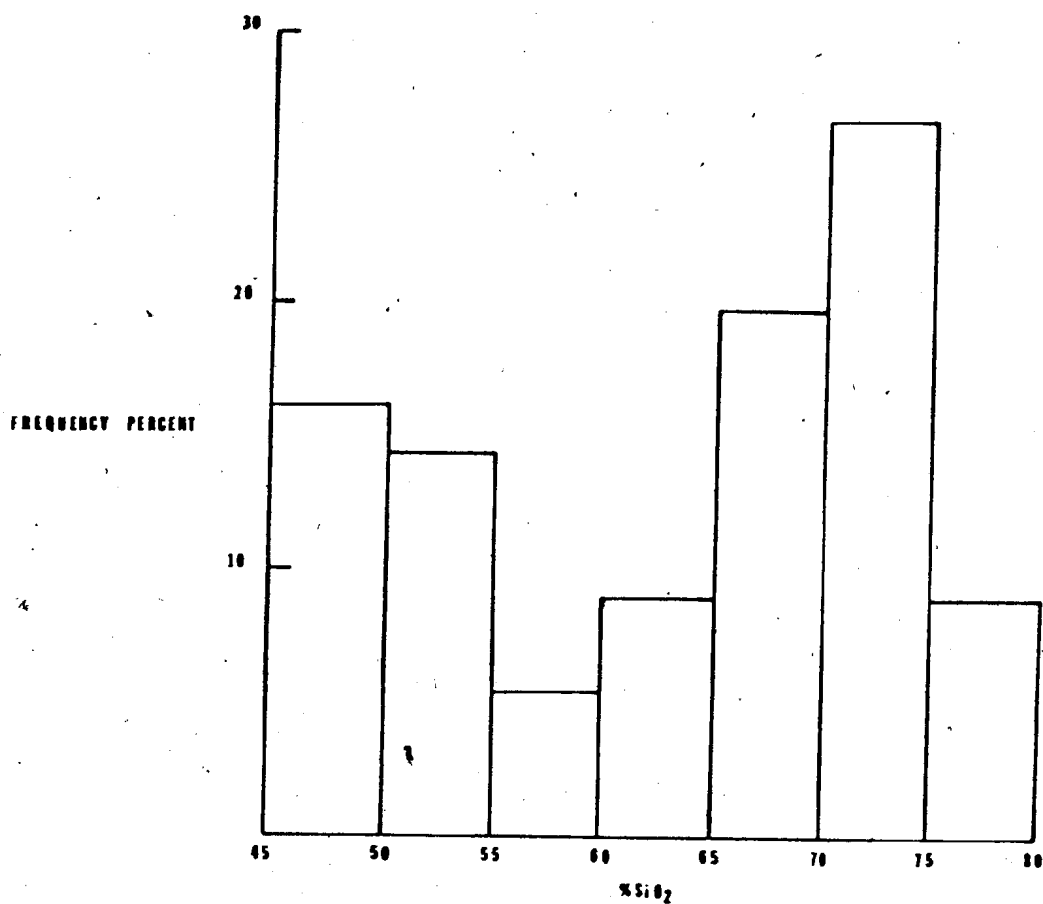
Figure 5-7: Histogram of SiO_2 contents of Buchans Group flows (n = 56). The relative lack of samples of intermediate composition is not a function of sampling error.

Table 5-2: Correlation matrix for Buchans Group flows (n=54). Decimal points are omitted.

	Fe_2O_3	TiO_2	SiO_2	CaO	K_2O	MgO	Al_2O_3	Na_2O	L.I.	MnO	Zr	Sr	Rb	Zn	Cu	Ba	Cu(s)	Pb(s)	Zn(s)	Pb	Ni	Co	Cr
TiO_2	85																						
SiO_2	-92	-81																					
CaO	85	76	-92																				
K_2O	-56	-60	50	-63																			
MgO	82	70	-91	84	-48																		
Al_2O_3	68	64	-74	58	-18	59																	
Na_2O	-46	-29	56	-58	04	-62	-33																
L.I.	45	33	-65	59	-30	59	29	-51															
MnO	76	64	-70	62	-51	60	48	-23	38														
Zr	-66	-38	65	-61	28	-59	-35	45	-47	-56													
Sr	49	47	-49	60	-48	39	41	-17	13	34	-05												
Rb	-62	-63	55	-60	88	-50	-27	00	-30	-47	37	-45											
Zn	40	42	-28	20	-43	21	22	11	18	56	-16	11	-37										
Cu	82	61	-77	78	-45	66	52	-46	35	56	-67	37	-49	20									
Ba	33	-31	38	-38	52	-39	-21	23	-41	-15	23	-11	47	-14	-14								
Cu(s)	73	56	-71	70	-40	65	47	-40	33	52	-60	29	-48	16	90	-18							
Pb(s)	-12	01	13	-14	04	-05	-02	07	-12	-02	23	-12	03	25	-11	11	-08						
Zn(s)	20	32	-08	04	-09	-02	14	13	-06	15	-05	07	-25	42	12	-06	24	27					
Pb	00	12	00	00	-07	05	06	01	-04	06	13	-05	-07	30	00	04	-01	98	23				
Ni	62	59	-78	78	-42	84	44	-56	59	49	-39	42	-41	05	51	-21	55	-08	-10	00			
Co	22	41	-20	30	-35	21	04	-07	-07	16	10	36	-36	01	23	-03	16	07	03	10	31		
Cr	60	57	-76	75	-38	77	44	-52	57	48	-39	46	-36	07	50	-14	44	-08	-11	01	87	25	
V	84	64	-78	78	-46	68	50	-48	46	53	-63	48	-52	31	78	-25	60	-16	03	-04	51	29	50

epidote, calcite, plagioclase) and also shows limited
substitution for Fe and Mg in these minerals. The correl-
ation of Zn to Zn(S) is not nearly as strong as the
previous associations suggesting a complex occurrence of
Zn both as minute sulphide and also widely substituted
for Fe in various phases.

The behavior of Ba in flows is important to
later discussions. K is the closest associate of Ba, with
other elements showing little consistent correlation.
This would seem to indicate that the major controlling
factor on Ba distribution is the abundance of K_2O and that
Ba most commonly occupies K lattice sites.

Harker diagrams, for Buchans Group flows, plotting
anhydrous weight percent and ppm of the various oxides,
elements and loss on ignition against silica, are presented
in Fig. 5-8. Also plotted on these diagrams are samples of
low-titanium diabase and the Feeder Granodiorite. Though
Harker diagrams were previously presented by the author
(Thurlow, 1973), the diagrams presented herein are considered
much more reliable as fragmental rocks and altered flows are
omitted from the data.

The Harker diagrams are, for the most part, self-
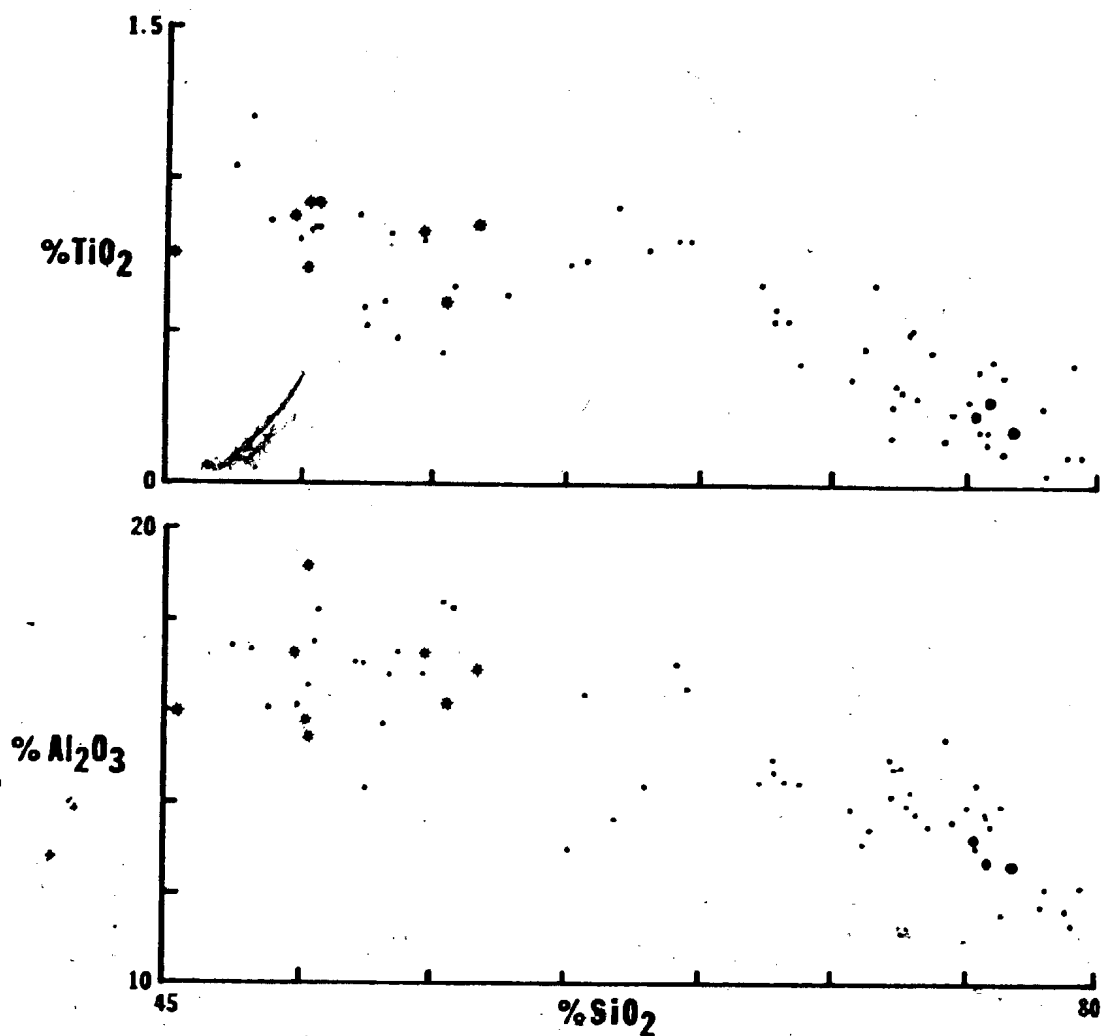explanatory and general comments are outlined in point form
below.

Figure 5-8:   Anhydrous Harker diagrams for Buchans Group
flows (small dots), low-titanium diabase
(stars) and Feeder Granodiorite (large dots).

Figure 5-8 (continued)
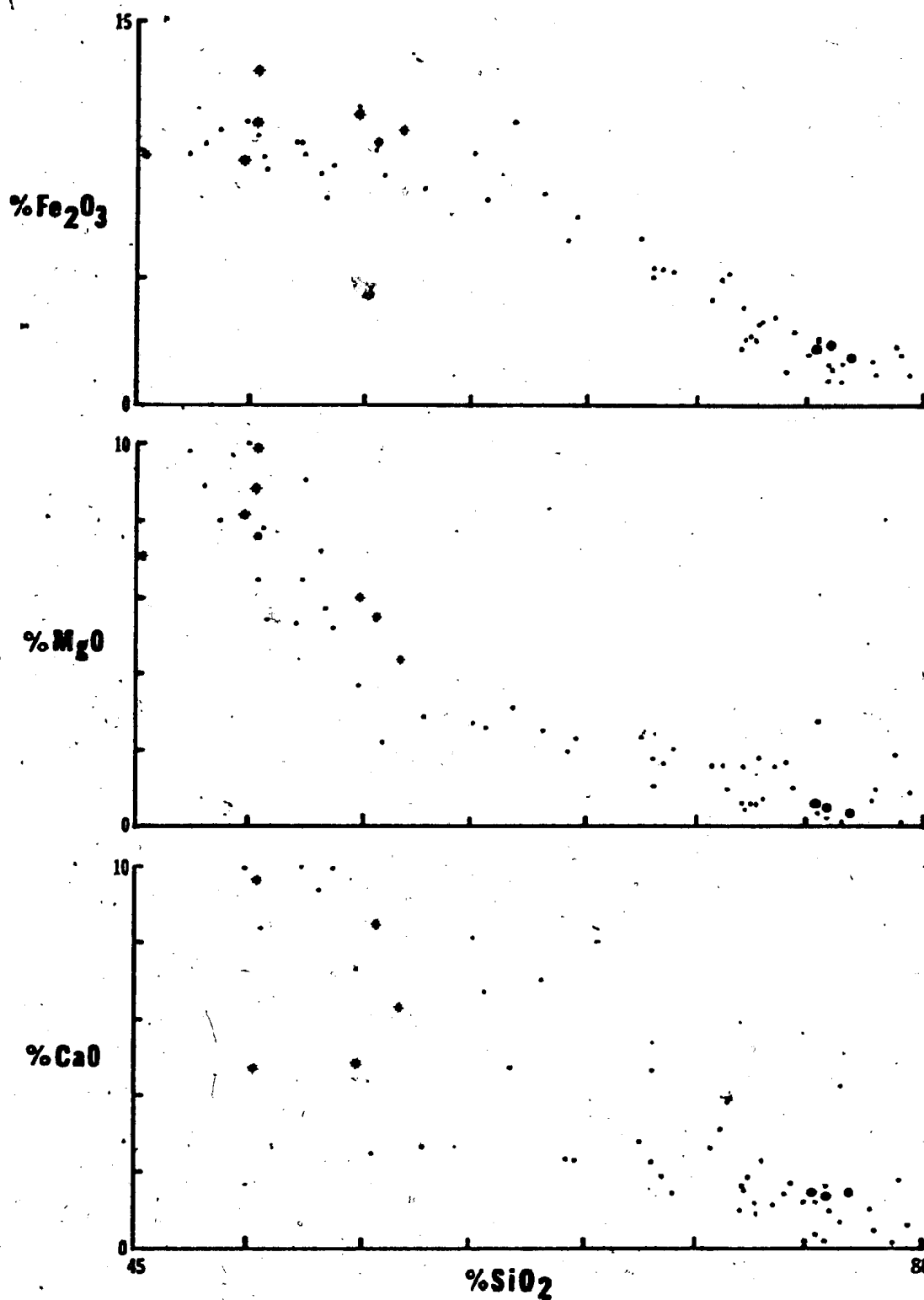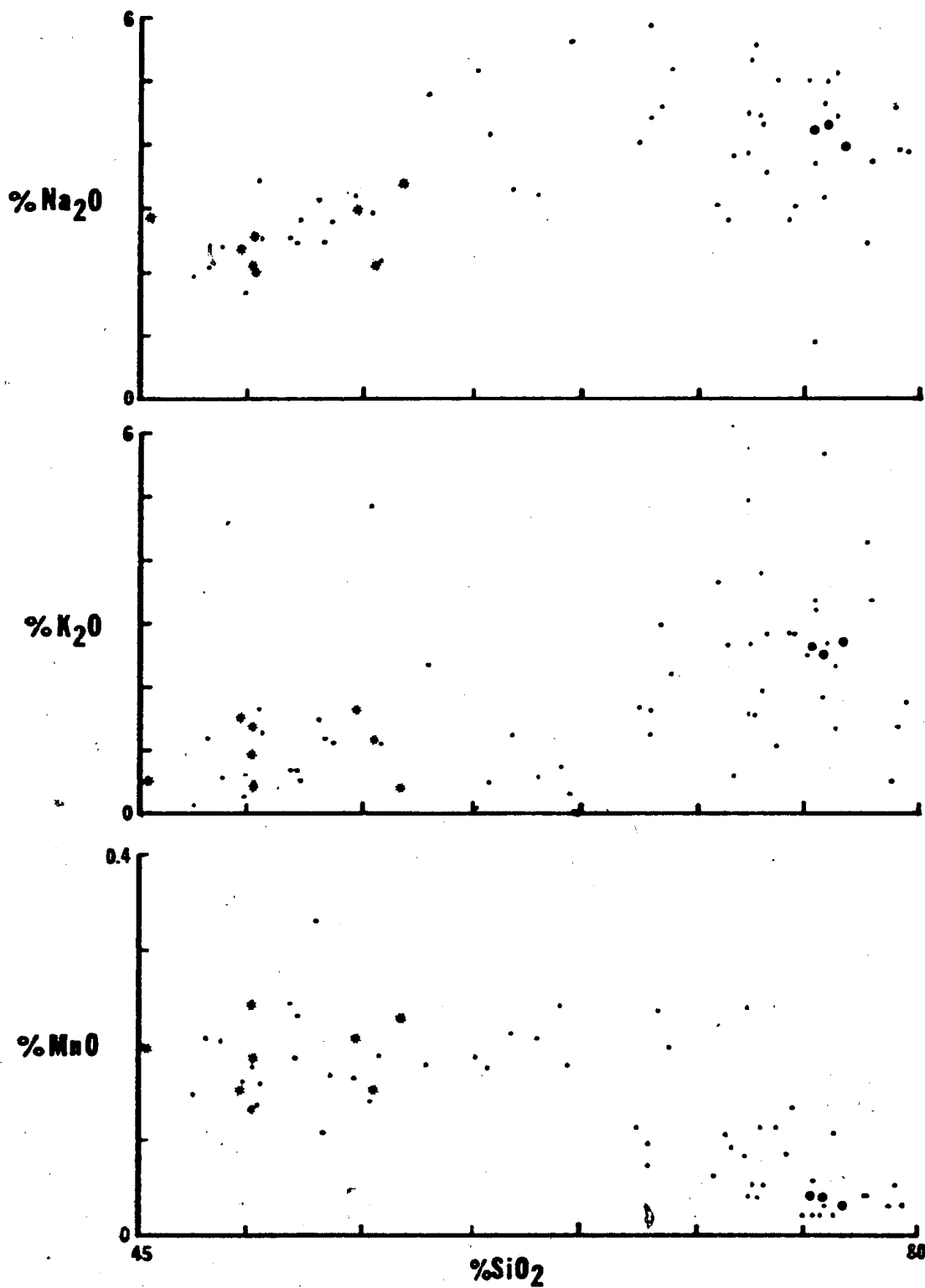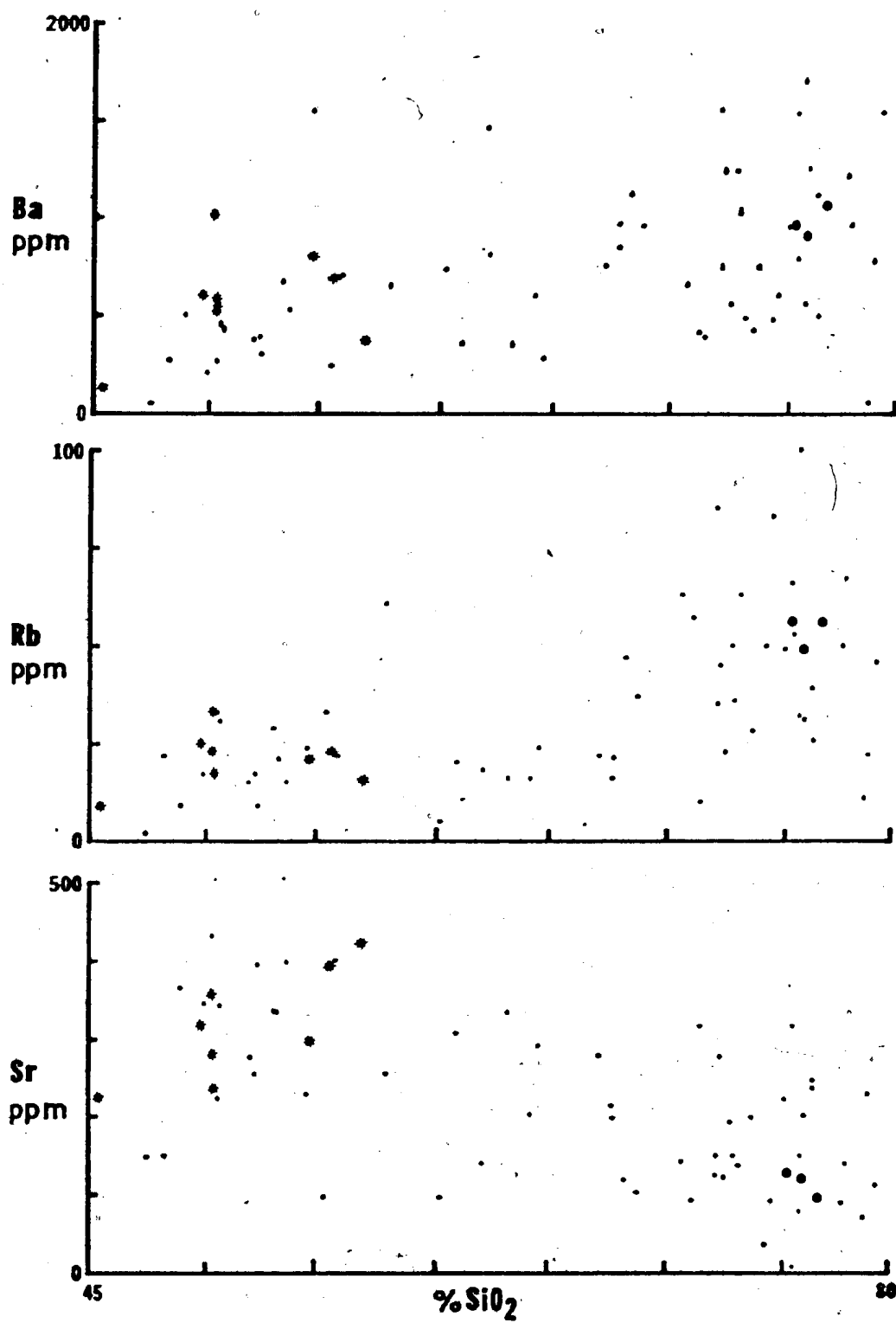
Figure 5-8 (continued)

%SiO_2

Figure 5-8 (continued)

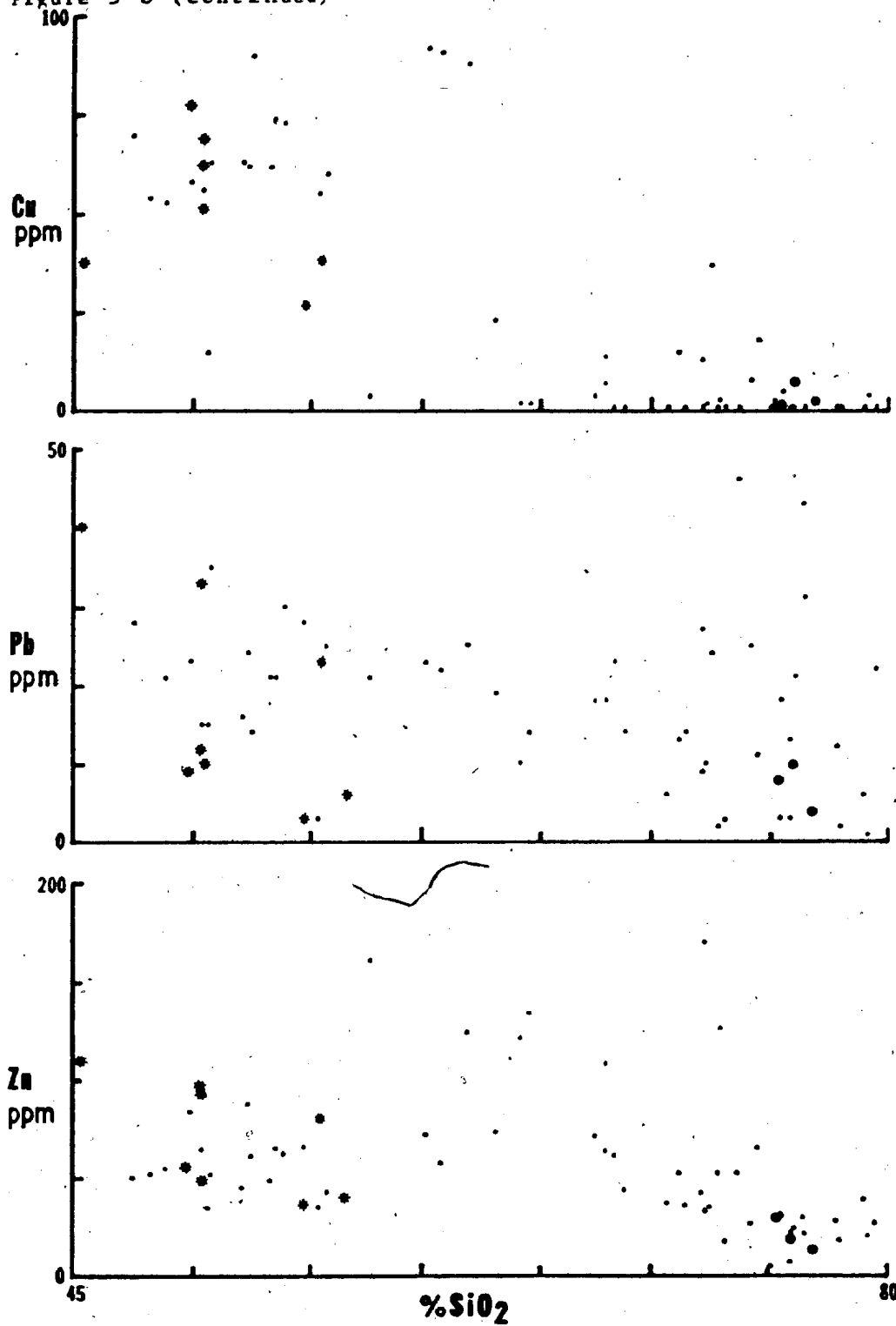Figure 5-8 (continued)

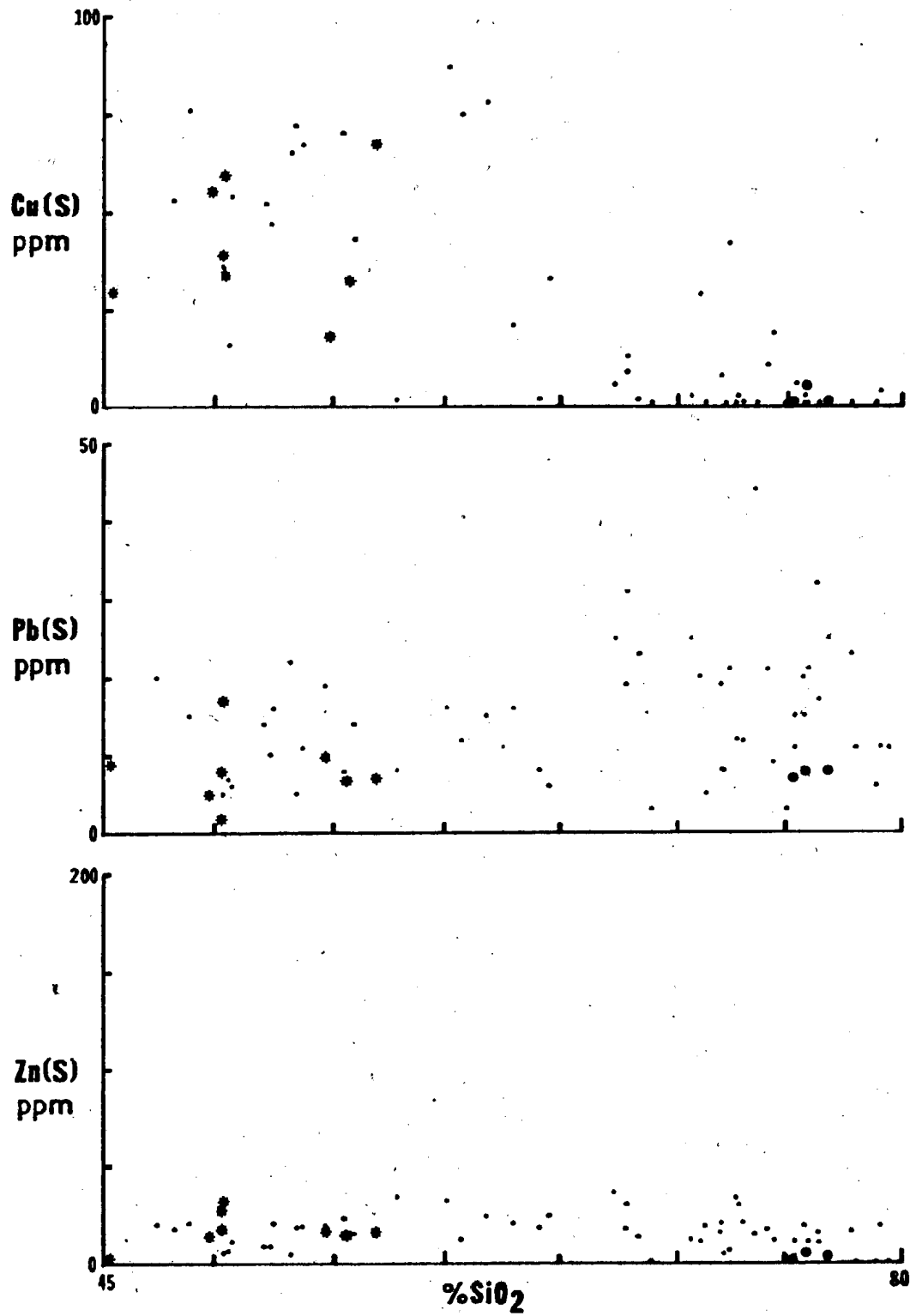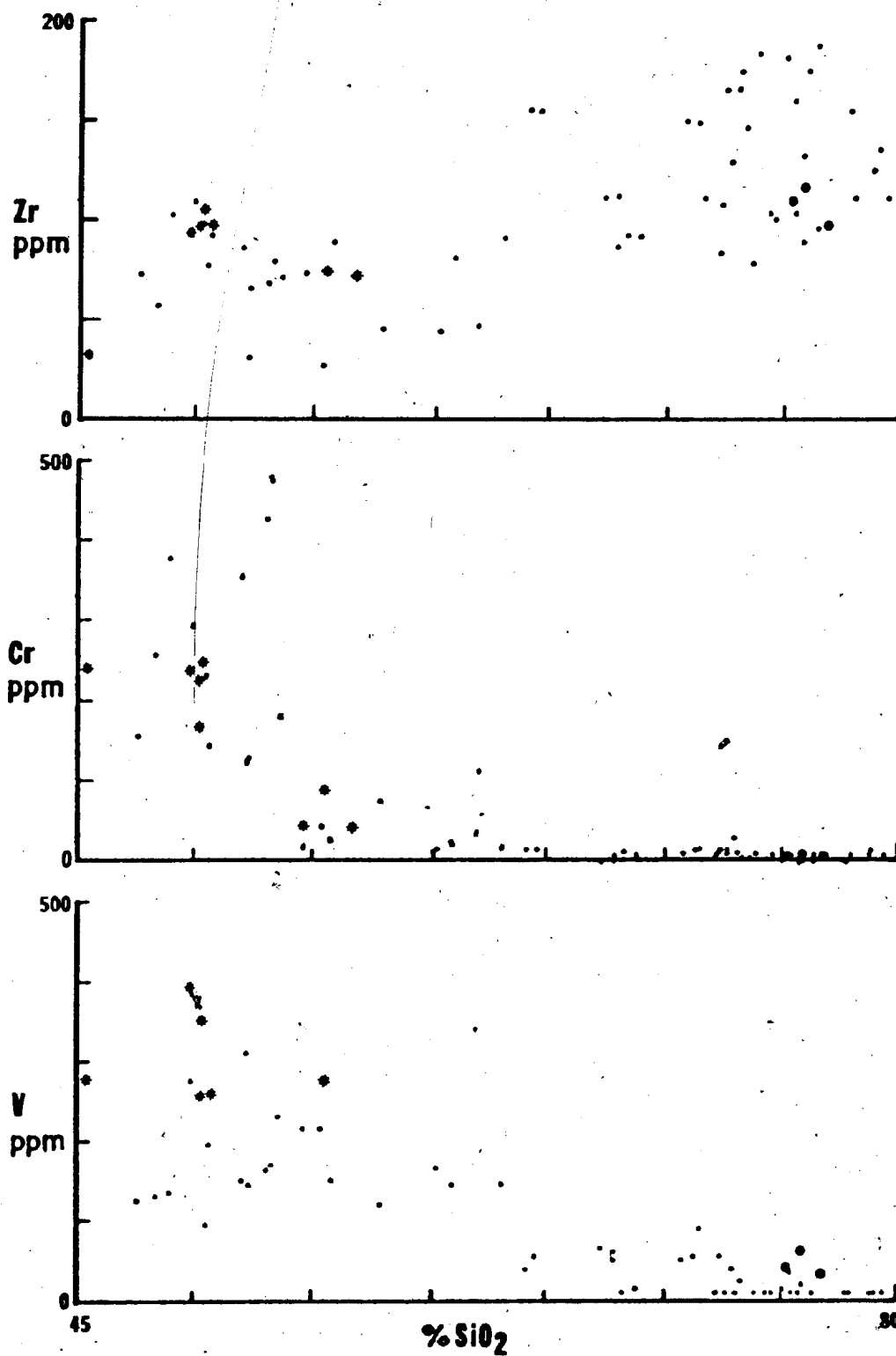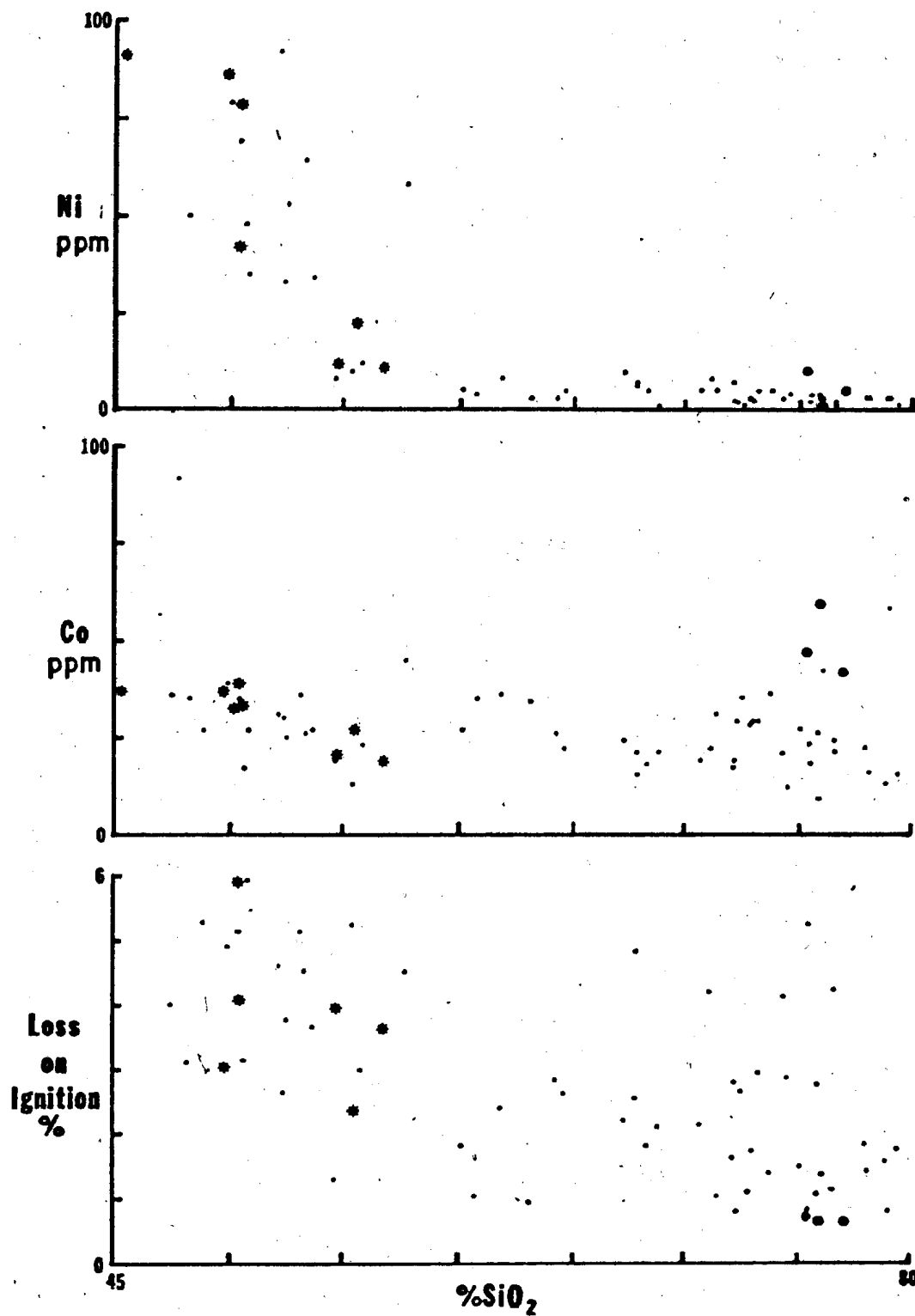Figure 5-8 (continued)

Figure 5-8 (continued)

Figure 5-8 (continued)

1) Buchans Group volcanic rocks span a compositional range
    from basalt to rhyolite but andesitic varieties are
    somewhat less common than more mafic and felsic end
    members.

2) The variation of all elements is that which is expected
    from normal petrological considerations. Most major
    elements decrease with increasing silica, in part
    because of simple dilution by silica (the "constant
    sum effect"). Only Na_2O and K_2O increase with increasing
    silica content. Among the trace elements, Ni, Cr, V,
    Sr, Cu and Cu(S) decrease and the large cations Rb, Ba
    and Zr increase with increasing silica. Somewhat
    surprisingly, Zn, Zn(S), Pb, Pb(S) and Co show little
    variation across the range of silica concentrations.

3) Anomalous scatter in some diagrams is probably largely
    due to post-depositional migration of elements. The
    elements most strongly affected (e.g. K, Rb, Ca, Sr)
    are those which are most easily mobilized in the secondary
    environment.

4) Despite scatter on some diagrams it is evident that all
    Buchans Group flows form a consanguineous mafic to felsic
    sequence. As such, there is no evidence to suggest that
    mafic and felsic members are not magmatically related
    nor is there any evidence to suggest that any portion of
    the Buchans Group has evolved from a magma distinct
    from the major magma source.

5) Both the low-titanium diabase and the Feeder Granodiorite
   plot entirely within the trends of the Buchans Group
   flows. This suggests a genetic link between these
   three lithologic groups.

6) Two types of variations are visible among elements which
   decrease in abundances with increasing silica. Some
   elements (e.g. Fe) show consistent and regular decrease
   whereas other elements (e.g. Mg, Ni, Cr, V) decrease
   rapidly at lower silica levels and less rapidly at
   higher silica levels. In the latter case this must
   indicate rapid removal of a specific phase(s) with
   increasing differentiation. Since no olivine has been
   identified at Buchans, this probably reflects fractiona-
   tion of augite.

5.3. Chemical Variations in Flows as a Function of
     Stratigraphic Position

The previous sections have dealt with overall
compositional variations within the Buchans Group. In this
section, variations in the composition of flows are examined
in order to determine whether variations in chemistry have
any stratigraphic significance. Such variations, if present,
presumably would reflect changing magmatic conditions. If
such variations are present, it is important to determine
whether they are of significance with respect to mineraliza-
tion or merely a result of normal petrologic processes. Of

particular interest in this study is whether unaltered
rhyolite flows in the ore-bearing Lucky Strike and Oriental
ore horizon sequences are chemically different from flows
elsewhere in the stratigraphic sequence.

Chemical data on mafic and intermediate flows of
the Footwall Basalt, Ski Hill Sequence, and Upper Buchans
Subgroup were plotted on one set of diagrams and data for
felsic flows of the Lucky Strike-Oriental Sequences, Prominent
Quartz Sequence and Upper Buchans Subgroup on a second series
of diagrams, yielding a total of over 50 diagrams. All
elements plotted were ratioed to Al_2O_3 based on the assump-
tion that significantly greater abundances of any element
in a given sample may "dilute" the abundances of elements
under scrutiny and consequently introduce apparent scatter
to the data.

5.3.1. Variations in Compositions of Mafic and Inter-
mediate Flows Through the Stratigraphic Sequence:
The distribution and number of samples (34) of these groups
of rocks is not wholly adequate to offer firm conclusions
as to whether any given stratigraphic unit differs significantly
from others. In general, as determined from extensive core
logging throughout the Buchans Group, there is no secular
change in the composition of flows through the stratigraphy.
Most mafic units are wholly basaltic and only the Ski Hill
sequence contains significant amounts of andesite. Within

the basaltic units, the chemical diagrams plotted indicate
that there is no significant difference for any elements
between units at differing stratigraphic levels. For
example, the large cations (e.g. K, Rb, etc.) do not
increase in abundance with stratigraphic height as has been
found in some island arc sequences (e.g. Kuno, 1966; Sugimura,
1968; Jakes and White, 1971; Kean and Strong, 1973). Samples
of more intermediate flows from the Ski Hill sequence form
a continuum on the variation diagrams with more mafic
counterparts from other units indicating that differences
in elemental abundances are not due to any geochemical
peculiarity but instead are a function of normal magmatic
processes.

In essence, the limited amount of geochemical data
seems to indicate that there is no geochemical anomaly
associated with any particular mafic unit. The Ski Hill
sequence, which is the mafic unit most closely associated
with mineralization, is "anomalous" only in that it contains
a greater abundance of truly intermediate rocks as opposed
to the other largely basaltic sequences.

5.3.2. Variations in Compositions of Felsic Flows
Through the Stratigraphic Sequence: Almost
all elements show no essential differences in composition
between felsic flows of the Lucky Strike-Oriental sequences,
Prominent Quartz sequence and Upper Buchans Subgroup. In

general, flows of the ore-bearing Lucky Strike-Oriental
sequences are compositionally more homogeneous than other
flows though this may only reflect the volumetrically
less abundant and spatially more restricted nature of these
flows. MgO and MnO tend to be less abundant in the ore
horizon flows than in the two other groups (Fig. 5-9). This
probably reflects lesser quantities of chlorite after
amphibole. CaO and Fe_2O_3 tend to be slightly more abundant
in the Prominent Quartz Sequence rhyolites than in the
other two groups (Fig. 5-9) probably reflecting the greater
abundance of epidote after plagioclase visible in these rocks.

Apart from the above-mentioned small differences,
felsic flows of the Lucky Strike-Oriental sequences are
similar to other felsic flows of the Buchans group. The major
ore-forming elements, Zn, Pb and Cu are not present in
greater abundances. Ba is marginally higher in ore horizon
rhyolites but shows a strong affinity to K_2O (correlation -
.87). K_2O is likewise marginally higher in the ore horizon
rhyolites.

Tasumi and Clark (1972) and Ishihara (1974) have
shown (on the basis of a limited number of analyses) that
felsic lavas genetically related to mineralization in the
Hokuroku district are somewhat more differentiated than
lavas unrelated to mineralization. A plot of silica vs.
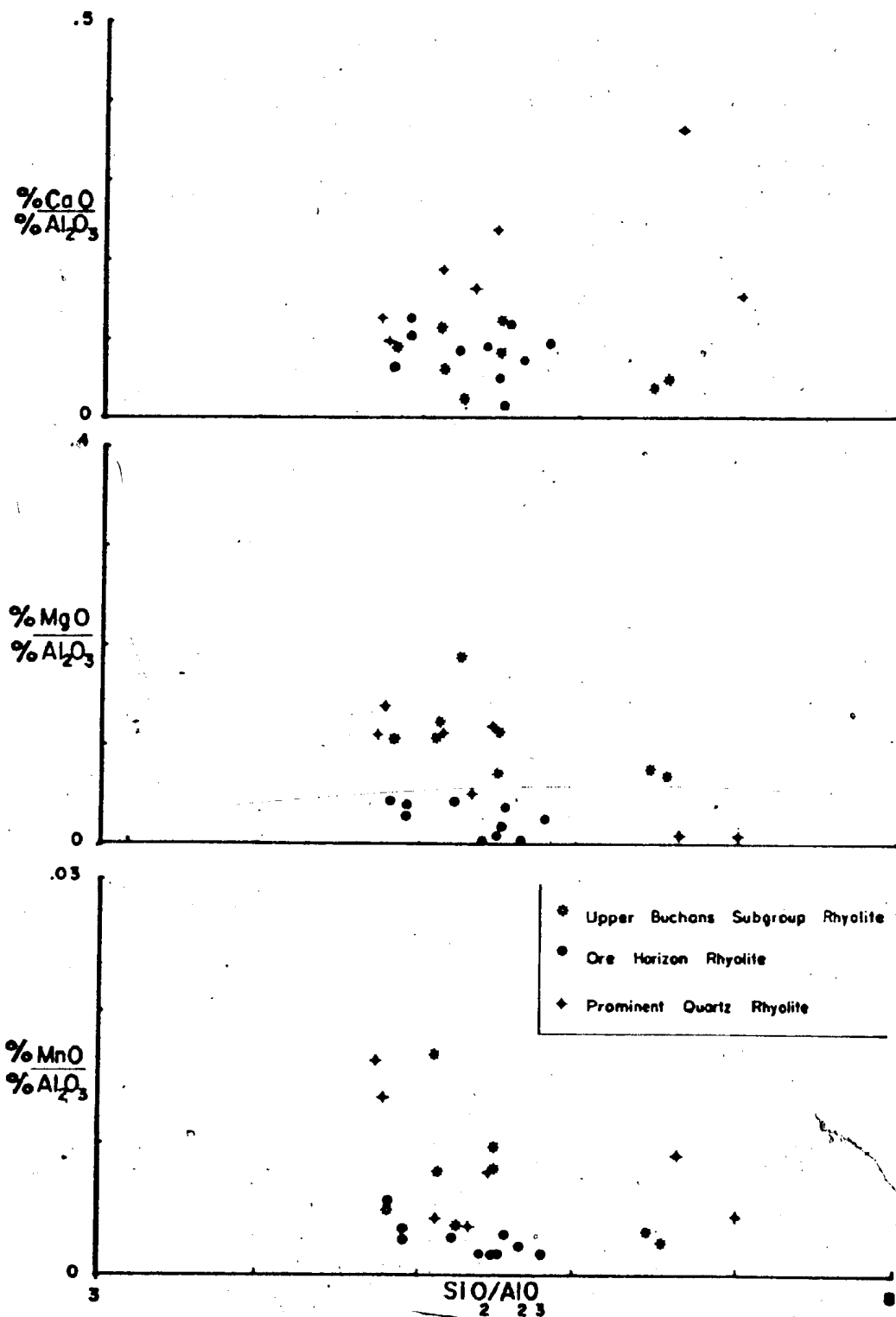Thornton and Tuttle's differentiation index for Buchans Group

Figure 5 - 9 :   CaO, MgO and MnO variations in flows as a
function of stratigraphic position.

felsic flows is presented in Fig. 5-10. On the basis of a limited number of analyses, it appears that for a given silica content, felsic flows of the ore-bearing Lucky Strike-Oriental ore horizon sequences are more "differentiated" than similar flows of other formations. The number of samples involved in this comparison is not sufficient, to firmly establish whether this distinction is actually statistically significant. Many more analyses combined with detailed petrographic work are required to determine the validity of this hypothesis. Such work could prove fruitful for the outcome would have a bearing on the overall source of metals, whether magmatic or leached from country rock.

5.3.3. Some Comments on the Chemistry of "White Rhyolite" at Buchans:

The presence of "white rhyolite" associated with many massive sulphide deposits is of theoretical and practical exploration interest. As indicated in Chapter Four, "white rhyolite" at Buchans displays a more tenuous relationship to mineralization than in the Kuroko deposits but, nonetheless, is generally linked to the presence of ore.

Two analyses of Buchans "white rhyolite" are presented in Table 5-3. Compared to associated unaltered rhyolite, and holding alumina constant, the "white rhyolite" has suffered massive introduction of K_2O, SiO_2 and Ba and removal of Fe_2O_3, Na_2O and CaO. Mineralogically this is

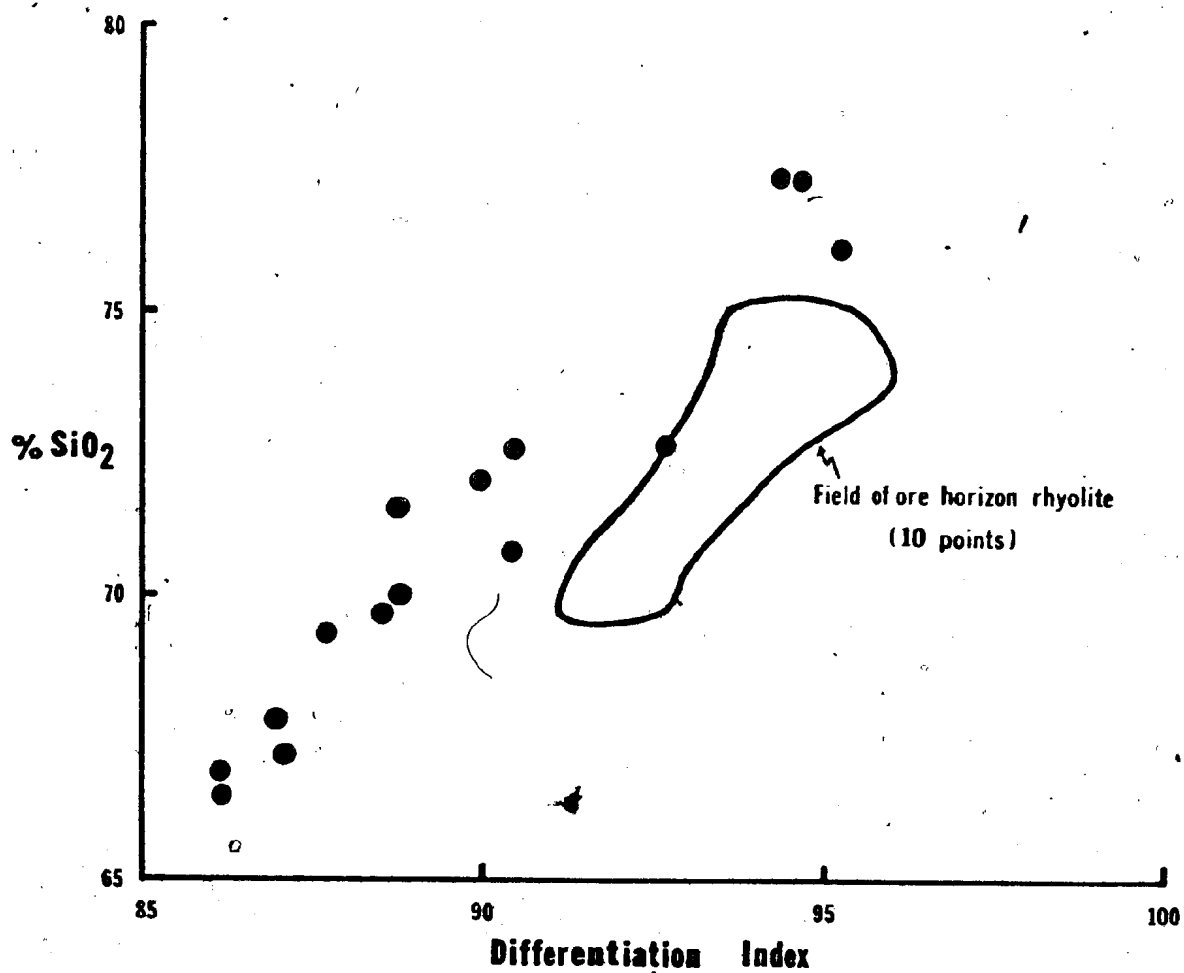Figure 5-10: SiO$_2$: differentiation index plot comparing un-
altered ore horizon rhyolites to rhyolites at
other stratigraphic positions.

Table 5-3: Composition of "white rhyolite" compared
to other ore horizon rhyolites

	WHITE RHYOLITE		
	1083-586	1730-1203	10 Ore Horizon Rhyolites
SiO_2	73.3	75.6	72.7
TiO_2	.39	.22	.31
Al_2O_3	12.91	10.29	13.68
Fe_2O_3	.03	.01	1.94
MnO	.01	.01	.04
MgO	.60	.01	.34
CaO	.44	.76	1.12
Na_2O	1.52	.36	4.47
K_2O	7.64	7.93	3.06
L.O.I.	1.68	1.62	1.49
Total	98.52	96.81	99.15
Ba	2982	4639	1175
Pb	3	32	15
Pb(S)	6	69	16
Zn	19	455	28
Zn(S)	22	460	13
Cu	1	1	6
Cu(S)	2	5	6
Rb	62	63	52
Sr	49	119	192
Zr	166	147	146
Ni	1	2	3
Co	27	42	26
Cr	0	0	9
V	10	15	22

reflected in conversion of normal rhyolite to an entirely
secondary assemblage composed essentially of quartz and K-
feldspar. This mineralogy contrasts with the quartz-
sericite-rich assemblage of the Japanese "white rhyolite"
(Date and Taniumura, 1974).

5.3.4. Summary: Based upon a limited number of
analyses of mafic intermediate and felsic flows (total 54
analyses) there appear to be no distinct changes in com-
position in Buchans Group volcanics throughout the strati-
graphic sequence. The mafic and felsic units most closely
associated with mineralization are chemically very similar
to other such units throughout the Buchans Group and do not
appear to contain abnormal amounts of base metal or barium.
As such, there appear to be no magmatic changes associated
with ore horizon rocks that have a bearing on the presence
of mineralization. Similar results to these were obtained
at Noranda by Larson and Webber (1977).

5.4. Geochemical Comparison of Flows and Cogenetic Fragmental
    Rocks

In any rock geochemical study it is important to
distinguish and separate those processes which cause chemical
change as a result of mineralization from other processes
unrelated to mineralization. In an effort to understand
the gross post-magmatic chemical changes involved in

pyroclastic rocks of the Buchans Group, a study was under-
taken to compare the chemistry of massive flows with associated
flanking pyroclastic rocks. This study was based on two
reasonably sound assumptions, i.e., 1) that flows and
stratigraphically related pyroclastic rocks were originally
derived from chemically similar magmas (i.e., are cogenetic),
and 2) that the composition of flows more closely approx-
imates that of the original magma. In view of the overall
chemical coherence of all Buchans Group volcanic rocks and
in view of similarities of phenocryst composition between
flows and associated pyroclastics, assumption No. 1 appears
valid. Petrographic comparison of flows and related pyro-
clastics indicates that the more permeable fragmental rocks
have invariably undergone greater degrees of alteration
than related flows and thus, assumption No. 2 also appears
valid.

Chemical data on flows and related pyroclastics
were plotted for five groups of lithologies, i.e., mafic
and intermediate rocks of the Footwall Basalt and Ski Hill
horizons and felsic rocks of the Lucky Strike-Oriental
sequences, Prominent Quartz sequence and Upper Buchans
Subgroup, yielding a total of over 100 diagrams. Flows
and related fragmentals were plotted on the same diagrams
to assist visual comparison. All elements were ratioed to
Al_2O_3 based on the assumption that Al_2O_3 remained relatively
inert during chemical change. The effect of this ratio is

to eliminate effects of variable addition of extraneous
elements (and consequent variable dilution of elements
under scrutiny) which would cause apparent increased scatter
of data points.

In virtually all cases, flows form more coherent
groups than related pyroclastics, supporting the contention
that they have undergone less post-magmatic chemical change.
Apart from differences in scatter, differences in general
abundances between the two groups were normally not signifi-
cant. Only Co showed consistent behavior in all groups,
being higher in flows relative to cogenetic pyroclastic
rocks.

Among the mafic and intermediate rocks of the
Footwall Basalt and Ski Hill sequence, Ca is generally
higher in flows (unavoidable calcite amygdules) as is Mn
and Co. There is a tendency for Zn and K to have been
added to the related fragmentals in each case.

Among felsic sequences compared, all had higher
Na and Co in felsic flows as compared to cogenetic crystal-
vitric tuffaceous rocks. Apart from these general tendencies,
the felsic rocks of the Prominent Quartz sequence and Upper
Buchans Subgroup showed no essential differences for all
other elements.

In contrast, the Lucky Strike-Oriental felsic flows
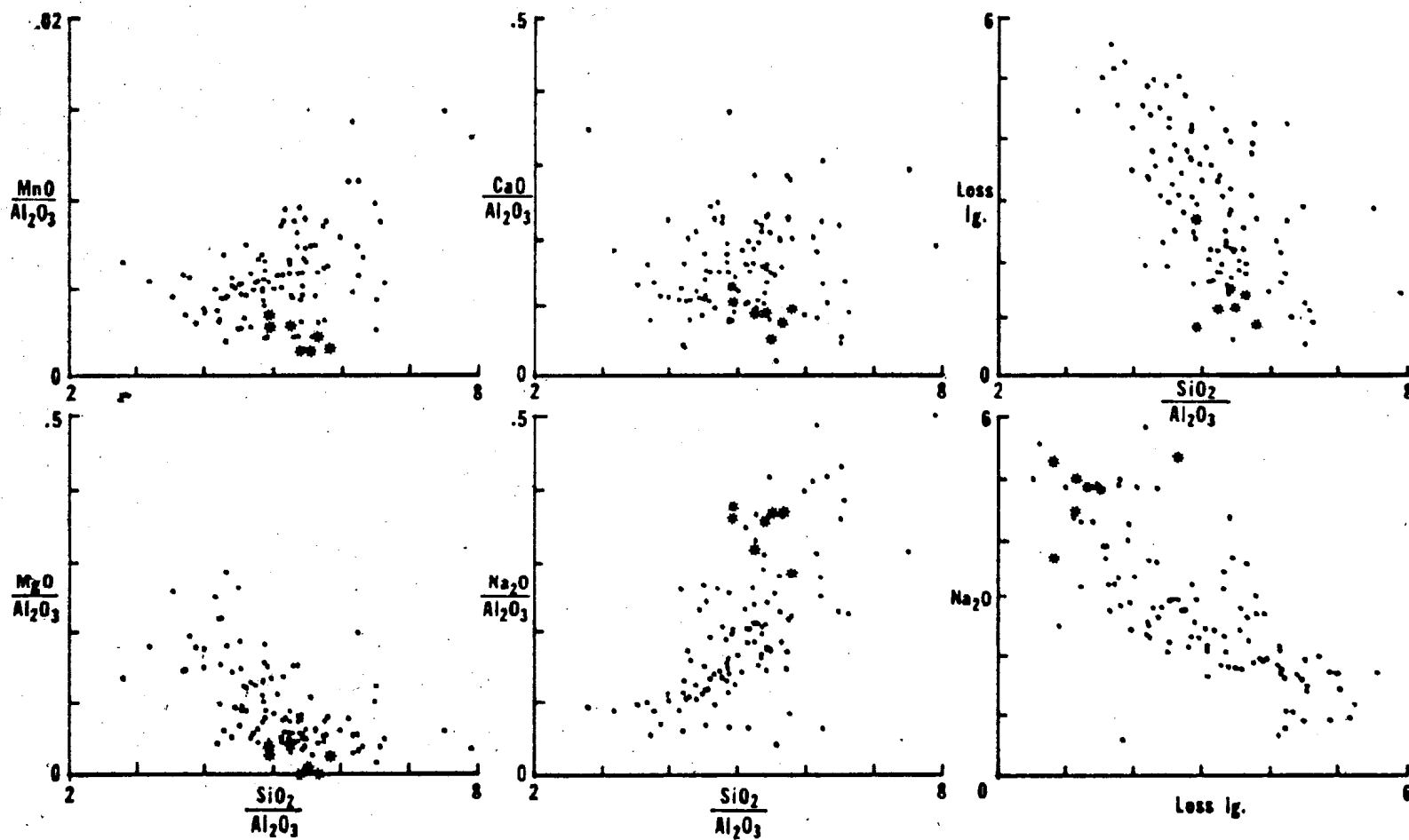and crystal-vitric tuffs show a number of additional

Figure 5-11:   Geochemical comparison of ore horizon dacitic tuffs (dots) and
rhyolite flows (stars).

differences. Dacitic crystal-vitric tuffs tend to be higher than flows in Mn, Mg, Ca, loss on ignition, Rb and Cu and lower in Co, Si and Na (the more significant of these are shown in Fig. 5-11). In view of the similar phenocryst mineralogy and proportions, and similar alteration of phenocrysts in these two groups of rocks, it can be reasonably assumed that all of these elemental differences reflect post-magmatic changes in chemistry of matrix glass in the crystal-vitric tuffaceous rocks. From Fig. 5-11 it can be seen that hydration and subsequent diagenetic-metamorphic alteration of groundmass glass to sericite and chlorite has resulted in addition of volatiles (principally H_2O) and MgO and removal of Na_2O from the glass. In Section 6.4. it is demonstrated using factor analysis that variations in the degree of these chemical changes are responsible for a large proportion of the total chemical variation within the dacite.

These results bear a strong similarity to those of Sopuck (1977), who compared matrix and clasts in the same rocks, from a sequence of unmineralized volcanics. His data show very marked differences in silica content between matrix and clasts either because they were not similar originally and/or because the matrix has undergone extreme alteration. Clast-matrix study at Buchans is not possible as coarse fragmental rocks are normally polylithic. It is emphasized that flows and related pyroclastics in this

study have essentially similar silica contents allowing
meaningful comparison.

CHAPTER SIX

GEOCHEMISTRY OF THE ORE HORIZON DACITIC TUFFS

6.1. Introduction

Dacitic crystal-vitric tuffs of the Lucky Strike-Oriental ore horizon sequences are the most widespread litho-logic unit which display intimate relationships to massive sulphide mineralization. These units therefore represent the lithologic units most likely to exhibit regional chemical variations which may be a function of mineralization and thus of interest to exploration. The chemistry of the ore horizon tuffs is examined somewhat more closely in this chapter in an effort to understand the processes responsible for chemical variation and to derive geochemical criteria of use in exploration.

6.2. General Chemical Abundances in the Ore Horizon Dacitic Tuffs

The average chemical abundances of the ore horizon dacitic tuffs from the Lucky Strike, Clementine and Oriental areas is presented in Table 6-1 and histograms of abundances for each element in Fig. 6-1. Most elements show normal population distributions with the exceptions of more lognormal Cu, Cu(S), Pb, Pb(S), Zn, Zn(S), Mg, Ni, Co and V.

Table 6-1: Average chemical composition of ore horizon dacitic tuffs.

	Lucky Strike Horizon Dacitic Tuffs	Oriental Horizon Dacitic Tuffs	Clementine Area Dacitic Tuffs
SiO_2	71.0	67.0	71.7
TiO_2	.23	.32	.24
Al_2O_3	13.68	15.56	13.25
Fe_2O_3	2.23	2.66	2.15
MnO	.08	.06	.06
MgO	1.23	2.56	1.20
CaO	2.17	2.05	1.97
Na_2O	2.69	2.17	1.79
K_2O	2.82	2.72	3.20
P_2O_5	.06	–	–
Loss. Ig.	2.97	3.90	3.76
Total	99.16	99.00	99.32
Ba	1657	1380	1042
$Ba(SO_4=)$	–	–	–
Pb	29	41	14
Pb(S)	24	77	24
Zn	109	160	25
Zn(S)	34	120	8
Cu	5	13	1
Cu(S)	2	16	2
S	–	–	–
Ag	–	–	–
Hg	–	–	–
Rb	70	83	99
Sr	222	250	127
Zr	122	156	140
Mo	<3	–	–
Ni	3	4	4
Co	5	16	19
Cr	24	9	2
V	19	16	15
Th	16(12)	19(23)	16
U	4(12)	4(23)	4
Ga	13(12)	16(23)	13

Fig. 6-1: Histogram for all elements determined in ore horizon dacitic tuffs.
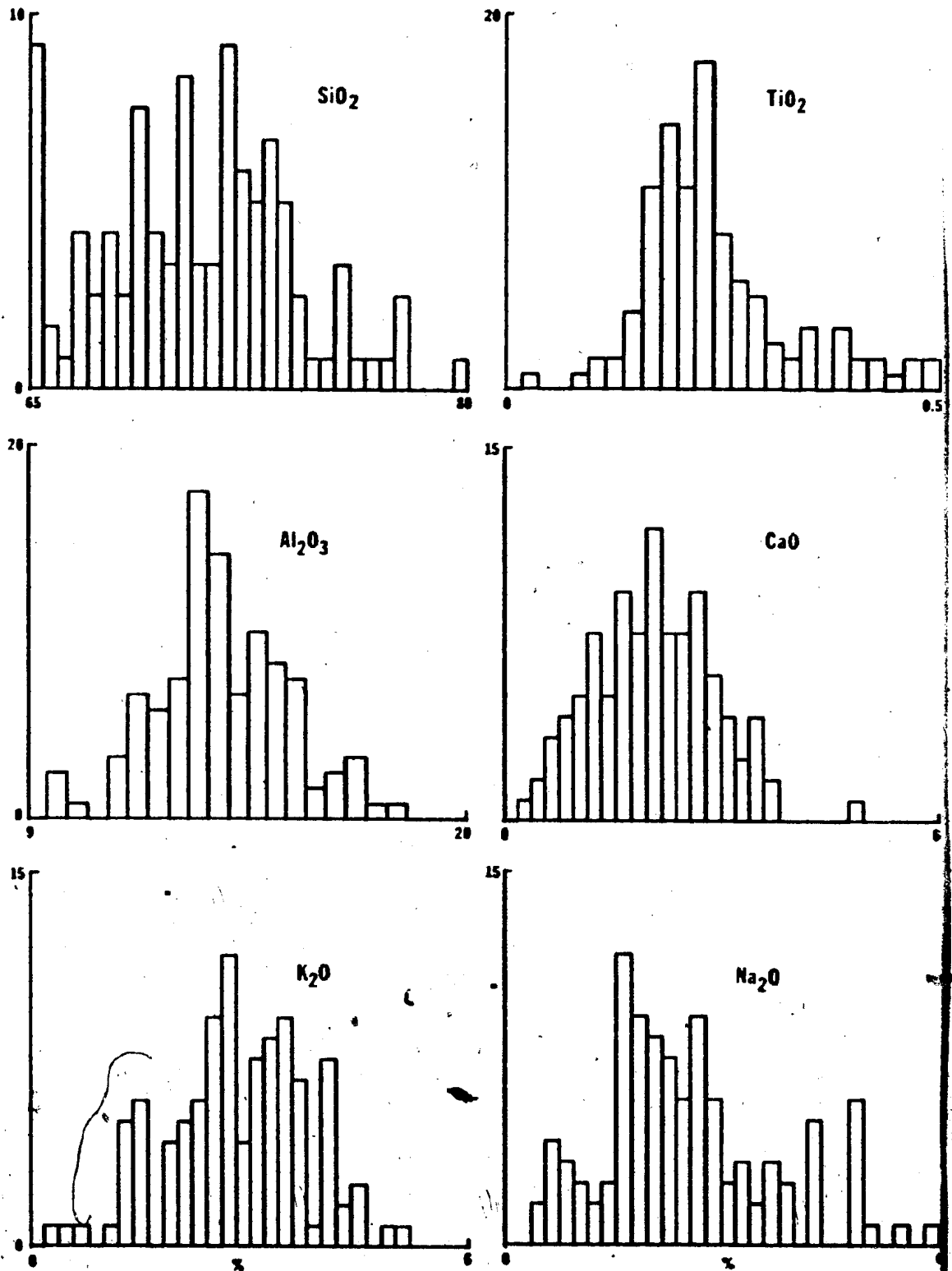
Fig. 6-1 (con't)
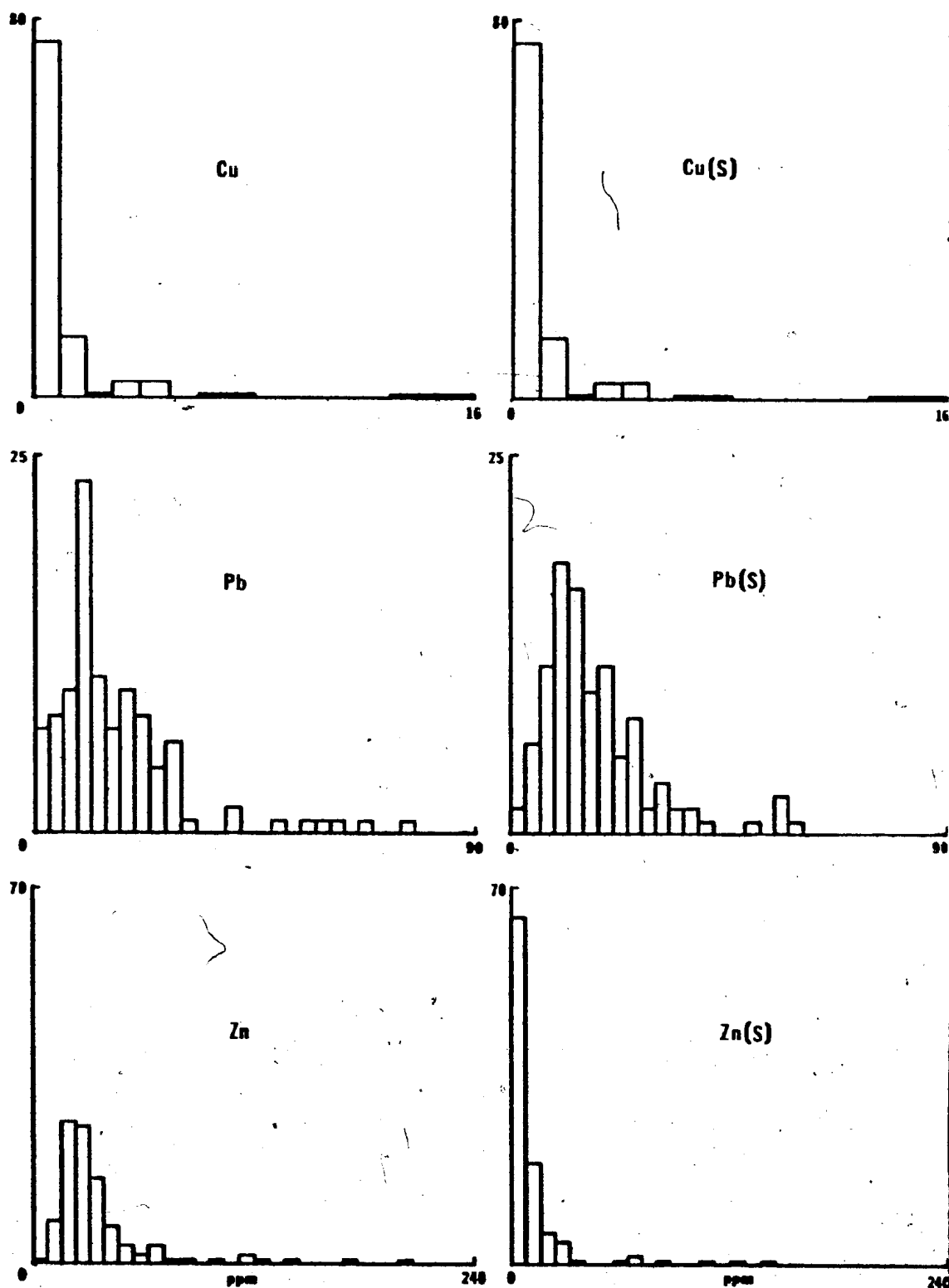
Fig. 6-1 (con't)
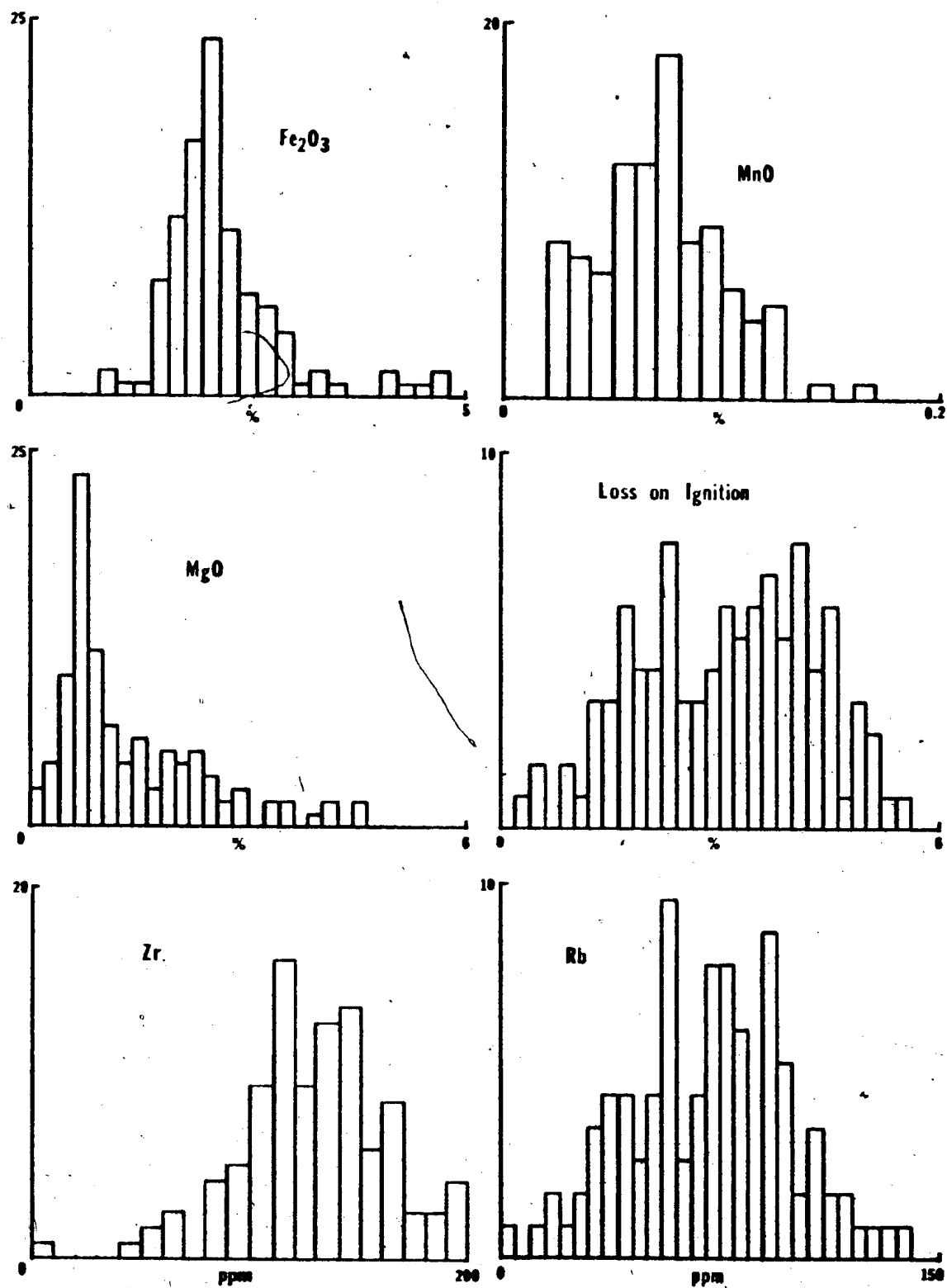
Fig. 6-1 (con't)
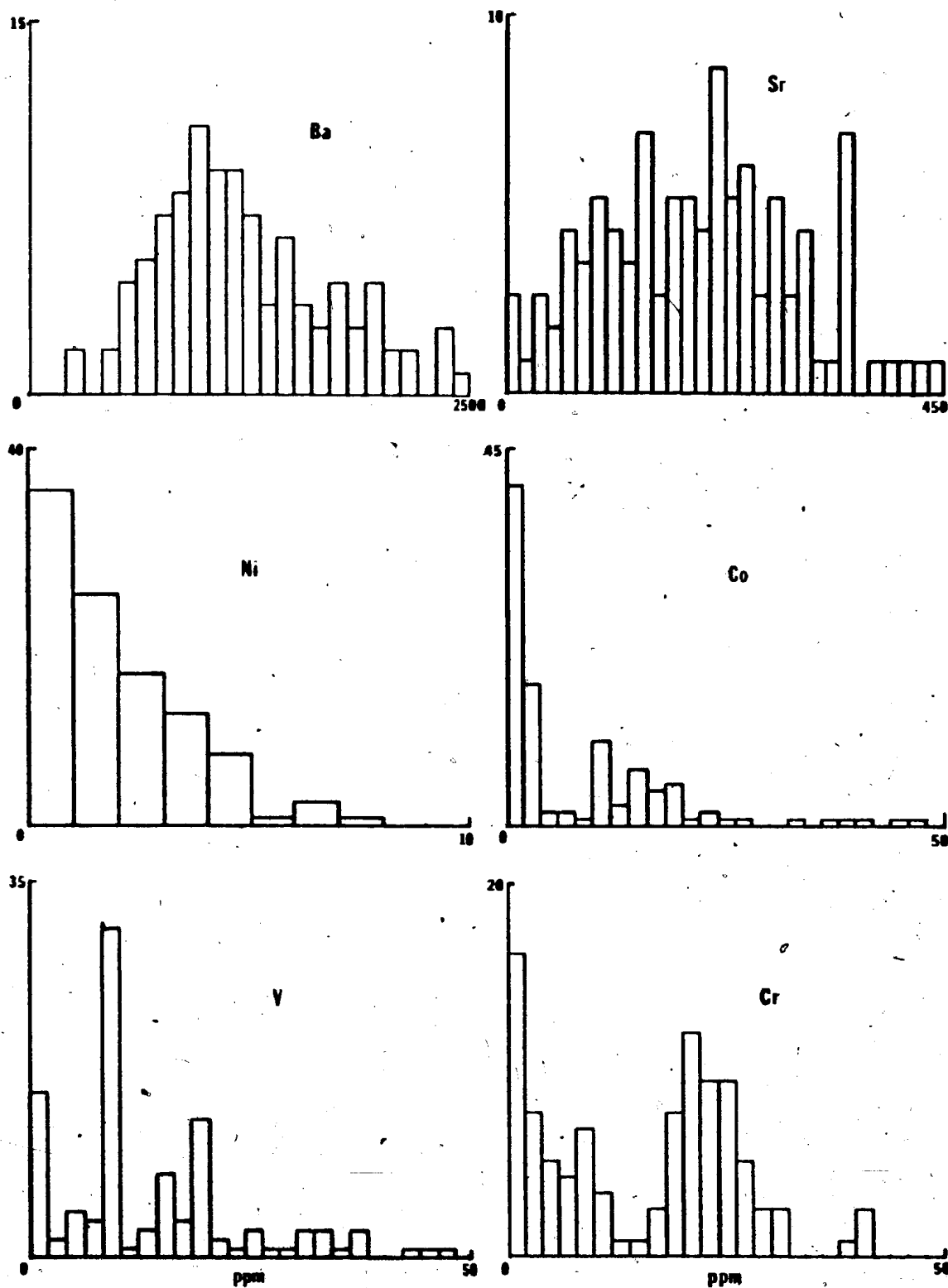
6.3. Correlation Matrix for Ore Horizon Dacitic Tuffs

A correlation matrix for ore horizon dacitic tuffs is given in Table 6-2. In general, most elemental associations are those normally predictable on petrochemical grounds. Nonetheless, there exist a few unusual features including a complete lack of Ba correlation with all other elements including K_2O. This is anomalous in view of the strong Ba: K_2O coherence in associated rhyolites and indicates that the process(es) controlling Ba distribution are quite different in these two suites of closely related rocks. Among the base metals, there is little correlation between Cu and the strongly correlative Pb-Zn pair.

Lengthy study of the correlation matrix reveals many element interactions which can be related to geochemical processes which acted upon the dacitic tuffs. Due to the complexity of these interactions, factor analyses was undertaken to better understand inter-element associations.

6.4. R-Mode Factor Analysis of the Ore Horizon Dacitic Tuffs - Major Elements

A large number of geochemical studies have proven the merit of factor analysis as a valuable tool in understanding processes responsible for geochemical variations. In order to identify geologic processes associated with various factors, it is necessary to understand the mode of

	Fe₂O₃	TiO₂	SiO₂	CaO	K₂O	MgO	Al₂O₃	Na₂O	L.I.	MnO	Zr	Sr	Rb	Zn	Cu	Ba	Cu(s)	Pb(s)	Zn(s)	Pb	Ni	Co	Cr
TiO₂	64																						
SiO₂	-50	-35																					
CaO	25	-01	-46																				
K₂O	09	20	-46	00																			
MgO	22	13	-30	-08	13																		
Al₂O₃	20	31	-73	07	50	29																	
Na₂O	00	-04	24	-24	-56	-53	-27																
L.I.	10	-07	-57	57	30	51	34	-68															
MnO	29	-15	04	31	-20	-16	-27	21	-10														
Zr	33	48	-36	-03	28	00	48	03	-07	-20													
Sr	03	04	-04	29	-13	-04	08	10	-20	19	35												
Rb	10	16	-45	13	75	18	56	-62	37	-19	48	05											
Zn	-13	-09	08	-27	-03	66	01	-30	25	-13	-23	-21	-10										
Cu	-05	04	-11	-11	85	24	16	04	-03	-01	-03	06	-01	17									
Ba	-13	-01	-05	20	02	05	02	-16	15	09	-01	22	-03	04	-01								
Cu(s)	03	11	-13	-01	-07	02	02	19	-02	-11	-04	-06	-13	-05	49	-16							
Pb(s)	08	00	-23	22	01	42	02	-30	47	-10	04	-06	05	32	05	16	12						
Zn(s)	-15	-04	28	-27	-09	34	-28	-17	07	-19	-29	-26	-23	62	-01	04	-04	23					
Pb	-11	-08	-07	-04	00	63	09	-35	37	-08	-05	01	-01	86	14	16	-08	57	54				
Ni	03	06	-14	-04	15	24	21	-10	04	01	12	10	15	04	82	04	01	01	-05	05			
Co	-05	12	07	-11	07	05	-03	-09	00	-34	01	03	05	01	24	-06	-04	-03	31	-06	42		
Cr	-02	-06	08	06	-04	-08	-07	04	-02	31	-13	-02	-02	02	07	-05	-02	-08	-07	01	01	-26	
V	04	05	-16	-02	15	25	19	-09	05	01	07	06	15	06	85	03	09	06	-04	05	97	39	01

occurrence of the various elements. Certainly, in most geo-. chemical studies, the mode of occurrence of the major elements is much better understood than that of the trace elements. For this reason, R-mode factor models were computed first for the major elements in order to facilitate identification of geochemical processes responsible for chemical variation in the dacites. Apart from this reason, major elements only were included in the first factor models in order to reduce the number of factors required to reasonably explain the variance in the dacite (factor analysis treats all variables as statistical equals, though in geochemical studies, the major elements comprise, by definition, the bulk of the elements of which the rock is composed). Factor matrices presented have undergone a varimax rotation similar to that described by Koch and Link (1971).

A variety of major element factor models were computed for the ore horizon dacite. The six factor model accounting for 94% of the variance in the dacite was selected as (by far) the most geologically explicable model. The rotated factor matrix is presented in Table 6-3.

Factor 1 (accounting for 16% of the total variance) accounts for almost all the MgO variation and a significant proportion of the Na_2O and loss on ignition in the ore horizon dacite. Microprobe examination of the dacite indicates that the bulk of the MgO occurs in chlorite after matrix glass

Table 6-3: Rotated factor matrix for dacitic tuffs of the Lucky Strike ore horizon sequence. The six factor matrix accounts for 94% of the data variability.

Variable	1 Chlorite After Glass (15.73%)	2 Hematite, Leucoxene, etc. (16.95%)	3 Secondary Calcite (17.17%)	4 Silica-Alumina (17.49%)	5 Sericite After Glass (14.78%)	6 MnO (11.96%)
Fe_2O_3	.15	.83	-.14	-.19	.04	.35
TiO_2	-.02	.93	.06	-.13	-.09	-.20
SiO_2	-.15	-.30	.41	.80	.15	-.05
CaO	-.09	.07	-.95	-.09	.01	.20
K_2O	-.01	.08	.04	-.38	-.90	-.05
MgO	.96	.10	.03	-.15	-.06	-.05
Al_2O_3	.13	.12	.01	-.89	-.23	-.18
Na_2O	-.54	.03	.34	-.05	.71	.16
L.O.I.	.53	-.11	-.71	-.26	-.25	-.10
MnO	-.09	.01	-.12	.11	.10	.96

(minor amounts also occur as chlorite after hornblende).
In Section 5.4. it was demonstrated that devitrification
of matrix glass involved hydration, removal of soda and
addition of MgO. This factor is thus easily identified as
representing alteration of original matrix glass to chlorite
with release of Na_2O.

Factor 2 (accounting for 17% of the total variance)
contains large loadings for Fe_2O_3 and TiO_2. These elements
occur almost exclusively in trace quantities of rutile,
ilmenite, leucoxene, hematite and pyrite, all of which, in
the author's experience, are randomly distributed in the
unaltered tuffs. Factor 2 indicates that the occurrence
of these minerals is not related to any geochemical process
which has affected the dacitic tuffs nor is their occurrence
linked to the presence of any other minerals.

Factor 3 (accounting for 17% of the total variance)
accounts for almost all the CaO variation in the dacite and
half of the loss on ignition variation. Calcite is the only
mineral which can satisfy the loadings of this factor with
only a minor contribution from prehnite. Calcite occurs
principally as alteration of plagioclase and as minute
calcite veinlets transecting all rocks. Factor 3 is thus a
"secondary calcite factor".

Factor 4 (accounting for 17% of the total variance)
has high antipathetic loadings for SiO_2 and Al_2O_3 and accounts

for most of the variation of these two elements. As no other
elements are significantly affected, this factor represents
substitution of Al_2O_3 for SiO_2 (and vice versa) as a result
of the varying presence of some mineral or as a result of
some secondary geochemical process. Such substitutions are
possible as a result of variation in both plagioclase and
chlorite compositions and this factor is tentatively correlated
to such compositional variations. Variations in the propor-
tions of quartz and plagioclase may also contribute to this
factor.

Factor 5 (accounting for 15% of the total variance)
accounts for almost all the K_2O variation in the dacite.
Potash occurs mainly in sericite (after matrix glass) with
only minor amounts in the much less abundant K-feldspar.
Indentification of this factor as a "sericite after glass"
factor satisfactorily explains the sympathetic relationship
between K_2O, loss on ignition and Al_2O_3. Their antipathetic
relationship with Na_2O indicates that soda has been expelled
from glass during sericitic alteration, a fact confirmed by
electron microprobe scans.

Factor 6 (accounting for 12% of the total variance)
accounts for virtually all MnO variation with no other elements
significantly affected. As such, it must be interpreted as
post depositional solution and redistribution of MnO.

The release of Na_2O during alteration of matrix
glass to chlorite and sericite (factors 1 and 5 above) is of

interest because none of the other factors involve addition
of soda. It must be concluded that soda originally present
in glass was largely removed from the dacitic tuffs during
alteration. In this regard, it is interesting to refer
back to Figure 5-12 (Section 5-4) in which it was demonstrated
that soda has been significantly depleted from the dacitic
tuffs as compared to the rather sodic cogenetic rhyolite
flows. Since none of the lithologies overlying or underlying
the dacite have undergone spilitic alteration it appears that
loss of soda from the dacite must have occurred at deposition,
with soda in glass being released to sea water. Thus it
appears that alteration of glass (probably originally to
clay minerals) occurred shortly after deposition and prior
to deposition of overlying basalt flows. Regional deposition-
al soda depletion of originally glassy pyroclastics has been
suggested as a process possibly operative in the vicinity of
the New Brunswick massive sulphide deposits (Govett et al.,
1974, p. 83). In Section 7.2. it is shown that this process,
though operative at Buchans, bears no relationship to
mineralization.

A consequence of this interpretation is that the
inverse correlation between Na_2O and K_2O in the dacitic tuffs
is not a function of local redistribution in glass of Na_2O
and K_2O as previously suggested by the author (Thurlow, 1973;
Thurlow et al., 1975). Instead, glass-rich samples contain
high K_2O and low Na_2O whereas glass-poor samples (i.e., crystal-

rich samples) contain relatively lower K_2O and higher Na_2O

(Na_2O in plagioclase). Consequently the inverse soda:

potash correlation is a function of the glass:crystal ratio

in the dacite. It follows that anomalously low soda:potash

ratios in the dacite are a function both of the degree of

depositional alteration of glass and of the glass:crystal

ratio and that low values of this ratio may not bear any

relationship to the presence of mineralization. It is demon-

strated in Section 7.2. that none of the above six factors

display any spatial distribution related to the presence of ore.

It is evident from the above that factor analysis

is a powerful aid in identifying and understanding processes

causing chemical variation.

6.5. R-mode Factor Analysis of the Ore Horizon Dacitic Tuffs -
   Major and Trace Elements

In this section, the behavior of trace elements is

considered with regard to the processes responsible for

chemical variation in the dacite as determined in the previous

section. Factor models were computed first for all major

elements and barium and subsequently for all major and trace

elements combined.

When barium is included in the major element factor

models it forms a factor independant of all other elements.

When the number of factors is reduced so as to reveal barium

associations with other elements, it does not show
correlation with any of the previously determined factors.
It is concluded that the process(es) responsible for
variation in barium concentration is not among those processes
mentioned in the previous section.

The remainder of the trace elements behave fairly
predictably in the combined major and trace elements factor
models (a representative nine factor model is shown in Table
6-4). Rubidium variation is virtually entirely incorporated
into the "sericite after glass" factor and zirconium enters
the "rutile-leucoxene" factor. Strontium forms a weak inde-
pendent factor which, in some factor models, also accounts
for up to one third of the barium variation. The meaning
of this factor is obscure, as Buchans barite is Sr-poor.

Factor analysis reveals that the variation in
the base metals Pb and Zn is quite independent from that
of Cu. Pb, Zn and Zn(S) show moderate to strong coherence
with the "chlorite after glass" factor. Pb(S) variation is
somewhat more complex than that of Zn(S) as it is associated
with both the "chlorite after glass" and "calcite" factors.
It is concluded that silicate zinc and lead are largely
incorporated into the chlorite lattice, that sulphide zinc
occurs primarily in association with chlorite and that sulphide
lead occurs primarily in association with chlorite and
calcite.

In contrast, Cu variation is strongly linked to
that of Ni and V as these elements form a strong factor
which is mildly linked to a Cu(S)-Cu factor (Table 6-4).
This may indicate that these factors represent variations
in proportion of a submicroscopic sulphide phase.

Table 6-4: Rotated factor matrix for dacitic tuffs of the
Lucky Strike ore horizon sequence. The nine
factor matrix accounts for 83% of the data variability.

FACTOR

	1	2	3	4	5	6	7	8	9
Fe_2O_3	00	-02	00	23	90	03	12	04	-15
TiO_2	-18	-02	01	-16	86	04	-13	-09	10
SiO_2	53	-03	-08	-50	-42	-14	-04	27	02
CaO	00	-17	-03	89	07	14	11	04	13
K_2O	-85	-04	08	00	08	-17	-03	07	07
MgO	-21	78	20	17	18	-02	-04	00	-07
Al_2O_3	-74	07	12	06	21	27	00	-22	-03
Na_2O	60	-37	-03	-37	06	24	12	-27	-12
L.I.	-40	35	-01	75	-02	-20	-05	-03	03
MnO	36	-14	08	25	13	05	67	26	05
Zr	-44	-08	-01	-18	40	62	-12	-03	-02
Sr	10	-08	11	10	-01	82	02	15	18
Rb	-87	-03	06	13	03	10	-03	15	-06
Zn	02	91	05	-13	-08	-15	03	02	-01
Cu	01	11	89	07	-03	00	05	-37	00
Ba	00	07	01	11	-04	09	02	05	96
Cu(s)	11	-05	16	02	06	-11	-03	-86	-07
Pb(s)	01	56	-03	43	04	06	-12	-23	11
Zn(s)	24	62	-02	-17	00	-37	-30	16	08
Pb	-02	93	02	06	-08	10	04	00	10
Ni	-10	02	96	00	02	06	-06	08	00
Co	06	-04	44	-02	-06	-11	-70	27	-04
Cr	-01	00	08	-09	-04	16	73	08	-02
V	-09	04	97	03	02	02	04	01	00

CHAPTER SEVEN

APPLIED ASPECTS OF THE GEOCHEMISTRY OF ORE HORIZON DACITIC TUFFS

7.1. Geochemical Comparison of Ore Horizon Dacitic Tuffs to Other Dacitic Tuffs

The average chemical composition of ore horizon dacitic tuffs as compared to dacitic tuffs at other non ore-bearing horizons is given in Table 5-1. A quick scan of this table reveals little visible difference in composition for most elements except possibly for Zn and Pb and a strong apparent enrichment of Ba in ore horizon dacitic tuffs. Histograms were prepared in order to more accurately assess the validity of these comparisons.

A histogram of Ba abundances in ore horizon dacitic tuffs as compared to other petrographically similar dacitic tuffs is given in Fig. 7-1. For reasons given in subsequent sections, all samples of ore horizon tuff from within 30 m of ore were excluded from this comparison. The histogram shows two distinct normally distributed Ba populations, highest in the ore horizon dacitic tuffs.

Discriminant functions analysis was undertaken in order to enhance the distinction between ore horizon and non ore horizon dacitic tuffs, and to identify other elements which might significantly differ between these groups. First, using dacitic tuffs from the Oriental and Lucky Strike
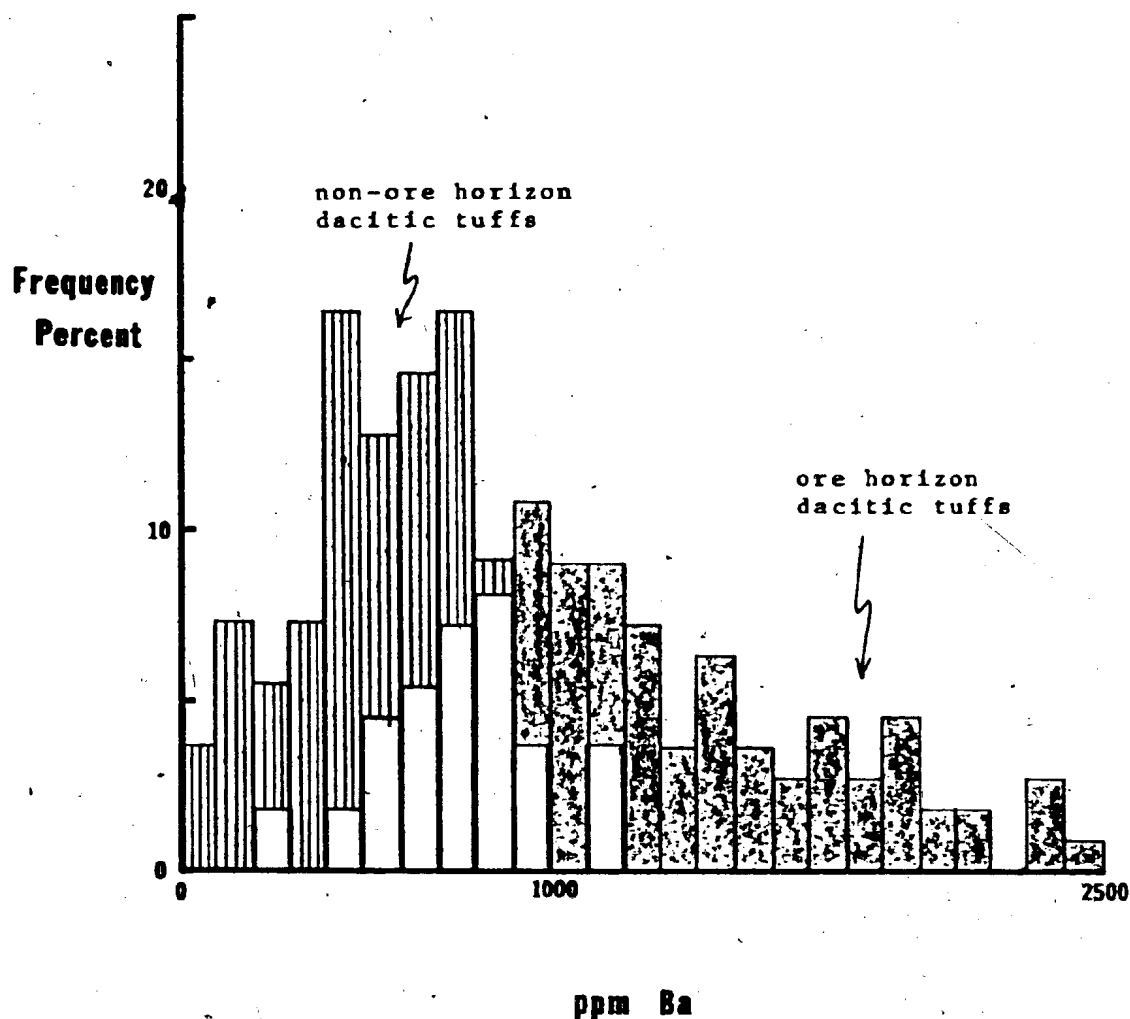
Figure 7-1: Histogram of Ba abundances in ore horizon dacitic
tuffs (n=111) as compared to non-ore horizon
dacitic tuffs (n=55).   Ore horizon samples from
within 30 m of ore are omitted.   Nine samples of
ore horizon tuff exceed 2500 ppm and are not
plotted.   Area of overlap not coloured.

areas, a discriminant function was calculated which indicated
that ore horizon tuffs could be distinguished with a high
degree of confidence from non-ore horizon tuffs. In order
to test this practical validity of this formula, discriminant
scores of 13 samples of Clementine area tuff (from areas
3 or more kilometers from Lucky Strike) were calculated.
The results show that all of these samples were successfully
classified as ore horizon tuffs. A new discriminant function
was thus calculated including the samples of Clementine
area dacitic tuff.

A histogram of discriminant scores, given in Fig. 7-2
shows the separation of ore horizon and non-ore horizon dacitic
tuffs. The data from this plot (Table 7-1) indicates that
lower Fe_2O_3 and higher Mn in the ore horizon dacitic tuffs
are significant as well as Ba in contributing to the
discrimination.

From these data, it is evident that ore horizon
dacitic tuffs can be distinguished from other lithologically
similar dacitic tuffs with a fair degree of confidence either
by simply comparing Ba abundances or by using a 24 element
discriminant function. The latter can be easily computed for
any new samples using any calculator. The degree of confidence
ascribed to classification of unknowns can be empirically
determined from the existing test cases. Using Ba abundances
only, it can be stated that any sample in excess of 1000 ppm
Ba belongs to the ore horizon, with 95% confidence. Using
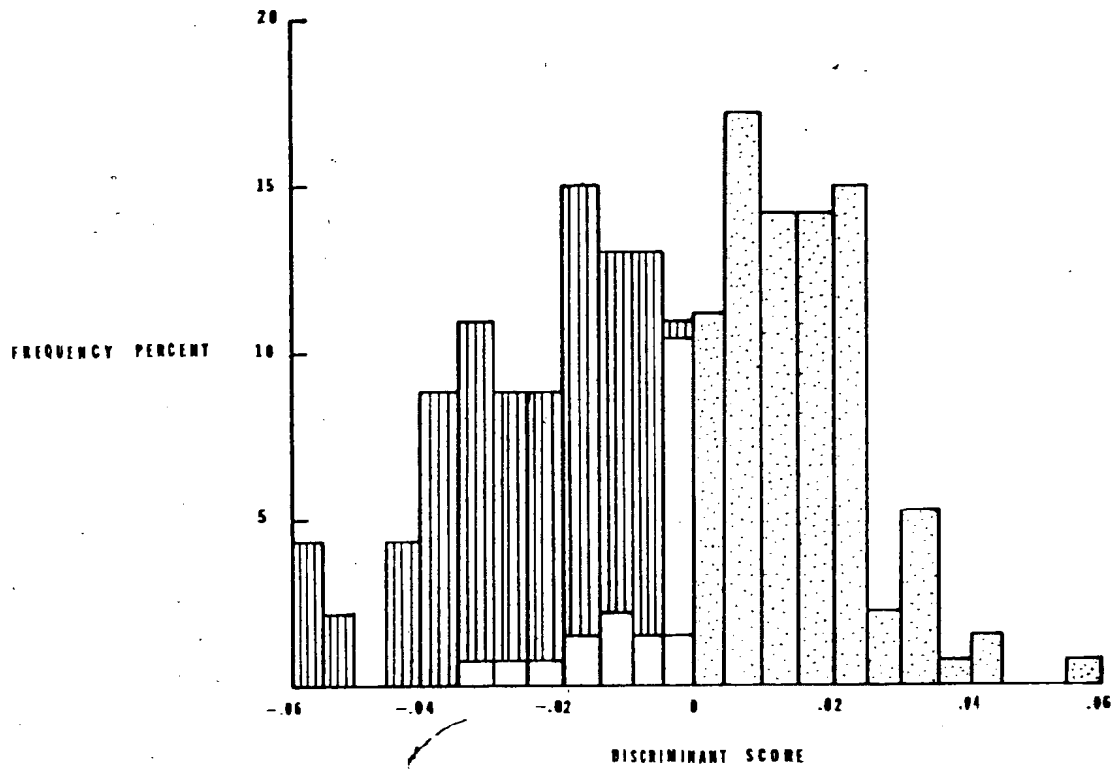
Figure 7-2: Histogram of discriminant scores.
Ore horizon dacitic tuffs, stippled (n = 134)
Non-ore horizon dacitic tuffs, ruled (n = 46)

Table 7-1: Discriminant fuction data. Sign convention in
first column; elements with positive values are
more abundant in the ore horizon dacitic tuffs.

Variable	Difference Of Means	Discriminent Function Coefficents	Percentage Contribution To Discrimination
Fe_2O_3	-000.863%	-1.45400	26.387
TiO_2	-000.066%	-2.12364	2.945
SiO_2	000.674%	-0.13161	0.445
CaO	000.080%	0.71228	1.189
K_2O	000.441%	0.28694	2.639
MgO	-000.053%	0.95599	1.050
Al_2O_3	-000.192%	-0.37748	1.512
Na_2O	-000.100%	0.58322	1.212
L.O.I.	000.004%	-0.23810	0.022
MnO	000.017%	26.66167	9.540
Zr	005.300 ppm	0.02850	3.154
Sr	024.718 ppm	-0.00462	2.387
Rb	015.453 ppm	0.02783	8.979
Zn	060.314 ppm	0.00023	0.291
Cu	-003.152 ppm	0.01215	0.800
Ba	988.062 ppm	0.00056	11.648
Cu(s)	-006.523 ppm	-0.02070	2.819
Pb(s)	020.354 ppm	-0.01330	5.653
Zn(s)	033.407 ppm	0.00258	1.802
Pb	019.005 ppm	0.01415	5.615
Ni	-002.117 ppm	-0.10467	4.626
Co	-004.909 ppm	0.03095	3.173
Cr	007.093 ppm	0.01159	1.716
V	-002.971 ppm	0.00639	0.396

the discriminant functions, the probability of an ore horizon
sample being classified as non-ore horizon is 7.5% whereas
the probability of a non-ore horizon sample being classified
as ore horizon is 10.9%.

The exploration applications of this are fairly
obvious. Already, the stratigraphy has been re-examined
and revised to account for two anomalous "non-ore horizon"
samples such that the member from which these come is now
known to form part of the ore horizon.

7.2. Chemical Variations in the Ore Horizon Dacitic Tuffs
as a Function of Distance to Ore

7.2.1. Introduction: In an effort to further under-
stand the nature and distribution of anomalous chemical
characteristics of the ore horizon dacite, studies were
undertaken to determine whether consistent and significant
chemical variations exist with proximity to ore. If such
relationships could be established, then the distance to ore
of unknown samples (e.g. Clementine area samples) could be
approximated from observed data.

Plots of chemical variations versus lateral strati-
graphic distance to ore were constructed for the ore horizon
dacite in two steps: 1) Plots of distance to nearest orebody,
whether transported or in situ, and 2) plots of distance
to nearest in situ orebody (a measure of the distance to
centers of ore-forming stockwork activity). Plots for all

elements determined were constructed as well as a wide
variety of elemental ratios which could conceivably bear
a relationship to proximity to ore. Also plotted versus
distance to ore were factor scores for each sample as derived
in previous sections. In total, over 100 plots of chemical
variations as a function of distance to ore were constructed.

7.2.2. Chemical Variations versus Distance to Nearest
Ore (whether transported or in situ): Plots
of this nature were constructed largely to ascertain whether
widespread post-depositional dispersion of elements has
occurred from the orebodies. Data plotted consisted of 120
samples of ore horizon dacitic tuff ranging from 1 m to
2.9 km from ore. Plots constructed included single element
plots as well as numerous combinations and ratios of variables
(e.g. Cu(S)/Cu, Fe/Mn, Mg/Ca, Na/K, etc.) as well as the
factor scores as determined in a previous section.

The resultant plots show that virtually no consistent
variations exist with proximity to ore (some typical examples
are shown in Fig. 7-3). Interestingly, none of the plots
of the scores for the six factors accounting for most of
the chemical variations in the dacitic tuffs show any
apparent spatial relationship to ore, e.g., chlorite after
glass and sericite after glass are not related to the ore-
forming process. However, in plots involving Ba, Pb and Zn,
samples within 50 m of ore display erratic behavior with a
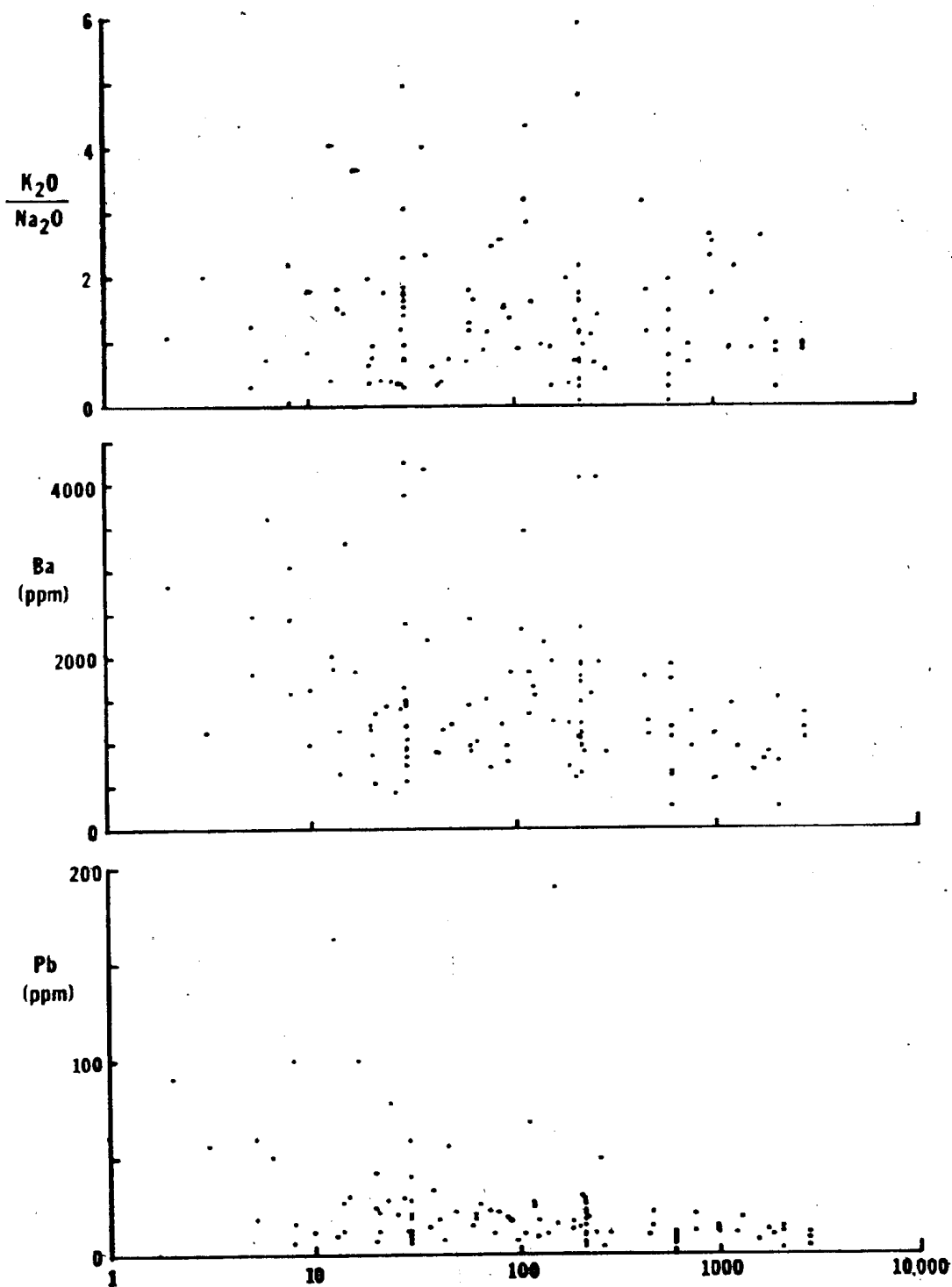
Distance to Nearest Ore   (log meters)

Figure 7-3:   Lateral variations of elements in ore horizon
dacitic tuffs as a function of distance to nearest ore.
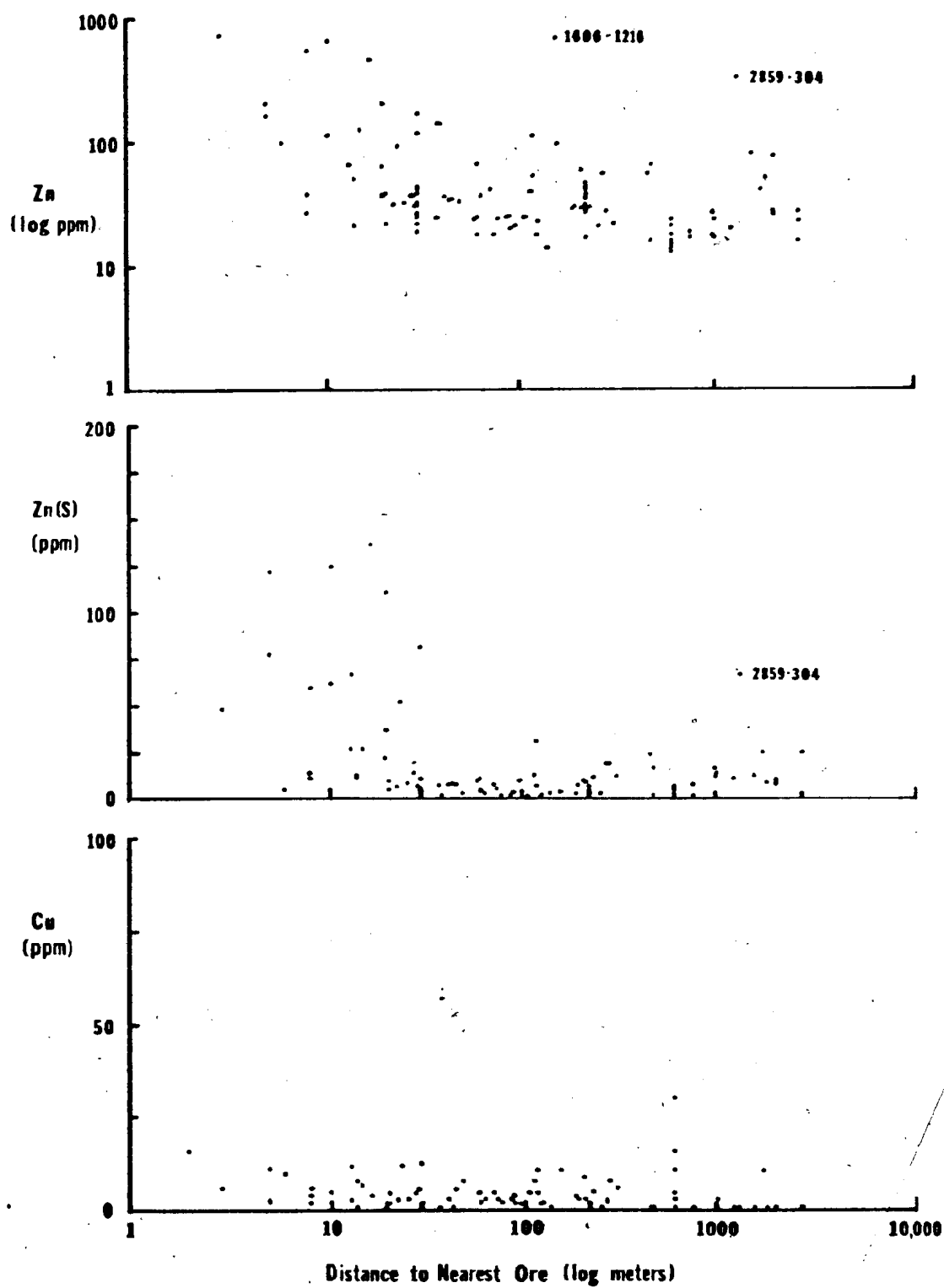
Figure 7-3 (con't)

large proportion of anomalously high values (Fig. 7-3). Zn
displays the "best" trend of all elements with virtually
all values in excess of 100 ppm occurring within 50 m of ore.
In this regard, it is interesting that all samples obtained
from the thick sequence of dacitic tuffs south of the
Clementine prospect contain less than 50 ppm Zn. Unlike the
other major ore-forming elements, Cu gives no indication
of nearby ore (Fig. 7-3). It is interesting to note that
Ba also shows no relationship to proximity to ore and thus
the anomalous Ba content of the ore horizon is a regional
characteristic of the unit.

The "nearest ore" for most samples within 50 m,
and all samples with 10 m of ore, is mechanically transported
ore. Since some of these deposits occur beyond the limits
of significant alteration associated with the main stockworks,
and since these samples are derived from both footwall and
hangingwall rocks, it is logical to conclude that small
amounts of Ba, Pb and Zn have migrated limited distances from
mechanically transported ores. It is also logical to conclude
(though it cannot be proven) that such migrations occurred
during compaction - diagenesis when the host dacitic crystal-
vitric tuffs were water-saturated and more permeable than
they were after lithification.

7.2.3. Chemical Variations versus Distance to in situ
ore: The occurrence of mechanically transported
ore at Buchans provides an excellent opportunity to study

dispersion of ore-forming elements from massive sulphide
as all evidence indicates that wall rock anomalies can
conceivably be caused only by post-ore dispersion directly
from the orebodies. It is demonstrated in the previous
section that such dispersion is erratic and limited only
to areas within 50 m of ore. Nevertheless, it is possible
that other dispersion processes not related to proximity to
transported ores may have acted upon the ore horizon dacite.
Dispersion patterns related to such processes would be super-
posed upon local dispersion from transported ore.

A number of alteration studies (e.g. papers in
Ishihara, 1974) have demonstrated that hydrothermal activity
and alteration of host rocks continues after massive sulphide
deposition, affecting both footwall and hangingwall rocks
alike. Such activity raises the possibility of lateral
dispersion of elements in unconsolidated crystal-vitric tuffs
as a function of the distance to the center of the geothermal
activity. If post-ore hydrothermal activity reached the
sea water - sediment interface, local sea water may be
slightly enriched in ore-forming constituents which may
subsequently be adsorbed on to clay minerals or deposited
syngenetically. Such processes could yield widespread
anomalies whose intensity would presumably be some function
of distance to the hydrothermal center.

In order to test such possibilities, chemical
variations of dacitic tuff samples were plotted as a function

of distance to in situ ore. In order to eliminate local dispersion effects from mechanically transported ores, all samples within 50 m of transported ore and displaying evidence of enrichment related to their proximity to such ore were eliminated from consideration. Samples in this study range from less than 100 m to more than 3.6 km from in situ ore.

The results of these plots are similar to the results of the previous section. No meaningful consistent trends are visible for any element, element ratios or for the six factors causing the bulk of the geochemical variation in the dacitic tuffs. Typical results are shown in Fig. 7-4.

Previous work by the author (Thurlow, 1973) in the immediate vicinity of the orebodies showed that there were no visible trends across stratigraphy within dacitic tuffs except within 30 m of ore. The results of this work appear to show that there are correspondingly no consistent lateral trends relating to the presence of ore.

7.2.4. Discriminant Scores as a Function of Distance to Ore: The discriminant function which effectively separates ore horizon dacitic tuffs from non-ore horizon dacitic tuffs did not yield a perfect 100%-separation. A number of samples of ore horizon were effectively "misclassified" as non-ore horizon dacitic tuff (see Section 7-1). In checking which samples were misclassified, it was noticed that some of these were samples relatively remote
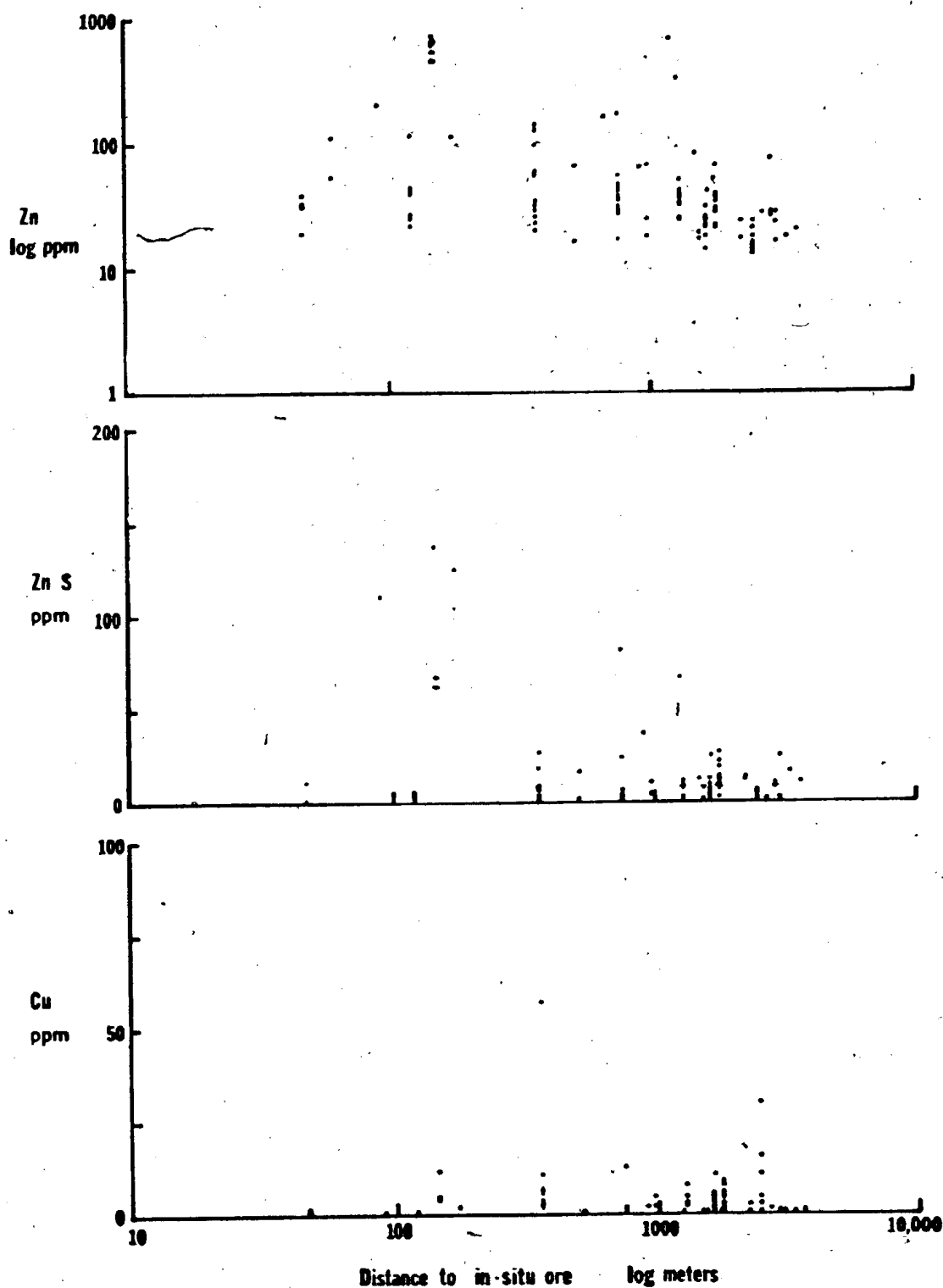
Figure 7-4: Lateral variations of elements in ore horizon dacitic tuffs as a function of distance to nearest in situ ore.
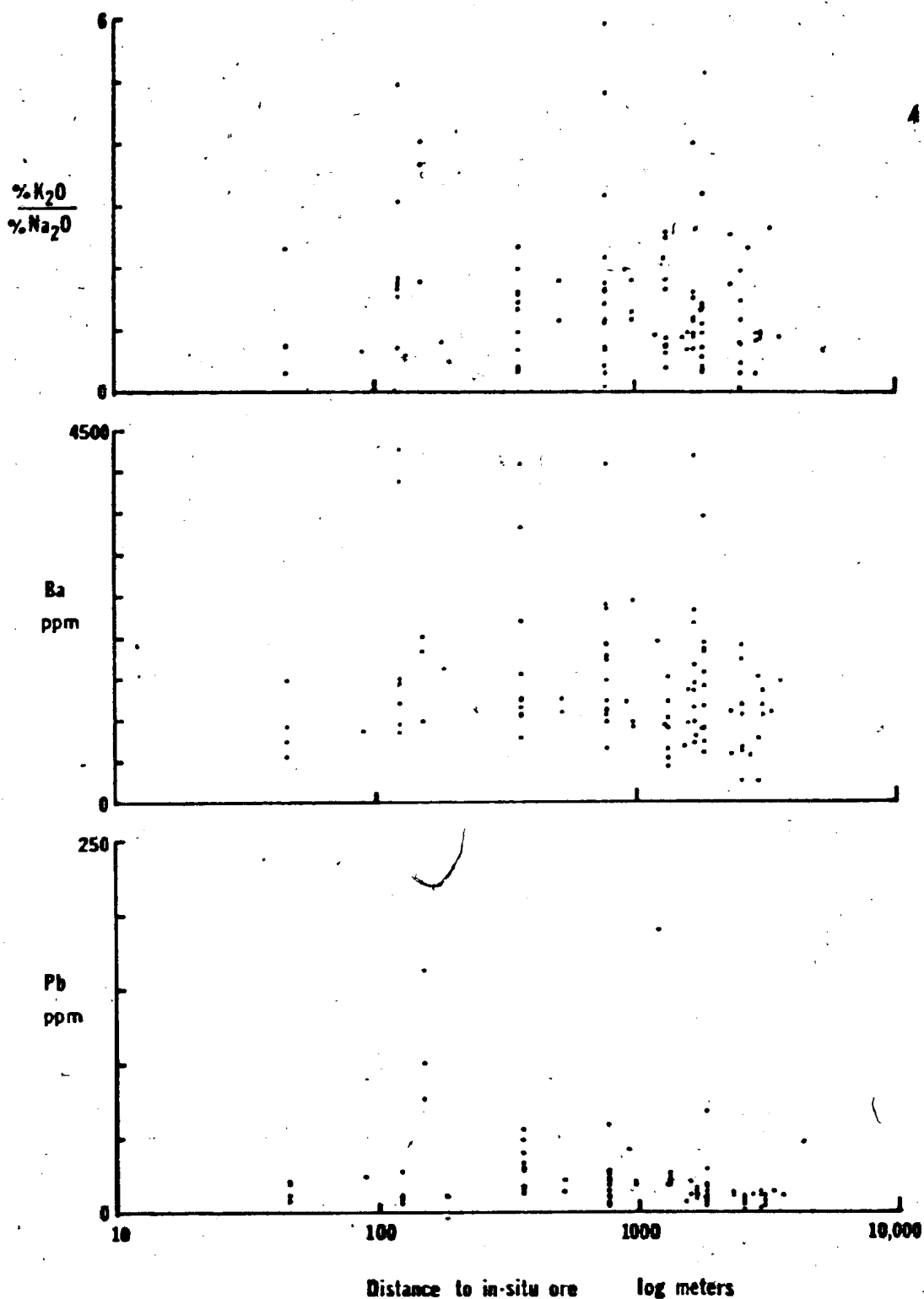
Figure 7-4 (con't)

from ore; i.e., several hundred meters or more. Plots were
constructed (Fig. 7-5) to determine whether in fact the ore
horizon dacitic tuffs actually become chemically more like
non-ore horizon dacitic tuffs with increasing distance
from ore. The diagrams show no obvious trend but, with
some imaginative license, one could say that ore horizon
dacitic tuffs become slightly more like non-ore horizon tuffs
with increasing distance from ore. If one could prove
this more convincingly, it would be possible to state that
the anomalous chemistry of the ore horizon dacitic tuffs
is indeed related to the presence of ore.

7.3. The Cause of the Ba Anomaly in Ore Horizon Dacitic Tuffs

The anomalous Ba content of ore horizon dacitic
tuffs is the most important geochemical distinction between
the ore horizon and other similar horizons throughout the
Buchans Group. Some pertinent facts regarding the distribution
of Ba, as outlined in previous sections are:

1) Ba in cogenetic rhyolite is controlled by K_2O distribution
    (correlation coefficent = .87)

2) Ba in other Buchans Group dacitic tuffs is also largely
    controlled by K_2O distribution (correlations coefficients
    for three such felsic units are .62, .46 and .58)

3) Ba in ore horizon dacitic tuffs shows no correlation
    with K_2O (correlation coefficient = .02)
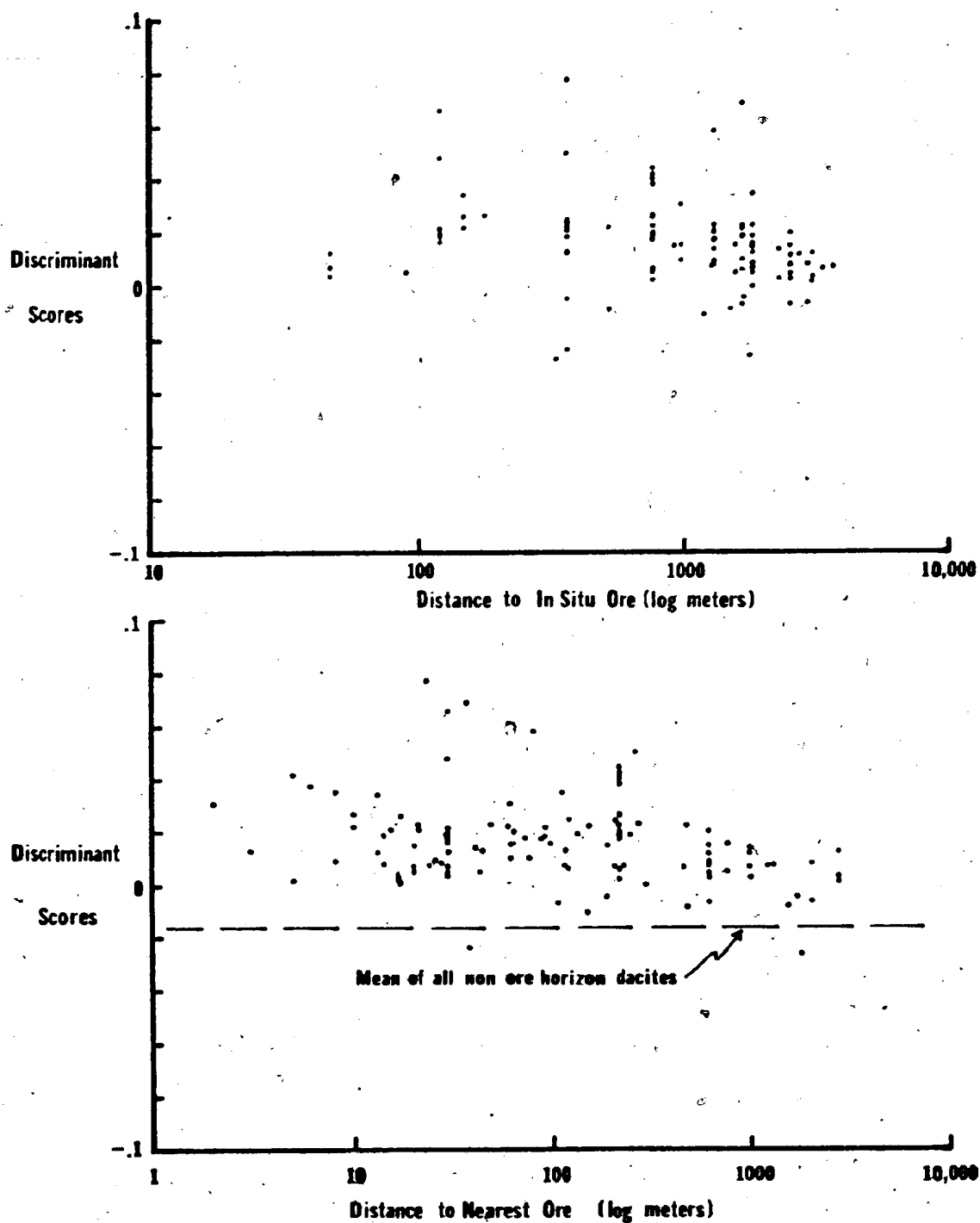
Figure 7-5: Lateral variations of discriminant scores in ore
horizon dacitic tuffs as a function of distance to ore.

4) Barium variation is apparently not related to any of the major post-depositional chemical changes that have affected the dacitic tuffs.

These criteria seem to suggest that Ba in the ore horizon tuffs has been enriched by a unique process. Though it cannot be proven, it is reasonable to suggest that this process might have some connection with the formation of the barite-rich orebodies.

In an attempt to identify the cause of the Ba anomaly a number of ore horizon and non-ore horizon dacitic tuffs were examined under the scanning electron microprobe. The following observations were recorded:

1) Ba is evenly and randomly distributed in non-ore horizon tuffs both in plagioclase and altered sericitic matrix glass

2) Ba has two modes of occurrence in samples of ore horizon tuffs: a) evenly and randomly distributed, as above and
    b) as tiny isolated concentrations

3) The isolated concentrations are composed of a Ba and sulphur-bearing mineral; probably barite

4) The isolated concentrations occur: a) as specks in matrix glass, b) as inclusions? in plagioclase, c) in small fractures in quartz, plagioclase and amphibole crystals (these relationships are schematically shown in Fig. 7-6).
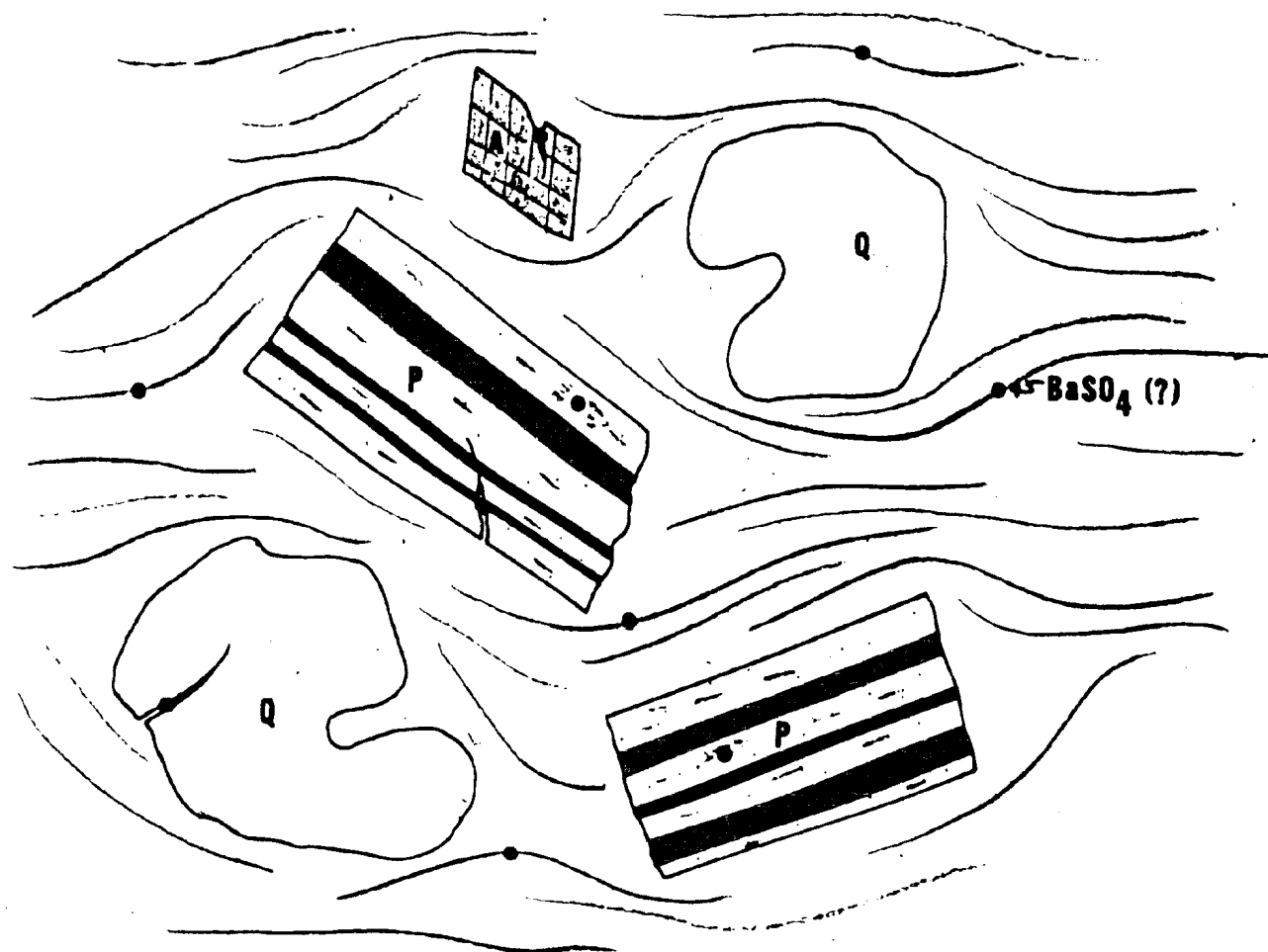
Figure 7-6:   Schematic diagram of thin section showing modes of occurrence of barite in ore
horizon dacitic tuffs as determined from electron microprobe scans.   Plagioclase
(P), quartz (Q), and hornblende (A) sit in matrix of glass shards altered
to sericite and chlorite.

It is evident from the above that the barium anomaly in the ore horizon tuffs is likely caused by trace amounts of very fine grained disseminated barite.

The origin of this barite is enigmatic. Any model must explain the widespread distribution of barite throughout the ore horizon with no apparent enrichment except very close to ore, take into account the extreme insolubility of barite in sea water, and account for the lack of a concomitant base metal anomaly.

Many of the ore horizon tuffs were deposited from subaqueous pyroclastic flows which locally contain minor concentrations of sulphide and barite clasts and grains (see Section 4.5,1.). Such clasts occur in the ore horizon at distances exceeding 4 km from the nearest known in situ deposit. It is very probable that, in addition to the visible clasts, microscopic barite and sulphide were also transported and homogenized by these density flows. Once emplaced, the sulphide and barite grains and clasts were distributed throughout porous tuff in contact with matrix sea water with a temperature, Eh and pH probably similar to that of ambient sea water. Compaction of the unit would result in a slow upward movement of sea water through the unit.

Sea water is a powerful oxidizing electrolyte capable of attacking and breaking down the common sulphides pyrite, sphalerite, galena and chalcopyrite. Constantinou (1976) has described several of the Cyprus orebodies as being

Plate 7-1: Drill core sample showing yellow ore clast in pyroclastic breccia of Lucky Strike ore horizon sequence. Note dark rim around margin of the clast, dark fracture cutting clast and dark spots within the clast. Enlargement approximately 2X.

in an advanced stage of leaching due to oxidation by sea
water. Complete destruction of the ores was prevented by
deposition of the ochre and overlying pillow lavas. It is
likely that the Buchans ores were subject to the same
attack, though almost immediate burial by thick pyroclastics
would have halted this process at a very early stage. It is
likely that the base metal anomalies recorded within 30 m
of transported ore are related to this process combined with
simple expulsion of matrix water and possible electro-
chemical dispersion as described by Sato and Mooney (1960).

Tiny sulphide grains and larger clasts throughout
the ore horizon pyroclastics would also have been subject
to this relatively brief period of oxidation. Conversely,
barite would remain stable. It is proposed that the barium
anomaly and lack of associated base metal enrichment in the
ore horizon pyroclastics is related to this process.

This proposal finds support in field evidence.
Many of the larger sulphide clasts display a dark sooty
margin which merges into the host pyroclastics (Plate 7-1).
Smaller Pb-Zn grains in tuff commonly have a thin, anomalous,
blue-grey halo. Instances of anomalous blue-grey specks
with no visible sulphide are common in several areas. The
material sampled in this study contained none of the above
features and thus may represent the complete-removal end
member of this process.

CHAPTER EIGHT

SUMMARY AND EXPLORATION APPLICATION

8.1. Summary of Thesis

The purposes for undertaking this study, as out-lined in Chapter 1, have been largely achieved though many old and new questions remain unresolved.

The relationships of the Buchans Group to adjac-ent rock units has been newly established in some cases, and clarified in others. The superposition of the Hungry Mountain Complex upon the Buchans Group by southeastward-directed thrusting has been established and the signific-ance of thrusting within the Buchans Group has been documented. The recognition of thrusting has resulted in the establishment of a new stratigraphic succession based upon indisputably conformable contacts. A plausible plutonic equivalent of the Buchans Group volcanics has been identified and suggested as a source for the enigmatic granitoid boulders within the Buchans Group. The peralka-line nature of a large part of the Topsails Granite has been recognized and the intrusive relationship with the Buchans Group of all phases of the granite and related gabbro has been clarified.

Study of the Buchans ores has resulted in a genetic model comprising stockwork, in situ and transported

ores. The latter are particularly well developed and
preserved at Buchans. Their nature has been documented
and their origin interpreted as a result of brecciation
at source, transport downslope in paleotopographic
channels by gravity-driven debris flows and preferential
deposition in depressions.

Whole-rock chemical analyses of unaltered Buchans
Group volcanics was undertaken largely to determine whether
this geochemical approach has exploration applications.
It has been shown that Buchans Group volcanic rocks
are similar in chemical abundances and variations to other
calc-alkaline volcanic suites. There was apparently
little chemical evolution in Buchans Group flows through
the stratigraphic column and flows within the ore horizon
sequences are essentially similar to their counterparts
elsewhere in the Buchans Group. Study of flows and cogenet-
ic pyroclastics at various stratigraphic horizons has
indicated some chemical differences between these groups,
probably due to greater permeability of pyroclastics
during diagenesis and metamorphism. Ore horizon pyroclas-
tics are chemically similar to those at other stratigraphic
horizons and show no anomaly related to mineralization
with the exception of anomalously high Ba concentrations
in the ore horizon.

The major causes of geochemical variations in
the ore horizon pyroclastic rocks have been quantified by
factor analysis and shown to bear no relationship to
mineralization. A variety of other elemental abundances
and ratios within unaltered ore horizon pyroclastics
similarly show no relationship to ore, whether in situ
or transported. Erratic base metal anomalies are present
in ore horizon pyroclastics within 50 m of ore and appear
to be the result of clastic concentration combined with
chemical and electrochemical dispersion.

The anomalous abundances of Ba in ore horizon
pyroclastics is a regional feature which provides a means
of distinguishing ore horizon pyroclastics from similar
lithologies at other stratigraphic horizons. The Ba
anomaly is caused by microscopic barite which was widely
distributed by subaqueous pyroclastic flows which transport-
ed most ore horizon pyroclastics.

8.2. Exploration Applications

Assuming that no ore remains undiscovered within
the depth capability of current geophysical technology, then
geological observation, interpretation and application
is the most powerful exploration tool at Buchans. (This
statement is substantiated by the recent discovery of
the MacLean Extension deposit.) An understanding of the

stratigraphy and of the myraid of new exploration possibil-
ities posed by thrust faults is essential. A detailed
knowledge of the nature and distribution of significant
lithologies, alteration and paleotopography in the vicinity
of the known ores is a prerequisite to effective exploration.
Recognition of analogous lithologies and alteration in
new exploration areas constitutes an important exploration
lead.

Rock geochemistry, as studied in this thesis,
has only limited exploration application. The relatively
fresh rocks of the Buchans Group provide an excellent
opportunity to determine whether geochemically anomalous
conditions existed in rocks which are not anomalous in
hand specimen. The anomalous Ba content of ore horizon
pyroclastics is a regional feature related to the presence
of ore and serves to distinguish pyroclastics which host
mineralization from those which do not. Accurate rock
analysis for Ba in the Buchans and Roberts Arm Groups,
and their correlatives, should be seriously considered as
a viable reconnaissance method of identifying potentially
mineralized felsic volcanic horizons.

Previous work by the author (Thurlow, 1973;
Thurlow, et al., 1975) showed that altered rocks of the
Intermediate Footwall were depleted in Na_2O, CaO and K_2O,
and enriched in SiO_2, MgO and many trace elements. These

results are typical of many massive sulphide terranes
(see Table 1-1). The application of these parameters
in exploration has become widespread, especially in areas
where subsequent deformation and metamorphism have masked
the appearance of altered rocks. However, at Buchans,
the relatively pristine condition of the rocks makes
even incipient stages of alteration evident in hand specimen.

A problem more common than identifying alteration
at Buchans is the significance of the recognized alteration.
The experienced eye can identify some alteration types as
having no economic importance. However, some instances
of interesting alteration occur at horizons known to be
barren and there is at least one instance of alteration of
uncertain significance in ore horizon pyroclastics. A
fruitful line of future research would be an integrated
mineralogical and geochemical study of clay mineral
alteration related to ore as compared to alteration at the
known barren horizons. This type of study may provide an
important means of assessing instances of alteration of
uncertain significance.

REFERENCES

ABBEY, S., 1968. Analysis of rocks and minerals by atomic
absorption spectroscopy; Part 2; Determination
of total iron, magnesium, calcium, sodium and
potassium. G.S.C. Paper 68-20.

ABBEY, S., 1975. Studies in "standard samples". Geol. Surv.
Can. Pap. 74-41.

ALCOCK, J.B.,.1961. Oriental No. Two Orebody. Unpub. B.Sc.
Thesis, Royal School of Mines, London, 56p.

AMSTUTZ, G.C. (Ed.), 1974. Spilites and spilitic rocks.
International Union of Geological Sciences,
Series A, Number 4; Springer-Verlag, Berlin,
471p.

ANDERSON, F.D., 1972a. Unpublished Geological Survey of
Canada maps (Buchans 12A/15, Badger 12A/16).

ANDERSON, F.D., 1972b. Buchans and Badger areas, Newfoundland.
Geol. Surv. Can. Pap. 72-1, Part A, p. 2.

ANGER, C., 1963. The lead-zinc-copper deposits of Buchans,
middle Newfoundland. Neues Jahrbuch fur
Minerologie, Montashefte, pp. 126-136.

BAIRD, D.M., 1960. Massive sulphide deposits in Newfoundland.
Can. Inst. Min. Metall. Bull., 53, pp. 77-80.

BELL, K. and BLENKINSOP, J., 1981. A geochronological study
of the Buchans Area, Newfoundland. In: "The
Buchans Orebodies – Fifty Years of Mining and
Exploration", E.A. Swanson, D.F. Strong and
J.G. Thurlow (eds.). Geol. Assoc. Can. Special
Paper No. 22, (in press).

BELT, E.S., 1969. Newfoundland Carboniferous stratigraphy
and its relation to the Maritimes and Ireland.
In: "North Atlantic – Geology and Continental
Drift", M. Kay (ed.). Am. Assoc. Petro. Geol.
Mem. 12, pp. 734-753.

BENNETT, R.A. and ROSE, W.I., 1973. Some compositional
changes in Archean felsic volcanic rocks related
to massive sulphide mineralization. Econ. Geol.,
68, pp. 886-891.

BISCHOFF, J.L. and DICKSON, F.W., 1975. Seawater-basalt
interaction at 200°C and 500 bars: implication
for origin of sea-floor heavy-metal deposits
and regulation of seawater chemistry. Earth
and Planet Sci. Lett., 25, pp. 385-397.

BOSTOCK, H.H., 1978. The Roberts Arm Group, Newfoundland: Geological notes on a Middle or Upper Ordovician island arc environment. Geol. Surv. Can. Pap. 78-15, 21p.

BOSTOCK, H.H., CURRIE, K.L., and WANLESS, R.K., 1979. The age of the Roberts Arm Group, north-central Newfoundland. Can. Jour. Earth Sci., 16, pp. 599-606.

BOYLE, R.W. and GARRETT, R.G., 1970. Geochemical Prospecting - A review of its status and future. Earth Sci. Rev., 6, pp. 51-75.

BRADSHAW, P.M.D., CLEWS, D.R., and WALKER, J.L., 1970. "Exploration Geochemistry - Part 4: Primary dispersion". Mining in Canada 1970.

BUCHANS STAFF, 1955. Buchans operation, Newfoundland. Can. Inst. Min. Metall. Bull., 48, pp. 349-353.

CADY, W.M., 1975. Tectonic setting of the Tertiary volcanic rocks of the Olympic Peninsula, Washington. Jour. Research U.S. Geol. Surv., 3, (5), pp. 573-582.

CALHOUN, T., 1979. A study of a fragmental ore occurrence, Clementine prospect, Buchans, Newfoundland. Unpub. M.Sc. Thesis, University of Western Ontario, 95 p.

CALHOUN, T.A. and HUTCHINSON, R.W., 1981. Determination of flow direction and source of fragmental sulphides, Clementine deposit, Buchans, Newfoundland. In: "The Buchans Orebodies - Fifty Years of Mining and Exploration", E.A. Swanson, D.F. Strong and J.G. Thurlow (eds.). Geol. Assoc. Can. Special Paper No. 22, (in press).

CANN, J.R., 1970. "Rb, Sr, Y, Zr and Nb in some ocean floor basaltic rocks". Earth and Planet. Sci. Let., 10, pp. 7-11.

CARLISLE, D., 1963. Pillow breccias and their aquagene tuffs, Quadra Island, British Columbia. Jour. Geol., 71, pp. 48-71.

CATHERALL, D.J., 1960. Engine House Orebody. Unpub. B.Sc. Thesis, Royal School of Mines, London, 92p.

CLARKE, D.B., 1975. Tertiary basalts dredged from Baffin
        Bay. Can. J. Earth Sci., 12, pp. 1396-1405.

COBBING, E.J. and PITCHER, W.S., 1972. The coastal batholith
        of central Peru. Jour. Geol. Soc. Land., 128,
        pp. 421-460.

CONSTANTINOU, G., 1976. Genesis of the conglomerate structure,
        porosity and collomorphic textures of the massive
        sulphide ores of Cyprus. In: "Metallogency
        and plate tectonics", D.F. Strong (ed.). Geol.
        Assoc. Can. Spec. Paper 14, pp. 187-210.

COOMBS, D.S., 1960. Lower grade mineral facies in New Zealand.
        Int. Geol. Congress, 21st. Copenhagen, Pt. 13,
        pp. 339-351.

DATE, J. and TANIMURA, S., 1974. Dacite and rhyolite assoc-
        iated with the Kuroko mineralization. In:
        "Geology of Kuroko Deposits", S. Ishihara (ed.).
        Soc. Min. Geol. Japan Spec. Issue 6, pp. 261-266.

DAVENPORT, P.H. and I. NICHOL, 1972. Bedrock geochemistry
        as a guide to areas of base metal potential in
        volcano-sedimentary belts of the Canadian Shield.
        In: "Geochemical Exploration 1972, Proceedings
        of the fourth International Geochemical Explor-
        ation Symposium, London", M.J. Jones (ed.).
        pp. 45-57.

DAVIES, I.C. and WALKER, R.G., 1974. Transport and deposition
        of resedimented conglomerates: the Cap Enrage
        Formation, Cambro-Ordovician, Gaspé, Quebec.
        J. Sed. Petro., 44, pp. 1200-1216.

DEAN, P.L., 1977. A report on the geology and metallogeny
        of the Notre Dame Bay area. Nfld. Dept. of
        Mines and Energy, 77-10, 17p.

DESCARREUX, J., 1973. A petrochemical study of the Abitibi
        volcanic belt and its bearing on the occurrence
        of massive sulphide ores. Can. Inst. Min.
        Metall. Bull., 66, pp. 61-69.

DUNNING, G.R. and HERD, R.K., 1980. The Annieopsquotch
        ophiolite complex, southwest Newfoundland and
        its regional relationships. In: "Current
        Research, Part A". Geol. Surv. Can. Paper
        80-1A, pp. 227-234.

ELLISTON, J., 1963. Gravitational sediment movements in the Warramunga Geosyncline. In: "Syntaphral Tectonics and Diagenesis, A Symposium (S.W. Carey: Convener)", University of Tasmania, pp. C1-C18.

ENTWISTLE, L.P. and BARNES, M.P., 1971. Report on exploration possibilities at the Buchans unit, Newfoundland. ASARCO unpub. company paper.

FISHER, R.V., 1960. Classification of volcanic breccias. G.S.A. Bull., 71, pp. 973-982.

FISKE, R.S., 1963. Subaqueous pyroclastic flows in the Ohanapecosh formation, Washington. G.S.A. Bull, 74, pp. 391-406.

FISKE, R.S., 1969. Recognition and significance of pumice in massive pyroclastic rocks. Bull. Geol. Soc. Amer., 80, pp. 1-8.

FISKE, R.S. and MATSUDA, T., 1964. Submarine equivalents of ash flows in the Tokiva Formation, Japan. Amer. Jour. Sci., 262, pp. 76-106.

FISKE, R.S., HOPSON, C.A., and WATERS, A.C., 1963. Geology of Mt. Ranier National Park, Washington. U.S.G.S. Prof. Pap. 444, 93p.

FRANKLIN, J.M., KASARDA, J., and POULSEN, K.H., 1975. Petrology and chemistry of the alteration zone of the Mattabi massive sulphide deposit. Econ. Geol., 70, pp. 63-79.

GABRIELSE, H. and REESON, J.E., 1974. Nature and setting of granitic plutons in the central and eastern parts of the Canadian Cordillera. In: "Pacific Geology", 8, Tokai Univ. Press., pp. 109-138.

GALE, G.H., 1969. The primary dispersion of Cu, Zn, Ni, Co, Mn and Na adjacent to sulphide deposits, Springale Peninsula, Newfoundland. Unpub. M. Sc. Thesis, Memorial University.

GEORGE, P.W., 1937. Geology of lead-zinc-copper deposits at Buchans, Newfoundland. Amer. Inst. Min. Met. Eng., T.P. 816 (Class I, Mining Geology, No. 70).

GJELSVIK, T., 1968. Distribution of major elements in wall rocks and the silicate fraction of the Skorovass pyrite deposit, Grong area, Norway. Econ. Geol., 63, pp. 217-231.

GOODFELLOW, W.D., 1975. Major and minor element haloes in
        volcanic rocks at Brunswick No. 12 sulphide
        deposit, N.B., Canada. In: "Geochemical
        Exploration", 1974, Amsterdam, Elsevier,
        pp. 279-295.

GOODWIN, A.M., 1968. Archean protocontinental growth and
        early crustal history of the Canadian Shield.
        Int. Geol. Congr., 23rd, 1, pp. 69-89.

GOVETT, J.G.S., 1972. Interpretation of a rock geochemical
        exploration survey in Cyprus - statistical and
        graphical techniques. J. Geochem. Explor., 1,
        pp. 77-102.

GOVETT, G.J.S. and GOODFELLOW, W.D., 1975. Use of rock
        geochemistry in detecting blind sulphide
        deposits: a discussion. Transactions Institu-
        tion of Mining and Metallurgy, Section B,
        85, pp. 134-140.

GOVETT, G.J.S. and NICHOL, I., 1979. Lithogeochemistry in
        mineral exploration. In: "Geophysics and
        geochemistry in the search for metallic ores",
        P.J. Hood (ed.). Geol. Surv. Can., Econ.
        Geol. Report 31, pp. 339-362.

GOVETT, G.J.S. and PANTAZIS, Th. M., 1971. Distribution
        of Cu, Zn, Ni and Co in the Troodos Pillow
        Lava Series, Cyprus. IMM Trans., 80, pp.
        B27-B46.

GOVETT, G.J.S., WHITEHEAD, R.E.S., CROSBY, R.M., and
        AUSTRIA, V.B., 1974. Exploration geochemistry
        in New Brunswick. Can. Inst. Min. Metall.,
        67, pp. 76-84.

GRAF, J.L., 1977. Rare earth elements as hydrothermal
        tracers during the formation of massive sulphide
        deposits in volcanic rocks. Econ. Geol., 72,
        527-548.

HAJASH, A., 1975. Hydrothermal processes along mid-ocean
        ridges: an experimental investigation. Contrib.
        Mineral. Petrol., 53, pp. 205-226.

HART, R., 1970. Chemical exchange between sea water and
        deep ocean basalts. Earth Planet Sci. Lett.,
        9, pp. 269-279.

HART, R.A., 1973. A model for chemical exchange in the basalt-seawater system of oceanic layer II. Can. Jour. Earth Sci., 10, pp. 799-816.

HART, S.R., 1969. K, Rb, Cs contents and K/Rb, K/Cs ratios of fresh and altered submarine basalts Earth Planet Sci. Lett., 6, pp. 295-303.

HART, S.R., 1973. Submarine basalts from Kilauea rift, Hawaii: nondependence of trace element composition on extrusion depth. Earth Planet Sci. Lett., 20, pp. 201-203.

HAWKES, H.E. and WEBB, J.S., 1962. Geochemistry in mineral exploration. Harper and Row, N.Y., 415p.

HELWIG, J. and SARPI, E., 1969. Plutonic-pebble conglomerates, New World Island, Newfoundland, and history of eugeosynclines. In: "North Atlantic - Geology and Continental Drift", M. Kay (ed.). Amer. Assoc. Petrol. Geol., Mem. 12, pp. 443-466.

HENLEY, R.W. and THORNLEY, P., 1981. Low grade metamorphism and the geothermal environment of massive sulphide ore formation, Buchans, Newfoundland. In: "The Buchans Orebodies - Fifty Years of Mining and Exploration", E.A. Swanson, D.F. Strong and J.G. Thurlow (eds.). Geol. Assoc. Can. Special Paper No. 22, (in press).

HIRABAYASHI, T., 1974. On the Kuroko-type orebodies in the Yokota mine area, Mishi-Aizu district, Fukushima Prefecture. In: "Geology of Kuroko Deposits", S. Ishihara (ed.). Soc. Min. Geol. Japan Spec. Issue 6, pp. 195-202.

HONISHI, O., 1974. Geology of the Wanibuchi gypsum deposits, Shimane Prefecture. In: "Geology of Kuroko Deposits", S. Ishihara (ed.). Society of Mining Geologists of Japan, Spec. Issue 6, pp. 213-220.

IRVINE, T.N. and BARAGAR, W.R.A., 1971. A guide to the chemical classification of the common volcanic rocks. Can. Jour. Earth Sci., 8, pp. 523-548.

ISHIHARA, S. (Ed.), 1974. Geology of the Kuroko deposits. Society of Mining Geologists of Japan, Spec. Issue No. 6, 435p.

ISHIKAWA, Y. and YANAGISAWA, Y., 1974. Geology of the
        Ainai mine, with special reference to syngenetic
        origin of the Daikoku deposits. In: Geology
        of Kuroko deposits", S. Ishihara (ed.). Soc.
        Min. Geol. Japan, Spec. Issue 6, pp. 79-88.

ITO, T., TAKAHASHI, T., and OMORI, Y., 1974. Submarine
        volcanic-sedimentary features in the Matsumine
        Kuroko deposits, Hanaoka mine, Japan. In:
        "Geology of the Kuroko deposits", S. Ishihara
        (ed.). Soc. Min. Geol. Japan, Spec. Issue 6,
        pp. 115-130.

JAKES, P. and WHITE, A.J.R., 1971. Composition of island
        arcs and continental growth. Earth and Planetary
        Sci. Lett., 12, pp. 224-230.

JOLLY, W.T., 1972. Degradation (hydration) - aggradation
        (dehydration) and low-rank metamorphism of mafic
        volcanic sequences. 24th Int. Geol. Cong.,
        Section 2, pp. 11-18.

JOLLY, W.T., 1974. Behavior of Cu, Zn and Ni during prehnite-
        pumpellyite rank metamorphism of the Keweenawan
        basalts, Northern Michigan. Econ. Geol., 69,
        pp. 1118-1125.

JOLLY, W.T. and SMITH, R.E., 1972. Degradation and metamorphic
        differentiation of the Keweenawan Tholeiitic
        Lavas of Northern Michigan, USA. Jour. Pet.,
        13, (2), pp. 273-309.

JONES, J.G., 1969. Pillow lavas as depth indicators. Amer.
        Jour. Sci., 267, pp. 181-195.

KAJIWARA, Y., 1970. Syngenetic features of the Kuroko ore
        from the Shakanai. In: "Volcanism and
        Ore Genesis", Tatsumi, T. (ed.). Univ. of
        Tokyo Press, pp. 197-206.

KALLIOKOWSKI, J., 1955. Gull Pond, Newfoundland. Geol.
        Surv. Can. Paper 54-4.

KEAN, B.F., 1977. Geology of the Lake Ambrose sheet,
        west half. In: "Report of Activities, 1976",
        R.V. Gibbons (ed.). Newfoundland Dept. of
        Mines and Energy, Report 77-1, pp. 21-26.

KEAN, B.F., 1979. Buchans map area (12A/15), Newfoundland.
        In: "Report of Activities for 1978", R.V. Gibbons
        (ed.). Newfoundland Dept. of Mines and Energy,
        Report 79-1, pp. 18-24.

KEAN, B.F., 1980. Buchans map sheet (12A/15), Newfoundland.
     Nfld. Dept. of Mines and Energy, Map 79-125.

KEAN, B.F. and JAYASINGHE, N.R., 1980. Badger map area
     (12A/16) Newfoundland. In: "Current research",
     O'Driscoll, C. and Gibbons, R. (eds.). Newfound-
     land Dept. of Mines and Energy, Report 80-1,
     pp. 37-43.

KEAN, B.F., DEAN, P.L. and STRONG, D.R., 1981. Regional
     geology of the central volcanic belt in Newfound-
     land. In: "The Buchans Orebodies - Fifty Years
     of Mining and Exploration", E.A. Swanson,
     D.F. Strong and J.G. Thurlow (eds.). Geol.
     Assoc. Can. Special Paper No. 22, (in press).

KOCH, G.S. and LINK, 1971. "Statistical Analysis of
     Geological Data",

KOWALIK, J., RYE, R.O., and SAWKINS, F.J., 1981. Stable
     isotope study of the Buchans polymetallic
     sulphide deposits. In: "The Buchans Orebodies -
     Fifty Years of Mining and Exploration", E.A.
     Swanson, D.F. Strong and J.G. Thurlow (eds.).
     Geol. Assoc. Can. Special Paper No. 22, (in press).

KUNO, H., 1966. Lateral variation of basalt magma type
     across continental margins and island arcs.
     Bull. Volcan., 29, pp. 195-222.

LAMBERT, I.B. and SATO, T., 1974. The Kuroko and associated
     ore deposits of Japan: a review of their features
     and metallogenesis. Econ. Geol., 69, pp.
     1215-1236.

LANGMHYR, F.J. and PAUS, P.E., 1968. The analysis of
     inorganic siliceous materials by atomic absorb-
     tion spectrophotometry and the hydrofluoric
     acid decomposition technique, Part I: The
     analysis of silicate rocks. Anal. Chim. Acta.,
     43, pp. 397-408.

LARGE, R.R., 1977. Chemical evolution and zonation of
     massive sulphide deposits in volcanic terrains.
     Econ. Geol., 72, pp. 549-572.

LARSEN, K.B., 1973. The formation and penecontemporaneous
     deformation of tuffaceous sediments in Buchans,
     Newfoundland. Unpub. ASARCO report.

LARSON, L. and WEBBER, G.R., 1977. Chemical and petro-
     graphic variations in rhyolitic zones in the
     Noranda area, Quebec. Can. Inst. Min. Metall.
     Bull., 70, pp. 80-93.

LAVIN, O.P., 1976. Lithogeochemical discrimination between
        mineralized and unmineralized cycles of volcanism
        in the Sturgeon Lake and Ben Nevis areas of
        the Canadian Shield. Unpub. M.Sc. thesis,
        Queens University, 249p.

LEE, M.S., MIYASIMA, T., and MIZUMOTO, H., 1974. Geology of
        the Kamaikita mine, Aomori Prefecture, with
        special reference to genesis of fragmental ores.
        In: "Geology of Kuroko Deposits", S. Ishihara
        (ed.). Soc. Min. Geol. Japan, Spec. Issue 6,
        pp. 53-66.

LEVINSON, A.A., 1974. Introduction to exploration geochem-
        istry, Second Edition, Applied Publishing,
        Illinois, 924p.

LUNDBERG, H., 1957. The discovery of large lead-zinc deposits
        at Buchans, Newfoundland. Mining Geophysics,
        6th Commonwealth Min. Met. Congress., 1957,
        pp. 141-154.

MACKENZIE, D.E. and CHAPPELL, B.W., 1972. Shoshonite and
        calc-alkaline lavas from the highlands of
        Papua, New Guinea. Contrib. Min. Petrol., 35,
        pp. 50-62.

MACLEAN, H.J., 1941. Memorandum on prospecting in the Little
        Sandy Brook area. Unpub. ASARCO report.

MACLEAN, H.J., 1943. Memorandum on prospecting in the
        Woodman's Brook - No. 2 Siding area. Unpub.
        ASARCO report.

MARCOTTE, D. and DAVID, M., 1978. Targets definition of
        Kuroko type deposits in Abitibi by statistical
        analysis of geochemical data. Paper presented
        to Can. Inst. Min. Metall.

MCCONNEL, J.W., 1976. Geochemical dispersion in wallrocks
        of Archean massive sulphide deposits. Unpub.
        M.Sc. thesis, Queens University, 230p.

MOTEGI, M., 1974. Kuroko deposits of the Kurosawa mine,
        Fukushima Prefecture. In: "Geology of Kuroko
        deposits", S. Ishihara (ed.). Soc. Min. Geol.
        Japan, Spec. Issue 6, pp. 203-208.

MURRAY, A., 1871. Annual report. Newfoundland Geological
        Survey.

MUTTI, E., 1965. Submarine flood tuffs associated with turbidites in Oligocene deposits of Rhodes Island, Greece. Sedimentology, 5, pp. 265-288.

NAIRIS, B., 1971. Endogene dispersion aureoles around the Rudtjebacken sulphide ore in the Adak area, Northern Sweden. In: "Geochemical Exploration", Can. Inst. Min. Metall., Spec. Vol. 11, pp. 357-374.

NEALE, E.R.W. and NASH, W.A., 1963. Sandy Lake (East Half), Newfoundland. Geol. Surv. Can. Paper 62-28.

NEARY, G.N., 1981. Mining History of the Buchans Area. In: "The Buchans Orebodies - Fifty Years of Mining and Exploration", E.A. Swanson, D.F. Strong and J.G. Thurlow (eds.). Geol. Assoc. Can. Special Paper No. 22, (in press).

NEWHOUSE, W.H., 1931. Geology and ore deposits of Buchans, Newfoundland. Econ. Geol., 26, pp. 399-414.

NILSSON, C.A., 1968. Wall rock alteration at Boliden deposit, Sweden. Econ. Geol., 63, pp. 472-494.

OHTAGAKI, T., ONO, T., and KIMURA, A., 1974. Geology of the Tashiro mine, Fukushima Prefecture. In: "Geology of Kuroko deposits", S. Ishihara (ed.). Soc. Min. Geol. Japan, Spec. Issue 6, pp. 189-194.

OSADA, T., ABE, M., and DAIMARU, K., 1974. Geology of the Yoshino mine, Yamagata Prefecture. In: "Geology of Kuroko deposits", S. Ishihara (ed.). Soc. Min. Geol. Japan, Spec. Issue 6, pp. 183-188.

OSHIMA, T., HASHIMOTO, T., KAMOND, K., KAWABE, S., SUCA, K., TANIMURA, S., and ISHIKAWA, Y., 1974. Geology of the Kosada mine, Akita Prefecture. In: "Geology of Kuroko deposits", S. Ishihara (ed.). Soc. Min. Geol. Japan, Spec. Issue 6, pp. 89-100.

PANTAZIS, T.L.M. and GOVETT, G.J.S., 1973. Interpretation of a detailed rock geochemical survey around Mathiati mine, Cyprus. Jour. Geochem. Exploration, 2, pp. 25-36.

PEARCE, J.A. and CANN, J.R., 1973. Tectonic setting of basic volcanic rocks determined using trace element analysis. Earth. Planet. Sci. Lett., 19, pp. 290-300,

PEARCE, T.H., 1974. Quench plagioclase from some Archean basalts. Can. J. Earth Sci., 11, pp. 715-719.

PHILPOTTS, J.A., SCHNETZLER, C.C., and HART, S.R., 1969.
Submarine basalts: some K, Rb, Sr, Ba, rare
earth, H_2O and CO_2 data bearing on their alter-
ation, modification by plagiclase and possible
source materials. Earth. Planet. Sci. Lett.,
7, pp. 293-299.

RELLEY, B.H., 1960. The geology of the Buchans mine. Unpub.
Ph.D. Thesis, McGill University, 281p.

RIDLER, R.H., 1973. Exhalite concept, a new tool for explor-
ation. Northern Miner, Nov. 29, pp. 59-61.

RILEY, G.C., 1957. Red Indian Lake (west half) map area,
Newfoundland. Geol. Surv. Can. Map 8-1957.

SAKRISON, H.C., 1967. Chemical studies of the host rocks of
the Lake Dufault mine, Quebec. Unpub. Ph.D.
thesis, McGill University.

SAKRISON, H.C., 1971. Rock geochemistry - its current useful-
ness on the Canadian Shield. CIM Bull., Nov.,
pp. 28-31.

SANGSTER, D.F., 1972. Precambrian volcanogenic massive
sulphide deposits in Canada: A review. Geol.
Surv. Can. Paper 72-22, 44p.

SANGSTER, D.F. and SCOTT, S.D., 1976. Precambrian, stratbound,
massive Cu-Zn-Pb sulfide ores of North America.
In: "Handbook of stratabound and stratiform
ore deposits", K. Wolf (ed.), 6, pp. 129-222.

SATO, M. and MOONEY, H.M., 1960. The electrochemical
mechanism of sulphide self potential. Geophysics,
25, pp. 226-249.

SATO, N. and KUSAKA, H., 1974. Geology of the Matsuki mine,
Ohdate city, Akita prefecture. In: "Geology
of Kuroko deposits", S. Ishihara (ed.). Soc.
Min. Geol. Japan, Spec. Issue 6, pp. 141-146.

SATO, T., 1968. Ore showing graded bedding from Uchinotai
western ore body, Kosaka mine, Akita prefecture.
Bull. Geol. Surv. Japan, 19, pp. 7-20.

SATO, T., 1972. Behaviors of ore-forming solutions in sea
water. Mining Geology, 22, pp. 31-42.

SATO, T., 1974. Distribution and geological setting of the
Kuroko deposits. In: "Geology of Kuroko
deposits", S. Ishihara (ed.). Soc. Min. Geol.
Japan, Spec. Issue 6, pp. 1-10.

SCHERMERHORN, L.J.G., 1970. The deposition of volcanics and pyritite in the Iberian pyrite belt. Mineral. Deposita, 5, pp. 273-279.

SCHERMERHORN, L.J.G., 1971. Pyrite emplacement by gravity flow. Bull. Geol. Min., 72, pp. 304-308.

SHAPIRO, L. and BRANNOCK, W.M., 1962. Rapid analysis of silicate, carbonate and phosphate rocks. U.S.G.S. Bulletin, 1144A, A31.

SIMMONS, B.D. and the GEOLOGICAL STAFF, Lake Dufault Divin, Falconbridge Copper Ltd., 1973. Geology of the Millenbach massive sulphide deposit, Noranda, Quebec. Can. Inst. Min. Metall. Bull., 66, pp. 67-78.

SINCLAIR, W.D., 1971. A volcanic origin for the No. 5 zone of the Horne mine, Noranda, Quebec. Econ. Geol., 66, pp. 1225-1231.

SMITH, R.E., 1968. Redistribution of major elements in the alteration of some basic lavas during burial metamorphism. Jour. Petrol., 9, pp. 191-219.

SNELGROVE, A.K., 1928. The geology of the central mineral belt of Newfoundland. Can. Min. and Met. Bull., 21, pp. 1057-1127.

SOPUCK, V.J., 1977. A lithogeochemical approach in the search for areas of felsic volcanic rocks associated with mineralization in the Canadian Shield. Unpub. Ph.D. thesis, Queens Univ.

SPENCE, C.D., 1975. Volcanogenic features of the Vauze sulfide deposit, Noranda, Quebec. Econ. Geol., 70, pp. 102-114.

SPITZ, G. and DARLING, R., 1978. Major and minor element lithogeochemical anomalies surrounding the Louvem copper deposit, Val d'Or, Quebec. Can. Jour. Earth Sci., 15, pp. 1161-1169.

STAUFFER, P.H., 1967. Grain-flow deposits and their implications., Santa Ynez Mountains, California. Jour. Sed. Petrology, 37, pp. 487-508.

STRECKEISEN, A., 1976. To each plutonic rock its proper name. Earth Sci. Rev., 12, pp. 1-33.

STRONG, D.F., 1973. Lushs Bight and Roberts Arm Groups of central Newfoundland: possible juxtaposed oceanic and island-arc volcanic suites. Bull. Geol. Soc. Amer., 84, pp. 3917-3928.

STRONG, D.F., 1977. Volcanic regimes of the Newfoundland
        Appalachians. Geol. Assoc. Can. Spec. Pap.
        16, pp. 61-90.

STRONG, D.F., 1981. Mineralographic notes on ore samples
        of the Buchans district. In: "The Buchans
        Orebodies - Fifty Years of Mining and Exploration",
        E.A. Swanson, D.F. Strong, and J.G. Thurlow (eds.).
        Geol. Assoc. Can. Special Paper No. 22, (in press).

SUFFEL, G.G., 1965. Remarks on some sulphide deposits in
        volcanic extrusives. Can. Inst. Min. Metall.
        Bull., 58, pp. 1057-1063.

SUGIMURA, A., 1968. Spatial relations of basaltic magmas.
        In: "Basalts", H.H. Hess and A. Poldervaart
        (eds.). New York, Interscience, pp. 573-577.

SWANSON, E.A. and BROWN, R.L., 1962. Geology of the Buchans
        orebodies. Can. Inst. Min. Metall. Bull., 55,
        pp. 618-626.

SWANSON, E.A., PERKINS, E.W., and HIGGINS, W.H., 1956.
        Diamond drill electrical surveys, Oriental #2
        orebody, Buchans mine. Paper presented at A.I.M.E.
        meeting, Feb. 1956.

TAKAHASHI, T. and SUGA, K., 1974. Geology and ore deposits
        of the Hanaoka Kuroko belt, Akita Prefecture.
        In: "Geology of Kuroko deposits", S. Ishihara
        (ed.). Soc. Min. Geol. Japan, Spec. Issue 6,
        pp. 101-114.

TANIMURA, S., SHIMODA, T., and SAWAGUCHI, T., 1974. On the
        Fukazawa orebodies, Akita Prefecture. In:
        Geology of the Kuroko deposits", S. Ishihara (ed.).
        Soc. Min. Geol. Japan, Spec. Issue 6, pp. 147-156.

TATSUMI, T. and CLARKE, L.A., 1972. Chemical composition of
        acid volcanic rocks genetically related to
        formation of the Kuroko deposit. Jour. Geol.
        Soc. Japan, 78, pp. 191-201.

TAYLOR, R.P., STRONG, D.F., and KEAN, B.F., 1980. The
        Topsails igneous complex: Silurian-Devonian
        peralkaline magmatism in western Newfoundland.
        Can. Jour. Earth Sci., 17, pp. 425-439.

THURLOW, J.G., 1973. Lithogeochemical studies in the vicinity
        of the Buchans massive sulphide deposits, central
        Newfoundland. Unpub. M.Sc. thesis, Memorial
        Univ., 172p.

THURLOW, J.G., 1975. Buchans area report. In: Geology, mineral deposits and mineral potential of the Buchans volcanic belt", by B.F. Kean and J.G. Thurlow. Report submitted to the Buchans Task Force, 56p.

THURLOW, J.G., 1977. The occurrence, origin and significance of mechanically transported ores at Buchans, Newfoundland. In: "Volcanic processes in ore genesis". Special Pub., 7, Geol. Soc. London., p. 127.

THURLOW, J.G., SWANSON, E.A., and STRONG, D.F., 1975. Geology and lithogeochemistry of the Buchans polymetallic sulphide deposits, Newfoundland. Econ. Geol., 70, pp. 130-144.

TONO, N., 1974. Minor elements distribution around Kuroko deposits in northern Akita, Japan. In: "Geology of Kuroko deposits", S. Ishihara (ed.). Soc. Min. Geol. Japan, Spec. Issue 6, pp. 399-420.

TUTTLE, O.F. and BOWEN, N.L., 1958. Origin of granite in the light of experimental studies in the system $NaAlSi_3O_8 - KAlSi_3O_8 - SiO_2 - H_2O$. Geol. Soc. Amer. Memoir, 74, 153p.

URABE, T. and SATO, T., 1978. Kuroko deposits of the Kosaka Mine, northeast Honshu, Japan - products of submarine hot springs on Miocene sea floor. Econ. Geol., 73, pp. 161-179.

WAHL, J.L., GOVETT, G.J.S., and GOODFELLOW, W.D., 1975. Anomalous element distribution in volcanic rocks around Key Anacon, Heath Steele B-zone and Brunswick No. 12 sulphide deposits (abstract). Can. Inst. Min. Metall. Bull., 68, p. 49.

WALKER, P.N. and KING, J., 1975. Preliminary report, Buchans Project. Unpub. ASARCO report, 4p.

WALKER, R.R., MATULICH, A., AMOS, A.C., WATKINS, J.J., and MANNARD, G.W., 1975. The geology of the Kidd Creek mine. Econ. Geol., 70, pp. 80-89.

WHITEHEAD, R.E., 1973. Environment of stratiform sulphide deposition; variation in Mn:Fe ratio in host rocks at Heath Steele mine, New Brunswick, Canada. Mineralium Deposita, 8, pp. 148-160.

WHITEHEAD, R.E.S. and GOVETT, G.J.S., 1974. Exploration
          rock geochemistry - detection of trace element
          haloes at Heath Steele mines (N.B., Canada)
          by discriminant analysis. J. Geochem. Explor.,
          3, pp. 371-386.

WILLIAMS, H., 1967. Silurian rocks of Newfoundland. G.A.C.
          Special Paper 4, pp. 93-137.

WILLIAMS, H., 1970. Red Indian Lake (east half), Newfound-
          land. Geological Survey of Canada, Map 1196A.

WILLIAMS, H., 1979. Appalachian orogen in Canada. Can.
          Jour. Earth Sci., 16, pp. 792-807.

WOAKES, M., 1954. A microscopic study of the ore sulphides
          from Buchans mine, Buchans, Newfoundland. Unpub.
          B.Sc. thesis, Royal School of Mines, London,
          59p.

YAMADA, E., 1973. Subaqueous pumice flow deposits in the
          Orikobe caldera, Miyaji Prefecture, Japan.
          J. Geol. Soc. Japan, 79, pp. 585-597.

APPENDIX I

Classification of Plutonic Rocks (after Steckeisan, 1976)
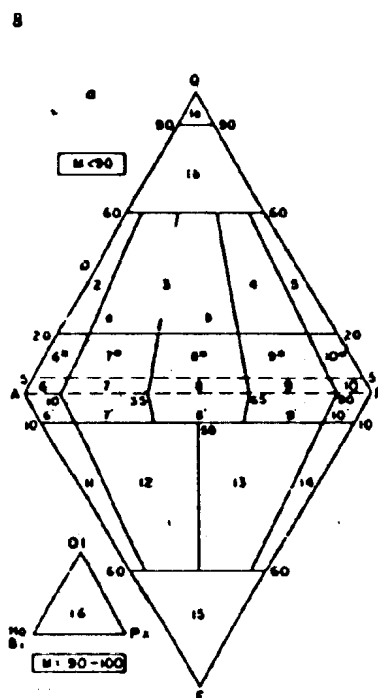
Fig. 1a. General classification and nomenclature of plutonic rocks according to mineral content (in vol. %).

Q + A + P = 100, or A + P + F = 100.

1a, quartzolite (silexite); 1b, quartz-rich granitoids; 2, alkali-feldspar granite; 3, granite; 4, granodiorite; 5, tonalite, 6°, quartz alkali-feldspar syenite; 7°, quartz syenite; 8°, quartz monzonite; 9°, quartz monzodiorite/quartz monzogabbro; 10°, quartz diorite/quartz gabbro/quartz anorthosite; 6, alkali-feldspar syenite; 7, syenite; 8, monzonite; 9, monzo-diorite/monzogabbro; 10, diorite/gabbro/anorthosite; 6', foid-bearing alkali-feldspar syen-ite; 7', foid-bearing syenite; 8', foid-bearing monzonite; 9', foid-bearing monzodiorite/monzogabbro; 10', foid-bearing diorite/gabbro; 11, foid syenite; 12, foid monzosyenite (syn. foid plagisyenite); 13, foid monzodiorite/foid monzogabbro (essexite = nepheline monzodiorite/monzogabbro); 14, foid diorite/foid gabbro (theralite = nepheline gabbro, teschenite = analcime gabbro); 15, foidolites; 16, ultramafic plutonic rocks (ultramafitol-ites).

APPENDIX II

FIELD AND LABORATORY METHODS

(i)   Sample Collection

(ii)   Sample Preparation

(iii)   Analytical Procedures - Major elements

(iv)   Analytical Procedures - Trace elements

(1)   Sample Collection

A small (less than 1 kg) reference sample was collected from almost all outcrops visited. The decision to take larger samples for geochemical analysis was based on a number of factors, i.e., the stratigraphic and aerial coverage desired, suitability of the lithology for geochemical analysis and accessibility of the outcrop. Samples taken for geochemical analysis ranged from one to five kilograms (varying with sample grain size) and were collected with a 3 kg sledge hammer. Visibly altered samples were not collected unless the alteration was characteristic of the area or the specific unit sampled. Similarly, samples were not collected from outcrops displaying lithologic heterogeneity, deep weathering, secondary veining, abundant amygdules, etc. Where pillow lava was sampled, care was taken to ensure that no selvedge or interpillow material was included. Samples were trimmed of weathering as best as possible in the field and remaining weathering was removed with

the diamond saw at Buchans. All field samples, regardless
of weathering, were slabbed with the diamond saw in order
to macroscopically assess their suitability for analysis.

The philosophy governing sample collection from
core was similar to that in the field except that weathering
was not a factor. The visual assessment of the suitability
of core samples for geochemical analysis was based on a
number of factors. Sections of core containing veins,
alteration or sulphides were not sampled. Some sections of
core contain a visible sheen of steel (or rust) derived
from abrasion with the core barrel during drilling. Samples
were not taken from such sections. Core samples taken were
deemed to be representative of the section of core under
study. Sampling of felsic pyroclastic rocks was especially
critical as these rocks were known to best distinguish
between mineralized and barren sequences (Thurlow, 1973).
Pyroclastic rocks sampled were fine grained (1-5 mm) and
homogeneous. Crystal-vitric tuffs (the most widespread
pyroclastic type) were sampled in preference to other
types such that texturally and mineralogically similar
lithologies were being geochemically compared. Pyroclastic
rocks containing numerous lithic fragments were not sampled.

In general, diamond drill core allows a better
visual estimation of the suitability for analysis than does
outcrop and also provides more exact stratigraphic positioning.

For these reasons, core samples were analysed in preference to surface samples where both were available from the same stratigraphic unit in the same area.

(ii) Sample Preparation

Samples selected for analysis were washed, logged, dried and put into clean bags before crushing. One half to two thirds of each sample was subjected first to a coarse crush, then a fine crush on a Denver steel jaw crusher. The crushed samples were rolled, quartered and placed in glass jars to await pulverizing.

Pulverizing was effected by two different methods. Those samples prepared during the previous study (Thurlow, 1973) were pulverized in alumina ball mills by a method described by Thurlow (op. cit.).

Additional samples prepared during the present study were pulverized in a Tema swing mill with a tungsten carbide liner. Approximately 50 grams of sample was pulverized for two minutes which yielded a powder of minus 200 mesh.

Contamination during sample reduction is inevitable but all possible efforts were taken to ensure that it was minimized. Samples were ordered according to lithology before crushing and pulverizing to ensure that the effects of inter-sample contamination were minimized. Samples

containing sulphides were crushed and pulverized after the
sulphide-free samples. After each sample was crushed,
the removable jaw of the crusher was taken off and the
entire appartus was brushed and blown clean with compressed
air. The internal parts of the swing mill were scrubbed
with water after each sample was pulverized. Pulverized
samples were stored in new glass jars. Care at all inter-
vening stages of the crushing and grinding procedure ensured
that inter-sample contamination was negligible.

Contamination from the crushing and pulverizing
apparatus is inevitable. The removable steel jaw of the jaw
crusher at Buchans was weighed prior to, and after crushing.
The jaw weighed 12 grams less after 625 samples were crushed,
an average contamination of approximately 20 ppm steel per
sample from that jaw. Alumina contamination from the alumina
ball mills used for pulverizing was determined by a similar
method and found to be approximately 0.1% Al_2O_3 per sample.
As tungsten was not determined in the present study tungsten
carbide contamination from the Tema swing mill was not
estimated.

(iii)   Analytical Procedures - Major Elements

All major elements were determined by the author
using a Perkin Elmer 303 atomic absorption spectrophotometer
equipped with a recorder readout. The digestion technique
used was similar to that described by Langmhyr and Paus (1968).

Exactly 0.1000 g of sample was weighed and placed in a poly carbonate digestion bottle. Digestion was effected by addition of 5 ml of concentrated HF and heating on a water bath for 20 minutes. Samples were subsequently cooled and 50 ml boric acid added to complex undissolved fluorides. Following a second heating, samples were diluted with 145 ml distilled and de-ionized water. Standards were prepared in a manner similar to that described by Abbey (1968).

Calcium and magnesium were determined using a air-acetelyne flame by adding a lanthanum oxide – HCl solution to supress interferences by aluminum. Phosphorus was determined by a colormetric method similar to that described by Shapiro and Brannock (1962). Loss on ignition was determined by heating a known weight of sample at 1050°C for 90 minutes and measuring the weight loss due to escape of volatiles (principally H_2O, CO_2 and SO_2).

Precision of major element analyses was determined by choosing a sample of intermediate composition and preparing solutions of this sample at intervals throughout the analytical period. The results of thirteen such runs are as follows:

PRECISION OF ATOMIC ABSORPTION MAJOR ELEMENT DETERMINATIONS

Element	Number Of Determinations	Mean (Weight %)	Standard Deviation	Coefficient of Variation (%)
SiO_2	13	65.4	.82	1.25
TiO_2	13	.40	.01	2.50
Al_2O_3	13	14.29	.21	1.47
Fe_2O_3	13	4.59	.10	2.18
MnO	13	.11	.01	9.09
MgO	13	1.71	.03	1.76
CaO	13	3.47	.05	1.44
Na_2O	13	1.88	.03	1.60
K_2O	13	3.40	.05	1.47
P_2O_5	13	.05	.03	60.0
Loss Ig.	13	3.89	.14	3.60

Accuracy was determined by comparison to the U.S.

G.S. standard BCR-1. The results of five analyses are as follows:

ACCURACY OF ATOMIC ABSORPTION MAJOR ELEMENT DETERMINATIONS

Wt. %	A*	Mean (Weight %)	Standard Deviation
SiO_2	54.85	55.38	0.37
TiO_2	2.22	2.35	0.18
Al_2O_3	13.68	13.50	0.27
Fe_2O_3	13.52	13.00	0.28
CaO	6.98	6.63	0.07
MgO	3.49	3.57	0.06
Na_2O	3.29	3.23	0.05
K_2O	1.68	1.73	0.05
MnO	0.19	0.18	0.01

*Proposed values after Abbey (1975).

(iv) Analytical Procedures - Trace Elements

Rock chips sent to the ASARCO laboratory at
Salt Lake City for trace element analysis were ground at
-50°C to prevent loss of Hg vapour. Hg was subsequently
determined on a modified Perkin Elmer 303 using a flameless
method. Zn, Mo, Cu, Pb, Ni, Co, V and Ag were determined
by conventional atomic absorption methods using a back-
ground correction for non-specific absorption (L.D. James,
personal communication).

Precision of trace element analyses were deter-
mined by replicate analysis of every tenth sample. The
results of the precision test are as follows:

PRECISION OF ATOMIC ABSORPTION TRACE ELEMENT DETERMINATIONS

Element	Number of Determinations	Range of Analysed Samples (ppm)	Average Coefficient of Variance (5)
Cu	25	2 - 9700	2.39
Pb	23	1 - 23000	5.30
Zn	26	10 - 115000	4.74
Mo	9	3 - 124	14.57
Ag	12	0 - 140	4.37
Hg	24	4 - 3466 (ppb)	11.21
Co	24	2 - 48	3.35
Ni	26	0 - 80	1.74
V	23	0 - 520	6.31

Rb, Ba, Sr, Zr and Cr were determined at Memorial University by X-Ray fluorescence. Ten g of sample powder was mixed with 1.3 g of phenolformaldehyde binding agent and pressed into a 40 mm pellet at 25 tons pressure.

Precision and accuracy data are as follows:

PRECISION AND ACCURACY OF XRF TRACE ELEMENT ANALYSES (13 DETERMINATIONS, SINGLE PELLET, W-1)

Element	Accepted* Value	Mean	Standard Deviation	Difference
Zr	105	98	2	-6.7%
Sr	190	189	6	-0.5
Rb	21	22	2	+4.8
Ba	160	171	12	+6.9
Cr	120	92	6	-23.3

*Abbey (1975)

FOOTWALL BASALT FLOWS

MAJOR ELEMENTS (WT%)

SAMPLE	JGT75139	JGT75219	9781479
SiO2	47.90	48.50	50.20
TiO2	.84	.84	.82
Al2O3	17.18	16.79	15.77
Fe2O3	8.70	9.32	7.65
MnO	.15	.13	.10
MgO	5.12	7.48	5.36
CaO	10.90	8.04	10.70
Na2O	2.39	3.29	2.33
K2O	1.22	1.59	1.11
LOI	5.90	3.10	4.50
TOTAL	100.30	99.08	98.54

TRACE ELEMENTS (PPM)

	JGT75139	JGT75219	9781479
Zr	92	77	79
Sr	343	223	334
Rb	31	33	21
Zn	52	35	65
Cu	63	15	74
Ba	435	461	678
CuS	54	16	72
PbS	6	7	5
ZnS	12	7	19
BaSO4	0	0	0
Pb	35	15	21
Ni	35	48	64
Co	27	17	26
Cr	144	231	478
V	195	95	170
Hg			
Ag			
Nb	10	6	2

FOOTWALL BASALT - ALTERED MAFIC FLOWS

MAJOR ELEMENTS (WT%)

SAMPLE	JBT75134	SK-5 350	542 550	542 625	14062440
SiO2	46.70	46.10	44.80	54.10	43.30
TiO2	1.18	1.18	.90	.63	1.00
Al2O3	15.83	15.26	16.28	11.75	15.89
Fe2O3	12.19	9.89	9.84	6.06	11.44
MnO	.20	.08	.20	.14	.21
MgO	5.42	14.32	8.78	4.18	6.85
CaO	5.16	1.86	9.84	10.03	9.85
Na2O	3.51	2.65	2.10	3.91	3.08
K2O	1.07	.10	.97	.11	.83
LOI	7.70	7.10	5.10	7.30	6.10
TOTAL	98.96	98.54	98.81	98.16	98.55

TRACE ELEMENTS (PPM)

	JBT75134	SK-5 350	542 550	542 625	14062440
Zr	60	50	96	46	66
Sr	92	41	352	144	239
Rb	25	6	20	9	18
Zn	96	47	105	94	72
Cu	28	72	53	44	64
Ba	270	71	614	162	318
CuS	28	85	42	34	51
PbS	9	5	20	11	5
ZnS	20	2	12	8	17
BaSO4	0	0	0		0
Pb	27	33	33	28	24
Ni	4	80	80	35	58
Co	25	45	37	27	28
Cr	27	622	208	103	262
V	235	230	275	260	165
Hg			12	12	
Ag			16	13	
Nb	8	6			6

FOOTWALL BASALT - MAFIC FRAGMENTALS

MAJOR ELEMENTS (WT%)

SAMPLE	542 700	5421000	05421150	5421225	05421350
SiO2	37.90	48.00	48.10	46.50	44.70
TiO2	.81	.86	.85	.80	.93
Al2O3	14.15	16.48	16.00	15.22	17.97
Fe2O3	10.32	11.64	11.89	10.15	12.27
MnO	.21	.12	.13	.15	.12
MgO	7.64	8.22	7.99	8.72	8.48
CaO	13.34	4.53	5.00	7.25	4.45
Na2O	1.98	1.98	2.29	1.94	1.63
K2O	.40	1.05	.63	.24	1.18
LOI	11.70	6.40	6.30	8.30	7.50
TOTAL	98.45	99.28	99.18	99.27	99.23

TRACE ELEMENTS (PPM)

Zr	82	87	75	75	83
Sr	244	283	223	254	224
Rb	18	26	17	16	33
Zn	91	88	80	73	91
Cu	50	66	59	58	55
Ba	257	373	340	276	429
CuS	32	23	38	32	31
PbS	12	2	7	3	2
ZnS	11	8	14	13	10
BaSO4	0				
Pb	30	34	36	42	34
Ni	42	59	54	40	64
Co	32	41	40	30	43
Cr	157	188	161	151	188
V	278	320	260	270	290
Hg	10	8	16	11	17
Ag	15	12	13	13	11
Nb					

FOOTWALL BASALT - MAFIC FRAGMENTALS

MAJOR ELEMENTS (WT%)

SAMPLE	05421475	12141450	12141475
SiO2	50.40	52.40	44.50
TiO2	.94	.78	.99
Al2O3	17.65	16.28	20.69
Fe2O3	10.96	10.70	14.41
MnO	.07	.12	.16
MgO	2.66	4.12	5.96
CaO	4.22	6.24	5.10
Na2O	.75	1.89	2.14
K2O	3.44	1.92	2.35
LOI	7.50	4.40	4.50
TOTAL	98.59	98.85	100.80

TRACE ELEMENTS (PPM)

	05421475	12141450	12141475
Zr	83	68	90
Sr	128	292	318
Rb	73	40	49
Zn	75	95	127
Cu	18	94	128
Ba	495	1619	1981
CuS	8	81	112
PbS	6	12	6
ZnS	2	31	38
BaSO4	0	.	0
Pb	28	16	20
Ni	39	13	16
Co	28	28	32
Cr	155	37	43
V	420	381	390
Hg	8	40	50
Ag	9	2	1
Nb			

FOOTWALL BASALT - ALTERED MAFIC FRAGMENTALS

MAJOR ELEMENTS (WTZ)

SAMPLE	02021225	542 775	5421075	05421575	05421625
SiO2	31.90	59.90	42.10	31.80	42.50
TiO2	.37	.36	.83	.77	.65
A1203	8.25	10.89	14.63	13.27	11.30
Fe203	5.47	10.67	9.52	6.34	15.24
MnO	.20	.24	.17	.15	.20
MgO	3.62	4.22	6.81	5.04	3.16
CaO	27.40	1.22	13.30	20.70	12.50
Na20	1.22	1.82	2.29	1.13	.85
K20	.43	.96	.65	.94	1.29
LOI	21.60	6.60	9.30	20.20	12.10
TOTAL	100.46	96.88	99.60	100.34	99.79

TRACE ELEMENTS (PPM)

Zr	36	52	88	90	57
Sr	121	61	285	194	101
Rb	19	29	18	29	34
Zn	78	125	87	75	77
Cu	44	33	66	39	31
Ba	129	2010	285	205	436
CuS	29	27	28	21	29
PbS	24	10	5	15	15
ZnS	17	19	8	14	6
BaSO4	0		0		
Pb	38	15	44	38	40
Ni	36	50	51	28	47
Co	20	42	33	33	27
Cr	76	50	171	105	110
V	163	161	270	290	168
Hg	43	15	10	21	19
Ag	15	0	15	13	14
Nb					

FOOTWALL BASALT - ALTERED MAFIC FRAGMENTALS

MAJOR ELEMENTS (WT%)

SAMPLE	05421700	05421875	05421950	05422025	05422100
SiO2	35.50	34.50	44.20	43.90	35.50
TiO2	.80	.66	.97	.73	.71
Al2O3	14.62	11.82	17.65	14.60	11.65
Fe2O3	8.39	8.67	12.47	9.41	9.93
MnO	.17	.17	.13	.19	.18
MgO	7.02	4.76	2.98	5.04	6.65
CaO	15.33	19.36	6.00	13.30	16.85
Na2O	1.37	1.82	1.19	2.66	1.50
K2O	1.05	.72	6.25	.99	1.17
LOI	15.70	17.10	7.30	7.70	15.80
TOTAL	99.95	99.58	99.14	98.52	99.94

TRACE ELEMENTS (PPM)

	05421700	05421875	05421950	05422025	05422100
Zr	76	103	87	94	66
Sr	162	619	196	472	161
Rb	31	26	110	27	37
Zn	73	59	62	85	68
Cu	41	24	55	47	52
Ba	203	164	969	406	150
CuS	37	19	41	38	51
PbS	11	10	2	8	11
ZnS	4	1	2	11	5
BaSO4					0
Pb	33	36	31	37	30
Ni	21	94	82	77	56
Co	26	37	29	36	32
Cr	94	224	231	205	170
V	310	290	310	255	300
Hg	40	32	23	28	27
Ag	12	13	11	13	11
Nb					

FOOTWALL BASALT - ALTERED MAFIC FRAGMENTALS

MAJOR ELEMENTS (WTZ)

SAMPLE	05422150	05422200	08692020	14930000	14930100
SiO2	37.80	39.60	33.50	36.00	42.10
TiO2	.59	.79	.63	.63	.94
Al2O3	11.96	14.34	11.50	14.10	16.90
Fe2O3	7.56	10.36	5.30	8.84	15.26
MnO	.14	.18	.15	.11	.06
MgO	6.67	8.48	2.60	1.76	1.70
CaO	15.74	13.63	23.24	19.86	9.00
Na2O	.64	2.45	1.95	2.59	1.90
K2O	1.90	.50	.99	1.13	3.35
LOI	16.30	9.27	19.60	15.00	8.70
TOTAL	99.32	99.60	99.46	100.02	99.91

TRACE ELEMENTS (PPM)

Zr	38	93	69	81	95
Sr	152	411	253	342	260
Rb	41	19	27	34	66
Zn	64	87	59	63	38
Cu	21	54	91	43	4
Ba	669	230	125	148	328
CuS	11	43	77	34	1
PbS	11	7	17	12	10
ZnS	3	9	15	9	11
BaSO4			0	0	
Pb	29	35	23	19	17
Ni	56	97	45	55	53
Co	28	44	26	20	17
Cr	164	257	127	170	248
V	270	260	290	178	129
Hg	23	23	33	16	9
Ag	11	10	0	0	0
Nb					

FOOTWALL BASALT - ALTERED MAFIC FRAGMENTALS

MAJOR ELEMENTS (WT%)

SAMPLE   14930250

SIO2	36.70
TIO2	.62
Al2O3	11.67
Fe2O3	7.25
MnO	.11
MgO	1.65
CaO	21.39
Na2O	2.34
K2O	2.01
LOI	16.80

TOTAL   100.54

TRACE ELEMENTS (PPM)

Zr	82
Sr	28
Rb	50
Zn	49
Cu	22
Ba	327
CuS	15
PbS	9
ZnS	8
BaSO4	
Pb	19
Ni	37
Co	13
Cr	123
V	16
Hg	14
Ag	2
Nb	

FOOTWALL BASALT SEQUENCE - RHYOLITE FLOWS

MAJOR ELEMENTS (WT%)

SAMPLE	JGT 169B
SIO2	77.38
TIO2	.18
A1203	11.48
Fe203	2.28
MnO	.83
MgO	1.82
CaO	.16
Na2O	4.49
K2O	.58
LOI	1.58
TOTAL	99.58

TRACE ELEMENTS (PPM)

Zr	125
Sr	72
Rb	11
Zn	39
Cu	1
Ba	68
CuS	1
PbS	6
ZnS	1
BaSO4	8
Pb	6
Ni	3
Co	13
Cr	11
V	18
Hg	
Ag	
Nb	6

BASALT FLOWS BELOW PROMINENT QUARTZ SEQUENCE

MAJOR ELEMENTS (WT%)

SAMPLE	21051526	2820 153
SiO2	45.30	46.70
TiO2	1.04	1.20
Al2O3	16.61	16.75
Fe2O3	9.38	9.90
MnO	.14	.20
MgO	9.36	8.59
CaO	11.55	10.35
Na2O	1.85	2.00
K2O	.12	1.15
LOI	4.00	3.10
TOTAL	99.35	99.94

TRACE ELEMENTS (PPM)

Zr	73	57
Sr	148	150
Rb	2	22
Zn	50	52
Cu	70	54
Ba	57	276
CuS	135	53
PbS	20	62
ZnS	20	18
BaSO4		0
Pb	28	92
Ni	133	50
Co	36	35
Cr	157	258
V	125	130
Hg		
Ag		
Nb		1

ALTERED BASALTIC FLOWS BELOW PROMINENT QUARTZ SEQUENCE

MAJOR ELEMENTS (WT%)

SAMPLE   2867 143

SIO2	49.68
TIO2	.01
AL2O3	15.24
Fe2O3	10.95
MnO	.16
MgO	8.03
CaO	4.69
Na2O	4.85
K2O	.09
LOI	5.40
TOTAL	98.42

TRACE ELEMENTS (PPM)

Zr	144
Sr	166
Rb	5
Zn	136
Cu	16
Ba	97
CuS	19
PbS	14
ZnS	26
BaSO4	0
Pb	35
Ni	27
Co	31
Cr	156
V	205
Hg	
Ag	
Nb	5

FOOTWALL ARKOSE SEQUENCE - DACITIC TUFFS

MAJOR ELEMENTS (WT%)

SAMPLE	JGT75216	R1-5 153
SiO2	72.80	64.20
TiO2	.24	.24
Al2O3	12.55	17.97
Fe2O3	2.52	2.57
MnO	.07	.08
MgO	1.18	3.49
CaO	1.24	1.10
Na2O	3.59	1.27
K2O	2.57	3.78
LOI	1.70	4.80
TOTAL	98.46	99.50

TRACE ELEMENTS (PPM)

Zr	71	140
Sr	138	248
Rb	49	102
Zn	66	41
Cu	2	2
Ba	615	989
CuS	1	3
PbS	4	6
ZnS	5	8
BaSO4	0	0
Pb	17	17
Ni	1	8
Co	8	6
Cr	12	8
V	25	15
Hg		
Ag		
Nb	7	12

WILWY'S SEQUENCE - FLOWS

MAJOR ELEMENTS (WT%)

SAMPLE	JGT75243	JGT75307	724 303	2622 60	2622 335
$SiO2$	72.60	66.50	66.80	59.20	70.40
$TiO2$	.11	.40	.54	.86	.12
$Al2O3$	10.96	13.92	14.13	15.30	15.49
$Fe2O3$	1.57	5.00	5.23	6.14	2.09
MnO	.10	.19	.23	.16	.02
MgO	.11	1.95	1.50	2.99	.01
CaO	4.00	1.38	1.83	3.76	1.10
$Na2O$	4.22	4.99	4.49	4.39	2.18
$K2O$	1.29	2.13	2.91	2.61	3.59
LOI	4.20	2.10	1.80	3.60	3.50
TOTAL	99.16	98.64	99.54	99.09	99.30

TRACE ELEMENTS (PPM)

	JGT75243	JGT75307	724 303	2622 60	2622 335
Zr	96	91	92	218	78
Sr	247	103	119	418	95
Rb	26	37	47	49	82
Zn	21	44	61	73	7
Cu	1	1	1	33	1
Ba	506	966	1127	819	432
CuS	1	1	2	3	2
PbS	17	3	23	4	7
ZnS	10	1	14	15	8
BaSO4	4	0	0	0	0
Pb	31	14	23	17	5
Ni	1	1	5	58	8
Co	21	21	18	22	11
Cr	10	8	14	115	7
V	10	15	10	120	30
Hg					
Ag					
Nb	9	9	5	17	12

WILWY'S SEQUENCE - FLOWS

MAJOR ELEMENTS (WT%)

SAMPLE   2622 365

SIO2	55.90
TIO2	.62
Al2O3	19.26
Fe2O3	8.97
MnO	.17
MgO	2.74
CaO	2.54
Na2O	4.55
K2O	2.22
LOI	4.50

TOTAL   99.61

TRACE ELEMENTS (PPM)

Zr	45
Sr	255
Rb	61
Zn	161
Cu	4
Ba	657
CuS	2
PbS	8
ZnS	35
BaSO4	0
Pb	21
Ni	58
Co	45
Cr	77
V	120
Hg	
Ag	
Nb	0

PROMINENT QUARTZ SEQUENCE - RHYOLITE FLOWS

MAJOR ELEMENTS (WT%)

SAMPLE	19402111	2090 242	2105 177	2753 505	2762 101
SIO2	76.80	69.30	67.80	77.30	70.70
TIO2	.26	.35	.45	.40	.29
Al2O3	11.54	13.55	12.43	11.06	13.28
Fe2O3	1.73	4.08	4.70	1.97	3.20
MnO	.04	.06	.10	.05	.05
MgO	.64	1.49	1.51	.11	.71
CaO	1.00	2.57	2.96	1.72	2.21
Na2O	2.42	2.99	2.68	3.82	3.43
K2O	4.22	3.57	2.52	1.34	2.74
LOI	1.80	2.10	4.20	.80	2.90
TOTAL	100.45	100.06	99.35	98.57	99.51

TRACE ELEMENTS (PPM)

Zr	154	149	148	135	146
Sr	90	143	93	229	137
Rb	50	63	57	22	63
Zn	28	37	52	20	17
Cu	1	1	15	4	1
Ba	1216	662	419	782	491
CuS	1	3	29	4	1
PbS	23	25	20	11	12
ZnS	16	12	11	20	22
BaSO4					
Pb	12	6	13	1	3
Ni	3	5	8	3	5
Co	22	19	22	58	29
Cr	0	11	16	3	9
V	10	50	55	10	25
Hg					
Ag					
Nb					

WILWY'S SEQUENCE - DACITIC TUFFS

MAJOR ELEMENTS (WT%)

SAMPLE	JGT75190	718 37	2622 242	2660 767	2754 728
SiO2	66.00	69.50	64.90	67.90	64.70
TiO2	.40	.56	.58	.33	.32
Al2O3	13.82	13.51	16.54	13.13	16.97
Fe2O3	5.14	3.96	3.75	3.88	3.26
MnO	.08	.05	.05	.08	.11
MgO	1.72	.95	.79	1.25	1.15
CaO	3.71	4.10	2.41	3.09	4.14
Na2O	1.24	3.01	1.77	2.66	3.93
K2O	3.04	1.04	3.52	2.65	2.72
LOI	4.30	3.00	5.40	4.20	2.10
TOTAL	99.45	98.78	99.71	99.12	99.40

TRACE ELEMENTS (PPM)

	JGT75190	718 37	2622 242	2660 767	2754 728
Zr	118	128	161	150	97
Sr	528	220	173	146	348
Rb	74	31	95	80	60
Zn	56	55	35	41	51
Cu	2	9	2	9	1
Ba	767	314	601	310	759
CuS	2	8	4	12	1
PbB	5	8	23	19	3
ZnS	6	11	18	17	12
BaSO4	6	0	0		0
Pb	17	14	7	4	13
Ni	5	12	24	7	3
Co	9	25	13	18	17
Cr	16	11	16	15	11
V	26	25	30	25	45
Hg					
Ag					
Nb	7	11	0		6

WILWY'S SEQUENCE - DACITIC TUFFS

MAJOR ELEMENTS (WT%)

SAMPLE	2769 219	2777 545	2880 311	BB 229	BB 232
SiO2	67.70	71.90	70.40	76.80	62.80
TiO2	.30	.51	.26	.02	.26
Al2O3	18.28	12.99	13.43	13.17	18.56
Fe2O3	1.95	2.38	2.31	.89	5.04
MnO	.01	.03	.06	.01	.18
MgO	1.01	.99	3.34	.61	1.54
CaO	.32	1.54	1.11	1.00	.54
Na2O	.43	1.93	.74	3.51	8.51
K2O	4.82	3.39	3.20	2.51	.69
LOI	4.20	3.80	4.60	2.50	1.50
TOTAL	99.02	99.46	99.45	101.02	99.54

TRACE ELEMENTS (PPM)

	2769 219	2777 545	2880 311	BB 229	BB 232
Zr	169	122	107		133
Sr	70	112	89	97	59
Rb	107	80	85	80	15
Zn	14	18	90		
Cu	1	2	11		
Ba	774	430	660	19	76
CuS	1	4	14		
PbS	17	20	30		
ZnS	17	17	22		
BaSO4					
Pb	1	11	28		
Ni	3	2	6		
Co	11	22	19		
Cr	8	5	6	0	10
V	15	10	20		
Hg					
Ag					
Nb					

WILWY'S SEQUENCE - DACITIC TUFFS

MAJOR ELEMENTS (WT%)

SAMPLE	BB 246	BB 247	BB 257
SiO2	69.40	69.10	76.90
TiO2	.28	.32	.14
Al2O3	13.71	14.65	11.45
Fe2O3	4.11	4.40	1.39
MnO	.05	.07	.03
MgO	1.29	1.37	2.63
CaO	2.03	2.84	.50
Na2O	2.94	3.55	.31
K2O	2.75	2.73	3.29
LOI	2.70	2.00	3.40
TOTAL	99.26	101.03	100.04

TRACE ELEMENTS (PPM)

	BB 246	BB 247	BB 257
Zr	154	147	111
Sr	170	217	69
Rb	67	54	91
Zn			
Cu			
Ba	558	648	482
CuS			
PbS			
ZnS			
BaSO4			
Pb			
Ni			
Co			
Cr	13	13	0
V			
Hg			
Ag			
Nb			

PROMINENT QUARTZ SEQUENCE - DACITIC TUFFS

MAJOR ELEMENTS (WT%)

SAMPLE	1908 85	1940 217	1960 233	2090 35	2490 527
SiO2	68.80	64.70	68.60	69.70	63.90
TiO2	.20	.44	.41	.30	.45
Al2O3	14.09	15.58	14.45	13.76	15.40
Fe2O3	3.69	4.46	3.66	3.64	5.46
MnO	.13	.05	.05	.07	.04
MgO	1.55	2.02	1.11	1.00	3.37
CaO	2.07	2.95	3.82	2.61	1.68
Na2O	2.59	2.24	2.82	3.42	1.63
K20	2.26	2.78	1.67	1.94	3.96
LOI	4.00	4.40	2.90	3.10	3.40
TOTAL	99.38	99.62	99.49	99.54	99.29

TRACE ELEMENTS (PPM)

	1908 85	1940 217	1960 233	2090 35	2490 527
Zr	99	170	158	153	140
Sr	91	144	199	191	177
Rb	53	66	46	46	143
Zn	227	65	29	35	23
Cu	1	2	1	1	4
Ba	663	515	469	482	923
CuS	1	9	4	1	5
PbS	10	19	12	22	11
ZnS	31	23	7	17	15
BaSO4	0				
Pb	1	11	4	7	1
Ni	6	9	4	6	7
Co	16	19	19	17	15
Cr	11	16	12	12	16
V	10	15	50	30	10
Hg					
Ag					
Nb	12				

PROMINENT QUARTZ SEQUENCE – DACITIC TUFFS

MAJOR ELEMENTS (WT%)

SAMPLE	2501 234	2501 469	2528 113	2530 110	2571 77
SiO2	74.20	72.30	68.40	62.90	69.20
TiO2	.34	.28	.33	.31	.24
Al2O3	12.21	14.43	13.79	16.97	13.31
Fe2O3	2.57	1.25	3.41	4.18	3.31
MnO	.03	.02	.07	.05	.05
MgO	1.43	1.24	1.87	1.84	.88
CaO	1.50	1.52	2.46	2.11	2.95
Na2O	1.68	2.12	2.85	1.91	2.05
K2O	3.76	3.80	2.02	2.97	2.67
LOI	2.00	1.90	3.80	5.30	4.70
TOTAL	99.72	98.86	99.00	98.54	99.36

TRACE ELEMENTS (PPM)

	2501 234	2501 469	2528 113	2530 110	2571 77
Zr	91	107	117	125	151
Sr	154	151	187	100	9
Rb	124	86	64	66	53
Zn	45	36	44	38	34
Cu	4	1	1	5	2
Ba	894	853	829	793	374
CuS	2	2	2	4	2
PbS	8	9	8	9	29
ZnS	17	13	14	12	10
BaSO4	0	0	6	0	
Pb	12	5	8	7	17
Ni	4	4	7	5	5
Co	8	8	11	18	17
Cr	16	11	14	13	11
V	10	10	10	50	15
Hg					
Ag					
Nb	11	7	10	15	

PROMINENT QUARTZ SEQUENCE - DACITIC TUFFS

MAJOR ELEMENTS (WT%)

SAMPLE	26660048	26660200	26660300	26660350	26660475
SiO2	66.50	76.60	74.40	73.60	71.90
TiO2	.37	.32	.20	.10	.36
Al2O3	15.17	14.88	12.60	13.60	13.35
Fe2O3	4.47	2.04	1.41	1.09	3.64
MnO	.10	.02	.02	.03	.04
MgO	1.72	.93	.64	1.37	1.48
CaO	2.27	3.55	3.15	1.22	1.98
Na2O	3.18	3.14	2.65	2.28	3.14
K2O	2.61	1.32	1.15	2.83	1.86
LOI	2.20	3.40	2.90	2.60	2.00
TOTAL	98.59	100.20	99.20	98.72	99.75

TRACE ELEMENTS (PPM)

Zr	181	171	120	126	114
Sr	211	401	514	597	342
Rb	60	43	38	74	69
Zn	20	22	20	22	34
Cu	27	4	5	5	4
Ba	696	564	519	832	619
CuS	25	1	1	2	1
PbS	6	7	3	8	8
ZnS	17	13	8	9	10
BaSO4					0
Pb	6	10	7	1	5
Ni	4	2	1	1	4
Co	4	2	2	1	4
Cr	30	22	23	17	31
V	54	24	10	0	39
Hg	20	14	20	27	8
Ag	0	1	0	0	0
Nb					

PROMINENT QUARTZ SEQUENCE — DACITIC TUFFS

MAJOR ELEMENTS (WT%)

SAMPLE	26660600	26660725	26660850	2680 267	28511475
SiO2	68.20	72.10	75.40	71.50	70.40
TiO2	.28	.24	.20	.25	.36
Al2O3	14.05	14.97	12.71	12.84	13.10
Fe2O3	2.23	1.88	1.82	3.17	3.40
MnO	.03	.03	.05	.03	.06
MgO	1.58	1.63	2.31	.63	2.39
CaO	2.10	2.71	1.17	1.84	1.11
Na2O	3.03	3.20	1.87	3.54	3.46
K2O	1.67	1.54	2.48	2.01	2.64
LOI	3.00	2.40	2.50	2.70	2.00
TOTAL	96.17	100.70	100.51	98.51	98.92

TRACE ELEMENTS (PPM)

	26660600	26660725	26660850	2680 267	28511475
Zr	117	120	126	146	111
Sr	248	365	233	134	98
Rb	52	47	58	40	48
Zn	12	8	13	17	28
Cu	6	1	3	3	5
Ba	748	744	670	226	545
CuS	3	0	1	4	8
PbS	7	8	15	17	13
ZnS	4	9	7	14	6
BaSO4	0		0		0
Pb	3	3	2	7	7
Ni	2	2	2	4	3
Co	2	2	1	20	21
Cr	23	21	20	8	13
V	15	9	2	35	30
Hg	8	6	7		
Ag	0	0	0		
Nb					13

PROMINENT QUARTZ SEQUENCE - DACITIC TUFFS

MAJOR ELEMENTS (WT%)

SAMPLE	28511955	2858 65
S102	69.30	68.90
T102	.40	.52
A1203	14.30	14.27
Fe203	4.76	3.98
MnO	.05	.05
MgO	.90	1.59
CaO	1.68	3.49
Na20	2.11	2.75
K20	3.12	1.43
LOI	3.50	2.70
TOTAL	100.12	99.68

TRACE ELEMENTS (PPM)

	28511955	2858 65
Zr	106	160
Sr	60	242
Rb	65	33
Zn	43	29
Cu	5	1
Ba	511	404
CuS	8	1
PbS	22	20
ZnS	18	4
BaSO4	0	
Pb	8	5
Ni	6	6
Co	17	21
Cr	12	14
V	30	10
Hg		
Ag		
Nb	15	

PROMINENT QUARTZ SEQUENCE - TUFFACEOUS SILTSTONE

MAJOR ELEMENTS (WT%)

SAMPLE	26661050	08691625	08691650	08691740	08691850
SiO2	76.50	67.20	67.10	75.20	70.30
TiO2	.10	.31	.47	.18	.21
Al2O3	12.67	14.20	13.60	11.10	13.60
Fe2O3	1.31	3.22	6.23	3.25	2.59
MnO	.03	.34	.14	.10	.14
MgO	2.29	1.34	1.82	1.34	.77
CaO	.55	1.71	1.94	.73	1.29
Na2O	.39	1.90	3.13	2.73	2.98
K2O	3.28	6.34	2.97	3.38	6.18
LOI	3.30	3.20	1.80	1.40	1.20
TOTAL	100.42	99.76	99.20	99.41	99.26

TRACE ELEMENTS (PPM)

Zr	54	136	135	116	128
Sr	11	77	224	87	110
Rb	62	91	38	66	79
Zn	23	43	51	23	29
Cu	52	17	6	10	4
Ba	811	1126	502	751	861
CuS	25	14	2	6	1
PbS	4	25	5	14	12
ZnS	1	12	17	8	8
BaSO4	6		0		4
Pb	1	29	11	19	19
Ni	1	4	4	4	2
Co	1	6	10	5	3
Cr	22	24	33	27	25
V	6	44	78	26	22
Hg	6	81	23	33	19
Ag	2	1	2	1	0
Nb					

PROMINENT QUARTZ SEQUENCE - TUFFACEOUS SILTSTONE

MAJOR ELEMENTS (WT%)

SAMPLE	26660150	26660900	08691477
SiO2	70.40	47.70	64.60
TiO2	.10	.90	.40
Al2O3	14.16	17.44	14.70
Fe2O3	1.70	10.80	4.70
MnO	.08	.20	.31
MgO	3.43	7.39	2.49
CaO	.92	7.63	1.71
Na2O	.06	3.31	1.20
K2O	4.61	1.02	5.26
LOI	4.90	4.10	3.70
TOTAL	100.44	100.49	99.15

TRACE ELEMENTS (PPM)

	26660150	26660900	08691477
Zr	71	103	134
Sr	0	530	114
Rb	114	25	95
Zn	41	14	72
Cu	3	2	19
Ba	1023	774	1135
CuS	1	0	11
PbS	4	7	10
ZnS	19	8	22
BaSO4	0		
Pb	5	4	21
Ni	2	1	8
Co	2	1	10
Cr	18	154	21
V	0	0	42
Hg	32	8	21
Ag	0	0	2
Nb			

PROMINENT QUARTZ SEQUENCE - MAFIC FRAGMENTALS

MAJOR ELEMENTS (WT%)

SAMPLE	26661325	26661725	26661850	26662000	26662125
SiO2	56.70	49.60	54.30	65.80	61.00
TiO2	.46	.40	.63	.33	.43
Al2O3	17.84	16.72	17.69	14.00	17.78
Fe2O3	9.15	10.48	3.66	5.70	5.34
MnO	.05	.08	.09	.09	.07
MgO	3.65	8.80	.92	5.20	5.62
CaO	2.71	4.02	7.45	.30	.30
Na2O	2.03	1.93	7.25	3.70	2.87
K2O	4.95	2.38	1.67	1.15	2.84
LOI	3.80	5.80	6.70	4.10	4.30
TOTAL	101.34	100.21	100.36	100.37	100.55

TRACE ELEMENTS (PPM)

Zr	54	43	50	23	30
Sr	188	272	181	3	0
Rb	113	53	24	15	27
Zn	24	38	43	52	58
Cu	9	54	16	10	9
Ba	463	246	115	74	96
CuS	4	48	17	4	8
PbS	5	7	7	30	7
ZnS	3	6	12	23	17
BaSO4	0				
Pb	4	0	0	13	1
Ni	50	178	1	3	3
Co	10	39	6	7	5
Cr	490	532	19	30	28
V	96	156	68	57	84
Hg	6	6	10	39	20
Ag	0	0	0	3	0
Nb					

PROMINENT QUARTZ SEQUENCE — MAFIC FRAGMENTALS

MAJOR ELEMENTS (WT%)

SAMPLE	26662450	26662575	26662700	26662825	26662950
SiO2	60.80	63.80	59.10	51.50	51.90
TiO2	.32	.32	.38	.40	.43
Al2O3	11.14	15.76	14.21	17.71	17.19
Fe2O3	12.03	4.54	7.70	9.37	9.34
MnO	.10	.17	.15	.12	.13
MgO	1.07	3.54	3.51	5.10	5.04
CaO	.82	1.41	2.70	2.75	2.31
Na2O	4.21	2.60	2.78	3.39	2.74
K2O	1.31	3.02	3.16	3.36	4.54
LOI	7.40	4.30	4.70	5.90	5.20
TOTAL	99.20	99.46	98.39	99.60	98.82

TRACE ELEMENTS (PPM)

Zr	58	42	31	28	27
Sr	98	62	79	97	97
Rb	23	30	25	31	33
Zn	24	24	35	29	35
Cu	43	13	36	56	55
Ba	71	111	201	201	245
CuS	23	11	44	68	70
PbS	40	13	4	9	8
ZnS	20	12	17	13	24
BaSO4		0		0	
Pb	46	3	1	2	3
Ni	4	2	4	5	10
Co	26	6	8	10	13
Cr	36	32	27	32	43
V	29	58	161	260	215
Hg	191	12	32	36	22
Ag	25	0	1	0	0
Nb					

PROMINENT QUARTZ SEQUENCE - ALTERED MAFIC FRAGMENTALS

MAJOR ELEMENTS (WT%)

SAMPLE	26661475	26661625	26662250	26662350
SiO2	53.30	41.10	40.30	19.60
TiO2	.32	.36	.28	.24
Al2O3	12.55	13.82	10.00	7.68
Fe2O3	7.32	6.96	23.10	37.30
MnO	.09	.28	.08	.08
MgO	6.15	5.11	8.51	9.21
CaO	10.18	15.62	.56	.65
Na2O	1.64	4.26	1.78	.40
K2O	.91	.51	1.34	.45
LOI	7.30	11.20	14.20	21.80
TOTAL	99.76	99.22	100.15	97.41

TRACE ELEMENTS (PPM)

	26661475	26661625	26662250	26662350
Zr	21	38	49	55
Sr	229	222	60	70
Rb	23	16	19	23
Zn	43	34	870	5600
Cu	62	6	59	101
Ba	112	78	94	83
CuS	45	3	31	61
PbS	7	8	167	1350
ZnS	7	12	680	6300
BaSO4		0	0	
Pb	2	2	185	1390
Ni	116	95	2	2
Co	26	23	12	10
Cr	277	317	36	72
V	166	151	57	32
Hg	10	8	426	2516
Ag	0	0	21	122
Nb				

INTERMEDIATE FOOTWALL - LUCKY STRIKE AREA

MAJOR ELEMENTS (WT%)

SAMPLE	02020650	02020700	02020750	02020800	02020875
SiO2	56.70	52.60	56.70	52.50	56.80
TiO2	.55	.29	.40	.49	.35
Al2O3	14.99	15.11	14.45	16.87	13.75
Fe2O3	7.81	11.05	8.01	8.58	9.90
MnO	.45	.44	.46	.64	.56
MgO	8.69	9.36	8.57	9.48	8.45
CaO	.35	.29	.65	.27	.69
Na2O	.09	3.31	2.36	2.67	1.86
K2O	1.64	.03	.59	1.27	.41
LOI	6.40	6.30	5.50	5.90	5.50
TOTAL	97.67	98.78	97.69	98.87	98.27

TRACE ELEMENTS (PPM)

Zr	46	33	28	33	22
Sr	0	9	9	17	2
Rb	42	11	18	30	15
Zn	310	284	260	450	270
Cu	25	5	117	260	55
Ba	1037	135	282	594	331
CuS	26	1	156	330	64
PbS	21	17	27	15	30
ZnS	49	35	44	74	42
BaSO4			0		
Pb	34	36	41	32	51
Ni	12	30	30	34	14
Co	16	23	22	27	20
Cr	70	112	91	100	69
V	180	234	264	258	242
Hg		25	27	29	19
Ag	7	10	6	7	11
Nb					

INTERMEDIATE FOOTWALL - LUCKY STRIKE AREA

MAJOR ELEMENTS (WT%)

SAMPLE	02020950	02021050	02021150	07U2 100	542 150
SiO2	56.70	45.20	55.00	61.40	54.10
TiO2	.31	.46	.40	.11	.42
Al2O3	12.00	12.00	14.99	14.25	17.60
Fe2O3	10.67	18.20	8.99	7.80	9.85
MnO	.53	.72	.58	.45	.67
MgO	8.53	11.19	8.63	5.12	5.91
CaO	.39	.68	.72	.23	.39
Na2O	1.89	.25	2.50	2.71	3.18
K2O	.12	.27	.43	1.26	1.57
LOI	6.00	10.20	5.60	4.40	5.10
TOTAL	97.14	98.87	97.84	97.73	98.79

TRACE ELEMENTS (PPM)

	02020950	02021050	02021150	07U2 100	542 150
Zr	28	40	36	93	85
Sr	6	19	10	45	65
Rb	12	18	19	28	32
Zn	294	740	295	280	280
Cu	7	100	14	13	5
Ba	143	212	196	652	856
CuS	2	119	12	1	1
PbS	17	120	16	100	22
ZnS	32	355	28	48	26
BaSO4	0		0		4
Pb	33	120	36	122	30
Ni	13	11	15	12	12
Co	23	29	24	17	17
Cr	64	54	63	77	60
V	268	274	300	132	230
Hg	27	70	33	82	17
Ag	10	15	10	10	10
Nb					

INTERMEDIATE FOOTWALL - LUCKY STRIKE AREA

MAJOR ELEMENTS (WT%)

SAMPLE	542 225	542 300	542 375	542 450	542 500
SiO2	55.00	37.80	74.10	53.80	51.00
TiO2	.59	.48	.15	.62	.77
Al2O3	17.42	20.54	12.36	18.75	17.16
Fe2O3	9.47	13.85	1.89	8.26	8.87
MnO	.20	.60	.04	.31	.16
MgO	5.13	12.57	.60	6.26	7.02
CaO	.25	1.09	.27	.76	1.48
Na2O	1.05	2.73	1.02	2.05	1.28
K2O	3.26	.90	3.15	2.42	5.08
LOI	6.00	8.10	2.80	5.50	5.20
TOTAL	98.37	98.66	96.38	98.73	98.02

TRACE ELEMENTS (PPM)

	542 225	542 300	542 375	542 450	542 500
Zr	40	55	119	40	50
Sr	17	52	0	59	93
Rb	62	23	58	39	53
Zn	162	340	930	270	360
Cu	13	5	48	40	127
Ba	1.101	470	1427	2943	3491
CuS	5	1	44	35	102
PbS	15	21	1085	210	86
ZnS	12	28	695	123	59
BaSO4		0		106	
Pb	24	34	1060	190	111
Ni	23	19	1	17	14
Co	35	26	3	25	30
Cr	68	74	19	61	37
V	290	420	16	260	330
Hg	21	23	70	70	25
Ag	8	11	10	16	15
Nb					

INTERMEDIATE FOOTWALL - LUCKY STRIKE AREA

MAJOR ELEMENTS (WT%)

SAMPLE	542 525	/7921428	07921575	07921649	08681655
SiO2	37.30	48.40	59.50	54.10	49.50
TiO2	.06	.76	.56	.50	.90
Al2O3	6.52	19.33	20.33	14.28	19.20
Fe2O3	25.40	10.86	3.16	9.30	12.30
MnO	.24	.20	.05	.47	.17
MgO	7.06	10.38	2.41	9.21	5.64
CaO	.61	.97	1.60	.43	3.76
Na2O	0.00	.64	1.77	.37	1.47
K2O	.24	2.94	5.19	1.32	4.72
LOI	15.80	6.70	5.00	5.90	4.30
TOTAL	93.23	101.18	99.57	95.88	101.36

TRACE ELEMENTS (PPM)

Zr	45	48	197	40	62
Sr	92	103	45	0	239
Rb	23	38	71	30	72
Zn	162	82	24	61	105
Cu	101	29	1	6	94
Ba	7550	1381	1615	509	3917
CuS	83	29	0	2	91
PbS	27	13	10	9	7
ZnS	42	24	9	22	23
BaSO4	51		7		
Pb	44	14	11	12	19
Ni	8	15	1	4	16
Co	38	18	2	5	28
Cr	40	48	19	38	40
V	310	490	17	175	470
Hg	46	18	12	13	25
Ag	23	0	6	0	1
Nb					

INTERMEDIATE FOOTWALL - LUCKY STRIKE AREA

MAJOR ELEMENTS (WT%)

SAMPLE	08681725	08681825	08681900	08681975	972 825
SiO2	55.80	49.10	51.20	48.70	64.80
TiO2	.82	1.02	.80	.83	.10
Al2O3	15.80	18.80	17.30	17.40	15.13
Fe2O3	10.88	13.49	11.64	13.87	5.08
MnO	.17	.19	.16	.20	.05
MgO	4.58	5.21	4.97	6.34	3.95
CaO	6.00	7.26	6.15	6.67	.58
Na2O	1.66	2.92	1.80	2.72	1.08
K2O	2.33	1.28	2.03	.73	4.08
LOI	3.20	4.20	3.90	4.90	3.90
TOTAL	101.24	103.47	99.95	102.36	98.75

TRACE ELEMENTS (PPM)

Zr	46	82	49	68	107
Sr	274	285	346	266	60
Rb	28	26	29	20	80
Zn	103	115	104	106	105
Cu	105	171	103	91	4
Ba	1407	985	1951	5632	1109
CuS	93	158	81	94	3
PbS	16	9	7	5	15
ZnS	28	27	27	24	24
BaSO4	0		0		
Pb	27	26	24	23	34
Ni	13	15	14	14	8
Co	30	31	30	33	18
Cr	38	45	42	52	14
V	380	350	340	360	15
Hg	25	19	27	29	
Ag	0	1	0	1	
Nb					

INTERMEDIATE FOOTWALL - LUCKY STRIKE AREA

MAJOR ELEMENTS (WT%)

SAMPLE	12141320	12141340	12141360	12141360	12141425
SiO2	56.20	67.00	61.40	66.00	54.20
TiO2	.67	.49	.56	.44	.82
Al2O3	21.10	16.44	17.74	15.43	15.60
Fe2O3	6.74	4.29	4.61	4.02	11.52
MnO	.10	.09	.12	.13	.14
MgO	3.00	1.79	2.09	1.50	4.83
CaO	2.17	2.19	2.78	2.04	5.43
Na2O	2.06	2.69	2.71	4.13	1.69
K2O	4.82	3.04	3.12	1.92	1.57
LOI	4.20	2.60	3.90	3.40	4.20
TOTAL	101.06	100.62	99.03	99.01	100.00

TRACE ELEMENTS (PPM)

Zr	249	218	202	224	65
Sr	213	367	433	426	243
Rb	103	71	74	55	31
Zn	86	72	79	79	110
Cu	5	8	4	218	92
Ba	1557	1138	1100	963	1116
CuS	1	3	1	218	72
PbS	9	12	7	67	16
ZnS	18	18	20	17	30
BaSO4	0		245		0
Pb	15	18	15	55	24
Ni	4	2	4	3	13
Co	3	3	3	5	25
Cr	21	24	34	26	38
V	12	25	32	21	420
Hg	28	50	29	308	52
Ag	0	0	0	28	2
Nb					

INTERMEDIATE FOOTWALL - LUCKY STRIKE AREA

MAJOR ELEMENTS (WT%)

SAMPLE	19111158	20431126	26663625	26663725	26663775
SiO_2	64.80	66.00	50.80	49.70	51.20
TiO_2	.58	.58	.82	.88	.77
Al_2O_3	13.97	13.91	17.76	18.13	17.95
Fe_2O_3	5.15	5.26	12.05	11.87	10.88
MnO	.09	.13	.08	.12	.16
MgO	.98	1.10	2.55	4.95	4.40
CaO	4.42	4.85	3.47	2.97	6.97
Na_2O	4.21	3.43	2.00	1.55	2.37
K_2O	1.20	.92	4.92	2.40	1.00
LOI	4.80	2.40	5.10	6.50	3.00
TOTAL	100.20	98.58	99.55	99.07	98.70

TRACE ELEMENTS (PPM)

Zr	112	107	70	71	64
Sr	198	402	200	204	266
Rb	21	19	90	55	21
Zn	108	74	48	58	113
Cu	14	2	15	103	127
Ba	856	731	938	864	797
CuS	13	5	6	89	85
PbS	31	7	13	12	8
ZnS	31	25	9	22	24
$BaSO_4$		0		0	
Pb	18	29	9	8	19
Ni	6	3	7	13	15
Co	15	17	11	23	33
Cr	0	10	43	41	42
V	50	45	820	574	512
Hg			0	10	15
Ag			0	0	0
Nb		5			

INTERMEDIATE FOOTWALL - LUCKY STRIKE AREA

MAJOR ELEMENTS (WTX)

SAMPLE   27040975

SiO_2 58.70
TiO_2 .60
Al_2O_3 15.90
Fe_2O_3 8.95
MnO .10
MgO 2.41
CaO 4.23
Na_2O 2.50
K_2O 2.42
LOI 2.70

TOTAL   . 98.51

TRACE ELEMENTS (PPM)

Zr   70
Sr   256
Rb   63
Zn   46
Cu   42
Ba   1075
CuS   37
PbS   4
ZnS   18
$BaSO_4$ 24
Pb   15
Ni   10
Co   10
Cr   37
V   301
Hg   22
Ag   0
Nb

INTERMEDIATE FOOTWALL - VARIABLY MINERALIZED AND ALTERED

MAJOR ELEMENTS (WT%)

SAMPLE	01750275	01750350	01750417	02020200	02020250
SIO2	71.90	50.60	73.10	29.10	16.70
TIO2	.28	.77	.17	.37	.01
Al2O3	7.91	17.21	11.86	15.05	1.15
Fe2O3	6.85	9.29	1.19	12.00	42.00
MnO	.07	.44	.04	.52	.38
MgO	1.81	1.87	1.51	23.30	1.02
CaO	.20	5.60	1.04	.39	8.78
Na2O	.05	.57	3.39	.01	0.00
K2O	1.99	3.50	2.50	0.00	.01
LOI	6.00	8.30	1.90	12.20	25.90
TOTAL	97.06	98.15	96.70	92.94	95.95

TRACE ELEMENTS (PPM)

	01750275	01750350	01750417	02020200	02020250
Zr	25	63	152	68	53
Sr	20	68	373	39	124
Rb	48	57	13	25	20
Zn	9999	9999	505	9999	890
Cu	2820	1790	76	2225	109
Ba	3184	2319	311	191	9999
CuS	1540	1350	84	1540	84
PbS	9999	3650	4500	999	1340
ZnS	9999	9999	200	9999	650
BaSO4		6750			999
Pb	999	2500	2300	9999	795
Ni	9	6	9	68	3
Co	14	13	17	43	14
Cr	69	35	61	351	54
V	61	98	173	270	16
Hg	278	144	36	1078	278
Ag	40	28	46	24	125
Nb					

INTERMEDIATE FOOTWALL - VARIABLY MINERALIZED AND ALTERED

MAJOR ELEMENTS (WT%)

SAMPLE	02020300	02020350	02020400	02020450	02020500
SiO2	16.00	26.30	48.70	53.40	53.30
TiO2	.16	.14	0.00	.26	.20
Al2O3	8.55	6.91	3.00	7.91	10.90
Fe2O3	42.30	31.60	23.70	17.19	12.31
MnO	.37	.28	.22	.39	.01
MgO	10.86	10.95	3.57	7.47	14.14
CaO	.10	.81	1.98	1.27	.35
Na2O	0.00	0.00	0.00	0.00	.02
K2O	0.00	0.00	.03	.38	.01
LOI	21.40	19.30	14.40	10.90	8.75
TOTAL	99.74	96.29	95.68	99.17	100.19

TRACE ELEMENTS (PPM)

	02020300	02020350	02020400	02020450	02020500
Zr	51	66	51	52	5
Sr	61	61	48	20	0
Rb	20	28	23	19	12
Zn	280	4800	9999	320	590
Cu	6650	2200	4000	1360	20
Ba	189	341	130	320	123
CuS	7600	1900	3100	1570	15
PbS	57	1100	8900	390	67
ZnS	55	2500	999	71	72
BaSO4			47		
Pb	99	8450	9500	305	80
Ni	14	3	6	3	136
Co	17	17	22	20	31
Cr	99	62	43	30	464
V	156	118	60	116	266
Hg	134	154	412	96	25
Ag	39	88	67	22	11
Nb					

INTERMEDIATE FOOTWALL - VARIABLY MINERALIZED AND ALTERED

MAJOR ELEMENTS (WTX)

SAMPLE	02020550	02020600	0542	0542 50	27853355
SiO2	48.00	56.00	56.20	61.10	42.30
TiO2	.06	.38	.02	.08	.90
Al2O3	7.65	11.37	5.05	5.90	15.20
Fe2O3	10.18	10.29	12.59	8.76	9.58
MnO	.71	.47	.13	.07	.17
MgO	9.31	9.44	3.64	1.50	7.24
CaO	6.45	1.79	.50	.02	12.37
Na2O	0.00	.01	.01	.03	2.69
K2O	.01	.67	.62	1.30	.84
LOI	11.60	7.80	9.30	6.90	7.90
TOTAL	93.97	98.22	88.06	85.66	99.19

TRACE ELEMENTS (PPM)

Zr	35	40	67	98	74
Sr	28	0	40	63	231
Rb	19	22	36	51	15
Zn	999	710	2900	9999	65
Cu	485	19	250	1360	56
Ba	87	599	366	4405	188
CuS	950	17	350	1100	42
PbS	7150	400	1090	9999	14
ZnS	360	270	3500	999	18
BaSO4	20		2600		0
Pb	2450	243	748	9999	27
Ni	72	24	15	3	85
Co	21	19	14	4	32
Cr	266	117	34	27	339
V	184	194	148	44	150
Hg	322	25	77	211	
Ag	23	14	16	32	
Nb					8

SKI HILL SEQUENCE FLOWS

MAJOR ELEMENTS (WT%)

SAMPLE	JGT75 41	JGT75 43	JGT75170	08680250	08680525
SiO2	58.90	61.20	53.60	61.40	51.30
TiO2	.73	.77	.80	.91	.58
Al2O3	15.81	13.90	16.46	13.50	16.70
Fe2O3	7.80	8.62	11.44	11.00	10.08
MnO	.17	.20	.16	.21	.18
MgO	2.49	2.40	3.61	3.05	6.32
CaO	6.50	6.82	7.18	4.68	9.79
Na2O	4.03	3.12	3.13	3.27	2.42
K2O	.47	.57	1.61	1.22	.65
LOI	1.00	.90	1.30	2.40	2.60
TOTAL	97.90	97.90	99.29	101.64	100.62

TRACE ELEMENTS (PPM)

Zr	81	91	73	47	31
Sr	305	334	228	140	255
Rb	20	16	24	18	17
Zn	57	73	65	124	87
Cu	91	23	136	88	62
Ba	363	351	1546	1465	398
CuS	75	21	125	78	47
PbS	12	16	19	15	10
ZnS	12	21	19	25	9
BaSO4	0	0	0		
Pb	22	19	28	25	24
Ni	4	3	8	8	33
Co	35	34	19	36	30
Cr	23	16	19	36	124
V	145	145	215	340	310
Hg				27	19
Ag				0	0
Nb	4	0	10		

SKI HILL SEQUENCE FLOWS

MAJOR ELEMENTS (WT%)

SAMPLE	08692100	14930150	27851517	28371950	28372575
SiO2	46.80	48.00	51.60	47.10	53.50
TiO2	.80	.83	.48	.88	.65
Al2O3	15.10	15.95	16.59	15.39	17.48
Fe2O3	10.42	10.19	9.81	9.31	8.63
MnO	.15	.17	.16	.22	.18
MgO	9.37	6.20	4.97	4.81	2.10
CaO	9.32	11.58	9.56	9.83	10.10
Na2O	1.57	2.44	2.69	2.30	2.09
K2O	.25	.49	1.07	.62	1.07
LOI	4.90	5.10	3.60	4.60	2.90
TOTAL	98.68	100.95	99.73	95.06	98.70

TRACE ELEMENTS (PPM)

	08692100	14930150	27851517	28371950	28372575
Zr	109	98	71	86	89
Sr	345	432	39	275	401
Rb	17	17	15	15	22
Zn	83	64	62	45	42
Cu	58	56	73	63	60
Ba	213	271	538	384	710
CuS		36	67	52	43
PbS		5	11	14	14
ZnS		6	19	9	16
BaSO4		0	0	0	0
Pb	23	15	30	18	25
Ni	79	69	34	92	12
Co	39	35	27	31	23
Cr	294	168	181	355	27
V	275	368	230	150	150
Hg	50	14			
Ag	0	2			
Nb			11	4	9

SKI HILL SEQUENCE FLOWS

MAJOR ELEMENTS (WT%)

SAMPLE	2841 50	2841 150	2851 283	2851 876	1925 100
SiO2	70.10	65.50	65.90	58.00	61.30
TiO2	.66	.66	.54	.72	.80
Al2O3	13.12	14.03	14.48	12.52	16.25
Fe2O3	5.07	6.38	4.89	9.53	6.19
MnO	.09	.11	.07	.18	.23
MgO	.96	2.27	1.71	2.62	1.85
CaO	3.75	2.70	2.17	7.86	2.23
Na2O	3.74	3.91	5.68	4.90	5.93
K2O	.58	1.63	1.56	.09	.71
LOI	1.00	2.20	2.50	1.80	2.80
TOTAL	99.87	99.39	99.56	98.22	98.29

TRACE ELEMENTS (PPM)

	2841 50	2841 150	2851 283	2851 876	1925 100
Zr	110	111	86	44	155
Sr	316	27	214	97	203
Rb	10	22	16	5	16
Zn	36	71	63	72	121
Cu	1	4	7	92	2
Ba	396	763	976	741	608
CuS	1	6	9	87	2
PbS	5	25	19	16	8
ZnS	19	37	18	33	19
BaSO4			0	0	0
Pb	14	18	18	23	18
Ni	5	10	7	5	3
Co	31	24	21	27	26
Cr	18		9	18	17
V	96	65	60	165	40
Hg					
Ag					
Nb			6	4	8

SKI HILL SEQUENCE FLOWS

MAJOR ELEMENTS (WT%)

SAMPLE   1925 140

SiO2	61.80
TiO2	.80
Al2O3	15.75
Fe2O3	7.07
MnO	.17
MgO	2.20
CaO	2.18
Na2O	5.37
K2O	.30
LOI	2.60

TOTAL	98.24

TRACE ELEMENTS (PPM)

Zr	154
Sr	291
Rb	24
Zn	134
Cu	2
Ba	288
CuS	33
PbS	6
ZnS	25
BaSO4	0
Pb	14
Ni	5
Co	22
Cr	16
V	55
Hg	
Ag	
Nb	5

SKI HILL SEQUENCE FRAGMENTALS

MAJOR ELEMENTS (WT%)

SAMPLE	JGT75 40	JGT75 42	07920050	07920150	08680150
SiO2	59.50	60.20	50.40	45.50	62.50
TiO2	.78	.77	.79	.75	.56
Al2O3	15.41	15.01	17.54	16.92	13.80
Fe2O3	7.92	8.01	11.48	11.13	7.25
MnO	.15	.15	.19	.21	.21
MgO	2.57	2.44	3.72	4.02	2.81
CaO	4.99	4.69	6.12	7.24	5.22
Na2O	2.73	2.78	2.87	3.81	2.47
K2O	1.88	1.90	2.68	.83	2.12
LOI	2.40	2.30	4.50	6.60	2.60
TOTAL	98.33	98.25	99.69	96.51	99.54

TRACE ELEMENTS (PPM)

Zr	110	105	76	81	83
Sr	320	321	284	288	340
Rb	47	36	35	24	39
Zn	69	74	111	119	85
Cu	41	39	90	94	48
Ba	1722	1697	1860	2238	9999
CuS	34	28	101	105	31
PbS	17	14	26	17	17
ZnS	17	8	42	27	21
BaSO4	0	0	3		0
Pb	31	25	31	33	29
Ni	3	8	12	12	14
Co	40	32	28	30	19
Cr	17	16	46	44	63
V	110	115	370	380	185
Hg			31	15	54
Ag			0	1	1
Nb	9	7			

SKI HILL SEQUENCE FRAGMENTALS

MAJOR ELEMENTS (WT%)

SAMPLE	08680325	08680425	08680625	08680725	08680825
SiO2	52.30	50.40	52.70	50.60	63.40
TiO2	.74	.74	.60	.63	.63
Al2O3	16.90	17.00	15.40	16.00	13.50
Fe2O3	11.00	11.09	10.08	9.00	9.63
MnO	.16	.17	.20	.16	.18
MgO	4.00	4.58	4.74	2.80	2.75
CaO	7.29	7.84	8.40	10.04	5.22
Na2O	2.15	2.15	2.08	4.09	2.78
K2O	1.43	1.12	.52	.50	.88
LOI	4.40	4.10	5.50	7.10	2.10
TOTAL	100.37	99.19	100.22	100.92	101.07

TRACE ELEMENTS (PPM)

	08680325	08680425	08680625	08680725	08680825
Zr	70	64	83	70	80
Sr	305	334	357	298	323
Rb	18	23	31	18	22
Zn	111	106	112	85	85
Cu	82	59	52	71	65
Ba	372	837	932	312	991
CuS	71	45	43	75	57
PbS	10	10	24	16	14
ZnS	23	16	21	23	18
BaSO4		0	0		0
Pb	26	26	40	25	23
Ni	14	13	10	8	5
Co	27	26	22	22	20
Cr	38	50	43	37	34
V	335	300	275	300	265
Hg	23	25	36	34	29
Ag	0	0	1	1	0
Nb					

SKI HILL SEQUENCE FRAGMENTALS

MAJOR ELEMENTS (WT%)

SAMPLE	08680925	08681125	08681225	08681325	08681425
SiO_2	43.90	47.70	61.50	49.20	52.50
TiO_2	.75	.72	.65	.75	.60
Al_2O_3	19.80	19.60	15.40	18.00	16.00
Fe_2O_3	13.35	12.15	7.61	11.90	8.92
MnO	.21	.18	.15	.15	.12
MgO	6.61	6.27	2.21	7.21	4.74
CaO	9.00	9.24	4.68	6.37	7.53
Na_2O	1.70	1.73	2.39	1.76	2.43
K_2O	1.51	1.24	2.03	1.22	.93
LOI	4.90	3.40	5.10	4.30	6.50
TOTAL	101.73	102.23	101.72	100.86	100.27

TRACE ELEMENTS (PPM)

Zr	87	60	88	77	75
Sr	393	341	252	314	393
Rb	31	28	46	28	27
Zn	150	101	113	104	87
Cu	73	52	18	70	81
Ba	1116	863	965	1056	580
CuS	71	36	18	61	84
PbS	13	4	10	19	20
ZnS	32	18	20	57	27
BaSO4		0		0	
Pb	30	21	21	25	31
Ni	18	22	3	22	32
Co	31	33	12	28	27
Cr	56	67	26	84	75
V	300	300	59	350	280
Hg	20	17	13	31	27
Ag	0	0	1	1	0
Nb					

SKI HILL SEQUENCE FRAGMENTALS

MAJOR ELEMENTS (WT%)

SAMPLE	08681450	08681475	08681525	08690075	08690260
SiO_2	74.40	65.70	65.00	54.50	51.30
TiO_2	.23	.46	.50	.77	.81
Al_2O_3	10.70	16.60	12.90	17.21	17.90
Fe_2O_3	4.17	4.58	5.34	10.15	11.07
MnO	.12	.13	.17	.16	.17
MgO	.64	1.50	.79	4.28	4.57
CaO	3.90	4.10	8.37	6.75	6.64
Na_2O	2.42	2.29	2.82	2.64	2.86
K_2O	1.44	3.16	.42	1.36	1.30
LOI	3.00	2.70	2.50	1.00	4.10
TOTAL	101.02	101.22	98.87	98.82	100.72

TRACE ELEMENTS (PPM)

Zr	128	233	136	93	76
Sr	244	422	443	430	39
Rb	42	80	16	30	26
Zn	18	50	55	96	105
Cu	3	3	11	65	111
Ba	375	854	224	1017	893
CuS	0	0	6	52	97
PbS	8	4	21	8	31
ZnS	2	8	13	28	22
BaSO4	0	0		0	
Pb	19	27	34	19	36
Ni	1	1	2	13	19
Co	1	2	7	24	31
Cr	21	21	37	46	43
V	5	31	68	275	305
Hg	10	10	15	41	52
Ag	0	0	0	2	1
Nb					

SKI HILL SEQUENCE FRAGMENTALS

MAJOR ELEMENTS (WT%)

SAMPLE	08690348	08690450	08690554	08690750	08690850
SiO2	57.40	55.80	49.40	52.70	48.80
TiO2	.58	.58	.54	.73	.73
Al2O3	16.00	15.70	16.80	17.00	18.90
Fe2O3	6.85	9.74	10.38	10.34	11.60
MnO	.18	.20	.23	.15	.15
MgO	3.41	4.28	6.10	4.37	5.85
CaO	8.21	8.03	9.56	8.32	8.94
Na2O	3.88	2.24	2.70	2.77	1.72
K2O	1.17	1.19	.66	.64	.59
LOI	2.90	2.40	3.10	4.60	4.20
TOTAL	100.58	100.07	99.47	101.62	101.48

TRACE ELEMENTS (PPM)

	08690348	08690450	08690554	08690750	08690850
Zr	72	79	78	81	72
Sr	384	306	421	355	387
Rb	31	28	25	22	21
Zn	83	92	96	114	89
Cu	72	62	114	59	73
Ba	695	741	533	526	451
CuS	60	51	120	54	57
PbS	4	16	5	21	8
ZnS	34	15	37	32	25
BaSO4	0			0	
Pb	16	20	20	26	20
Ni	28	16	35	21	12
Co	22	24	29	26	28
Cr	115	74	122	58	39
V	230	326	315	315	405
Hg	43	40	40	38	38
Ag	6	4	5	0	0
Nb					

SKI HILL SEQUENCE FRAGMENTALS

MAJOR ELEMENTS (WT%)

SAMPLE	08690950	08691050	08691150	08691250	08691325
SiO2	57.90	60.10	49.40	46.60	53.00
TiO2	.60	.58	.65	.72	.72
Al2O3	16.80	17.20	16.60	17.30	16.20
Fe2O3	8.59	8.13	10.68	12.57	8.70
MnO	.15	.15	.12	.11	.22
MgO	3.18	3.44	7.17	7.50	2.39
CaO	3.33	5.21	5.59	9.25	8.60
Na2O	7.24	2.92	1.59	2.34	5.00
K2O	.05	1.25	.73	.35	.05
LOI	1.90	2.70	4.50	3.60	4.50
TOTAL	99.74	101.68	97.03	100.34	99.38

TRACE ELEMENTS (PPM)

	08690950	08691050	08691150	08691250	08691325
Zr	70	125	91	65	53
Sr	151	533	409	279	215
Rb	12	27	26	17	2
Zn	86	97	107	113	89
Cu	24	42	53	55	72
Ba	141	1065	511	340	717
CuS	25	41	54	71	35
PbS	18	64	12	10	0
ZnS	24	23	38	20	82
BaSO4				0	7
Pb	21	61	23	23	1
Ni	6	5	20	28	9
Co	19	17	26	33	82
Cr	37	29	100	150	13
V	180	150	250	410	41
Hg	37	41	41	49	3
Ag	1	0	2	1	6
Nb					0

SKI HILL SEQUENCE FRAGMENTALS

MAJOR ELEMENTS (WT%)

SAMPLE	08691350	12140105	1214 195	12140300	12140500
SiO2	76.50	64.10	61.80	53.70	46.60
TiO2	.19	.35	.73	.74	.70
Al2O3	5.65	11.84	15.38	16.00	17.23
Fe2O3	5.74	4.83	5.21	9.97	11.46
MnO	.21	.12	.08	.21	.18
MgO	1.55	1.51	1.38	3.18	4.37
CaO	2.56	3.86	4.35	6.58	7.78
Na2O	.29	.52	.23	3.08	.78
K2O	1.67	1.97	3.31	1.20	3.10
LOI	3.00	6.00	6.80	4.40	9.90
TOTAL	97.36	95.10	99.27	99.06	102.10

TRACE ELEMENTS (PPM)

Zr	3	66	57	87	34
Sr		39	5	365	200
Rb		50	63	28	17
Zn		101	74	124	121
Cu		44	22	47	68
Ba		823	958	1121	241
CuS		32	17	42	58
PbS		19	2	17	9
ZnS		7	6	11	13
BaSO4			10		
Pb		45	25	51	35
Ni		6	1	9	31
Co		12	10	22	26
Cr		35	22	47	36
V		196	138	254	226
Hg		38	31	32	34
Ag		7	5	12	10
Nb					

SKI HILL SEQUENCE FRAGMENTALS

MAJOR ELEMENTS (WTZ)

SAMPLE	12140600	12140700	12140900	12140975	28371275
SiO2	49.40	56.10	49.40	64.30	55.70
TiO2	.45	.66	.85	.40	.89
Al2O3	16.67	17.28	20.60	13.07	16.45
Fe2O3	10.59	9.41	11.86	3.13	9.83
MnO	.16	.21	.22	.10	.13
MgO	6.00	3.35	3.90	.57	3.20
CaO	6.85	7.43	5.63	7.10	3.12
Na2O	1.89	2.81	3.35	5.18	1.19
K2O	.90	1.00	1.12	.37	2.72
LOI	3.70	2.20	1.40	4.60	3.80
TOTAL	96.61	100.45	97.73	98.82	97.03

TRACE ELEMENTS (PPM)

	Zr	Sr	Rb	Zn	Cu	Ba	CuS	PbS	ZnS	BaSO4	Pb	Ni	Co	Cr	V	Hg	Ag	Nb
12140600	58	304	24	112	69	978	53	7	20	0	39	27	29	85	241	32	11	
12140700	53	289	19	95	47	679	30	7	12		40	7	22	36	194	29	11	
12140900	114	505	29	151	89	801	75	7	21		44	5	29	43	202	95	11	
12140975	79	448	17	19	26	3763	24	8	8	0	32	1	6	27	130	103	7	
28371275	96	243	79	73	73	1869	57	12	20	0	27	7	35	38	215			9

SKI HILL SEQUENCE FRAGMENTALS

MAJOR ELEMENTS (WT%)

SAMPLE	28371398	28371500	28373200	28373550	2851 820
SiO2	58.10	57.00	52.90	48.00	58.20
TiO2	.60	.61	.68	.69	.78
Al2O3	17.20	16.90	17.07	19.09	15.07
Fe2O3	7.43	7.14	9.29	10.09	8.00
MnO	.12	.11	.17	.15	.19
MgO	2.81	2.89	4.21	4.43	3.24
CaO	6.70	6.69	8.49	8.51	4.68
Na2O	1.90	2.88	2.13	3.55	2.77
K2O	.71	.70	.74	.47	1.80
LOI	1.90	2.60	3.50	3.50	3.70
TOTAL	97.47	97.52	99.18	98.48	98.43

TRACE ELEMENTS (PPM)

Zr	93	75	80	71	77
Sr	424	373	318	276	263
Rb	17	31	19	20	23
Zn	52	70	57	82	84
Cu	41	62	78	83	32
Ba	65	718	688	424	874
CuS	38	39	58	69	34
PbS	15	14	20	20	25
ZnS	16	14	14	17	31
BaSO4	0	0	0	0	0
Pb	29	25	30	37	25
Ni	7	6	46	9	6
Co	24	23	32	26	23
Cr	27	39	78	44	13
V	140	165	170	280	85
Hg					
Ag					
Nb	5	4	3	2	2

ALTERED SKI HILL SEQUENCE FRAGMENTALS

MAJOR ELEMENTS (WT%)

SAMPLE	2851 882	28371500	28373200	28373550	2851 820
SiO2	51.40	57.00	52.90	48.00	58.20
TiO2	.96	.61	.68	.69	.78
Al2O3	15.33	16.90	17.07	19.09	15.07
Fe2O3	12.82	7.14	9.29	10.09	8.00
MnO	.22	.11	.17	.15	.19
MgO	3.39	2.89	4.21	4.43	3.24
CaO	6.12	6.69	8.49	8.51	4.68
Na2O	3.49	2.88	2.13	3.55	2.77
K2O	2.39	.70	.74	.47	1.80
LOI	2.80	2.60	3.50	3.50	3.70
TOTAL	98.92	97.52	99.18	98.48	98.43

TRACE ELEMENTS (PPM)

	2851 882	28371500	28373200	28373550	2851 820
Zr	56	75	80	71	77
Sr	167	373	318	276	263
Rb	21	31	19	20	23
Zn	78	70	57	82	84
Cu	117	62	78	83	32
Ba	691	718	688	424	874
CuS	108	39	58	69	34
PbS	20	14	20	20	25
ZnS	41	14	14	17	31
BaSO4	0	0	0	0	0
Pb	24	25	30	37	25
Ni	11	6	46	9	6
Co	29	23	32	26	23
Cr	21	39	78	44	13
V	240	165	170	280	85
Hg					
Ag					
Nb	0	4	3	2	2

SKI HILL SEQUENCE FRAGMENTALS

MAJOR ELEMENTS (WT%)

SAMPLE   2851 882

SiO2	51.40
TiO2	.96
Al2O3	15.33
Fe2O3	12.82
MnO	.22
MgO	3.39
CaO	6.12
Na2O	3.49
K2O	2.39
LOI	2.80

TOTAL   98.92

TRACE ELEMENTS (PPM)

Zr	76
Sr	167
Rb	21
Zn	78
Cu	117
Ba	691
CuS	108
PbS	20
ZnS	41
BaSO4	0
Pb	24
Ni	11
Co	29
Cr	21
V	240
Hg	
Ag	
Nb	0

LUCKY STRIKE ORE HORIZON SEQUENCE - HANGING WALL DACITIC TUFFS

MAJOR ELEMENTS (WT%)

SAMPLE	JGT75328	645 290	07920225	07920400	07920475
SiO2	79.90	71.90	69.20	70.80	70.20
TiO2	.23	.17	.35	.35	.23
Al2O3	9.92	12.55	13.27	13.26	15.44
Fe2O3	.81	2.14	2.85	2.99	2.14
MnO	.03	.04	.09	.11	.05
MgO	.11	.91	.93	.92	1.87
CaO	.73	2.85	3.78	2.87	1.65
Na2O	3.14	2.66	3.13	2.28	1.80
K2O	2.60	2.45	2.08	2.94	3.57
LOI	1.20	3.90	3.30	2.50	3.20
TOTAL	98.67	99.57	98.98	98.85	100.15

TRACE ELEMENTS (PPM)

Zr	70	93	162	187	187
Sr	95	133	280	354	334
Rb	38	57	53	77	87
Zn	115	28	56	60	29
Cu	2	1	3	3	4
Ba	1624	1437	4081	1070	1232
CuS	1	1	0	0	0
PbS	1	18	32	13	9
ZnS	125	11	19	9	3
BaSO4	4	6	3	0	
Pb	12	11	49	30	13
Ni	1	2	2	2	1
Co	56	15	2	3	2
Cr	10	11	31	21	22
V	18	18	2	0	0
Hg			18	13	11
Ag			1	2	1
Nb	7	15			

LUCKY STRIKE ORE HORIZON SEQUENCE - HANGING WALL DACITIC TUFFS

MAJOR ELEMENTS (WT%)

SAMPLE	07920575	07920675	07920775	07920925	07920950
SiO2	74.00	72.20	70.50	74.90	69.50
TiO2	.20	.20	.18	.20	.22
Al2O3	12.40	13.40	13.20	12.04	15.90
Fe2O3	1.85	2.19	2.25	1.67	1.86
MnO	.10	.09	.10	.09	.09
MgO	.72	1.19	1.03	.62	2.26
CaO	1.06	1.32	2.77	2.68	1.20
Na2O	4.93	2.53	2.13	3.34	1.62
K2O	1.57	4.00	3.34	1.28	3.00
LOI	1.40	2.20	4.10	1.70	3.00
TOTAL	98.23	99.32	99.60	98.52	98.65

TRACE ELEMENTS (PPM)

Zr	96	121	115	122	134
Sr	108	216	151	597	358
Rb	40	116	84	40	105
Zn	97	23	20	35	141
Cu	11	2	2	6	57
Ba	1260	1551	783	1152	2194
CuS	0	0	1	2	1
PbS	12	12	17	21	12
ZnS	4	2	4	8	2
BaSO4	0		0		5
Pb	16	18	18	56	33
Ni	1	1	1	1	57
Co	1	1	1	2	40
Cr	28	24	79	22	29
V	0	6	0	0	345
Hg	13	10	11	18	5
Ag	2	2	0	0	1
Nb					

LUCKY STRIKE ORE HORIZON SEQUENCE - HANGING WALL DACITIC TUFFS

MAJOR ELEMENTS (WT%)

SAMPLE	07920975	07921000	07921025	08681550	08681590
SiO2	69.90	73.30	70.10	74.40	72.10
TiO2	.22	.18	.25	.18	.22
A1203	15.23	13.08	14.87	13.20	13.50
Fe203	1.62	1.51	2.56	1.90	1.83
MnO	.07	.10	.08	.08	.08
MgO	1.20	.75	1.82	.56	.62
CaO	2.32	2.62	2.24	2.11	2.17
Na20	2.90	3.66	2.12	2.43	2.63
K20	2.70	1.47	3.09	3.12	3.09
LOI	2.50	2.20	2.80	1.90	2.30
TOTAL	98.66	98.87	99.93	99.88	98.54

TRACE ELEMENTS (PPM)

Zr	175	110	108	120	112
Sr	698	551	357	278	216
Rb	86	37	72	92	92
Zn	26	32	127	18	25
Cu	2	3	7	2	2
Ba	1042	7814	3316	975	2439
CuS	0	0	2	0	0
PbS	21	9	18	14	21
ZnS	1.	7	27	5	4
BaSO4				0	0
Pb	40	28	30	18	19
Ni	1	1	2	0	0
Co	2	2	2	1	1
Cr	22	22	28	27	19
V	0	0	27	9	10
Hg	8	6	12	11	13
Ag	0	0	0	0	0
Nb					

LUCKY STRIKE ORE HORIZON SEQUENCE - HANGING WALL DACITIC TUFFS

MAJOR ELEMENTS (WT%)

SAMPLE	08681630	08692190	08692215	08692240	08692265
SiO2	65.40	66.60	67.10	67.70	71.70
TiO2	.40	.21	.25	.27	.21
Al2O3	14.29	15.91	14.60	15.12	13.24
Fe2O3	4.50	2.09	2.17	2.44	1.63
MnO	.11	.05	.07	.08	.06
MgO	1.71	1.51	1.25	.98	.69
CaO	3.47	.64	2.09	1.65	.69
Na2O	1.80	1.77	1.74	4.00	2.29
K2O	3.40	4.58	4.32	3.50	3.79
LOI	3.80	3.30	4.10	1.90	2.80
TOTAL	98.88	96.66	97.69	97.64	98.22

TRACE ELEMENTS (PPM)

	08681630	08692190	08692215	08692240	08692265
Zr	179	164	174	166	145
Sr	263	32	147	221	139
Rb	95	123	106	76	95
Zn	67	25	24	42	37
Cu	5	3	2	5	3
Ba	905	1215	5058	1510	1018
CuS	2	1	1	2	1
PbS	12	14	37	18	23
ZnS	11	2	2	8	3
BaSO4					
Pb	21	19	22	23	26
Ni	2	3	4	4	3
Co	4	2	2	2	2
Cr	22	7	8	8	5
V	26	25	20	37	18
Hg	12	8	8	5	4
Ag	0	0	0	0	0
Nb					

LUCKY STRIKE ORE HORIZON SEQUENCE - HANGING WALL DACITIC TUFFS

MAJOR ELEMENTS (WT%)

SAMPLE	08692315	08692340	08692390	08692405	08692430
SiO_2	68.00	76.30	75.90	67.50	68.80
TiO_2	.24	.19	.23	.21	.24
Al_2O_3	16.38	12.40	13.40	14.94	13.62
Fe_2O_3	1.94	1.93	1.49	2.12	2.78
MnO	.06	.06	.04	.08	.08
MgO	.65	.67	.56	1.39	1.50
CaO	2.04	1.00	1.00	2.31	2.52
Na_2O	4.25	3.90	4.89	3.58	1.92
K_2O	3.12	2.40	1.90	2.76	3.50
LOI	1.90	1.60	1.70	3.60	3.80
TOTAL	98.58	100.45	101.19	98.49	98.76

TRACE ELEMENTS (PPM)

	08692315	08692340	08692390	08692405	08692430
Zr	197	143	168	167	142
Sr	233	105	167	81	138
Rb	86	62	50	66	100
Zn	33	37	32	39	51
Cu	8	3	3	5	8
Ba	1217	892	428	535	650
CuS	4	1	1	2	5
PbS	21	14	15	15	24
ZnS	3	8	9	10	12
BaSO4					
Pb	22	18	21	22	27
Ni	3	3	3	4	7
Co	2	2	2	2	2
Cr	6	9	8	11	23
V	21	14	24	19	47
Hg	5	5	6	11	5
Ag	0	0	0	0	0
Nb					

LUCKY STRIKE ORE HORIZON SEQUENCE - HANGING WALL DACITIC TUFFS

MAJOR ELEMENTS (WT%)

SAMPLE	9781260	12141000	12141025	12141050	12141075
SiO2	70.40	73.20	66.90	75.80	67.40
TiO2	.33	.22	.23	.13	.23
Al2O3	13.73	13.40	15.74	10.11	15.44
Fe2O3	2.98	2.06	2.25	2.00	1.83
MnO	.08	.10	.11	.15	.08
MgO	.99	.79	.92	.57	.70
CaO	2.23	2.79	3.12	2.96	3.20
Na2O	2.77	2.31	2.68	3.21	1.99
K2O	2.45	2.63	3.14	1.36	4.15
LOI	3.50	2.10	3.70	2.80	4.50
TOTAL	99.46	99.60	98.79	99.09	99.43

TRACE ELEMENTS (PPM)

	9781260	12141000	12141025	12141050	12141075
Zr	81	119	151	81	108
Sr	68	377	442	311	83
Rb	60	82	88	41	99
Zn	83	31	36	27	28
Cu	1	2	2	2	2
Ba	680	1060	177	1907	977
CuS	1	0	0	0	0
PbS	4	3	9	5	15
ZnS	13	2	7	2	2
BaSO4	4				3
Pb	7	28	29	22	26
Ni	2	1	1	0	0
Co	15	3	3	2	2
Cr	9	41	30	21	42
V	10	0	8	0	6
Hg		16	13	22	22
Ag		5	5	4	8
Nb	11				

LUCKY STRIKE ORE HORIZON SEQUENCE - HANGING WALL DACITIC TUFFS

MAJOR ELEMENTS (WT%)

SAMPLE	12141100	12141125	12141150	12141175	12141200
SiO2	70.20	69.00	72.70	73.60	73.50
TiO2	.23	.18	.18	.03	.15
Al2O3	14.53	13.23	12.72	11.96	11.78
Fe2O3	2.05	1.84	1.70	2.12	1.95
MnO	.07	.09	.11	.17	.13
MgO	1.04	.71	.64	.34	.39
CaO	2.42	2.15	3.62	2.17	3.58
Na2O	2.24	3.45	1.85	5.82	2.91
K2O	3.69	2.50	3.26	.52	1.98
LOI	3.60	3.30	3.70	2.10	2.60
TOTAL	100.07	96.45	100.48	98.83	98.97

TRACE ELEMENTS (PPM)

Zr	116	92	117	99	59
Sr	105	135	355	207	106
Rb	100	72	95	19	60
Zn	38	35	35	43	29
Cu	1	2	1	2	2
Ba	1124	967	2341	1712	649
CuS	0	0	0	0	0
PbS	6	11	13	6	13
ZnS	4	2	1	7	3
BaSO4					
Pb	21	22	23	18	10
Ni	0	0	1	1	1
Co	3	3	2	2	2
Cr	26	19	22	25	51
V	4	5	10	0	10
Hg	22	16	31	27	32
Ag	7	6	4	5	6
Nb					

LUCKY STRIKE ORE HORIZON SEQUENCE - HANGING WALL DACITIC TUFFS

MAJOR ELEMENTS (WT%)

SAMPLE	12141225	12141245	12141265	12141285	12141295
SiO2	72.00	70.30	77.20	72.70	71.10
TiO2	.18	.17	.23	.22	.17
Al203	13.63	13.69	13.90	12.68	13.96
Fe203	1.87	2.16	1.12	1.79	1.88
MnO	.12	.13	.03	.08	.07
MgO	.63	.79	.36	.57	.60
CaO	2.65	2.69	.29	2.85	2.28
Na2O	2.05	.86	.56	2.15	4.86
K2O	3.33	4.14	3.32	2.51	1.47
LOI	3.00	4.40	1.80	3.00	2.00
TOTAL	99.46	99.33	98.81	98.55	98.39

TRACE ELEMENTS (PPM)

Zr	110	90	116	130	113
Sr	268	50	27	393	35
Rb	91	104	75	74	45
Zn	42	47	17	38	44
Cu	1	1	2	2	2
Ba	1223	1472	1930	4077	1111
CuS	0	0	0	0	0
PbS	24	17	11	8	11
ZnS	3	4	1	4	5
BaSO4			9		
Pb	15	11	4	6	7
Ni	1	1	1	0	0
Co	3	2	1	1	2
Cr	21	18	24	27	31
V	4	6	0	0	0
Hg	32	31	137	31	22
Ag	5	6	4	5	6
Nb					

LUCKY STRIKE ORE HORIZON SEQUENCE - HANGING WALL DACITIC TUFFS

MAJOR ELEMENTS (WT%)

SAMPLE	14930400	14930450	14930500	14930550	14930600
SiO2	73.10	69.10	69.60	73.99	71.80
TiO2	.23	.21	.20	.18	.26
Al2O3	15.00	14.57	14.61	13.66	14.61
Fe2O3	1.70	1.99	2.06	1.75	2.05
MnO	.06	.08	.10	.07	.08
MgO	2.33	.88	.63	.45	.68
CaO	1.15	3.32	3.20	2.12	1.32
Na2O	2.42	1.95	2.00	2.38	2.93
K2O	2.33	3.16	2.68	3.64	3.39
LOI	3.00	4.70	3.70	3.10	2.90
TOTAL	101.32	99.96	98.78	101.25	100.02

TRACE ELEMENTS (PPM)

	14930400	14930450	14930500	14930550	14930600
Zr	133	62		154	130
Sr	212	0		192	41
Rb	60	51		94	81
Zn	14	18	25	26	18
Cu	1	2	5	4	3
Ba	2170	1654	2320	970	716
CuS	0	1	2	2	1
PbS	11	8	8	18	15
ZnS	3	1	2	4	6
BaSO4		9			0
Pb	11	9	11	17	11
Ni	1	1	1	1	1
Co	1	1	2	2	2
Cr	20	24		28	97
V	0	13	0	0	10
Hg	12	12	21	12	10
Ag	3	0	2	0	0
Nb					

LUCKY STRIKE ORE HORIZON SEQUENCE - HANGING WALL DACITIC TUFFS

MAJOR ELEMENTS (WT%)

SAMPLE	14930725	14930750	14930775	14930800	26103011
SiO_2	72.30	71.20	72.50	73.70	69.30
TiO_2	.29	.23	.27	.17	.29
Al_2O_3	12.54	14.00	13.37	13.46	14.03
Fe_2O_3	2.03	2.37	2.08	2.16	2.50
MnO	.11	.12	.08	.09	.04
MgO	.64	.68	.63	.64	1.86
CaO	3.50	1.42	2.19	2.02	2.00
Na_2O	1.03	3.21	3.20	2.30	1.74
K_2O	4.13	3.84	3.02	3.51	4.05
LOI	4.20	1.60	1.70	2.20	3.50
TOTAL	100.77	98.67	99.04	100.25	99.31

TRACE ELEMENTS (PPM)

Zr	146	106	158	148	133
Sr	128	163	275	309	143
Rb	110	81	75	93	137
Zn	25	31	22	21	28
Cu	1	6	2	1	2
Ba	4178	1649	1344	1140	567
CuS	0	2	0	0	1
PbS	15	15	8	12	27
ZnS	7	7	5	13	2
BaSO4		4			
Pb	14	12	12	12	13
Ni	2	2	1	1	2
Co	2	3	1	2	11
Cr	24	26	20	23	8
V	18	12	0	15	10
Hg	10	22	12	10	
Ag	0	2	3	6	
Nb					

LUCKY STRIKE ORE HORIZON SEQUENCE - HANGING WALL DACITIC TUFFS

MAJOR ELEMENTS (WT%)

SAMPLE	26663025	26663075	26663150	26 3250	26663325
SiO2	76.80	66.60	71.90	73.70	70.40
TiO2	.17	.31	.24	.24	.20
Al2O3	9.73	14.21	13.66	11.14	12.98
Fe2O3	2.02	2.37	1.87	1.72	2.40
MnO	.13	.07	.06	.06	.09
MgO	.33	.80	.76	.52	.63
CaO	1.86	3.53	1.30	.99	3.00
Na2O	4.86	3.68	5.00	2.47	2.27
K2O	.39	2.94	1.50	4.86	3.36
LOI	1.30	3.40	1.70	.80	2.20
TOTAL	97.59	97.91	97.99	96.50	97.53

TRACE ELEMENTS (PPM)

Zr	63	101	115	82	108
Sr	192	198	168	138	282
Rb	11	75	39	58	89
Zn	13	18	14	24	21
Cu	5	16	30	11	3
Ba	1062	619	260	1904	61
CuS	1	15	35	7	1
PbS	4	18	10	11	7
ZnS	7	7	2	3	1
BaSO4			0		
Pb	1	2	2	10	12
Ni	1	1	1	3	1
Co	2	2	3	4	2
Cr	25	25	23	22	23
V	20	33	18	37	10
Hg	8	10	10	10	8
Ag	2	0	1	0	0
Nb					

LUCKY STRIKE ORE HORIZON SEQUENCE - HANGING WALL DACITIC TUFFS

MAJOR ELEMENTS (WT%)

SAMPLE	26 3400	26663475	26 3550	26802856	27101053
SiO2	70.10	68.60	72.00	68.00	69.50
TiO2	.23	.15	.19	.11	.32
Al2O3	13.46	13.07	12.44	14.71	13.91
Fe2O3	2.67	1.58	1.56	2.15	2.68
MnO	.08	.06	.08	.04	.07
MgO	.67	.40	.97	.71	1.15
CaO	2.50	2.89	2.48	3.33	1.69
Na2O	2.82	4.35	2.72	1.40	2.31
K2O	3.30	2.06	2.14	3.72	4.03
LOI	1.80	3.40	2.60	5.00	3.30
TOTAL	97.63	96.56	97.18	99.17	98.96

TRACE ELEMENTS (PPM)

Zr	125	104	96	129	155
Sr	295	172	254	113	17
Rb	76	51	48	90	88
Zn	24	15	16	18	17
Cu	3	3	1	1	1
Ba	1177	1734	1179	1090	1106
CuS	1	0	0	1	1
PbS	7	12	10	28	14
ZnS	6	5	2	17	12
BaSO4	0		3		
Pb	6	5	8	15	13
Ni	2	2	1	3	2
Co	3	2	1	15	20
Cr	22	25	20	4	9
V	22	15	10	20	10
Hg	10	6	10		
Ag	0	0	0		
Nb					

LUCKY STRIKE ORE HORIZON SEQUENCE - HANGING WALL DACITIC TUFFS

MAJOR ELEMENTS (WT%)

SAMPLE	27101150	27711312	27711350	2800 182	2800 387
SiO2	68.80	71.70	72.90	71.00	66.70
TiO2	.26	.20	.26	.20	.44
Al2O3	14.24	13.28	13.00	14.63	15.88
Fe2O3	3.06	2.13	2.17	1.72	4.09
MnO	.08	.04	.06	.09	.07
MgO	1.42	.95	.78	1.12	2.41
CaO	2.17	2.10	2.58	2.20	2.62
Na2O	1.59	2.75	2.93	2.03	2.03,
K2O	4.06	2.63	2.01	3.67	2.35
LOI	4.20	2.70	2.50	2.40	3.30
TOTAL	99.88	98.48	99.19	99.06	99.89

TRACE ELEMENTS (PPM)

Zr	149	134	140	140	189
Sr	117	311	360	461	358
Rb	96	78	58	113	65
Zn	24	19	17	16	66
Cu	3	4	1	1	1
Ba	584	1359	955	1254	1094
CuS	4	1	1	1	1
PbS	25	32	27	28	18
ZnS	14	2	8	2	17
BaSO4					
Pb	11	21	12	15	22
Ni	4	2	2	1	5
Co	11	45	18	16	15
Cr	11	5	6	6	9
V	10	15	10	10	10
Hg					
Ag					
Nb					

LUCKY STRIKE ORE HORIZON SEQUENCE - HANGING WALL DACITIC TUFFS

MAJOR ELEMENTS (WT%)

SAMPLE 14930650

SiO2	72.60
TiO2	.29
Al2O3	13.51
Fe2O3	2.50
MnO	.13
MgO	.70
CaO	1.40
Na2O	3.92
K2O	2.75
LOI	1.50
TOTAL	99.30

TRACE ELEMENTS (PPM)

Zr	126
Sr	203
Rb	67
Zn	24
Cu	5
Ba	1437
CuS	2
PbS	17
ZnS	10
BaSO4	
Pb	15
Ni	2
Co	2
Cr	39
V	1.4
Hg	14
Ag	0
Nb	

ORIENTAL AND LUCKY STRIKE AREA RHYOLITE FLOWS

MAJOR ELEMENTS (WT%)

SAMPLE	JGT75327	158 584	158 617	885 195	1589 778
SiO2	69.80	71.50	74.90	72.80	75.00
TiO2	.31	.33	.38	.28	.36
Al2O3	14.21	14.55	12.90	13.49	13.68
Fe2O3	2.65	2.60	2.54	1.97	.95
MnO	.05	.04	.02	.02	.02
MgO	.53	.43	.33	.03	.14
CaO	1.78	1.50	1.19	1.19	.68
Na2O	5.34	5.26	3.67	4.85	5.02
K2O	1.50	2.65	3.35	2.42	2.27
LOI	2.60	.80	.80	1.50	1.10
TOTAL	98.77	99.66	100.08	98.55	99.22

TRACE ELEMENTS (PPM)

	JGT75327	158 584	158 617	885 195	1589 778
Zr	129	165	159	181	187
Sr	122	27	317	222	237
Rb	23	45	66	49	39
Zn	35	33	31	5	30
Cu	37	2	1	1	1
Ba	565	1242	1535	962	1126
CuS	42	1	1	1	1
PbS	21	8	11	3	32
ZnS	7	5	12	4	16
BaSO4	0				
Pb	24	10	3	1	43
Ni	1	2	2	2	2
Co	35	29	23	27	24
Cr	12	17	9	2	0
V	10	55	35	15	10
Hg					
Ag					
Nb	9				

ORIENTAL AND LUCKY STRIKE AREA RHYOLITE FLOWS

MAJOR ELEMENTS (WT%)

SAMPLE	1589 811	17301260
SiO2	73.80	71.00
TiO2	.41	.50
A1203	13.09	13.76
Fe203	1.38	2.57
MnO	.03	.04
MgO	.01	.59
CaO	.96	1.19
Na20	4.84	4.40
K20	2.61	3.75
LOI	1.30	1.10
TOTAL	98.43	98.90

TRACE ELEMENTS (PPM)

Zr	174	165
Sr	201	191
Rb	31	50
Zn	24	52
Cu	1	1
Ba	1259	1247
CuS	1	1
PbS	21	12
ZnS	11	34
BaSO4		
Pb	21	2
Ni	3	3
Co	42	28
Cr	0	32
V	20	40
Hg		
Ag		
Nb		

CLEMENTINE AREA RHYOLITE FLOWS

MAJOR ELEMENTS (WT%)

SAMPLE	1903 609	23491065	2866 516
SiO_2	69.90	73.50	73.90
TiO_2	.16	.18	.14
Al_2O_3	14.48	13.26	13.42
Fe_2O_3	2.19	1.50	.97
MnO	.08	.04	.02
MgO	.61	.49	.21
CaO	.96	1.59	.28
Na_2O	3.74	4.49	3.09
K_2O	4.78	1.70	5.53
LOI	1.60	2.70	1.00
TOTAL	98.50	99.53	98.48

TRACE ELEMENTS (PPM)

Zr	83	89	132
Sr	125	150	79
Rb	85	32	100
Zn	42	22	7
Cu	13	1	1
Ba	1553	568	1702
CuS	8	3	1
PbS	19	15	20
ZnS	16	20	5
$BaSO_4$	0	0	
Pb	27	13	3
Ni	7	3	4
Co	17	9	26
Cr	9	10	0
V	10	10	10
Hg			
Ag			
Nb	6	8	

ORIENTAL ORE HORIZON SEQUENCE 'WHITE RHYOLITE'

MAJOR ELEMENTS (WTZ)

SAMPLE	1083 586	17301203
SiO2	73.30	75.60
TiO2	.39	.22
Al2O3	12.91	10.29
Fe2O3	.03	.01
MnO	.01	.01
MgO	.60	.01
CaO	.44	.76
Na2O	1.52	.36
K2O	7.64	7.93
LOI	1.60	1.60
TOTAL	98.44	96.79

TRACE ELEMENTS (PPM)

Zr	166	147
Sr	49	119
Rb	62	63
Zn	19	455
Cu	1	1
Ba	2982	4639
CuS	2	5
PbS	6	69
ZnS	22	460
BaSO4		
Pb	3	32
Ni	1	2
Co	27	42
Cr	0	0
V	10	15
Hg		
Ag		
Nb		

LUCK STRIKE ORE HORIZON SEQUENCE - PYRITIC SILTSTONE

MAJOR ELEMENTS (WT%)

SAMPLE	02020150	02020175	07921080	07921093	07921100
SiO2	61.60	53.90	68.40	64.60	62.06
TiO2	.30	.28	.41	.49	.44
Al2O3	11.45	11.05	13.68	16.44	15.69
Fe2O3	2.46	2.37	4.22	3.94	2.90
MnO	.28	.33	.09	.08	.07
MgO	15.11	20.51	1.42	1.19	1.61
CaO	.28	1.86	1.23	2.60	2.73
Na2O	.06	.06	2.65	3.30	2.65
K2O	.74	.05	3.32	3.16	2.38
LOI	7.40	10.10	3.00	3.50	3.50
TOTAL	99.68	100.51	98.42	99.30	93.97

TRACE ELEMENTS (PPM)

	02020150	02020175	07921080	07921093	07921100
Zr	131	109	128	126	148
Sr	0	0	176	280	302
Rb	21	2	44	40	43
Zn	320	480	2900	345	1060
Cu	6	7	46	36	32
Ba	511	146	2013	2670	2209
CuS	2	1	40	32	35
PbS	26	35	530	56	530
ZnS	33	102	1070	410	2900
BaSO4	0				
Pb	48	132	580	46	171
Ni	2	2	5	6	4
Co	3	3	8	9	6
Cr	25	24	27	28	29
V	33	22	38	54	73
Hg	20	30	73	59	106
Ag	8	9	5	0	5
Nb					

LUCK STRIKE ORE HORIZON SEQUENCE - PYRITIC SILTSTONE

MAJOR ELEMENTS (WT%)

SAMPLE	07921117	07921140	07921190	07921240	07921300
SiO2	68.40	70.50	69.00	63.50	62.70
TiO2	.48	.18	.20	.20	.20
Al2O3	14.67	12.81	12.15	12.78	12.36
Fe2O3	2.92	2.10	4.13	4.00	5.67
MnO	.07	.08	.10	.22	.09
MgO	.97	.56	.67	.79	1.49
CaO	1.95	1.72	2.43	2.44	2.33
Na2O	4.24	2.16	3.74	2.67	2.51
K2O	1.64	3.31	1.32	3.11	2.79
LOI	2.00	3.10	2.50	2.80	4.20
TOTAL	97.34	96.82	96.24	92.51	94.34

TRACE ELEMENTS (PPM)

Zr	109	93	115	97	102
Sr	308	243	280	209	158
Rb	29	42	22	38	36
Zn	53	270	123	57	111
Cu	8	15	11	17	29
Ba	2111	6904	833	1586	1298
CuS	6	11	5	11	18
PbS	47	207	68	42	45
ZnS	28	510	107	69	78
BaSO4		3900			
Pb	29	128	44	25	33
Ni	3	4	4	4	8
Co	4	6	7	7	9
Cr	39	22	28	28	37
V	82	47	41	30	62
Hg	16	432	41	31	55
Ag	0	13	11	5	5
Nb					

LUCK STRIKE ORE HORIZON SEQUENCE - PYRITIC SILTSTONE

MAJOR ELEMENTS (WT%)

SAMPLE	07921360	07921400	08692550	08692590	14930950
SiO2	62.50	64.30	70.50	67.50	65.40
TiO2	.34	.32	.36	.41	.44
Al2O3	13.45	13.32	15.33	13.56	15.30
Fe2O3	4.68	4.29	3.47	4.78	4.30
MnO	.10	.12	.02	.04	.07
MgO	1.90	2.30	.83	1.86	1.21
CaO	2.37	3.46	.50	2.43	3.26
Na2O	2.55	2.38	1.86	4.00	4.60
K2O	2.30	2.25	3.93	1.24	1.64
LOI	4.30	5.40	3.70	3.80	3.80
TOTAL	94.49	98.14	100.50	99.62	100.02

TRACE ELEMENTS (PPM)

Zr	98	97	140	176	175
Sr	231	257	0	293	380
Rb	35	33	63	21	31
Zn	78	98	122	135	49
Cu	31	36	28	27	7
Ba	1943	4467	936	622	1375
CuS	11	35	34	23	3
PbS	41	6	56	124	27
ZnS	41	124	55	58	38
BaSO4					62
Pb	26	35	69	110	10
Ni	4	5	7	9	4
Co	7	7	2	2	5
Cr	28	34	17	17	28
V	68	65	81	60	49
Hg	45	51	28	27	33
Ag	3	3	5	3	0
Nb					

LUCK STRIKE ORE HORIZON SEQUENCE - PYRITIC SILTSTONE

MAJOR ELEMENTS (WT%)

SAMPLE	14930962	27040006	27040950
SiO2	68.00	66.60	67.80
TiO2	.40	.46	.38
Al2O3	13.46	13.66	13.36
Fe2O3	4.33	4.00	5.08
MnO	.06	.06	.13
M3O	.88	.84	?30
CaO	2.54	1.98	2.00
Na2O	4.10	3.35	4.92
K2O	1.41	2.95	1.07
LOI	3.00	2.80	2.30
TOTAL	98.18	96.70	97.84

TRACE ELEMENTS (PPM)

Zr	177	155	152
Sr	304	238	281
Rb	32	55	23
Zn	109	115	125
Cu	12	12	12
Ba	71	1766	1097
CuS	8	3	2
PbS	84	31	33
ZnS	105	96	64
BaSO4			
Pb	42	19	42
Ni	5	5	4
Co	6	21	7
Cr	36	28	30
V	71	52	39
Hg	56	46	58
Ag	2	0	0
Nb			

LUCK STRIKE ORE HORIZON SEQUENCE - FOOTWALL DACITIC TUFFS

MAJOR ELEMENTS (WT%)

SAMPLE	02020100	02020110	02020122	19170000	19170025
SiO2	77.90	68.70	74.40	74.30	72.30
TiO2	.13	.23	.15	.29	.31
Al2O3	9.60	16.44	11.93	11.32	13.28
Fe2O3	1.76	1.78	1.60	2.45	3.26
MnO	.08	.05	.07	.10	.12
MgO	4.10	3.51	2.31	.42	.53
CaO	.97	.68	1.59	1.56	1.05
Na2O	.64	.91	.75	4.35	5.56
K2O	1.14	3.67	2.74	1.53	1.99
LOI	4.10	4.80	4.20	1.10	.60
TOTAL	100.42	100.69	99.74	97.42	99.00

TRACE ELEMENTS (PPM)

Zr	44	107	51	113	132
Sr	43	66	0	16	93
Rb	28	77	53	24	32
Zn	650	1060	460	37	37
Cu	5	12	4	5	1
Ba	984	2009	1831	1397	1154
CuS	1	1	1	2	0
PbS	36	55	50	60	15
ZnS	62	67	137	14	22
BaSO4					6
Pb	76	163	100	29	7
Ni	1	1	1	2	3
Co	1	4	2	2	3
Cr	22	28	20	24	26
V	8	20	6	17	29
Hg	20	31	34	16	18
Ag	5	10	7	0	0
Nb					

LUCK STRIKE ORE HORIZON SEQUENCE - FOOTWALL DACITIC TUFFS

MAJOR ELEMENTS (WT%)

SAMPLE	19170050	27040050	27040225	27040275	27040525
SiO2	73.10	75.70	67.80	64.90	72.30
TiO2	.26	.26	.27	.20	.23
Al2O3	11.60	11.63	14.05	13.36	13.36
Fe2O3	2.72	2.21	2.42	2.69	2.06
MnO	.08	.05	.06	.09	.08
MgO	.42	.19	1.82	2.41	1.07
CaO	1.29	.63	2.52	4.95	3.04
Na2O	4.84	5.02	2.06	.86	1.93
K2O	2.00	1.56	2.83	2.76	.68
LOI	1.00	.50	4.10	7.00	3.90
TOTAL	97.23	97.75	97.93	99.22	98.65

TRACE ELEMENTS (PPM)

Zr	113	144	120	113	114
Sr	116	84	183	249	101
Rb	33	29	72	70	95
Zn	66	34	21	40	30
Cu	3	1	2	8	3
Ba	1862	885	1820	3454	733
CuS	1	0	1	8	2
PbS	19	12	17	131	38
ZnS	27	8	10	13	7
BaSO4		6		500	
Pb	10	7	7	68	17
Ni	1	2	3	3	3
Co	3	8	23	2	4
Cr	25	25	25	20	21
V	20	0	31	44	37
Hg	20	8	8	12	18
Ag	0	0	0	1	0
Nb					

LUCK STRIKE ORE HORIZON SEQUENCE - FOOTWALL DACITIC TUFFS

MAJOR ELEMENTS (WT%)

SAMPLE	27040575	27040650	27040725	27040800	27040875
SiO2	71.60	72.90	70.80	69.70	73.50
TiO2	.20	.20	.24	.23	.24
Al2O3	11.75	11.26	13.74	13.62	13.28
Fe2O3	2.26	2.40	2.82	2.90	2.53
MnO	.13	.11	.13	.12	.10
MgO	.86	1.12	1.04	1.84	1.38
CaO	2.36	2.45	2.09	1.42	1.50
Na2O	4.84	2.53	2.74	2.47	3.35
K2O	3.58	2.43	3.07	3.54	1.89
LOI	2.30	2.80	1.60	2.20	2.00
TOTAL	99.80	98.20	98.27	98.04	99.77

TRACE ELEMENTS (PPM)

	27040575	27040650	27040725	27040800	27040875
Zr	118	86	129	115	93
Sr	407	224	290	193	222
Rb	19	57	77	87	48
Zn	29	30	21	28	22
Cu	9	5	1	8	6
Ba	600	896	1568	1938	891
CuS	5	2	1	3	4
PbS	21	31	9	8	8
ZnS	10	12	3	19	12
BaSO4		10			2
Pb	14	19	11	4	11
Ni	5	4	2	3	3
Co	4	4	3	3	2
Cr	32	25	23	24	22
V	32	32	8	33	34
Hg	16	14	12	12	12
Ag	0	0	0	0	0
Nb					

LUCK STRIKE ORE HORIZON SEQUENCE - DACITIC TUFFS IN PROXIMITY TO ORE

MAJOR ELEMENTS (WT%)

SAMPLE	JGT75 44	01750025	01750125	02020070	02020075
SiO2	70.30	58.00	63.50	65.60	76.80
TiO2	.44	.34	.25	.24	.18
Al2O3	14.66	20.28	17.15	18.38	10.58
Fe2O3	2.76	3.18	2.92	1.00	1.66
MnO	.09	.07	.06	.03	.06
MgO	1.92	3.14	2.73	2.50	3.92
CaO	2.55	1.42	1.79	1.05	.68
Na2O	1.67	1.93	1.18	1.31	.73
K2O	2.05	5.51	5.11	3.84	1.47
LOI	3.00	5.30	4.00	5.50	4.10
TOTAL	99.44	99.17	98.69	99.45	100.10

TRACE ELEMENTS (PPM)

	JGT75 44	01750025	01750125	02020070	02020075
Zr	236	164	130	71	41
Sr	429	136	279	297	34
Rb	71	130	131	21	33
Zn	161	53	111	620	730
Cu	3	5	11	38	6
Ba	2476	1823	1341	1049	1132
CuS	2	0	1	9	1
PbS	17	31	24	86	19
ZnS	78	7	31	131	48
BaSO4	6	2	3	18	
Pb	18	25	27	410	56
Ni	3	2	2	1	2
Co	18	2	3	3	2
Cr	10	19	19	211	20
V	35	17	4	22	16
Hg		15	23	27	19
Ag		0	2	11	6
Nb	6				

LUCK STRIKE ORE HORIZON SEQUENCE - DACITIC TUFFS IN PROXIMITY TO ORE

MAJOR ELEMENTS (WT%)

SAMPLE	02020092	08692465	14930825	14930843	14930855
SiO2	67.80	78.00	73.30	70.60	62.10
TiO2	.16	.16	.17	.20	.44
Al2O3	14.46	10.13	13.51	14.61	17.35
Fe2O3	2.69	.84	1.45	1.86	5.37
MnO	.11	.03	.06	.08	.08
MgO	5.18	.68	.92	1.72	2.65
CaO	1.51	1.65	2.37	2.31	2.52
Na2O	.95	4.89	2.92	1.81	2.52
K2O	2.08	.31	2.13	2.50	2.70
LOI	5.60	1.80	2.20	2.50	3.00
TOTAL	100.54	98.49	99.03	98.19	98.73

TRACE ELEMENTS (PPM)

Zr	7	138	132	151	153
Sr	150	286	460	442	293
Rb	43	1	70	71	64
Zn	540	38	99	43	2600
Cu	6	4	10	4	16
Ba	2434	3040	3602	6614	2630
CuS	2	1	3	1	15
PbS	44	25	39	98	155
ZnS	60	11	5	10	1690
BaSO4	7		9	12	
Pb	100	16	50	61	91
Ni	2	2	2	2	4
Co	3	2	2	3	6
Cr	21	9	21	25	43
V	6	18	6	0	103
Hg	17	4	12	16	24
Ag	14	2	3	3	2
Nb					

LUCK STRIKE ORE HORIZON SEQUENCE - DACITIC TUFFS IN PROXIMITY TO ORE

MAJOR ELEMENTS (WT%)

SAMPLE	14930929	19170075	1917 118
SiO2	66.30	79.70	68.00
TiO2	.40	.36	.24
Al2O3	14.78	13.52	15.76
Fe2O3	3.54	3.56	2.09
MnO	.07	.11	.06
MgO	3.00	1.54	1.84
CaO	3.41	2.75	2.27
Na2O	1.61	4.39	1.67
K2O	2.87	1.34	3.70
LOI	5.20	1.30	3.50
TOTAL	101.18	99.57	99.13

TRACE ELEMENTS (PPM)

Zr	163	162	116
Sr	156	456	255
Rb	62	23	104
Zn	92	205	27
Cu	12	11	2
Ba	1434	1839	1580
CuS	7	4	1
PbS	132	87	8
ZnS	52	122	14
BaSO4			
Pb	78	59	6
Ni	5	10	2
Co	5	6	1
Cr	28	37	21
V	41	64	7
Hg	33	18	12
Ag	2	0	1
Nb			

ORIENTAL ORE HORIZON SEQUENCE - GRANITE BOULDERS

MAJOR ELEMENTS (WT%)

SAMPLE	1147 118	1202 104	1217 192	1261 230	1273 232
SiO2	72.30	71.00	70.50	73.70	76.30
TiO2	.24	.24	.30	.52	.20
Al2O3	13.04	13.22	12.62	12.45	10.92
Fe2O3	2.39	2.11	1.64	1.98	.13
MnO	.08	.05	.05	.08	0.00
MgO	1.25	.84	1.04	1.24	.18
CaO	1.23	1.86	1.90	.96	.42
Na2O	4.16	4.15	3.33	4.90	3.57
K2O	1.20	2.45	2.15	.53	1.36
LOI	2.20	1.60	2.70	1.80	2.40
TOTAL	98.09	97.52	96.23	98.16	95.48

TRACE ELEMENTS (PPM)

Zr	116	85	121	148	116
Sr	173	239	213	140	96
Rb	15	27	30	7	10
Zn	73	38	47	890	3200
Cu	3	12	4	83	200
Ba	909	1990	1551	958	3384
CuS	4	15	4	79	187
PbS	13	16	18	570	2800
ZnS	15	21	11	590	2300
BaSO4	104	0	86	440	3400
Pb	5	4	15	680	2150
Ni	7	4	4	3	3
Co	40	38	37	32	28
Cr	10	9	8	11	10
V	10	10	10	30	10
Hg					
Ag					
Nb	7	6	4	8	0

LUCK STRIKE ORE HORIZON SEQUENCE - ORE HORIZON BARREN BRECCIA

MAJOR ELEMENTS (WT%)

SAMPLE	07921050	07921065	19170092	19170100
SiO2	58.40	61.20	63.20	63.80
TiO2	.20	.50	.20	.21
Al2O3	13.51	14.63	11.53	11.78
Fe2O3	6.18	5.07	2.54	2.70
MnO	.14	.11	.07	.08
MgO	2.01	2.07	1.71	1.75
CaO	2.96	1.33	2.40	2.40
Na2O	2.63	3.15	1.80	1.87
K2O	2.36	2.51	2.12	2.21
LOI	6.10	4.40	6.10	6.10
TOTAL	94.49	94.97	91.67	92.90

TRACE ELEMENTS (PPM)

Zr	82	108	139	135
Sr	368	632	731	772
Rb	36	33	47	45
Zn	2700	1420	540	630
Cu	1490	480	280	134
Ba	9999	9999	999	999
CuS	1570	495	340	113
PbS	1550	490	450	530
ZnS	2800	1055	830	1040
BaSO4	999		999	
Pb	1010	270	670	285
Ni	5	5	6	5
Co	10	7	3	4
Cr	37	32	31	30
V	84	94	53	28
Hg	149	45	105	98
Ag	108	25	20	57
Nb				

LUCKY STRIKE AREA TRANSPORTED ORE

MAJOR ELEMENTS (WT%)

SAMPLE	02020025	2020050	07921075	08692480	08692528
SiO_2	1.20	1.20	1.90	20.30	25.50
TiO_2	0.00	0.00	.01	.19	.48
Al_2O_3	.36	.34	.31	5.98	8.21
Fe_2O_3	4.35	2.14	11.16	3.94	7.41
MnO	.03	.02	.03	.08	.18
MgO	.20	.33	.04	2.50	4.09
CaO	2.60	1.49	.03	1.42	4.71
Na_2O	0.00	0.00	0.00	.39	1.46
K_2O	.07	0.00	.05	1.04	.40
LOI	5.80	4.20	14.90	5.90	8.10
TOTAL	14.61	9.72	28.43	41.74	60.54

TRACE ELEMENTS (PPM)

Zr	154	203	75	218	94
Sr	1190	1527	74	1000	185
Rb	27	23	40	15	35
Zn					
Cu	132	61	295	57	155
Ba	0	0	3	500	1
CuS	6000	3050	2900	4800	1600
PbS	41	37	78	24	64
ZnS	180	245	12	46	9
$BaSO_4$	1	1	2501	120	952
Pb	9000	2300	8000	9200	6900
Ni	3	5	9	12	53
Co	2	2	3	2	2
Cr	29	28	61	0	109
V	16	20	15	98	129
Hg	2455	2820	1545	3222	1967
Ag	970	820	1100	820	410
Nb					

LUCKY STRIKE AREA TRANSPORTED ORE

MAJOR ELEMENTS (WT%)

SAMPLE, 14930848

SiO2	18.90
TiO2	.12
Al2O3	3.94
Fe2O3	5.47
MnO	.05
MgO	.44
CaO	.53
Na2O	.88
K2O	.46
LOI	11.20

TOTAL	41.99

TRACE ELEMENTS (PPM)

Zr	131
Sr	589
Rb	40
Zn	
Cu	107
Ba	0
CuS	9500
PbS	84
ZnS	96
BaSO4	4572
Pb	2500
Ni	5
Co	3
Cr	33
V	33
Hg	3466
Ag	1360
Nb	

LUCKY STRIKE ORE HORIZON SEQUENCE - CLEMENTINE DACITIC TUFFS

MAJOR ELEMENTS (WT%)

SAMPLE	1258 443	2866 325	2869 938	2879 437	2882 298
SiO_2	71.20	68.40	77.60	68.00	73.10
TiO_2	.23	.25	.16	.18	.19
Al_2O_3	12.41	15.00	11.80	14.88	12.87
Fe_2O_3	2.03	1.56	1.35	2.68	1.85
MnO	.06	.07	.04	.07	.05
MgO	.67	1.59	.44	2.14	2.41
CaO	3.20	1.85	1.70	1.21	.89
Na_2O	2.75	.67	1.50	.73	.43
K_2O	2.20	4.56	2.49	4.24	3.10
LOI	4.10	4.50	3.10	3.80	4.10
TOTAL	98.85	98.45	100.18	97.93	98.99

TRACE ELEMENTS (PPM)

Zr	129	14	123	149	135
Sr	235	80	64	129	66
Rb	54	157	70	154	90
Zn	34	28	8	14	20
Cu	1	1	1	1	1
Ba	2022	950	330	783	1431
CuS	1	1	1	1	1
PbS	34	24	15	57	21
ZnS	9	6	1	6	4
BaSO4					
Pb	26	10	3	61	6
Ni	5	2	2	2	5
Co	11	12	38	11	18
Cr	1	3	0	3	2
V	20	10	10	10	15
Hg					
Ag					
Nb					

LUCKY STRIKE ORE HORIZON SEQUENCE – CLEMENTINE DACITIC TUFFS

MAJOR ELEMENTS (WT%)

SAMPLE	2884 908	28851555	28861325	28861353	28971504
SiO2	75.60	71.80	61.30	71.50	71.90
TiO2	.25	.27	.47	.35	.20
Al2O3	12.06	13.35	17.03	12.91	13.12
Fe2O3	1.74	2.14	4.74	2.25	2.22
MnO	.03	.03	.11	.07	.08
MgO	.19	.83	2.99	1.61	.82
CaO	.44	2.60	2.07	2.00	2.61
Na2O	4.36	1.86	1.92	.75	1.82
K2O	3.54	2.98	4.12	3.79	3.23
LOI	.30	3.90	5.10	4.40	4.00
TOTAL	98.51	99.76	99.85	99.63	100.00

TRACE ELEMENTS (PPM)

Zr	146	166	163	132	135
Sr	57	214	139	62	171
Rb	61	126	169	131	87
Zn	11	27	69	28	25
Cu	3	1	1	1	4
Fe	788	791	752	1031	1055
CuS	4	1	1	1	5
PbS	21	25	25	25	26
ZnS	5	8	17	27	5
BaSO4					
Pb	6	1	21	25	11
Ni	3	4	7	2	5
Co	34	11	8	12	22
Cr	3	3	10	1	2
V	25	10	10	15	15
Hg					
Ag					
Nb					

LUCKY STRIKE ORE HORIZON SEQUENCE - CLEMENTINE DACITIC TUFFS

MAJOR ELEMENTS (WT%)

SAMPLE	2899 909	29001165	2901 753
SiO_2	73.50	75.50	71.80
TiO_2	.25	.10	.16
Al_2O_3	12.42	11.44	12.93
Fe_2O_3	2.06	1.57	1.70
MnO	.05	.06	.05
MgO	.48	.83	.61
CaO	1.78	2.33	2.93
Na_2O	2.23	1.80	2.04
K_2O	2.24	2.30	2.76
LOI	3.50	3.60	3.80
TOTAL	98.51	99.53	98.78

TRACE ELEMENTS (PPM)

Zr	134	125	138
Sr	91	161	105
Rb	43	59	81
Zn	21	24	17
Cu	1	1	1
Ba	431	768	1766
CuS	1	1	1
PbS	19	15	5
ZnS	2	5	4
BaSO4			
Pb	1	7	1
Ni	4	4	4
Co	41	19	14
Cr	4	0	0
V	20	20	10
Hg			
Ag			
Nb			

ORIENTAL ORE HORIZON SEQUENCE - DACITIC TUFFS

MAJOR ELEMENTS (WT%)

SAMPLE	1096 300	1475 1	1589 736	16061216	17301310
SiO2	60.90	68.60	68.90	67.80	67.80
TiO2	.36	.45	.43	.50	.40
Al203	17.36	15.24	15.24	14.03	14.03
Fe203	4.61	2.07	2.63	3.44	3.28
MnO	.08	.04	.04	.10	.07
MgO	4.42	2.79	2.20	1.51	1.78
CaO	2.27	2.75	1.74	2.51	2.72
Na20	1.65	2.29	1.01	2.62	1.81
K20	2.36	1.47	3.21	2.42	3.59
LOI	5.00	2.90	4.30	3.60	4.10
TOTAL	99.01	98.60	99.70	98.53	99.58

TRACE ELEMENTS (PPM)

Zr	193	186	196	150	168
Sr	271	424	226	243	149
Rb	56	32	75	56	87
Zn	171	206	55	690	64
Cu	13	1	1	120	2
Ba	2395	865	174	1934	1215
CuS	16	1	1	182	5
PbS	56	24	21	330	42
ZnS	82	111	24	710	37
BaSO4					
Pb	59	24	10	190	42
Ni	8	4	4	7	3
Co	15	12	6	20	13
Cr	16	20	3	17	10
V	45	20	15	35	20
Hg					
Ag					
Rb					

ORIENTAL ORE HORIZON SEQUENCE - DACITIC TUFFS

MAJOR ELEMENTS (WT%)

SAMPLE	1872 166	1872 223	1872 317	1872 393	1872 440
SiO2	69.90	70.20	64.10	66.10	66.80
TiO2	.11	.28	.21	.39	.22
Al2O3	15.06	15.93	17.36	16.62	15.79
Fe2O3	2.01	1.84	2.49	1.90	2.09
MnO	.09	.08	.06	.06	.07
MgO	1.89	1.43	2.52	2.88	3.41
CaO	1.44	1.78	1.35	1.89	1.67
Na2O	2.10	3.63	.92	1.69	1.65
K2O	3.44	2.60	4.56	2.92	2.54
LOI	3.00	2.30	5.10	4.10	4.30
TOTAL	99.04	100.07	98.67	98.55	98.54

TRACE ELEMENTS (PPM)

Zr	135	147	151	149	144
Sr	247	243	138	225	237
Rb	111	76	152	98	85
Zn	118	44	42	22	40
Cu	1	1	1	1	1
Ba	845	944	1495	1194	1295
CuS	1	1	1	1	1
PbS	24	13	19	13	11
ZnS	6	4	2	4	5
BaSO4					
Pb	10	6	8	11	12
Ni	2	2	1	3	3
Co	19	15	12	18	19
Cr	1	1	3	1	2
V	10	10	10	10	10
Hg					
Ag					
Nb					

ORIENTAL ORE HORIZON SEQUENCE - DACITIC TUFFS

MAJOR ELEMENTS (WT%)

SAMPLE	1872 465	1872 506	1872 649	2367 192	2367 273
SiO2	65.90	65.10	49.70	65.30	74.00
TiO2	.20	.33	.50	.30	.27
Al2O3	16.00	17.36	17.86	16.93	13.74
Fe2O3	2.32	1.86	.92	2.13	1.55
MnO	.08	.10	.12	.05	.06
MgO	3.94	3.31	2.34	2.99	.90
CaO	1.74	2.37	6.19	1.93	1.65
Na2O	1.37	1.48	1.66	1.15	4.30
K2O	2.43	2.75	5.10	2.65	1.28
LOI	4.50	4.50	10.10	5.20	1.30
TOTAL	98.48	99.16	94.49	98.63	99.05

TRACE ELEMENTS (PPM)

	1872 465	1872 506	1872 649	2367 192	2367 273
Zr	144	157	202	149	132
Sr	230	289	216	198	317
Rb	79	75	106	110	53
Zn	27	25	1910	31	19
Cu	1	1	161	1	1
Ba	1437	3876	4257	1473	1507
CuS	1	1	180	1	2
PbS	20	32	1220	17	5
ZnS	3	5	1950	11	1
BaSO4					
Pb	13	28	560	19	9
Ni	4	3	10	5	2
Co	10	4	7	6	19
Cr	2	2	17	3	3
V	10	15	20	20	20
Hg					
Ag					
Nb					

ORIENTAL ORE HORIZON SEQUENCE - DACITIC TUFFS

MAJOR ELEMENTS (WT%)

SAMPLE	2367 394	2367 412	2837 800	2837 900	28371050
SiO2	68.90	68.20	65.60	77.80	70.30
TiO2	.29	.21	.40	.20	.28
A1203	15.47	15.94	15.26	11.97	14.36
Fe203	1.62	1.92	4.08	1.59	2.32
MnO	.04	.03	.07	.03	.03
MgO	4.03	4.55	2.69	1.43	2.15
CaO	1.31	1.24	1.66	.54	1.14
Na20	1.70	1.66	2.42	4.30	2.78
K20	1.29	1.22	2.07	1.26	2.68
LOI	4.80	4.90	3.50	1.20	2.40
TOTAL	99.45	99.87	97.75	100.32	98.44

TRACE ELEMENTS (PPM)

	2367 394	2367 412	2837 800	2837 900	28371050
Zr	160	162	163	189	132
Sr	251	262	307	234	306
Rb	43	41	91	59	90
Zn	33	39	77	28	26
Cu	1	2	1	1	1
Ba	242	919	767	745	1015
CuS	1	1	1	1	2
FeS	27	11	10	10	15
ZnS	1	2	11	8	9
BaSO4			0	0	0
Pb	21	12	15	3	12
Ni	4	3	4	2	2
Co	13	12	18	47	24
Cr	2	2	19	30	41
V	20	10	10	10	10
Hg					
Ag					
Sb			0	0	2

ORIENTAL ORE HORIZON SEQUENCE - DACITIC TUFFS

MAJOR ELEMENTS (WT%)

SAMPLE	2839 529	2839 657	28391586	2853 672	2854 708
SiO2	72.40	72.60	70.80	57.40	63.50
TiO2	.24	.22	.19	.47	.41
Al2O3	13.71	13.57	14.59	18.14	16.00
Fe2O3	2.15	1.97	2.31	6.21	5.34
MnO	.03	.03	.03	.10	.06
MgO	2.04	2.05	1.25	3.22	2.33
CaO	1.48	1.14	1.14	3.36	3.59
Na2O	2.88	2.76	3.70	1.56	1.79
K2O	2.48	2.72	3.47	4.12	2.36
LOI	1.90	2.20	1.50	4.40	3.40
TOTAL	99.31	99.26	98.98	98.98	98.78

TRACE ELEMENTS (PPM)

Zr	111	113	120	283	11
Sr	246	218	185	272	347
Rb	76	82	96	161	67
Zn	23	16	28	42	52
Cu	1	1	1	11	1
Ba	1145	1339	104	43	9
CuS	2	1	1	14	1
PbS	7	11	10	20	16
ZnS	3	2	25	25	9
BaSO4					
Pb	11	8	4	13	10
Ni	5	2	2	5	6
Co	26	27	17	11	15
Cr	2	2	5	13	11
V	15	10	10	20	10
Hg					
Ag					
Nb					

ORIENTAL ORE HORIZON SEQUENCE - DACITIC TUFFS

MAJOR ELEMENTS (WTZ)

SAMPLE   2859 304

SiO2	62.00
TiO2	.41
Al2O3	16.97
Fe2O3	4.39
MnO	.10
MgO	2.40
CaO	2.76
Na2O	1.66
K2O	3.60
LOI	5.50

TOTAL   99.79

TRACE ELEMENTS (PPM)

Zr	193
Sr	236
Rb	119
Zn	330
Cu	1
Ba	943
CuS	1
PbS	27
ZnS	67
BaSO4	
Pb	19
Ni	5
Co	11
Cr	10
V	10
Hg	
Ag	
Nb	

LAKE SEVEN BASALT

MAJOR ELEMENTS (WT%)

SAMPLE   23491540

SiO2	50.10
TiO2	.52
Al2O3	13.67
Fe2O3	9.38
MnO	.22
MgO	8.65
CaO	9.87
Na2O	2.70
K2O	.50
LOI	3.70

TOTAL   99.31

TRACE ELEMENTS (PPM)

Zr	65
Sr	395
Rb	9
Zn	61
Cu	90
Ba	369
CuS	140
PbS	16
ZnS	21
BaSO4	
Pb	14
Ni	53
Co	25
Cr	130
V	145
Hg	
Ag	
Nb	

LAKE SEVEN BASALT ALTERED FLOWS

MAJOR ELEMENTS (WT%)

SAMPLE   932 367

SiO2	43.90
TiO2	.80
Al2O3	15.40
Fe2O3	10.00
MnO	.19
MgO	7.72
CaO	12.00
Na2O	2.50
K2O	.63
LOI	6.10

TOTAL	99.24

TRACE ELEMENTS (PPM)

Zr	101
Sr	425
Rb	9
Zn	55
Cu	64
Ba	208
CuS	72
PbS	7
ZnS	15
BaSO4	
Pb	10
Ni	39
Co	24
Cr	87
V	140
Hg	
Ag	
Nb	

SANDY LAKE BASALT FLOWS

MAJOR ELEMENTS (WT%)

SAMPLE	1352 477	2839 494
SiO_2	45.60	49.80
TiO_2	.86	.60
Al_2O_3	14.99	14.70
Fe_2O_3	10.05	8.51
MnO	.19	.31
MgO	7.45	6.72
CaO	11.40	8.76
Na_2O	2.23	2.93
K_2O	.53	1.39
LOI	5.20	5.10
TOTAL	98.50	98.82

TRACE ELEMENTS (PPM)

Zr	102	.68
Sr	36	334
Rb	9	29
Zn	55	48
Cu	53	62
Ba	539	2294
CuS	76	65
PbS	15	22
ZnS	22	5
BaSO4		
Pb	21	21
Ni	102	114
Co	27	36
Cr	379	429
V	135	163
Hg		
Ag		
Pb		

UPPER BUCHANS SUBGROUP - MAFIC TUFFS

MAJOR ELEMENTS (WT%)

SAMPLE	2837 125	2837 200	2837 350	2837 438	2837 550
SiO2	52.20	53.60	49.50	70.00	74.10
TiO2	.45	.53	.57	.36	.27
Al2O3	17.48	16.04	17.88	13.25	13.11
Fe2O3	8.54	9.35	10.90	3.66	2.63
MnO	.16	.15	.17	.08	.09
MgO	3.10	2.38	3.01	1.69	1.48
CaO	4.47	4.54	3.69	2.87	1.42
Na2O	4.55	4.30	4.91	3.57	2.07
K2O	1.01	.91	.05	1.39	1.76
LOI	6.00	5.60	6.20	3.40	3.20
TOTAL	97.96	97.90	96.88	100.27	99.93

TRACE ELEMENTS (PPM)

	2837 125	2837 200	2837 350	2837 438	2837 550
Zr	56	54	78	169	143
Sr	142	115	101	135	89
Rb	20	38	13	36	38
Zn	68	77	129	45	57
Cu	65	153	31	8	5
Ba	74	78	12	337	216
CuS	70	108	35	10	8
PbS	10	10	13	13	20
ZnS	13	15	17	7	9
BaSO4	0	0	0	0	0
Pb	22	15	25	11	21
Ni	17	11	18	5	2
Co	27	27	33	18	24
Cr	61	30	39	15	15
V	150	150	250	10	10
Hg					
As					
Sb	3	3	3	0	3

UPPER BUCHANS SUBGROUP - MAFIC TUFFS

MAJOR ELEMENTS (WT%)

SAMPLE   2837 725

SiO2	69.90
TiO2	.37
Al2O3	14.84
Fe2O3	3.88
MnO	.08
MgO	1.96
CaO	.53
Na2O	3.80
K2O	1.42
LOI	2.20

TOTAL   98.98

TRACE ELEMENTS (PPM)

Zr	143
Sr	142
Rb	50
Zn	88
Cu	1
Ba	228
CuS	1
PbS	6
ZnS	11
BaSO4	0
Pb	12
Ni	1
Co	20
Cr	11
V	10
Hg	
Ag	
Sb	3

UPPER BUCHANS SUBGROUP - RHYOLITE FLOWS

MAJOR ELEMENTS (WT%)

SAMPLE	BJ-9-80	BJ-10-46	BJ42 A47	BJ42 980	BJ421470
SiO_2	71.50	72.00	72.50	76.10	69.70
TiO_2	.51	.44	.24	.04	.26
$Al2O3$	13.96	13.15	13.21	11.82	13.64
$Fe2O3$	3.16	3.39	2.83	1.21	3.72
MnO	.11	.11	.13	.04	.23
MgO	1.74	1.51	.97	.93	1.51
CaO	.89	1.12	1.66	.47	1.59
Na2O	4.23	4.08	2.95	3.63	4.33
K2O	1.90	1.84	2.76	3.29	1.51
LOI	1.70	1.40	2.80	1.40	2.70
TOTAL	99.70	99.04	100.05	98.93	99.19

TRACE ELEMENTS (PPM)

	BJ-9-80	BJ-10-46	BJ42 A47	BJ42 980	BJ421470
Zr	174	183	120	111	107
Sr	151	199	92	110	51
Rb	36	28	83	67	35
Zn	126	52	65	18	170
Cu	3	1	18	10	1
Ba	1033	739	618	970	747
CuS	3	1	19	0	0
PbS	320	44	9	11	8
ZnS	30	15	12	1	21
FeSO4	0	0	0	0	0
Pb	350	16	11	2	9
Ni	2	5	4	-3	2
Co	29	16	12	16	19
Cr	12	11	10	10	13
V	10	10	10	10	10
Mg					
Ag					
Nb	3	9	9	5	9

UPPER BUCHANS SUBGROUP - RHYOLITE FLOWS

MAJOR ELEMENTS (WT%)

SAMPLE	BJ421658	BJ45 117	BJ46 100
SiO2	77.30	69.90	67.20
TiO2	.10	.15	.18
Al2O3	11.82	14.48	12.20
Fe2O3	1.18	1.28	2.37
MnO	.03	.08	.05
MgO	.83	1.52	2.44
CaO	.58	1.35	.32
Na2O	3.77	2.66	.80
K2O	1.72	2.68	2.86
LOI	1.70	4.10	5.20
TOTAL	99.03	98.25	93.42

TRACE ELEMENTS (PPM)

Zr	111	103	103
Sr	112	37	9
Rb	46	50	53
Zn	27	27	31
Cu	1	8	5
Ba	1023	484	795
CuS	3	11	6
FeS	11	21	15
ZnS	1	18	4
BaSO4	0		
Pb	22	25	18
Ni	1	3	4
Co	15	21	18
Cr	9	3	11
V	10	10	10
Hg			
Ag			
Cb	9		

UPPER BUCHANS SUBGROUP – DACITIC TUFFS

MAJOR ELEMENTS (WT%)

SAMPLE	1568 640	16061070	17821036	19201726	2842 762
SiO2	61.80	70.20	66.00	72.60	68.90
TiO2	.43	.33	.28	.10	.32
Al2O3	17.38	13.60	15.64	12.00	13.05
Fe2O3	4.14	2.89	4.64	2.01	4.88
MnO	.07	.07	.06	.04	.15
MgO	2.88	1.47	1.53	.99	2.24
CaO	2.11	2.14	1.68	1.72	1.19
Na2O	1.75	3.80	2.82	2.14	2.82
K2O	3.37	1.46	2.43	2.65	1.60
LOI	4.00	2.50	3.80	3.40	3.70
TOTAL	97.93	78.46	78.88	97.65	78.90

TRACE ELEMENTS (PPM)

Zr	281	167	144	77	112
Sr	283	360	101	68	56
Rb	112	33	58	58	41
Zn	62	65	78	57	61
Cu	1	17	1	200	1
Ba	1140	720	260	273	130
CuS	2	30	1	243	1
PbS	15	39	15	16	14
ZnS	18	31	33	17	11
BaSO4					
Pb	5	59	6	15	8
Ni	7	4	3	4	8
Co	11	19	23	19	15
Cr	10	6	8	0	0
V	10	20	10	10	10
Hg					
As					
Sb					

UPPER BUCHANS SUBGROUP - DACITIC TUFFS

MAJOR ELEMENTS (WT%)

SAMPLE	BJ42 685	BJ421975	BJ422228	BJ47 344	BJ48 135
SiO2	61.80	72.20	73.50	67.30	68.30
TiO2	.22	.18	.16	.45	.38
Al2O3	19.92	13.01	13.07	14.93	16.97
Fe2O3	2.26	3.19	2.98	3.75	2.02
MnO	.07	.13	.08	.07	.01
MgO	2.46	1.41	1.99	2.00	1.58
CaO	.24	.66	.39	1.04	1.19
Na2O	1.44	4.79	3.89	2.10	3.16
K2O	8.30	1.13	1.29	2.80	1.63
LOI	3.50	1.80	2.00	4.10	3.50
TOTAL	100.21	98.50	99.27	99.34	98.74

TRACE ELEMENTS (PPM)

	BJ42 685	BJ421975	BJ422228	BJ47 344	BJ48 135
Zr	148	160	137	128	130
Sr	68	108	93	45	133
Rb	216	21	34	58	39
Zn	86	90	88	52	51
Cu	1	1	1	11	1
Ba	1107	343	5	116	175
CuS	1	0	1	14	1
FbS	17	11	11	15	21
ZnS	24	12	5	6	9
BaSO4	0	0	0		
Pb	18	1	11	24	21
Ni	5	1	3	7	5
Co	7	14	15	14	14
Cr	7	10	9	5	2
V	10	10	10	15	15
Hg			A		
Ag					
Sb	11	6	8		

UPPER BUCHANS SUBGROUP - DACITIC TUFFS

MAJOR ELEMENTS (WT%)

SAMPLE	BJ49 263	1683 403	1730 602	2852 674	2855 110
SiO2	70.20	65.00	76.30	71.20	71.90
TiO2	.32	.23	.18	.32	.26
Al2O3	13.49	14.93	10.10	14.03	13.66
Fe2O3	3.73	5.80	.42	3.59	3.13
MnO	.08	.13	.02	.08	.04
MgO	1.21	2.79	.30	1.50	1.27
CaO	1.69	1.48	.64	2.24	2.08
Na2O	2.03	1.96	.19	3.68	4.49
K2O	2.28	2.14	2.94	1.85	1.27
LOI	3.70	4.20	3.70	1.70	1.40
TOTAL	98.73	98.66	94.79	100.19	99.42

TRACE ELEMENTS (PPM)

Zr	98	126	118	123	3
Sr	29	62	18	436	3
Rb	52	73	45	40	15
Zn	75	187	76	63	31
Cu	6	7	49	3	1
Ba	146	237	333	365	47
CuS	8	9	67	4	1
PbS	26	11	18	3	3
ZnS	24	29	52	14	12
FeSO4				0	0
Pb	20	17	6	21	3
Ni	4	8	4	5	1
Co	13	15	21	12	21
Cr	6	15	1	11	13
V	30	10	15	30	25
Hg					
As					
Sb				13	18

UPPER BUCHANS SUB GROUP - DACITIC TUFFS

MAJOR ELEMENTS (WT%)

SAMPLE   23551476

SiO2	69.98
TiO2	.48
Al2O3	14.99
Fe2O3	2.99
MnO	.07
MgO	1.43
CaO	2.71
Na2O	3.06
K2O	1.89
LOI	1.60

TOTAL   99.04

TRACE ELEMENTS (PPM)

Zn	115
Sr	17
Rb	52
Zn	17
Cu	2
Ni	3
CuS	3
FeS	3
ZnS	8
FeSO4	0
Pb	7
Ni	3
Co	26
Cr	16
V	45
Hg	
Ag	
Tb	13

LOW TITANIUM DAIBASE

MAJOR ELEMENTS (WT%)

SAMPLE	05421267	05421775	98691550	14970325	14930880
SiO2	45.98	39.08	54.80	48.90	48.90
TiO2	.92	.79	.68	.88	.20
Al2O3	17.49	13.46	16.08	12.90	14.95
Fe2O3	11.93	8.53	10.15	9.48	10.75
MnO	.12	.17	.15	.15	.18
MgO	6.95	4.05	5.49	7.73	9.58
CaO	4.31	14.79	8.33	13.04	7.76
Na2O	2.34	2.47	2.07	2.35	1.92
K2O	1.25	.46	1.18	1.51	.46
LOI	6.90	12.00	2.30	3.80	4.00
TOTAL	98.11	97.98	100.98	100.31	100.20

TRACE ELEMENTS (PPM)

Zr	185	32	74	94	124
Sr	354	226	391	317	235
Rb	33	9	23	25	17
Zn	93	111	80	56	50
Cu	69	78	38	77	51
Pb	0	13	10	12	13
CuS	59	29	43	45	54
PbS	2	9	7	5	17
ZnS	17	2	16	15	13
BaSO4	0	0	0	1	0
Fe	73	18	23	7	8
Ni	42	1	2	6	2
Co	59	57	47	57	43
Cr	173	240	59	203	209
V	350	278	275	392	258
Ba	18	34	13	16	8
La	1	13	2	3	0

POOR COPY
COPIE DE QUALITEE INFERIEURE

LOW TITANIUM DAIBASE

MAJOR ELEMENTS (WT%)

SAMPLE	19170290	26660780	26660975
$SiO2$	47.30	55.20	52.90
$TiO2$	.71	.85	.83
$Al2O3$	14.88	16.41	16.72
$Fe2O3$	10.48	10.48	11.06
MnO	.23	.22	.20
MgO	8.29	4.23	5.82
CaO	9.46	6.08	4.67
$Na2O$	1.93	3.27	2.89
$K2O$	.88	.41	1.60
LOI	5.90	3.60	3.90
TOTAL	1_0.06	100.55	100.59

TRACE ELEMENTS (PPM)

Zr	97	71	73
Sr	278	421	297
Rb	23	15	21
Zn	96	40	37
Cu	62	55	27
Ba	211	274	0
CuS	37	67	18
FeS	9	7	10
ZnS	29	17	19
FeSO4			
Pb	12	6	3
Ni	28	11	12
Co	33	19	23
Cr	226	43	45
V	256	512	530
Hg	12	14	10
Ag	0	0	0

POOR COPY
COPIE DE QUALITEE INFERIEURE

FEEDER GRANODIORITE

MAJOR ELEMENTS (WT%)

SAMPLE	JGT75227	JGT75228	JGT75229
SiO2	74.50	75.28	74.39
TiO2	.24	.18	.28
Al2O3	12.99	12.33	12.45
Fe2O3	2.19	1.86	2.36
MnO	.04	.03	.04
MgO	.50	.34	.52
CaO	1.42	1.49	1.32
Na2O	4.15	3.88	4.21
K2O	2.40	2.69	2.44
LOI	.70	.60	.60
TOTAL	98.83	98.58	98.52

TRACE ELEMENTS (PPM)

	JGT75227	JGT75228	JGT75229
Zr	159	97	116
Sr	127	97	123
Rb	56	56	49
Zn	30	14	21
Cu	1	2	7
Ba	521	1 13	512
CuS	1	1	5
PbS	7	8	8
ZnS	2	5	7
FeSO4	3	0	0
Pb	8	4	10
Ni	13	5	1
Co	37	42	37
Cr	8	9	13
V	40	55	40
Hg			
As			
U	5	3	31

HIGH TITANIUM DAIBASE

MAJOR ELEMENTS (WT%)

SAMPLE	JGT75218	01750200	542 804	542 850	542 925
SiO2	48.00	43.90	45.00	44.73	45.30
TiO2	2.28	1.80	1.59	1.56	1.52
Al2O3	14.70	17.63	16.73	16.17	16.57
Fe2O3	12.43	10.68	11.10	10.28	10.82
MnO	.20	.16	.19	.17	.17
MgO	6.32	6.70	7.04	5.86	6.67
CaO	9.40	9.32	9.45	6.66	8.67
Na2O	2.89	3.05	2.92	5.21	4.07
K2O	.70	.25	.24	.07	.10
LOI	1.60	4.10	4.10	7.10	5.00
TOTAL	98.52	97.59	98.36	98.78	98.89

TRACE ELEMENTS (PPM)

	JGT75218	01750200	542 804	542 850	542 925
Zr	142	145	154	1.8	156
Sr	24	142	369	361	427
Rb	16	51	15	14	14
Zn	42	117	98	92	87
Cu	57	52	29	27	27
S	276	755	373	245	117
CuS	19	43	29	13	23
FeS	11	25	5	2	3
ZnS	10	16	10	13	18
FeSO4	0	0		0	
Nb	15	25	42	39	42
Ni	32	43	76	65	9
Co	27	30	41	3	38
Cr	139	28	87	87	70
V	115	255	236	212	200
Hg		31	19	17	12
As		0	17	14	14
S	31				

HIGH TITANIUM DIABASE

MAJOR ELEMENTS (WT%)

SAMPLE	07920875	07921500	08681025	08690650	08692000
SiO2	45.08	45.83	54.80	46.28	55.20
TiO2	2.22	1.91	1.45	2.48	1.47
Al2O3	15.75	17.24	15.40	15.80	15.00
Fe2O3	13.90	12.33	9.70	13.39	8.18
MnO	.23	.21	.19	.20	.13
MgO	6.99	7.29	5.53	7.25	2.74
CaO	.96	9.43	9.17	9.54	7.83
Na2O	2.40	2.41	2.93	3.30	4.00
K2O	.24	.28	.80	.32	.38
LOI	3.60	3.90	3.10	3.20	5.80
TOTAL	91.29	99.95	103.07	101.68	103.23

TRACE ELEMENTS (PPM)

	07920875	07921500	08681025	08690650	08692000
Zr	167	151	219	146	206
Sr	325	347	248	302	491
Rb	17	14	18	17	17
Zn	126	63	101	110	84
Cu	62	49	27	18	19
Fe	239	3-S	272	114	114
As	61	52	26	62	11
Pb	17	11	12	6	15
Zn	26	11	25	27	22
BaSO4				0	
Pb	3	11	25	23	24
Ni	57	82	31	61	15
Co	45	38	33	41	22
Cr	61	58	52	128	45
V	354	253	230	330	170
Sg	21	18	25	54	23
3	0	3	1	5	1
5					

HIGH TITANIUM DAIBASE

MAJOR ELEMENTS (WT%)

SAMPLE	12149025	12143790	14930630	24461950	27648125
SiO2	45.60	44.60	49.50	47.40	48.90
TiO2	2.80	2.22	1.82	2.34	2.77
Al2O3	12.80	15.57	16.10	15.46	13.24
Fe2O3	13.32	12.44	10.70	11.70	14.05
MnO	.22	.19	.22	.20	.27
MgO	3.80	7.09	6.19	6.51	4.70
CaO	7.41	10.28	9.76	8.97	7.53
Na2O	3.22	2.43	2.42	2.57	4.24
K2O	.41	.16	.82	.92	.28
LOI	7.10	4.80	2.90	3.10	3.80
TOTAL	99.98	103.58	99.94	99.37	99.40

TRACE ELEMENTS (PPM)

Zr	192	176	173	174	151
Sr	510	438	419	421	145
Rb	16	13	19	19	13
Zn	161	109	55	77	95
Cu	15	47	58	41	14
Ba	476	43	113	77	173
CuS	12	41	14	9	12
NiS	11	7	11	8	14
ZnS	37	16	19	10	54
FeO4		0		0	
Pb	35	54	14	6	12
Ni	9	74	15	3	7
Co	29	43	49	43	2
Cr	26	170	76	13	5
V	312	184	242	28	768
Hg	49	36	18	7	12
As	12	11	4	3	9
S					

HIGH TITANIUM DAIBASE

MAJOR ELEMENTS (WT%)

SAMPLE	27040350	27040425	27040475
SiO2	44.80	45.70	41.60
TiO2	1.09	2.23	2.60
Al2O3	15.46	14.93	14.65
Fe2O3	11.70	13.05	11.70
MnO	.18	.19	.20
MgO	7.49	6.87	6.28
CaO	9.57	9.22	9.65
Na2O	2.92	2.42	2.43
K2O	.37	.40	.50
LOI	7.00	4.30	11.60
TOTAL	99.50	99.31	100.61

TRACE ELEMENTS (PPM)

Zr	141	136	128
Sr	332	39	228
Rb	18	16	22
Zn	91	105	123
Cu	59	56	45
Cu	372	41	2
CuS	46	61	48
NiS	13	19	54
ZnS	13	12	19
FeSO4			28
Pb	18	15	25
Ni	64	67	52
Co	5	23	33
Cr	65	36	28
V	313	437	265
Hg	8	12	14
Ag	3	3	1
Cb			

ALKALI FELDSPAR GRANITE

MAJOR ELEMENTS (WT%)

SAMPLE	BJ51 55	BJ52 60	JGT/5124	JGT 124A	JGT 233A
SiO2	74.50	73.80	76.59	76.93	75.70
TiO2	.20	.28	.06	.12	.10
Al2O3	12.99	13.53	11.18	11.53	12.05
Fe2O3	1.36	1.74	2.57	1.62	.97
MnO	0.00	.03	0.00	.03	.01
MgO	.02	.43	.01	.15	.01
CaO	.62	.71	.01	.31	.27
Na2O	4.10	4.21	3.45	3.93	3.57
K2O	4.33	4.25	4.12	4.40	5.03
LOI	1.00	1.50	.70	.50	.60
TOTAL	99.22	99.13	98.52	99.49	98.51

TRACE ELEMENTS (PPM)

Zr	115	142	116	464	142
Sr	72	67	15	14	23
Rb	126	117	72	148	153
Zn	14	15	122	65	7
Cu	1	1	2	1	1
Ba	7	4	5	5	9
S	2	4	1	2	1
S	10	11	12	01	2
Z S	1	1	33	97	1
PbSO4	0	0	0	0	0
b	8	7	28	47	5
i	3	3	3	3	1
Co	3	51	22	16	07
Cr	7	79	6	5	6
V	10	25	10	58	15
Hg					
F					
	13	18	2	2	2

ALKALI FELDSPAR GRANITE

MAJOR ELEMENTS (WT%)

SAMPLE	JGT75231	JGT 231A	JGT75276	JGT75277	JGT 315A
SiO2	76.50	76.99	70.78	73.10	75.68
TiO2	.16	.12	.36	.26	.10
Al2O3	12.38	12.05	14.83	13.22	12.78
Fe2O3	1.31	1.30	2.50	1.81	1.28
MnO	.01	.01	.04	.03	.01
MgO	.02	.02	.42	.35	.03
CaO	.35	.35	.49	.38	.31
Na2O	3.79	3.74	3.95	4.02	3.63
K2O	4.81	4.91	5.12	5.11	5.44
LOI	.50	.50	1.10	.80	.40
TOTAL	99.83	99.98	98.69	99.58	99.58

TRACE ELEMENTS (PPM)

	JGT75231	JGT 231A	JGT75276	JGT75277	JGT 315A
Sr	145	114	263	229	124
Cr	29	32	53	43	34
Rb	137	151	133	129	158
Zn	28	33	27	31	21
Cu	1	1	1	1	1
Ni	7	7	1	1	5
PbS	1	2	0	0	1
ZnS	8	5	1	1	5
FeS	18	15	5	14	2
S.SO4	0	0	0	0	0
Pb	7	13	8	5	11
Th	1	1	1	1	5
Co	59	58	58	59	57
Cr	7	10	8	7	8
V	10	10	10	10	10
	3	58	2	2	8

ALKALI FELDSPAR GRANITE

MAJOR ELEMENTS (WT%)

SAMPLE	J\\ 315B	JGT 315C
SiO2	74.20	72.20
TiO2	.26	.28
Al2O3	13.10	13.49
Fe2O3	1.59	1.83
MnO	.02	.01
MgO	.12	.20
CaO	.49	.78
Na2O	3.84	3.80
K2O	5.46	5.58
LOI	.50	.50
TOTAL	99.58	98.47

TRACE ELEMENTS (PPM)

	J\\ 315B	JGT 315C
Zr	178	185
Sr	42	77
Rb	172	147
Zn	21	29
Cu	1	1
Ba	893	9
CuS	3	2
NiS	3	3
ZnS	4	.8
FeSO4	0	0
Pb	29	21
Ni	1	1
Co	62	42
Cr	7	9
V	10	10
Hg		
As		
Sb	14	15

HYBIRD GRANITE

MAJOR ELEMENTS (WT%)

SAMPLE   JGT75279

SiO2	58.40
TiO2	1.62
Al2O3	13.74
Fe2O3	8.60
MnO	.16
MgO	3.36
CaO	4.88
Na2O	3.89
K2O	2.57
LOI	1.40

TOTAL   98.62

TRACE ELEMENTS (PPM)

Zr	208
Sr	164
Rb	64
Zn	56
Cu	17
Ba	48
CuS	15
PbS	5
ZnS	11
BaSO4	0
Pb	21
Ni	10
Co	32
Cr	38
V	175
Hg	
Ag	
Nb	20

RHYOLITE DYKES

MAJOR ELEMENTS (WT%)

SAMPLE	07920300	08681000	08690175	08691925
SiO2	71.40	73.00	65.80	67.60
TiO2	.38	.13	.11	.10
Al2O3	13.61	11.29	15.30	13.40
Fe2O3	2.88	3.24	1.27	1.45
MnO	.06	.11	.10	.08
MgO	.68	.20	.62	.51
CaO	1.79	1.42	5.26	5.48
Na2O	4.07	3.35	.57	4.39
K2O	1.91	3.49	3.59	1.87
LOI	2.50	2.10	7.30	5.50
TOTAL	99.28	98.33	99.92	100.38

TRACE ELEMENTS (PPM)

Zr	183	562	91	61
Sr	223	0	211	172
Rb	46	63	80	52
Zn	44	129	25	31
Cu	3	8	5	3
Ba	873	743	582	425
CuS	0	5	1	1
PbS	13	12	22	18
ZnS	13	55	11	3
BaSO4		0		0
Pb	19	19	20	27
Ni	2	3	2	1
Co	3	2	1	2
Cr	34	23	18	21
V	4	11	7	13
Hg	13	82	137	19
Ag	1	0	2	0
Nb				

PERALKALINE GRANITE

MAJOR ELEMENTS (WT%)

SAMPLE	BAFF 2	JGT75265	JGT75266	JGT75274	JGT75275
SIO2	75.00	76.90	74.00	77.20	76.90
TIO2	.32	.14	.16	.18	.12
Al2O3	11.69	11.42	11.46	11.01	11.01
Fe2O3	2.61	2.22	2.66	2.61	1.87
MnO	.06	.04	.08	0.00	.07
MgO	.01	.01	.01	.01	.01
CaO	.40	.09	.49	.05	.13
Na2O	4.27	3.88	3.94	3.46	3.97
K2O	4.79	4.53	4.41	4.06	4.70
LOI	.30	.40	1.20	.70	.30
TOTAL	99.45	99.63	98.41	99.28	99.08

TRACE ELEMENTS (PPM)

Zr		458	471	834	167
Sr	17	17	27	13	19
Rb	80	94	76	90	198
Zn	21	57	110	109	29
Cu	1	7	5	1	1
Ba		533	955	326	201
CuS	1	7	4	2	1
PbS	24	17	0	11	3
ZnS	21	45	107	46	2
BaSO4		0	0	0	0
Pb	26	28	19	28	18
Ni	3	3	4	2	1
Co	53	54	38	32	61
Cr		6	18	7	7
V	10	10	10	10	10
Hg					
Ag					
Nb		31	29	47	92

SPRINGDALE GROUP (?) IGNIMBRITE

MAJOR ELEMENTS (WT%)

SAMPLE   JGT 266A

SiO2	76.70
TiO2	.14
Al2O3	12.38
Fe2O3	1.18
MnO	.03
MgO	.01
CaO	.05
Na2O	5.18
K2O	1.58
LOI	1.30

TOTAL   99.35

TRACE ELEMENTS (PPM)

Zr	89
Sr	40
Rb	52
Zn	15
Cu	1
Ba	213
CuS	1
PbS	2
ZnS	1
BaSO4	0
Pb	12
Ni	1
Co	45
Cr	0
V	10
Hg	
Ag	
Nb	17

HUNGRY MOUNTAIN COMPLEX

MAJOR ELEMENTS (WT%)

SAMPLE	JGT 317A	2856 145	2856 317
SiO2	64.10	73.90	73.80
TiO2	.54	.14	.34
Al2O3	15.80	13.33	12.68
Fe2O3	5.21	1.59	2.38
MnO	.07	.03	.05
MgO	1.63	.62	1.09
CaO	4.04	1.00	1.86
Na2O	3.45	3.25	3.66
K2O	2.33	5.00	2.68
LOI	1.20	1.00	1.20
TOTAL	98.45	99.86	99.74

TRACE ELEMENTS (PPM)

	JGT 317A	2856 145	2856 317
Zr	166	97	86
Sr	352	218	197
Rb	68	119	67
Zn	31	25	28
Cu	1	6	1
Ba	1621	1858	885
CuS	1	6	2
PbS	6	15	22
ZnS	3	12	11
BaSO4	0	0	0
Pb	18	15	15
Ni	1	44	7
Co	38	40	30
Cr	12	10	10
V	60	15	30
Hg			
Ag			
Nb	6	7	5

MISCELLANEOUS SAMPLES

MAJOR ELEMENTS (WT%)

SAMPLE	08681612	12141315
SiO2	72.60	70.10
TiO2	0.00	.35
Al2O3	1.82	11.43
Fe2O3	19.12	6.64
MnO	.11	.20
MgO	.41	2.57
CaO	3.54	1.42
Na2O	.05	2.60
K2O	.25	1.35
LOI	2.60	2.70
TOTAL	100.50	99.36

TRACE ELEMENTS (PPM)

Zr	25	123
Sr	48	211
Rb	18	38
Zn	34	71
Cu	4	50
Ba	686	143
CuS	1	43
PbS	12	12
ZnS	2	13
BaSO4		
Pb	22	19
Ni	5	7
Co	9	7
Cr	34	36
V	21	48
Hg	15	245
Ag	0	1
Nb		

APPENDIX IV

FACTOR ANALYSIS

R-mode factor analysis used in this study was computed by
Newfoundland and Labrador Computer Services using program
BMDO8M. A general description from their program manual
is as follows:

General Description, Factor Analysis Program BMDO8M

This program performs a factor analysis of up to 198 input
variables. The factoring may be done using either covariance
or correlation matrices. Initial communality estimates may
be squared multiple or they may be specified by the user.
If requested, the program will iterate on the initial
communality estimates. Three types of rotation are available,
all based on the oblimin criterion. In the first, the
factors are restricted to be orthogonal which yields, among
others, quartimax and varimax rotations. In the second, the
criterion are applied to the reference factor structure and
the factors are allowed to be oblique which yields the standard
oblimin rotations. In the third, the criterion are applied
to the primary factor loadings, allowing the factors to be
oblique and yielding simple loadings rotations (1). Factor
scores may be estimated. Data input may be in the form of
raw data, a correlation matrix, a covariance matrix, or a
factor loading matrix.

Output from this program includes:

1) Means and standard deviations

2) Correlation or covariance matrix

3) Eigenvalues and cumulative proportion of total variance

4) Communalities

5) Factor loading matrix before rotation

6) Rotated factor loading matrix

7) Correlation matrix of the rotated factors

8) Factor scores

H 2501 (2

H 2528

JGT.-280
JGT.-279
JGT.-278
JGT.-277

JGT.-276

H·2622(4)

H 2530   H 2571

TOPSAILS   GRANITE

H 266

H 2820   H 2867

H 2769 ●
H 2777 ●

H 2880

JGT.-1568

H 2882●   ●H 2
H 2879●   ●M 2
H 2886(2)

JGT.-315
a   b   c

H 2350   H 2886(

H 2886

1 OF

JGT.-124

JGT.-317 A

HUNGRY MOUNTAIN COMPLEX

H 2856(2)

H 2501 (2)

H 2855(2)

H 2852

BUCHANS LAKE

H 2490

H 2528

H 2090(2)

H 2858

H 2851 (6)

H2530   H 2571

2622(4)

H2762   H1960

H 2841(2)

H2854

2867

H1940(2)

H2853

H 2105(3)

H 2680 H925

H2660

H 2610

H 2666(40)

H 2043

H1903

H1917 B2704

H1911

H1493   JGT.-170

H 2348

H869   H885

H1258

H868

H2769

H2785(2)   H1214   JGT.-40-43   H1083

H 2777

H 2710(2)

H2800 ● H1096
(2)

JGT.44

H782

H 2771(2)   H202   JGT.-328

H1406

H175

H 645(7)

H932   H542

H 2880

H1908

H 2901

●H2899

H 2882   ●N 2900

H978(2)

H 2879   ●H2897
H2895

H2868(2)

H2884

H 2350

H 2886(2)

H2885

COMPLEX

JGT.-113

JGT.-317

H 2856(2)

BUCHANS
LAKE

H2839 (4)

H 2837 (17)

H 2842

H 1920

H 2854

H 2853

H 1782

H 2859

H 1662

H1683

H 1589 (3)

H 1568

H1608(2)

H1730

H298

H 1352

JGT.-170

H665

H1062

H972

H158(2)

H2785(2)

H1214

JGT.-40-43

H1065

H1872

H2800

H1096

H1202

H2367

H792

(2)

H1479

H202

JGT.-328

JGT. 44

M175

H932

H642

H1908

BUCHANS
GROUP

B.J.-46

B.J.-4

B.J.-47

H1917

H2704

H1493

H559

H868

2771(2)

78(2)

TOPSAILS   GRANITE

●B.J.50

●B.J.51

B.J.-46
●
    B.J.-45
    ●
       ●B.J.-49
B.J.-47
●
   ●B.J.-48

      ●B.J.10

BUCHANS
GROUP

●B.J.-42(B)

ITE

JGT-265 ● ●JGT-266-266 A

B.J.50 ●

(1) JO
A
LO

(2) NU
HO
OR

B.J.51 ●

B.J.52 ●

HUNGRY

MOUNTAIN

COMPLEX

O

5 of

B.J-42(B) ●

N

JGT- 265

JGT-266-266 A
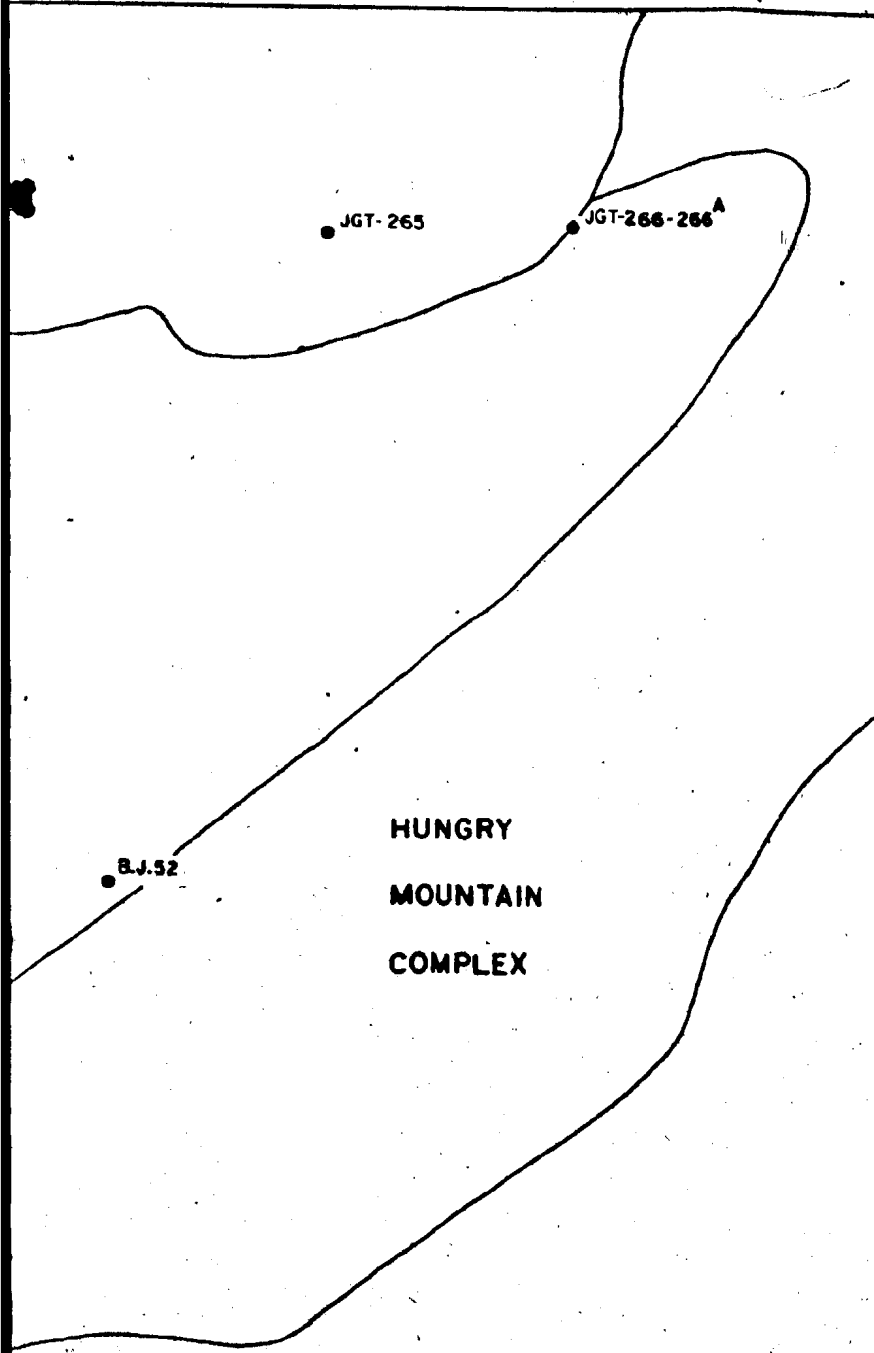
LEGEND

(1) JGT. SAMPLES ARE FROM OUTCROP
ALL OTHER ARE DRILL HOLE SAMPLE
LOCATIONS.

(2) NUMBER OF SAMPLES TAKEN FROM DRILL
HOLES IN BRACKETS, IF GREATER THAN
ONE.

HUNGRY

MOUNTAIN

COMPLEX

B.J.52

0   1000   2000   3000

Meters
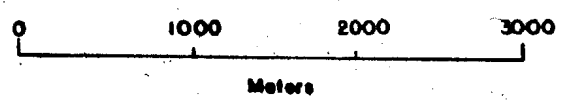
R.I.-5

JGT - 219

JGT-218

60F

JGT - 216

TOPSAILS GRANITE

FEEDER GRANODIORITE

JGT.-276
JGT.-279
JGT.-278
JGT.-277

H 2622(4)
H 2530
H 2571

H 2820
H 2867

H 2769
H 2777

JGT.-1668

H 2880

H 2882
H 2873
H 2866(2)
H 2886
H 2350

JGT.-315
a b c

JGT.-307
H 724 JGT.-305
H 718

JGT.-2271 & 231

JGT.-234

B.B.257

7₀F

B.B.246
B.B.247

B.B.229 B.B.232

H 2622(4)   H 2530   H 2371   H 2090(2)
                                  H 2858   H 2851(6)

                        H2762 H1960   H 2841(2)
                              H1940(2)

                              H2105(3)
                    H 2680 H925
H 2820   H 2867   H 2880   H 2810   H2666(40)

                        H 2043
                        H1903   H1917 & 2704
                        H1911   H 1493
                        H 2349   H969
                                          H868   JGT.-170
                    H 1258   H1214   JGT.-40-43
H 2769   H 2785(2)
H 2777   H 2710(2)   H2800
                                      H 792   (2)
                              H1406 H 2771(2) H202 JGT.-328
                                                H75
                    H 645(7)   H932   H542
H 2880   H1908
        H 2901
        H2899   H978(2)
H 2882 H 2900
H 2879 H2887
        H2869
H2866(2)
            H 2864
H 2350 H 2886(2)
        H 2885

JGT.-307
H 724 JGT.-305
    H 718
                                              H2754

                                H2753
                                          JGT.-190

GRANODIORITE

JGT.-234

B.B.257   JGT.-1608

B.B.246
B.B.247

B.B.229   B.B.232   8.0F

BUCHANS
GROUP

9 oF

BUCHANS
GROUP

B.J.-46
B.J.-45
B.J.-49
B.J.-47
B.J.-48
B.J.10

B.J.-42(8)

JGT.-134

RED INDIAN LAKE

100f

J.IO

B.J.-42(8)

JCT-216

AN LAKE

SAMPLE LOCATION MAP

0   1000   2000   3000

Meters

R.I.-5

JGT.-219

JGT.-218

JGT.-216

12•F12

FIGURE 1 — 2

SAMPLE LOCATION MAP

1" = 3333' OR 1 : 40,000

48°57'

HIND'S
LAKE

Sugarloaf
Mt.
1250'

9a

Little
Hind
Lake

River

55'

Orchid
Lake

Bluff

Hills

5A₀ ?

5A₀ ?

1 oF

9a

5A₀ ?

8b

White

Hills

Ken's Brook

Noah's
Ballast

50'

5A

9a

T   H

HIND'S
LAKE

Sugarloaf
Mt.
1250

9a

Little
Hind's
Lake

9a

9c

Orchid
Lake

Bluff
Hills

5A₀

Hungry Mt.

5A₀?

8b

5A₁?

Buchans

Lake

Wharf

50'   45'

T H E   T O P

9c

Barren Mt.

9c

9c

9a

Airport
Hill
1250

Buchans
Lake

Pond

P

Pond

45'

40'

T O P S A I L S

Barren Mt.

9a

Stag
Ridge

9c

9a

Mt. Lomas

1250

9a

Peyton's
Pond

9a

Little S.
Lake

Sof

S

9a

9a

Mt. Lomas

8b

Brook

Little Sandy
Lake

8a

Seal Pond

8b

Brook

Mary March

ndy

SYMBOLS

Geological boundary (defined, approximate, assumed)

Bedding, tops known (inclined, vertical) . . . .

Bedding, tops unknown (inclined, vertical) . . . .

Pillow bedding, tops known (inclined, vertical) . . . . . .

Flow banding (inclined, vertical) . . . .

Schistosity, foliation (inclined, vertical) . . . .

Foliation due to thrusting (inclined, vertical) . . . .

Anticline (approximate) . . . .

Syncline (approximate) . . . .

Thrust fault (defined, approximate or assumed) . . . . .

Fault (defined, approximate, assumed) . . . .

In situ and transported sulfides, extreme outline projected

Geology compiled by Asarco Inc. and Price Company Limited
remote areas compiled in consultation with Department
Newfoundland and Labrador.

Lake

Wharf

8c

5C

8b

8b

8a

BM 793

Woodman's Brook

8c

8b

BM 716

River

Tower

8b

SA

RED

INDIAN

GEO

9oF

SYMBOLS

Geological boundary (defined, approximate, assumed) ....

Bedding, tops known (inclined, vertical) 90

Bedding, tops unknown (inclined, vertical) ....

Pillow bedding, tops known (inclined, vertical) ....

Flow banding (inclined, vertical) ....

Schistosity, foliation (inclined, vertical) ....

Foliation due to thrusting (inclined, vertical) ....

Anticline (approximate) ....

Syncline (approximate) ....

Thrust fault (defined, approximate or assumed) ....

Fault (defined, approximate, assumed) ....

In situ and transported sulfides, extreme outline projected to surface ....

Geology compiled by Asarco Inc. and Price Company Limited (now Abitibi-Price Inc.). Geology in remote areas compiled in consultation with Department of Mines and Energy, Government of Newfoundland and Labrador.

Whole rock Rb/Sr isochrons determined by Bell and Blenkinsop using the decay constant λ 87

CARBONIFEROUS

Poorly indurated red sandstone and conglomerate

SILURIAN AND DEVONIAN

Reddish subaerial ignimbrite, flow banded rhyolite and pyroclastics. Extrusive equivalents of the Topsails Granite. 10a, subvolcanic quartz feldspar porphyry

TOPSAILS GRANITE

9a Alkali Feldspar Granite (387 ± 16 Ma): Fine grained, brick-red granite. Locally approaches syenite. Locally associated bodies of fine grained quartz-feldspar porphyry.

Mafic Intrusives (associated with Topsails Granite): Fine to coarse grained diabase ($9b_1$) and gabbro ($9b_2$).

Peralkaline Granite (421 ± 7 Ma): Medium to coarse grained, equigranular white-weathering granite.

Little Sandy Lake

8c

8a

8b

8b

River

BM 716

INDIAN LAKE

ED

GEOLOGICAL MAP OF BUCHANS. ARE
NEWFOUNDLAND

Scale 1:50,000 Échelle

Miles 1   0   1   2   3 Miles

Metres 1000   0   1000   2000   3000   4000 Mètres
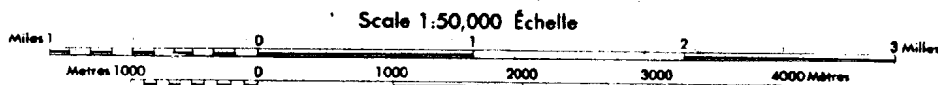
LEGEND

ORDOVICIAN - SILURIAN

BUCHANS GROUP (447 ± 18 Ma)

Upper Buchans Subgroup

US

indurated red sandstone and conglomerate

DEVONIAN

sh subaerial ignimbrite, flow-banded rhyolite and pyroclastics. Extrusive
lents of the Topsails Granite. 10a, subvolcanic quartz-feldspar porphyry.

NITE

Feldspar Granite (387 ± 16 Ma): Fine grained, brick-red granite. Locally
ches syenite. Locally associated bodies of fine grained quartz-feldspar
ry.

intrusives (associated with Topsails Granite): Fine to coarse grained
e (9b$_1$.) and gabbro (9b$_2$).

line Granite, (421 ± 7 Ma): Medium to coarse grained, equigranular,
weathering granite.

Lake Seven Basalt: Basaltic, amygdaloidal, feldsparphyric, hematitized lava,
pillow lava, breccia and minor tuff ; 6a, arkosic interbeds

Lower Buchans Subgroup

Lucky Strike Ore Horizon Sequence: Predominantly felsic sequence of
pyroclastics, flows, breccias and clastic sediments; 5A, small rhyolite units at
base, flanked by pyritic siltstone and wacke, followed by 5A, dacitic crystal-vitric
tuffs gradational with 5A, lithic-rich pyroclastic breccias and in situ massive and
fragmental transported sulfides; 5A, granite-bearing breccia-conglomerate;
5A, mafic interbeds.

Intermediate Footwall: Complex assemblage of mafic to felsic pyroclastics,
breccias, minor flows. Locally altered, mineralized.

Little Sandy Lake

8b

LAKE

L MAP OF BUCHANS AREA
NEWFOUNDLAND

Scale 1:50,000 Échelle

0   1   2   3 Miles

0   1000   2000   3000   4000 Mètres

LEGEND

(± 18 Ma)

up

lt: Basaltic, amygdaloidal, feldsparphyric, hematitized lava,
e and minor tuff ; 6a, arkosic interbeds

p

re Horizon Sequence: Predominantly felsic sequence of
n, breccias and clastic sediments; 5A, small rhyolite units at
yritic siltstone and wacke, followed by 5A, dacitic crystal-vitric
with 5A, lithic-rich pyroclastic breccias and in situ massive and
ported sulfides; 5A, granite-bearing breccia-conglomerate.
s.

hult: Complex assemblage of mafic to felsic pyroclastics,
ws. Locally altered, mineralized.

8b
8a
Little Sandy Sequence: Interfingered and inter
felsic volcanic rocks with the latter predom
pillow lava, breccia, pyroclastic flows and
volcanics; 8b, dacitic breccia and quartz-fe
quartz-feldspar crystal tuffs, breccias, tuffs, p
massive flows; 8d, dominantly intermediate fra
and mineralized.

Upper Arkose: Resedimented arkosic conglo
graywacke, siltstone; 7a, interbeds of mafic vo
6

Oriental Ore Horizon Sequence: Complex as
breccias, flows and clastic sediments. Similar i
to Lucky Strike Ore Horizon Sequence; 5B, cac
flows, flanked and overlain by 5B, pyritic siltsc
dacitic crystal-vitric tuffs greisenized with poly
situ massive and fragmental transported sulfi
with 5B, granitoid-bearing breccia-conglomera

Old Mill Sequence: Stratigraphic equivalent o
pillow lava, porphyritic and amygdaloidal ba

HANS AREA

3 Miles

4000 Mètres

Mary March

Mary March
Provincial Park

12 0F

Little Sandy Sequence: Interfingered and interbedded mafic, intermediate and felsic volcanic rocks with the latter predominant; 8a, basaltic and andesitic pillow lava, breccia, pyroclastic flows and tuff, minor unseparated felsic volcanics; 8b, dacitic breccia and quartz-feldspar crystal tuff; 8c, rhyolitic quartz-feldspar crystal tuffs, breccias, tuffs, pyroclastic flows, flow-banded to massive flows; 8d, dominantly intermediate fragmental volcanics, locally altered and mineralized.

Upper Arkose: Resedimented arkosic conglomerate, lithic arkose, siliceous graywacke, siltstone; 7a, interbeds of mafic volcanics, possibly correlative with 6.

Oriental Ore Horizon Sequence: Complex assemblage of felsic pyroclastics, breccias, flows and clastic sediments. Similar lithologically and stratigraphically to Lucky Strike Ore Horizon Sequence; 5B_a, coalescing rhyolite breccia domes at base, flanked and overlain by 5B_b, pyritic siltstone and wacke, followed by 5B_c, dacitic crystal-vitric tuffs gradational with polylithic breccia-conglomerate and in situ massive and fragmental transported sulfides which in turn are associated with 5B_d, granitoid-bearing breccia-conglomerate.

Ski Hill Sequence: Stratigraphic equivalent of Intermediate Footwall. Basaltic pillow lava, porphyritic and amygdaloidal andesitic flow breccias and fine to coarse pyroclastics. Includes minor polylithic breccias near stratigraphic top,

9D₁

Hoognose Mt.

9D₁

9D₁

9a

3A₁ₐ

3A₁ₐ

3A₁ₐ

3A₁ᵦ

3A₁ᵦ

3Aₐ

3A₁ₐ

3A₁ₐ

3A₁ᵦ

3A₁ₐ

3Aₐ

3A₁ᵦ

9D₁

4A

Lake 15

5Aₐ

5Aᵦ

5Aₑ

5Aₐ

5Aᵦ

5Aₑ

5Aₐ

5Aᵦ

5Aₑ

3A₁ᵦ

5Aₐ

Brook

13

11

9a

9a

9a

48°42

57°04

57°00

13 DF

Geological boundary (defined, approxim...

Bedding, tops known (inclined, vertica...

Bedding, tops unknown (inclined, vertic...

Pillow bedding, tops known (inclined, v...

Flow banding (inclined, vertical)

Schistosity, foliation (inclined, vertical...

Foliation due to thrusting (inclined, vertic...

Anticline (approximate)

Syncline (approximate)

Thrust fault (defined, approximate or as...

Fault (defined, approximate, assumed)

In situ and transported sulfides, extrem...

Geology compiled by Asarco Inc. and Pr...
remote areas compiled in consultation...
Newfoundland and Labrador.

Whole rock Rb/Sr isochrons determined...
Rb of 1.42×10^{-11} yr^{-1}

Map accompanies manuscript "Geolo...
Newfoundland", by J.G. Thurlow and...
Thurlow, J.G., eds., The Buchans Oreb...
Canada Spec. Paper 22, in press.

Geological cartography by Mineral De...
Government of Newfoundland and Labr...

Base maps at same scale published by...
Mines and Resources, Ottawa

Approximate magnetic declinations, 1...
annually.

Elevations in feet above mean sea level

Hooknor Mt.

Willy's Lakes

Willy's Brook

Lake 4

3A₂

3A₁ₐ

R E D

SYMBOLS

Geological boundary (defined, approximate, assumed) ....

Bedding, tops known (inclined, vertical) ....

Bedding, tops unknown (inclined, vertical) ....

Pillow bedding, tops known (inclined, vertical) ....

Flow banding (inclined, vertical) ....

Schistosity, foliation (inclined, vertical) ....

Foliation due to thrusting (inclined, vertical) ....

Anticline (approximate) ....

Syncline (approximate) ....

Thrust fault (defined, approximate or assumed) ....

Fault (defined, approximate, assumed) ....

In situ and transported sulfides, extreme outline projected to surface ....

Geology compiled by Asarco Inc. and Price Company Limited (now Abitibi-Price Inc.). Geology in remote areas compiled in consultation with Department of Mines and Energy, Government of Newfoundland and Labrador.

Whole rock Rb/Sr isochrons determined by Bell and Blenkinsop using the decay-constant for ^{87}Rb of 1.42×10^{-11} yr^{-1}

Map accompanies manuscript "Geology and Ore Deposits of the Buchans Area, Central Newfoundland", by J.G. Thurlow and E.A. Swanson in Swanson, E.A., Strong, D.F. and Thurlow, J.G., eds., The Buchans Orebodies: Fifty Years of Geology and Mining: Geol. Assoc. Canada Spec. Paper 22, in press.

Geological cartography by Mineral Development Division, Department of Mines and Energy, Government of Newfoundland and Labrador.

Base maps at same scale published by the Surveys & Mapping Branch, Department of Energy, Mines and Resources, Ottawa.

Approximate magnetic declinations, 1969, for center of map, 28°39'W, decreasing 3.0' annually.

Elevations in feet above mean sea level.

CARBONIFEROUS

Poorly indurated red sandstone and conglomerate

SILURIAN AND DEVONIAN

Reddish subaerial ignimbrite, flow-banded rhyolite equivalents of the Topsails Granite. 10a, subvolcanic

TOPSAILS GRANITE

9a Alkali Feldspar Granite (387 ± 16 Ma): Fine grained approaches syenite. Locally associated bodies of porphyry.

Mafic Intrusives (associated with Topsails Granite) diabase (9b₁) and gabbro (9b₂).

9c Peralkaline Granite (421 ± 7 Ma): Medium to coarse white-weathering granite.

50'

49'

RED INDIAN LAKE

8b

BM 726

GEOLOGICAL MAP OF BUC

NEWFOUNDLAND

Scale 1:50,000 Échelle

Miles 1   0   1   2

Metres 1000   0   1000   2000   3000

LEGEND

CARBONIFEROUS

Poorly indurated red sandstone and conglomerate

SILURIAN AND DEVONIAN

Reddish subaerial ignimbrite, flow-banded rhyolite and pyroclastics. Extrusive equivalents of the Topsails Granite. 10a, subvolcanic quartz-feldspar porphyry.

TOPSAILS GRANITE

Alkali Feldspar Granite (387 ± 16 Ma): Fine grained, brick-red granite. Locally approaches syenite. Locally associated bodies of fine grained quartz-feldspar porphyry.

Mafic Intrusives (associated with Topsails Granite): Fine to coarse grained diabase ($9b_1$) and gabbro ($9b_2$).

Peralkaline Granite (421 ± 7 Ma): Medium to coarse grained, equigranular, white-weathering granite.

ORDOVICIAN - SILURIAN

BUCHANS GROUP (447 ± 18 Ma)

Upper Buchans Subgroup

Lake Seven Basalt: Basaltic, amygdaloidal, feldsparphyric, hematitized lava, pillow lava, breccia and minor tuff ; 6a, arkosic interbeds

Lower Buchans Subgroup

Lucky Strike Ore Horizon Sequence: Predominantly felsic sequence of pyroclastics, flows, breccias and clastic sediments; 5A, small rhyolite units at base, flanked by pyritic siltstone and wacke, followed by 5A, dacitic crystal-vitric tuffs gradational with 5A, lithic-rich pyroclastic breccias and in situ massive and fragmental transported sulfides; 5A, granite-bearing breccia-conglomerate; 5A, mafic interbeds.

Intermediate Footwall: Complex assemblage of mafic to felsic pyroclastics, breccias, minor flows. Locally altered, mineralized.

Footwall Arkose: 3A, Lithic arkose, with local thin, widely separated interbeds of mudstone, siltstone, siliceous graywacke, conglomerate; 3A, sequence of pumiceous felsic pyroclastics and interbedded tuffaceous sediments, underlying lithic arkose east of Buchans; 3A, basaltic lava, pillow lava, pillow breccia, lesser pyroclastics and lenses of bedded chert.

Footwall Basalt: 2a, Basaltic lava, pillow lava and pillow breccia, weakly to strongly amygdaloidal, feldsparphyric and hematitized, with lesser pyroclastics and discontinuous lenses of multicolored bedded chert. Host for Skidder Brook massive sulfide deposit; 2b, felsic flows, breccia and tuff; 2c, rhyolite.

ORDOVICIAN OR OLDER

Hungry Mountain Complex (860 ± 70 and 400 ± 60 Ma): Massive to foliated biotite granodiorite, hornblende diorite, gabbro and amphibolite with less abundant foliated granite.

45'   40'

L A K E

GICAL MAP OF BUCHANS AREA
NEWFOUNDLAND

Scale 1:50,000 Échelle

Fertes 1000   0   1000   2000   3000   4000 Metres

0 _____ 1 _____ 2 _____ 3 Miles

LEGEND

DVICIAN - SILURIAN

HANS GROUP (447 ± 18 Ma)

Upper Buchans Subgroup

Lake Seven Basalt: Basaltic, amygdaloidal, feldsparphyric, hematitized lava, pillow lava, breccia and minor tuff ; 8a, arkosic interbeds

Lucky Strike Ore Horizon Sequence: Predominantly felsic sequence of pyroclastics, flows, breccia and clastic sediment; 5A, small rhyolite units at base, flanked by pyritic siltstone and wacke, followed by 5A, dacitic crystal-vitric tuffs gradational with 5A, lithic-rich pyroclastic breccia and in situ massive and fragmental transported sulfides; 5A, granite-bearing breccia-conglomerate; 5A, mafic interbeds.

lower Buchans Subgroup

Intermediate Footwall: Complex assemblage of mafic to felsic pyroclastics, breccia, minor flows. Locally altered, mineralized.

Footwall Arkose: 3A, Lithic arkose, with local thin, widely separated interbeds of mudstone, siltstone, siliceous greywacke, conglomerate; 3A, sequence of pumiceous felsic pyroclastics and interbedded tuffaceous sediment, underlying lithic arkose east of Buchans; 3A, basaltic lava, pillow lava, lesser pyroclastics and lenses of bedded chert.

Footwall Basalt: 2a, Basaltic lava, pillow lava and pillow breccia, weakly to strongly amygdaloidal, feldsparphyric and hematitized, with lesser pyroclastics and discontinuous lenses of multicolored bedded chert. Host for Skidder Brook massive sulfide deposit; 2a, felsic flows, breccia and tuff; 2c, rhyolite.

OVICIAN OR OLDER

Hungry Mountain Complex (460 ± 70 and 400 ± 60 Ma): Massive to foliated biotite granodiorite, hornblende diorite, gabbro and amphibolite with less abundant sulfide deposit; 2a, felsic flows, breccia and tuff; 2c, rhyolite.

Wiley's Prominent Quartz Sequence: Stratigraphic volcanic equivalent of 3A, felsic pyroclastics characterized by quartz crystals commonly exceeding 10 mm in diameter; 3A, rhyolite flows and tuffs; 3A, dacitic pyroclastics; 3A, interbeds of basaltic lavas; pillow lavas; 3A, multicolored tuffaceous siltstone, siltstone, mudstone and chert.

Feeder Granodiorite (410 ± 80 Ma): Pink, medium to coarse grained, biotite granodiorite, probably synchronous with 3A, and other Buchans Group rocks.

Ski Hill Sequence: Stra... pillow lava, porphyritic coarse pyroclastics. Inc... overlain in subsurface pumiceous pyroclastics

Prominent Quartz Seq... rhyolitic (3A,) pyrocla... subaqueous pyroclastic... important basaltic mem...

Oriental Ore Horizon S... breccias, flows and clas... to Lucky Strike Ore Hor... base, flanked and over... dacitic crystal-vitric tuf... situ massive and fragm... with 5A, granitoid bear...

Upper Arkose: Resed... greywacke, siltstone. 7a...

Little Sandy Sequence: ... felsic volcanic rocks w... pillow lava, breccia, ... volcanics; 8b, dacitic b... quartz-feldspar crystal ... massive flows; 8d, dom... and mineralized.
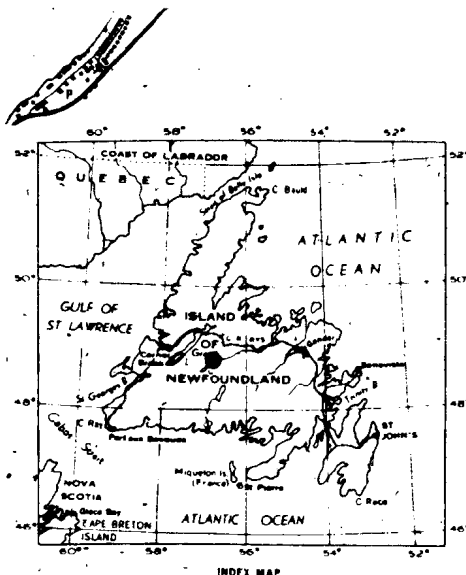
HANS AREA

3 Miles

4000 Metres

Little Sandy Sequence: Interfingered and interbedded mafic, intermediate and felsic volcanic rocks with the latter predominant; 8a, basaltic and andesitic pillow lava, breccia, pyroclastic flows and tuff, minor unseparated felsic volcanics; 8b, dacitic breccia and quartz-feldspar crystal tuff; 8c, rhyolitic quartz-feldspar crystal tuffs, breccias, tuffs, pyroclastic flows, flow-banded to massive flows; 8d, dominantly intermediate fragmental volcanics, locally altered and mineralized.

Upper Arkose: Resedimented arkosic conglomerate, lithic arkose, siliceous graywacke, siltstone; 7a, interbeds of mafic volcanics, possibly correlative with 6.

Oriental Ore Horizon Sequence: Complex assemblage of felsic pyroclastics, breccias, flows and clastic sediments. Similar lithologically and stratigraphically to Lucky Strike Ore Horizon Sequence; 5B$_a$, coalescing rhyolite breccia domes at base, flanked and overlain by 5B$_b$, pyritic siltstone and wacke, followed by 5B$_c$, dacitic crystal-vitric tuffs gradational with polylithic breccia-conglomerate and in situ massive and fragmental transported sulfides which in turn are associated with 5B$_d$ granitoid-bearing breccia-conglomerate.

Ski Hill Sequence: Stratigraphic equivalent of Intermediate Footwall. Basaltic pillow lava, porphyritic and amygdaloidal andesitic flow breccias and fine to coarse pyroclastics. Includes minor polylithic breccias near stratigraphic top, overlain in subsurface by altered intermediate to felsic flows, breccias and pumiceous pyroclastics (Oriental Intermediate).

Prominent Quartz Sequence: Stratigraphic equivalent of 3A : Dacitic (3B$_a$) to rhyolitic (3B$_b$) pyroclastics; 3B$_c$ interbedded lenses of graded pumiceous subaqueous pyroclastic flows, cherty mudstone and siltstone; 3B$_d$ locally important basaltic members.

Wiley's Prominent Quartz Sequence: Stratigraphic volcanic equivalent of 3A; felsic pyroclastics characterized by quartz crystals commonly exceeding 10 mm in diameter; 3A$_a$, rhyolite flows and tuffs; 3A$_b$, dacitic pyroclastics; 3A$_c$, interbeds of basaltic lavas; pillow lavas; 3A$_d$, multicolored tuffaceous siltstone, siltstone, mudstone and chert.

Feeder Granodiorite (410±80 Ma): Pink, medium to coarse grained, biotite granodiorite, probably synchronous with 3A$_1$ and other Buchans Group rocks.

FIG. 2-2

45'

48°42'

35'

56°30'